HUMAN CONVECTIVE BOUNDARY LAYER AND ITS IMPACT ON PERSONAL EXPOSURE

DUSAN LICINA

NATIONAL UNIVERSITY OF SINGAPORE

TECHNICAL UNIVERSITY OF DENMARK

2015

HUMAN CONVECTIVE BOUNDARY LAYER AND ITS IMPACT ON PERSONAL EXPOSURE

DUSAN LICINA

(Bachelor of Eng., University of Belgrade;
Master of Eng., University of Belgrade)

A THESIS SUBMITTED

FOR THE DEGREE OF DOCTOR OF PHILOSOPHY

DEPARTMENT OF BUILDING
NATIONAL UNIVERSITY OF SINGAPORE

DEPARTMENT OF CIVIL ENGINEERING
TECHNICAL UNIVERSITY OF DENMARK

2015

DECLARATION

I hereby declare that this thesis is my original work and it has been written by me in its entirety. I have duly acknowledged all the sources of information which have been used in the thesis.

This thesis has also not been submitted for any degree in any university previously.

_____

Dusan Licina
09 January 2015

“Man cannot discover new oceans

unless he has the courage to lose sights of the shore”

-- Andre Gide

ACKNOWLEDGEMENTS

I would like to express my sincere gratitude to my advisors and mentors Professors Tham Kwok Wai and Chandra Sekhar from National University of Singapore. They provided me not only the inspiration for the ideas and concepts in research, but also their patience, guidance, encouragement and the freedom they allowed in my research. I would also like to express my sincere thanks to my advisor and mentor, Professor Arsen Krikor Melikov from Technical University of Denmark, for his continuous support and vital guidance. His encouragement, positive attitude, enthusiasm and immense knowledge made me inspired to be a better researcher and person. A very few students are fortunate enough to be guided through PhD journey by three advisors and mentors and I am very grateful for this opportunity.

I would like to thank to Dr. Jovan Pantelic, my good friend, colleague and mentor, whose knowledge and passion for science helped me develop more open approach towards scientific problems through numerous discussions we had.

I acknowledge the constructive suggestions given by my PhD thesis committee members: Prof. Atila Novoselac, Prof. Jørn Toftum and Prof. Harn Wei Kua. I would like to thank to Ms. Snjezana Skocajic, Ms. Patt Choi Wah, Ms. Christabel Toh and Ms. Stephanie Ong Huei Ling and other administrative staff who provided me with generous assistance beyond the scientific tasks. I express my gratefulness to the laboratory technicians: Mr. Zaini bin Wahid, Ms. Wu Wei Yi, Mr. Tan Cheow Beng, Mr. Peter Simonsen and Mr. Nico Henrik Ziersen who lent their expertise to realize my efforts in the experimental work.

My sincere gratitude goes to all the people who helped me in accomplishing my work and inspired me with their ideas and professional attitude. Special thanks to David Cheong, Willie Tan, Michael Khoo, Andre Nicolle, Christian Klettner, Zhecho Bolashikov, Gabriel Beko and Pawel Wargocki for inspiring discussions and their help on various tasks. I would also like to

thank to Professor Bjarne Olesen, the head of the International Center for Indoor Environment and Energy, for his helpfulness and admitting me into the joint PhD program. I thank to Professors Branislav Todorovic and Marija Todorovic for encouraging me to pursue the academic career and for enlightening me at the first glance of research.

Gratitude also goes out to the National University of Singapore and Technical University of Denmark for funding this effort and providing much needed apparatus and opportunity to participate at scientific conferences during the course of my doctoral research. I also acknowledge ASHRAE for awarding me with the Graduate Grant-in-Air for 2013.

I also owe a large debt of gratitude to all my fellow PhD students, especially Veronika Foldvary, Mariya Bivolarova and Ongun Kazanci, for stimulating discussions and all the fun we have had in the past several years. I would also like to thank to my colleagues Pawel Mioduszewski, Charalampos Angelopoulos and Kiriyaki Gialedaki, master students from Technical University of Denmark, for their kind assistance during the experimental measurements.

Another huge thanks goes to all my friends that have provided the real support in the form of necessary distractions that have kept me sane throughout my PhD research. There are many of you to name, but you certainly know who you are, and I cannot express my gratitude enough for the time and memories that we now share. I thank to my sister and brother-in-law Jelena Sreckovic and Milan Sreckovic, and to the future Dr. Stefan Sreckovic, for their enduring support and unconditional love.

Most of all, I would like to thank to my father Zarko Licina and my mother Ljiljana Licina who always believed in me and gave me all the support I could ever ask for. They taught me how to be persistent and not to turn away from difficulties, but to face them and overcome them. Thank you!

TABLE OF CONTENTS

SUMMARY

People spend most of their time indoors and they are constantly exposed to pollution that affects their health, comfort and productivity. Due to strong economic and environmental pressures to reduce building energy consumption, low air velocity design is gaining popularity; hence buoyancy flows generated by heat sources are gaining more prominent influence in space airflow formation and on the indoor environment overall. In such spaces with low air supply velocity, air mixing is minimized and the pollution emitted from localized indoor sources is non-uniformly distributed. The large spatial differences in pollution concentration mean that personal exposure, rather than average space concentration, determines the risk of elevated exposure. Current room air distribution design practice does not take into account the air movement induced by the thermal flows from occupants, which often results in inaccurate exposure prediction. This highlights the importance of a detailed understanding of the complex air movements that take place in the vicinity of the human body and their impact on personal exposure.

The two objectives of the present work are: (i) to examine the extent to which the room air temperature, ventilation flow, body posture, clothing insulation/design, table positioning and chair design affect the airflow characteristics (velocity, turbulence and temperature) around the human body; and (ii) to examine the pollution distribution within the human convective boundary layer (CBL) and personal exposure to gaseous and particulate pollutants as a function of the factors that influence the human CBL, and of different locations of the pollution sources. In this work, the empirical results were obtained primarily by using a thermal manikin to simulate a human in the indoor environment.

In spaces with low air mixing, an increase of the ambient temperature from 20 to 26 ˚C widened the CBL flow in front of a seated manikin, but did not influence the shape of the CBL in front

of a standing manikin. The same temperature increase caused a reduction of the peak velocity from 0.24 to 0.16 m/s in front of the seated manikin. Dressing the nude manikin in a thin-tight clothing ensemble reduced the peak velocity in the breathing zone by 17%, and by 40% for a thick-loose ensemble. A lack of hair on the head increased the peak velocity from 0.17 to 0.187 m/s. Apart from their thermal insulation, clothing and chair design had a minor influence on the velocity profile beyond 5 cm distance from the body. Closing the gap between the table and the manikin reduced the peak velocity from 0.17 to 0.111 m/s. At a room air temperature of 23 ˚C, with the manikin leaning backwards the peak velocity was 0.185 m/s, which is 45% above the case with the manikin leaning forward.

The direction and magnitude of the surrounding airflows considerably influence the airflow distribution around the human body. Downward flow with a velocity of 0.175 m/s at a room air temperature of 23 ˚C did not influence the convective flow in the breathing zone, while the flow at 0.30 m/s affected the CBL at the nose level, reducing the peak velocity from 0.185 to 0.10 m/s. In order to completely break away the human CBL, downward flow had to be supplied with a velocity of 0.425 m/s. Transverse horizontal flow disturbed the CBL at the breathing zone even at 0.175 m/s. With a seated manikin exposed to airflow from below with a velocity of 0.30 and 0.425 m/s assisting the CBL, the peak velocity in the breathing zone was reduced and the flow pattern around the body was affected, compared to the assisting flow of 0.175 m/s or quiescent conditions. In this case, the airflow interaction was strongly affected by the presence of the chair. The results also show that Particle Image Velocimetry (PIV) and Pseudo Color Visualization (PCV) techniques can be adequately employed for the human CBL investigation.

The results show that reducing the room air temperature from 23 to 20 ˚C increased the fluctuations of air temperature close to the surface of the body. Large standard deviation of air

temperature fluctuations, up to 1.2 ˚C, was measured in the region of the chest, and up to 2.9 ˚C when the exhalation was applied. Leaning the manikin backwards increased the air temperature and standard deviation of air temperature fluctuations in the breathing zone, while a forward body inclination had the opposite effect. Exhalation through the mouth created a steady temperature drop with increasing distance from the mouth, without disturbing conditions in the region of the chest. Exhalation through the nose did not affect the air temperature in front of the chest due to the physics of the jets flow from the nose. Only very small discrepancies between the results obtained with the breathing thermal manikin and a real human subject were found. This suggests that the thermal manikin can be used for accurate measurements of an occupant's thermal microenvironment.

The results also suggest that a detailed understanding of the distribution of pollutants in the vicinity of a human body is essential for understanding exposure in spaces with low air mixing. The pollution source location had a considerable influence on the pollution concentrations measured in the breathing zone and on the extent to which the pollution spread to the surroundings. The highest breathing zone concentrations were measured when the pollution source was located at the chest, while there was negligible exposure to any the pollution emitted from the upper back or behind the chair. Based on the results obtained in a single plane, it was shown that a decrease in personal exposure to pollutants released from or around the human body increased the extent to which the pollution spread to the surroundings. Reduced room air temperature and backward body inclination both intensified the transport of pollution to the breathing zone and increased personal exposure. The front edge of a table positioned at zero distance from the human body reduced pollution/clean air transport to the breathing zone, but when it was positioned 10 cm from the body it increased the transport of pollution/clean air from beneath.

For accurate predictions of personal exposure, the characteristics of the CBL must be considered, as it can transport pollution around the human body. The best way to control and reduce personal exposure when the pollution originates at the feet is to employ transverse flow from in front and from the side, relative to the exposed occupant. Airflows from above opposing the CBL and from behind transverse to the CBL, create the most unfavourable velocity field that exhibits a non-linear dependence between the supply airflow rate and personal exposure. Without a better understanding of the airflow patterns in a room the ventilation rate may therefore be increased in vain.

RESUMÉ

Vi opholder os alle indendørs for det meste og som resultat er vi kontinuerligt udsatte for de luftforureninger som findes i indeklimaet, med negative konsekvenser for vore helbred, komfort og produktivitet. Stærke økonomiske faktorer og et nyligt opdaget miljøhensyn driver på en mindskning af alle bygningers energiforbrug, som leder til at ventilationdesign idag er beregnet for alt lavere lufthastigheder. Som resultat betyder de statiske opdrift som foranlediges af varmekilder alt mere for luftrørelserne indendørs og for indeklimaet generelt. I lokaler med en lav indblæsningshastighed er luftblanding minimal og den befindlige pollution fordeles ujævnt. De store forskeld som derved opstår betyder at personlig eksponering, i stedet for den gennemsnitlig pollutionsnivå, bestemmer risikoen for en forhøjede negativ effekt af pollution. Den nuværende ventilationspraktik tager ikke hensyn til at statisk opdrift fra menneskekroppen kan påvirke luftens strømming, og derfor leder til forkerte beregninger af pollutionens negative effekter på de mennesker som opholder sig i bygningen. En meget detaljeret forståelse af de komplekse luftstrømmer som opstår omkring menneskekroppen er nødvendig hvis disse effekter skal kunne forudsiges.

Målsætningen med det nuværende arbejde er: 1) at undersøge hvor meget luftrørelserne omkring menneskekroppen (i termer af deres lufthastighed, turbulens og lokaltemperatur) er påvirket af rumsluftens temperatur, luftmængden som tilføres af ventilationssystemet, kroppens holdning, beklædningens termiske isolationsevner og drapering, arbejdsbordets lokalisering og arbejdsstolens udformning; og 2) at undersøge hvordan luftforureninger fordeler sig indenfor Kroppens Konvektive Grænselag (KKG, en term modsvarende CBL på engelsk) og den resulterende menneskelige eksponering til skadelige forureninger i form af gaser eller partikler, som en funktion af alle de faktorer som påvirker KKG og af forureningskildernes lokalisering. I den nuværende undersøgelsen stemmer de empiriske

resultater hovedsagelige fra målinger som udførtes i nærheden af en elektrisk opvarmet termisk mannequin, som blev brugt som en simulering af hvordan et menneske påvirker og er påvirket af indeklimaet. Udover at mannequinen hade den fysiologisk rette fordelingen af overfladernes temperaturer var den også i stand til at simulere indånding og udånding.

I lokaler med lav opblandning af rumsluften ledte en stigning af rummets lufttemperatur fra 20 til 26 °C til en udbredning af KKG foran en termisk mannequin i siddende stilling, men ikke til nogen ændring i KKGs omformning for en stående mannequin. Den maksimale lufthastigheden foran den siddende mannequin mindskedes derved fra 0.24 til 0.16 m/s. Når den nøgne mannequinen beklædtes med tynd og tætsiddende tøj mindskedes den maksimale lufthastigheden i indåndingszonen med 17%; tykke og løstsiddende tøj ledte til at den blev 40% mindre. Uden hår på hovedet blev den maksimale lufthastigheden 0.187 i stedet for 0.17 m/s. Bortset fra deres termisk isoleringsevne, hverken tøjets eller stolens udformning hade en målbar effekt på lufthastighederne som opmåltes mer end 5 cm væk fra kroppen. Når bordskanten flyttedes nærmere kroppen blev den maksimale lufthastigheden i KKG 0.11 i stedet for 0.17 m/s. Om rumsluftens temperatur var 23 °C, den maksimale lufthastigheden som blev målt var 0.185 m/s når mannequinen var tilbagelænet, 45% højre end når mannequinen var fremadlænet.

Luftstrømningernes retning og hastighed i nærheden af kroppen hade en stor indflydelse på KKG. En nedadrettet luftstrømning med en hastighed af 0.175 m/s ved en rumstemperatur af 23 °C hade ingen effekt på KKG i indåndningszonen, men da den blev øget til 0.30 m/s mindskedes den opadrettede maksimale hastigheden i denne zone fra 0.185 til 0.10 m/s. En horisontale luftstrømning fejede bort KKG i indåndningszonen allerede ved 0.175 m/s. Luftstrømning nedefra en siddende mannequin, det vil sige en luftstrømning i samme retning som KKG, sat konvektionen ud af spil så meget at de maksimale lufthastigheder i indåndningszonen blev mindre, ikke større, når luftrømningens hastighed var 0.30 eller 0.425

m/s end når den var 0.175 m/s eller udeblev. Interaktionen med KKG var i dette fald stærkt påvirket af om mannequinen var placeret på en stol.

Når rumslufttemperaturen mindskedes fra 23 til 20 °C observeredes en stigning af temperaturfluktuationerne indenfor KKG. I brøsthøjde blev disse fluktuationer så stor som 1.2 °C, og de blev så stor som 2.9 °C når udånding blev simuleret. Lufttemperaturen i indåndingszonen øgedes hvis mannequin var fremadlænet og mindskedes om den var tilbagelænet. Udånding gennem munden hade den effekt at temperaturerne blev gradvis mindre med stigende afstand fra munden, uden at KKG fremfor bålet blev påvirket. Udånding gennem næsen, det vil sige i to meget tyndere luftstråle, hade ingen effekt på temperaturene fremfor bålet. En sammenligning mellem mannequinen og en levende person i samme tøj og stillinger afslørede meget få og meget små diskrepanser, bekræftende at en mannequin af denne type kan bruges for at undersøge mikroklimaet omkring menneskekroppen.

Resultaterne af den nuværende undersøgningen demonstrere at der er meget vigtigt at forstå hvordan luftens forureninger fordeles i nærheden af kroppen om det skal være muligt at forudse en bestemt persons eksponering til dem. Forureningskildens nøjagtige placering hade en stor indflydelse på den koncentrationen af forureninger som opmåltes i indåndingszonen og på hvordan de spredtes til omgivelserne. Koncentrationen var størst om forureningskilden var på fremsiden af overkroppen, og mindst om den var på øvre del af ryggen eller bagved stolen. Baseret på målinger i kun to dimensioner, mindsket eksponering til forurening fra kilder på eller i nærhed af kroppen var associeret med øget spredning af forurening til omgivelsene. En lavere rumslufttemperatur og en tilbagelænet holdning ledte hver for sig til en øget transport af forurening til indåndingszonen og til øget personlig eksponering. Med fremkanten af arbejdsbordet i kontakt med kroppen blev mindre forurening transporteret til indåndingszonen, og med fremkanten 10 cm fra kroppen blev mere luft transporteret op til indåndningszonen fra under bordet, uanset om den var ren luft eller forurenet luft.

Konklusionen er at om personlig eksponering skal kunne forudses mere precist, skal man tage KKG med i beregningen, fordi den er i stand til at transportere forurening både til og fra og omring kroppen. Hvis forureningskilden er i gulvhøjde, den mest effektive ventilationsstrategi for at mindske personlig eksponering er at etablere en horisontale luftstrømning skråt mod fremsiden af kroppen. Luftstrømning nedad mod gulvet, i opposition til KKG, eller horisontalt bagfra kroppen, leder til den mindst gunstige hastighedsfordeling omkring kroppen, med en ikke-linear relation mellem den indblæste luftens mængde og personlig eksponering. Uden en bedre indsigt i hvordan ventilationsluften fordeler sig i den ventilerede volumen kan man øge ventilationen forgæves.

LIST OF TABLES

LIST OF FIGURES

NOMENCLATURE

Abbreviations

ACH	Air exchange rate
AHU	Air Handling Units
ASHRAE	American Society of Heating, Refrigerating and Air-Conditioning Engineers
CBL	Convective Boundary Layer
CCD	Charge-coupled Device
CDC	Center for Disease Control and Prevention
CFD	Computational Fluid Dynamic
IAQ	Indoor Air Quality
ISO	International Organization for Standardization
LDA	Laser Doppler Anemometry
PBL	Pollution Boundary Layer
PCV	Pseudo Color Visualization
PDA	Phase Doppler Anemometry
PIV	Particle Image Velocimetry
RMS	Root Mean Square
SARS	Severe Acute Respiratory Syndrome

SBS		Sick Building Syndrome
TBL		Temperature Boundary Layer
VOC		Volatile Organic Compounds

Symbols

Gr		Grashof number
Ra		Rayleigh number
Ri		Richardson number
ν	[m^2/s]	Kinematic viscosity
β		Thermal expansion coefficient
g	[m/s^2]	Acceleration due to gravity
ΔT	[K]	Temperature difference
T_{TBL}	[˚C]	Temperature at the outer edge of the TBL
T_{surf}	[˚C]	Temperature of the surface
T_{amb}	[˚C]	Temperature of the ambient air
α	[m^2/s]	Thermal diffusivity

CHAPTER 1: INTRODUCTION

1.1 Background and motivation

The purpose of ventilation system is to ensure acceptable indoor environment that refers to thermal environment and air quality. These two factors have to be considered with a great attention as people in a modern society spend from 80% to 90% of their time in artificial environments (Spengler and Sexton, 1983), and indoor pollution levels are often much higher than outdoors (Wallace, 2000). The indoor environment has been associated with numerous long-term and immediate health issues such as respiratory diseases, transmission of infectious disease, cancer, allergies, sensory irritations and "sick building syndrome" (SBS) symptoms (Awbi, 2003). It has attracted an increased attention in recent decades since the appearance of SBS in early 1970s. As a result of energy-saving measures by tightening the building envelope and decreasing the amount of outdoor air supplied, the quality of indoor air has deteriorated substantially and the risk of potential spread of infectious diseases has increased. On the other hand, increased ventilation rates, up to 25 l/s per person, are associated with reduced SBS symptoms (Sundell et al. 2011). With the present total volume ventilation strategy, ensuring an acceptable indoor climate often requires increased ventilation rates which inevitably increases energy input. This creates a potential conflict between ensuring a comfortable and healthy indoor environment and building energy consumption.

The change of climatic factors has been increasingly associated with global health and occurrence of airborne diseases such as respiratory syncytial virus, tuberculosis and influenza epidemics (Louis and Hess, 2008). In the near future, it is reasonable to expect more frequent occurrence of existing airborne diseases and emergence of new, potentially more hazardous, diseases. Outbreaks such as certain biohazards such as influenza pandemic and severe acute

respiratory syndrome (SARS), global resurgence of tuberculosis and concerns of anthrax have resulted in tremendous efforts to control the spread of infectious diseases. In densely populated spaces such as offices, schools, hospitals and vehicles, the spread of infectious diseases is even more rapid than in less populated environments, which causes a significant burden on health care system and economy. Considering the office workers in the United States, the economic loss estimated is up to $160 billion because of the impairment of occupants' productivity and healthcare cost (Fisk, 2000).

Since building occupants are constantly exposed to numerous pollutants, there is a need to identify the sources of pollution and to establish their acceptable concentration levels. In general, particulate matter and gaseous pollutants are commonly encountered in indoor environments. Particulate pollutants can be classified based on their size and the main external forces acting on them. Particle size is important factor that is subjected to gravity, inertia, turbulent diffusion, Brownian forces, electrical forces, electromagnetic radiation, temperature and relative humidity. Thereby, different forces will have different impact on the particle depending on its size. Some representatives of particulate pollutants are potentially infectious bioaerosols such as viruses and bacteria, as well as other commonly encountered particulate pollutants such as smoke, dust, products of combustion from gas burners and particles resuspended from indoor surfaces. Bioaerosols could cause infectious disease transmission such as influenza, tuberculosis or SARS (Qian et al. 2006; Li et al. 2007), while other common particles have been associated with cardiovascular and respiratory diseases, asthma, as well as the damage to electrical appliances. Typical representatives of gaseous pollutants in indoor environment are ozone (indoor and outdoor sources), radon (infiltrated from soil), volatile organic compounds (formaldehyde from building materials and products), nitrogen dioxide (from gas appliances), carbon-monoxide (from incomplete combustion), moisture and different

odours (Awbi, 2003). Such gaseous pollutants are able to cause respiratory irritation and illness, lung cancer, asthma and eye irritation (Ernst and Zibrak, 1998).

Other than the general transmission pathways through the diet (contaminated food or water sources) or through the skin (directly or indirectly), there are three main routes of how respiratory infectious diseases can be transmitted: direct contact, large droplet and aerosols (droplet nuclei, airborne). When people are the source of infection, their respiratory secretion becomes aerosolized through expiratory activities such as coughing, sneezing, vomiting, talking and breathing. Although the former two are more frequent, activities such as coughing and sneezing generate substantially higher number of droplets. Droplets of smaller size quickly evaporate forming droplet nuclei that can remain suspended in the air for a long period of time. They interact with momentum induced airflows generated by ventilation system and buoyancy driven airflows generated by internal heat sources and surfaces which make them scattered broadly across the indoor environment.

Transmission of potentially infectious aerosols in an indoor environment requires the recognition of many factors, such as room air distribution, location of pollution source and recipient, droplet momentum, size, generation and survival mechanism, number and density, personal protection etc. Apart from droplet size which is the most important factor influencing their dispersion, survival and deposition, airflow patterns in the indoor environment generated by mechanical ventilation systems, occupants or other heat sources are of critical importance (Morawska, 2006). This emphasizes that room airflow patterns have important role in spreading the pollution in an indoor environment. The ability of airflow patterns to mitigate (prevent) exposure to airborne pollutants is not studied comprehensively enough till date.

One of the most common ways to reduce human exposure to airborne pollutants is to use mechanical ventilation. Majority of the ventilation systems, as well as the occupied space

layouts, are not suitably designed to prevent the spread of pollution across the room. The required amount of outdoor air supplied to the room is usually determined based on the room area and the number of occupants. Once supplied to the room, the airflow patterns and the amount of clean air that ends up in the breathing zone are generally not considered, which often leads to impaired indoor air quality. Mixing ventilation system is the main total volume air distribution principle used in buildings. Its main feature is to have large airflow rates supplied to condition the entire space (including unoccupied spaces), which leads to a high energy penalty. Air is supplied far away from occupants and is mixed with a warm and polluted surrounding air before it reaches inhalation zone. In case that pollution originates in the room itself, it is difficult to remove it before it is mixed with the surrounding air. In fact, total volume air distribution strategy can enhance the transport of pollutants from unoccupied zone into the occupied zone (Melikov, 2011).

In the existing ventilation standards, it is commonly accepted that the improvement of inhaled air quality can be achieved by increasing outdoor ventilation rates. Recent studies, however, have shown that providing a minimally recommended ventilation rates does not necessarily ensure adequate air quality in the occupied zone. Li et al. (2007) found that there is not sufficient evidence to support the quantification of the minimum ventilation requirements in relation to the spread of airborne infectious diseases for the context of offices, schools and other non-hospital environments. Moreover, several recent studies have challenged existing ventilation standards by showing that in some cases increase of the ventilation rates can lead to a higher exposure and an increased risk of airborne disease transmission (Melikov et al. 2010; Bolashikov et al. 2012; Popiolek et al. 2012; Pantelic and Tham, 2013). These studies emphasize the importance of understanding the complex airflow interaction in the rooms generated by mechanical ventilation and heat sources.

Due to strong economic pressures to reduce building energy consumption and carbon footprint, low air velocity design is gaining popularity. Therefore, buoyancy flows generated by heat sources often have prominent role in the formation of airflow patterns in an indoor environment. In the typical office spaces, occupants are major internal heat sources. This will especially be the case in the future since the airflows generated by thermal sources such as lighting and equipment will be less important due to the increasing use of low-power devices. In that regard, the volume flux of the air in microenvironment around human body is comparable to that created by the total ventilation flow. Velocities measured within the free convection flow around the human body are comparable to the upper limits of the room air velocity. Several studies reported that the airflow induced by the human body heat affects air distribution in the room, spread of airborne infectious diseases and air pollution control, inhaled air quality and occupants' thermal comfort (Craven and Settles, 2006; Rim and Novoselac, 2009). This emphasizes importance of understanding air movement induced by the building occupants.

In the current room air distribution design practice, airflows induced by the building occupants are not taken into account resulting in inaccurate prediction of the personal exposure. Different exposure models have been developed over the years which mostly assume uniform concentrations of the pollution across the space. Nevertheless, in many indoor environments, especially in those that operate with low supply velocity, air mixing is not efficient and pollution concentration gradients occur. These concentration gradients may occur near a person forming a "personal cloud" that tends to have different pollution levels in the breathing zone then in the surroundings of the room (Wallace, 2000). Thus, assuming "well mixed" condition may lead to incorrect exposure prediction.

It is, therefore, necessary to comprehend both the airflow characteristics and the pollutant dispersion in occupied spaces for analysis of personal exposure in order to design a healthy

indoor environment that minimizes human exposure to indoor air pollution. The primary objective of this study is to investigate the complex air distribution in the microenvironment around a human body and its impact on personal exposure. The results of this study make contribution to the knowledge of the airflow characteristics and patterns in the microenvironment around the human body and their impact on personal exposure.

1.2 Scope of work

This study belongs to an engineering aspect of ventilation and indoor environment through a detailed understanding of airflow characteristics and patterns in the microenvironment around the human body. Furthermore, understanding pollutant transport mechanisms in occupied spaces and the personal exposure makes this study applicable to the medical practice.

Chapter 2: Literature review chapter presents previous research work on indoor airflow characteristics with a focus on the buoyancy induced airflows around the human body. Subsequently, the indoor pollutants and their transport around the human body are presented in relation to personal exposure. Furthermore, the mechanisms of transmission of airborne infectious diseases are highlighted in the indoor environment. The knowledge gap, research objectives and study design are provided at the end of this chapter.

The following five chapters (3 - 7) present the study results published in five peer-reviewed research papers (Appendix B) that contribute to the knowledge of the airflow characteristics and patterns in the microenvironment around the human body, as well as, to the knowledge of personal exposure. Parameters such as room air temperature, body posture, clothing and chair insulation/design and table positioning are studied in indoor environments with little or no air movement and the results apply only to environments with low air mixing. Most of the results are obtained from steady-state conditions, even though several experiments involve transient

flow of exhalation and the real human subject. The scope of this study does not extend to a consideration of occupant movement which needs to be studied in the future. In addition, the results are applicable only to gaseous pollutants and to smaller particles that naturally follow the room airflows. More details about each of the chapters are given in the section 2.8.

Chapter 8: This chapter merges the findings of chapters 3 - 7 into an overall discussion and finds the correlation factors between parameters such as airflow characteristics and mechanisms of pollution transport.

Chapter 9: The last chapter summarizes the key findings of this study, highlights study limitations and gives a brief summary of future research directions.

CHAPTER 2: LITERATURE REVIEW

2.1 Air distribution in ventilated spaces

Room air distribution has a very complex nature as there is a transfer of momentum among the numerous airstreams within the same enclosure. In confined spaces, primary airstreams alter their own flow characteristics and therefore, it is very difficult to generalize their behaviour. In general, room airflow patterns are influenced by the complex interaction between buoyancy induced airflows generated by the internal heat sources/surfaces and momentum induced airflow generated by the mechanical ventilation.

2.1.1 Buoyancy induced airflows

Buoyancy driven airflows, also known as "natural convection", originates from heat sources such as occupants, equipment, lighting, radiant panels (cooling and heating) and other surfaces that cause thermal gradient. The surface of the heat source is delimited from the cooler ambient air in the room with a layer of upward convective flow known as a convective boundary layer (CBL). The driving force of the CBL flow is the buoyancy force caused by the difference in the temperature between a warm surface and cooler surrounding air. After it detaches itself from the surface of the heat source, the CBL develops into a thermal plume. The mass flow of a thermal plume increases with height as a result of entrainment of surrounding air. The entrainment of the ambient air into CBL can be defined as a process whereby the fluid with less turbulence and lower velocity is introduced into the region of the entraining fluid. Along the interface between the plume and the environment there are growing vortex motions that give rise to the engulfment of the surrounding air (Etheridge and Sandberg, 1996). Depending on the heat source, the thermal plume can be developed into different shapes. In principle, a

symmetrical shape is formed at a certain height above the heat source, unless constrained by the ceiling height or other physical obstacle. Nevertheless, the irregularly shaped heat sources usually do not develop into symetrical thermal plumes. This is especially the case with seated occupants where the asymmetry is formed due to the additional buoyant flow araised from thighs and lower legs which generates asymmetrical velocity and temperature distribution profiles (Zukowska et al. 2010). It should be noted that the buoyant flows have predominantly upward airflow direction; however, in some cases buoyant flows move downwards (e.g. airflow near the chilled ceiling; cold window, etc.).

The influence of the thermal plume on the room air distribution is a function of many other factors, such as an inherent strength of the heat source, mechanical ventilation parameters (air temperature, velocity, thermal stratification, turbulence, etc.), room dimensions (particularly ceiling height) and furniture arrangement which can restrict entrainment of fluid from the surroundings (Kofoed, 1991; Craven and Settles, 2006). Most of the research on the thermal plumes in ventilated spaces has been done in rooms with displacement ventilation since the effect of plumes is more prominent due to low air mixing (Awbi, 2003). Also, rooms with little air movement (<0.1 m/s) or no mechanical ventilation that create quiescent environmental conditions are found to have prominent thermal plumes due to little disruption from the surroundings (Murakami et al., 2000). Nevertheless, it has been documented that even in rooms with high air mixing, the thermal plumes can have a prominent role in airflow patterns formation (Cho and Awbi, 2002; Zukowska et al. 2010).

2.1.2 The momentum induced airflows

Building ventilation is primarily induced by mechanical ventilation and infiltration. Unlike the infiltration, the mechanical ventilation has an ability to control the supplied airflow rate and therefore, to control occupants' health and thermal comfort. Mixing ventilation is the most

commonly employed total volume air distribution strategy. It uses a dilution principle by supplying the air at high initial velocity to ensure good mixing in the room. Air distribution in the room using mixing ventilation is highly unpredictable and influenced by the momentum flux at the supply terminal, type and location of supply and exhaust terminals, room geometry, occupants' movement, obstacles and furniture, thermal loads in the room (Etheridge and Sandberg, 1996). This suggests that the mechanical ventilation creates different airflow patterns in every room, hence any generalization of the airflow patterns and/or pollution distribution is challenging. In such a homogeneous environment with high air mixing, indoor pollutants are typically mixed with the room air and inhaled by the occupants. This air distribution principle has been associated with high energy usage and increased initial cost due to larger AHU, ducts and fans.

Apart from mixing ventilation, rooms are ventilated with displacement air distribution that supplies the clean air at 3-6 ºC below the room temperature at relatively low velocity and turbulence intensity at the floor level (Melikov and Langkilde, 1990; Nielsen, 1993). The clean air is displaced upwards due to the natural buoyancy forces and transported to the upper part of the room and then exhausted at the ceiling level. The airflow in such spaces can be divided in two zones: lower zone or "clean zone" in which clean air enters the plume; and upper zone or "contaminated zone" where warmer and more polluted air has more turbulent nature. The height of the room at which air volume flux induced by the heat sources is equal to the supply flow rate defines a border between lower and upper zone. Since the buoyant upward flow around occupants is predominant, airborne cross-infection can be reduced because indoor pollution can be brought above the breathing zone by means of a thermal plume. However, in densely populated spaces, as well as in dynamic environments (where people move extensively), natural convection flow around the human body is disturbed. For instance, a person walking (speed above 1 m/s) in the room equipped with displacement ventilation is

causing air mixing close to that in the room with mixing ventilation, thus increasing the probability of cross-infection (Bjørn et al. 1997; Halvonova and Melikov, 2010). Lastly, since the buoyant force is a predominant mechanism of air movement, any pollution source originating at the "clean zone" can be easily brought into the human breathing zone.

2.2 Convective boundary layer around the human body

2.2.1 Human body thermoregulation

A human body heat is generated in its organs, especially in the brain, heart and liver, as well as in the skeletal muscles during recreation. The human body heat is transferred to the skin from deep organs and tissues by means of blood flow. As a part of the thermoregulatory process, the skin is constantly exchanging heat with its surrounding environment. As a result, the normal body temperatures are maintained which is critical for comfort and health. Excessive heat loss cools the body which can result in hypothermia, while insufficient heat loss may result in hyperthermia. Average skin temperature at normal activity level is about 33 ˚C (Etheridge and Sandberg, 1996), while the body core temperature is at approximately 37 ˚C. In a thermally comfortable state, there may be substantial differences in the skin temperatures across the body.

A human body heat loss to the surroundings is governed by the combination of several heat transfer mechanisms: sensible heat loss from the skin, sensible heat loss during exhalation, latent heat loss from sweat evaporation, latent heat loss from evaporation of moisture diffused through the skin and latent heat loss from moisture evaporation during exhalation (ASHRAE, 2009). At comfortable room air temperatures, the sweat heat loss from evaporation is negligible compared to sensible heat exchange. The sweat heat loss from evaporation becomes dominant at elevated room air temperatures (i.e. 32 ˚C). Murakami et al. (2000) reported that heat rejected

to the environment by the unclothed human body with the metabolic heat production of 1.7 Met includes 29% through convection, 38.1% through radiation, 8.7% through respiration and 24.2% by evaporation, in a stagnant indoor environment. Both the convective and the radiant heat exchange mainly depend on the temperature difference between the surface of the human body and the surroundings. Thereby, a relevant parameter for the convective heat transfer is the temperature of the surrounding air, while for the radiant heat transfer it is the temperature and relative proximity of surrounding surfaces. In that sense, elevated surrounding air temperature mitigates the convective heat transfer from the human body while amplifying other means of heat transfer. In the same way, reduction of the temperature of the surrounding surfaces increases the radiant heat transfer from the human body. Kulpmann (1993) reported that in rooms equipped with chilled ceiling, radiant heat loss from the human body increases up to 50%, while the convective heat loss decreases. These changes in the ratio between different heat rejection mechanisms play an important role in formation of airflow patterns in the human microclimate.

2.2.2 Human convection flow

Design indoor air temperature range is 20-26 ˚C (ISO, 2005; ASHRAE, 2013a) which is approximately 7-13 ˚C colder than the temperature of the human skin. Consequently, temperature gradients exist between the ambient air and the surface of the human body which causes a steady natural process of convective heat loss to the surrounding space. The convective heat loss from the human body induces upward movement of the surrounding air, thus forming a convective boundary layer (CBL) around it and a free-convection thermal plume above the head. This flow is visually described by Settles (2001) using the Schlieren photography technique.

Lewis et al. (1969) were the first to conduct a systematic analysis of the air movement in the vicinity of the human body using the Schlieren photography and hot wire anemometer. It was found that at a background temperature of 15 ˚C, a natural flow in front of a standing nude man begins to change from laminar to turbulent at the height of 1 m and becomes fully turbulent at about 1.5 m from the floor. Other studies (Clark and Toy, 1975; Homma and Yakiyama, 1988) documented that the surrounding air is entrained into the laminar free-convection flow around the human body which after some distance accelerates progressively developing into a thicker turbulent flow with a relatively high velocity at the mouth level. As a result of the entrainment of the surrounding air, the mass flow in the human CBL increases with height. A nude standing human can induce as much as 60 l/s of surrounding convection flow, measured at 20 ˚C ambient temperature (Homma and Yakiyama, 1988; Zukowska et al. 2010). In that regard, the volume flux of the air surrounding the human body can be comparable to the total ventilation flow, thus having a prominent role in the formation of the airflow patterns in an indoor environment.

Once the convection flow reaches the head region, it is influenced by facial features (nose, eyes and ears) as well as the jaw and the neck. The part of the air that flows under the surface of the chin will reach inhalation zone, while the rest of the flow passes over the cheeks, eyes and forehead and subsequently merges with rising flow from the shoulders, sides and the back of the head. As a result, a human thermal plume is formed that stretches across a certain distance above the head. For a seated occupant, a thermal plume is not symmetrical due to a stronger convection flow that arises from its front side, compared to the one that arises behind the back. However, this flow becomes nearly symmetrical at the height of 1.5 m above the head (Zukowska et al. 2007). It should be noted that not all the flow enveloping the human body is constantly moving upwards. Still regions may occur if the convection flow is blocked by a horizontal surface such as axilla, nasal septum or lobe of the ear.

2.2.2.1 Velocity field of the convective boundary layer

The velocity and the thickness of the human CBL can strongly differ under different ambient conditions and at different heights of the body. Lewis et al. (1969) found that in the region of lower legs the thickness of the CBL is 0.03 m and maximum velocity of the CBL is 0.25 m/s, measured at 0.05 m distance from the skin, while the ambient temperature was kept at 15 ˚C. In the same region, but at the ambient temperature range of 19-21 ˚C, Homma and Yakiyama (1988) reported the CBL thickness in range of 0.01-0.03 m and the velocity in range of 0.10-0.15 m/s. As the ambient air became entrained into the CBL, it spread to about 0.075 m in the mid-chest region of a nude person, i.e. 0.15 m of the clothed person, with a wide velocity range from 0.05 to 0.25 m/s.

A definition of CBL physical thickness is somewhat arbitrary since the transition from zero velocity at the surface (assuming no slip) to the velocity in the free-stream outside the CBL is non-linear. For instance, in computational and experimental investigation performed by Craven and Settles (2006), the outer edge (thickness) of the human CBL was defined as 10% of the maximum velocity within the plume. Clark and Toy (1974) related the thickness of the human CBL to the heat loss from the body. Where the CBL was thinner, the convective heat loss was larger due to a steep thermal gradient. On the other hand, thicker CBL suggested a lower thermal gradient and convective heat loss.

Özcan et al. (2005) obtained the mean velocity data around the head of the breathing thermal manikin by using Particle Image Velocimetry (PIV) technique. There were two cases explored: no breathing and continuous nose exhalation. In the first case, the mean velocity was 0.16 m/s, while exhalation through the nose increased the mean velocity to 1.85 m/s. Both cases created a similar velocity profile above the head, with a maximum velocity of around 0.25 m/s. Other studies have also shown that velocity in the CBL can go up to 0.25 m/s at the head level with

the thickness of 0.2 m (Homma and Yakiyama 1988; Melikov and Zhou 1996; Özcan et al. 2003).

Murakami et al. (2000) performed a numerical simulation on the airflow transport around the human body. The predicted velocity field showed very good agreement with experimental results obtained. The maximum velocity in the head region obtained from the numerical simulation was 0.23 m/s, while the measurements using the thermal manikin and the real human body showed velocities of 0.21 m/s and 0.20 m/s, respectively. Similar study was performed by Sørensen and Voigt (2003) by using unclothed, unwigged and non-breathing computational manikin. Predicted velocity distribution was fairly high with a peak value of 0.5 m/s above the manikin's head.

Salmanzadeh et al. (2012) performed CFD analysis on a heated and unheated manikin. In a non-isothermal case, the convection flow generated by the heated manikin was able to draw the floor supplied airflow at 0.1 m/s and 0.2 m/s towards itself. This was not the case when the inlet velocity was increased to 0.8 m/s, since the thermal plume of the manikin was unable to draw the supplied air towards itself. The maximum velocity of 0.3 m/s above the manikin's head was found to be in a good agreement with the measurements performed by Marr et al. (2005). Furthermore, Craven and Settles (2006) performed the PIV measurements and CFD simulations to obtain time-averaged velocity data around a standing male volunteer. Maximum velocity values were 0.24 m/s (measured case) and 0.20 m/s (simulated case), reported approximately at 0.42 m above the head.

A flow regime of the CBL can be described by Grashof number, *Gr* that approximates the ratio of the buoyancy to a viscous force acting on a fluid. The value of the Grashof number below $2x10^9$ indicates a laminar flow regime that closely follows the body contours. When the Grashof number exceeds 10^{10} the flow regime is fully turbulent. As shown in Fig. 2.1, for the

ambient temperature of 20 ˚C and a naked standing human with a skin temperature of 33˚C, the flow regime remains laminar up to 0.9 m height while developing into a fully turbulent flow above 1.5 m. This phenomenon was studied in experiments that involved Schlieren photography (Clark and Edholm, 1985; Lewis et al. 1969).

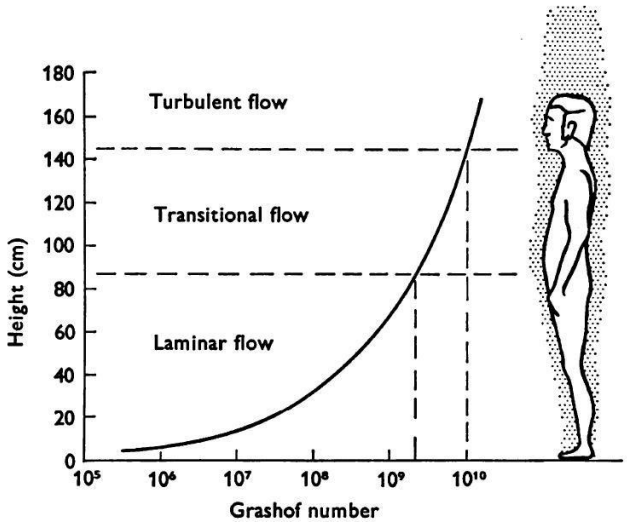

Figure 2.1 Human CBL flow regime in relation to Grashof number (Clark and Toy, 1975).

Other dimensionless parameters that can be used to describe flow field around the human body are Richardson number (*Ri*), defined as a ratio of free and forced convection (Murakami et al, 1999), and Rayleigh number (*Ra*) associated with purely buoyancy driven flow, described by Tavoularis (2005). If the Richardson number is greater than the unity, the natural convection, i.e. pure buoyant flow, is dominant. Rayleigh number below 10^8 indicate a buoyant laminar flow, while transition to a turbulent regime occurs within a range $10^8<Ra<10^{10}$. In the pure natural convection, the Rayleigh number is given as:

$$Ra = \frac{g\beta\Delta T L^3}{v\alpha}$$

where v is kinematic viscosity ($1.6\text{x}10^{-5}$ m^2/s), β is thermal expansion coefficient and α is thermal diffusivity ($2.4\text{x}10^{-5}$ m^2/s).

2.2.3 Factors influencing the human CBL

Apart from the temperature gradient between warm surface of the body and the cooler surrounding air, there are number of factors which influence the development of the human CBL such as room air distribution, thermal stratification, metabolic rate, posture of the body, clothing insulation and design, as well as furniture arrangement (Kofoed, 1991; Mundt, 1995; Craven and Settles, 2006). In addition, occupants sometimes move across indoor environment and change posture (sitting or standing). All these factors cause changes in the CBL intensity, shape and flow regime and they have not been studied extensively in the past.

2.2.3.1 The impact of breathing

A human unsteady respiratory cycle is known to impact the formation of the human CBL. Average occupant takes about 12 breaths per minute (around 6 litres of air), which constantly alters the airflow patterns in the vicinity of the human body (Hyldgaard, 1994). Exhalation activity may create different jets, depending on whether it takes place through the mouth or the nose. Both exhalation through the mouth and the nose have an initial momentum capable of passing through the human CBL, so that only a small amount of such a flow is re-inhaled (Melikov and Kaczmarczyk 2007; Hyldgaard, 1994). Mouth exhalation generates a single jet that rapidly rises after being exhaled (Özcan et al. 2005), unlike nose exhalation that creates two separate jets (angle between them 30˚) with the initial momentum of 2 m/s and 45˚ angle against the horizontal plane (Hyldgaard, 1994). One study found that exhalation flow increased the value of local turbulence intensity three times due to the interaction between the shear layers of the human CBL and the air jets from the human nose (Marr et al. 2005). On the other hand, inhalation process has no prominent effect on the surrounding airflows since the airflow enters into the nose and mouth equally from all sides (Hyldgaard, 1994).

Study done by Melikov and Kaczmarczyk (2007) suggested that respiratory flow affects airflow patterns, pollutant concentration and local temperature in the breathing zone. Rim and Novoselac (2009) found that respiratory cycle of the thermal manikin had considerable effect on the airflow patterns in the breathing zone. Findings also showed that breathing activity increase or decrease particle concentration in the inhalation zone, depending on the source location and particle size. The concentration change was approximately 30% for larger particles of 3.2 μm and 15% for smaller particles of 0.77 μm, suggesting that the effect of breathing is more important for evaluation of exposure to larger particles. They also found that impact of respiratory cycle and localized hand movement on the thermal plume 0.25 m above the head was small, as confirmed by Hyldgaard (1998). Zukowska et al. (2012) also assessed the impact of breathing on the thermal plume above a seated thermal manikin. It was found that the exhalation through the nose created a negligible effect on the thermal plume. Nevertheless, exhalation through the mouth generated a substantial change causing wider thermal plume with 40% higher mean volume flux.

2.2.3.2 The impact of thermal insulation

Apart from the respiratory cycle, the airflow characteristics of the human CBL are influenced by the level of clothing insulation. Thermal manikins were used to assess the impact of clothing insulation (McCullough et al. 1985), chairs (McCullough et al. 1994a), bedding system (McCullough et al. 1987) and sleeping bags (Anttonen, 2001). Some studies measured clothing insulation for manikins in motion and found that a body in motion decreased clothing insulation while enhancing convective heat loss (Olesen et al. 1982; McCullough et al. 1994b). Typically, the temperature of the human clothing is about 27-28 ˚C, which is lower than the temperature of the human skin. The decrease in the clothing insulation increases the temperature of the clothing and thus, the temperature gradient between clothing and ambient air, i.e. the

convection heat loss is increased. In addition, the reduction in clothing insulation increases the velocity and turbulence of the CBL and reduces its thickness, as found by Homma and Yakiyama (1988). It was also reported that the thickness of the CBL at the chest level is about 7.5 cm for a nude standing person, whereas in the case of a dressed person the thickness is about 15 cm.

Several researchers reported that clothing insulation can be a function of the body posture (McCullough et al., 1994; Olesen et al. 1882). It was documented that a seated person had a lower clothing insulation than a standing person. One recent study explored impact of clothing and chair design on the thermal plume above a seated occupant (Zukowska et al. 2012). Findings showed that the occupant dressed in loose clothing generated a wider thermal plume measured in horizontal plane, 0.7 m above the head. Loosely dressed occupant had a lower velocity of the thermal plume and 24% greater volume flux compared to a tightly dressed occupant. The loose clothing also increased the width of the thermal plume. The same study found that the occupant's wig significantly intensifies the mixing of the CBL flow at the head level, thus increasing the volume flux in the plume by 15%.

2.2.3.3 The impact of a body posture

The human body posture has a prominent influence on the development of the CBL. Several researchers (Clark and Edholm, 1985; Clark R.P. and de Galcina-Goff, 2009) employed Schilieren photography technique to visualize the development of the CBL under three body postures: standing, sitting and lying. The visualization showed that a supine body position generates a weaker convection flow compared to a standing posture, and consequently, different heat output rates from the human head. Sedentary occupants might not be necessarily seated in the upright position, but may lean backwards or forwards depending on their

preference. Understanding the physics of the flow around a sedentary person is more important as most of the building occupants are predominantly seated throughout the day.

Clark and Toy (1975) reported that the CBL of a seated occupant starts to form only from the lower part of the abdomen interacting with additional airstreams that rise from thighs and lower legs. As a result, the velocity in the breathing zone of the seated occupant differs from that of a standing occupant. The body heat loss was also assessed in relation to the body posture. Findings showed that standing occupant was thermally more protected than the lying occupant. A head of a lying occupant had 30% greater heat loss than the head of a standing occupant.

2.2.3.4 The impact of furniture arrangement

In indoor spaces, seated occupants are customary surrounded with the furniture that can alter the airflow characteristics around their body. In the case of a seated occupant, part of the thighs, buttocks and back are in the contact with a chair. This limits the convective heat exchange and weakens the CBL at the back side of the body (Zukowska et al. 2012). Bolashikov et al. (2011a) employed Particle Image Velocimetry (PIV) to study the strength of the human CBL and its interaction with a personalized ventilation jet. The results show that placing a cardboard between the front edge of the desk and abdomen of the occupant reduced the peak velocity in the mouth region from 0.19 m/s to 0.10 m/s. This weakening of the human CBL allowed the personalized ventilation jet to penetrate the breathing zone at the flow rate of 4 l/s, which was otherwise achieved at 6 l/s.

Zukowska et al. (2012) assessed the impact of the blocking effect of a table in front of the seated occupant on the airflow characteristics of the thermal plume 0.7 m above the head. Two distances between the edge of the table and occupant's abdomen were explored: 0 and 10 cm. Both cases were compared to the base case without the table. Findings showed that 10 cm case had a minor effect in the thermal plume while closing the gap between occupant and the table

generated wider plume with 50% greater volume flux. These findings suggested that furniture design can play an important role in controlling airflow distribution in the microenvironment around human body.

2.2.3.5 The impact of the ventilation flow

As earlier shown, several studies investigated the CBL in a quiescent indoor environment (Lewis et al. 1969; Homma and Yakiyama, 1988; Clark and Toy, 1975; Craven and Settles, 2006). These studies provide a basic knowledge of the airflow behaviour in the vicinity of a human body. In spaces that operate with a high airflow mixing, the ventilation flow strongly interacts with the CBL and modifies its characteristics. This interaction is influenced by factors that define both the CBL flow (body posture, clothing, breathing, ambient temperature, furniture arrangement, etc.) and the ventilation flow (velocity, turbulence, airflow direction, etc.). As the mixing air distribution generates different airflow patterns in every room, any generalization of airflow patterns is challenging. In order to understand the phenomenon and increase generalization of the results, a simplified approach is needed which is based on the physics of the interaction between the CBL and the ventilation airflows. In such an approach, the interacting flows can be assisting, opposing or transverse to each other. So far, little is known about the true nature of the interaction between these flows.

The study that used the combination of two personalized ventilation systems coupled with mixing or displacement ventilation highlighted the importance of airflow interaction around the human body on inhaled air quality (Melikov et al. 2003). Interaction between the CBL and locally supplied personalized ventilation airflow from the front (Bolashikov et al. 2011a), assisting from below (Bolashikov et al. 2011b) and opposing from above (Yang et al. 2009) has been studied and reported. Frontally supplied airflow at 6 l/s was able to penetrate the CBL, while personalized jet at the lower flow rate was deflected upwards by the CBL without

penetrating into the breathing zone. In the study with two assisting confluent jets, increased airflow from below led to an increase of the velocity in the breathing zone. The velocity increase from 0.17 m/s to 0.34 m/s was recorded across the mouth, when the airflow of 4 l/s increased to 10 l/s. These studies investigated only the local airflow interaction in the breathing zone and did not focus on how airflow patterns in the occupied spaces globally affect the development of the CBL.

Melikov and Zhou (1996) studied the airflow interaction between the human free convection flow and uniform horizontal airflow from behind. The results indicate that the convection flow with the maximum velocity of 0.13 m/s measured at the neck of a seated manikin was penetrated by invading flow with the velocity of 0.1 m/s. This also resulted in 4 ˚C lower air temperature near the skin. Similar study performed in a low speed environment with uniform airflow direction revealed that a heated and a non-heated manikin create very distinctive airflow patterns with respect to the free air stream (Johnson et al. 1996). Both studies focused only on the interaction between the human convection flow and the airflow approaching from behind of the manikin. In another, low speed wind tunnel study, it was found that the human metabolic heat considerably alters the airflow patterns on the leeward side of the child-sized manikin and that the increased wind velocity reduces the existence of the human convection flow (Heist et al. 2003).

2.3 Temperature field of the convective boundary layer

Human convective heat loss generates the CBL that has a higher temperature than the ambient air. The human CBL is naturally warmer very close to the surface and becomes cooler with increasing the distance from the human body. Air that is in contact with a warm human body is warmer that the one which is further away. The distance at which the temperature of the air

enveloping the human body equals or closely approaches to the temperature of the ambient air defines the outer edge (thickness) of a temperature boundary layer (TBL).

Murakami et al. (1997) found that the thickness of the TBL around a standing person is relatively small at the level of the feet (0.05 m) and increases as it rises upwards. Large body parts, such as the back and chest are enveloped with a thicker TBL that reduces the convective heat loss. In the same study it was reported that the thickness of the TBL in the neck region was 0.19 m. Homma and Yakiyama (1998) performed visualization of the TBL around a seated and standing human body and found that seated body generates wider thickness of the TBL. Study done by Voelker et al. (2014) confirmed that the human TBL is thinner at the lower part of torso and expands going up. Other researchers (Melikov and Zhou, 1996) reported that the thickness of the TBL at the neck was 0.3-0.35 m and it dropped down to 0.1 m when the uniform horizontal ventilation flow from the back was applied. They also reported the highest standard deviation close to the surface of the body, which was decreased when the invading flow was applied. Homma and Yakiyama (1998) used infrared camera to study air temperature distribution around a standing and clothed body. At 0.025 m distance from the ankle, the air temperature excess in relation to ambient temperature was 0.5 ˚C. The air temperature excess of 1 ˚C was recorded at 0.3 m above the head. Closer to the head, at 0.1-0.15 m distance, the temperature excess was 1.5 ˚C. These results, however, include the effect of radiation, which should be removed in order to accurately measure the air temperature.

2.4 Personal exposure and transmission of infectious diseases in the indoor environment

2.4.1 Indoor pollutants and their transport around the human body

The human CBL plays two important roles. The first role, as already discussed earlier, is its contribution to the convective heat loss from the human body. The second role is to transport the pollution around the human body. This role is especially important in indoor environments that operate with low supply velocity, where pollution concentration gradients occur. These concentration gradients may occur near a person forming a "personal cloud" that tends to have different pollution levels in the breathing zone than in the surroundings of the room (Wallace, 2000). Lewis et al. (1969) documented that content of microorganisms is substantially higher (30-400%) in the microenvironment of the nude standing man than in the ambient air. Thus, assuming "well mixed" room air condition may lead to incorrect exposure prediction.

Several studies have shown that building occupants are substantial contributors to total aerosol mass indoors (Thatcher and Layton, 1995; Ferro et al. 2004). The occupancy associated airborne pollutants can originate from the human body itself or can become aerosolized through occupancy activities such as walking or sitting on the furnishings (Qian et al. 2014). Pollution generated by the human body (bioeffluence) is one of the major IAQ concerns as numerous volatile compounds can be emitted from different body parts (e.g. feet, groins, armpits, etc.) that are disposed to odor generation (Wysocki and Preti, 2004). Human skin shedding plays substantially influences the amount of microbiological aerosols indoors (Noble et al. 1976). Human beings shed the entire layer of their skin every 2-4 weeks and the shedding rate is very large and equivalent to 0.2-1 billion skin cells per day (Roberts and Marks, 1980) which makes them major contributors of dust in indoor environments occupied by humans. Clark and Cox

(1973) revealed that the human skin released from 10^6 to 10^7 skin particles in 24 h, with the average diameter of 14 μm and the size range from below 1 μm up to 50 μm. The level of wall shear stress in human CBL flow is not sufficiently strong to cause detachment of the particles from the human skin. This is also usually the case with momentum induced airflows generated by mechanical ventilation. On the other hand, particles can be easily detached from the human body by rubbing the skin or by body movement. Very large particles are likely to fall on the ground after detaching from the skin, while particles with smaller diameter can be easily transported upwards by the CBL. This indicates that all indoor particles relevant to the airborne disease transmission can be transported by the human CBL.

Apart from the pollution that origins from the human body itself in the process of skin shedding, the source of pollution can come from surroundings as potentially infectious suspended aerosols or aerosols released through respiratory activities such as talking, coughing or sneezing (Morawska, 2006). In addition, the source of pollution can be emissions from indoor sources (VOCs from furnishings or personal care products) and infiltration of outdoor pollutants into buildings (e.g. ozone and other photochemical oxidants). These pollutants can be entrained by the CBL and inhaled by the occupant. Therefore, it is necessary to focus on both the pollutants from the skin/clothing and the ones near the occupant, as well as to identify to what extent their location influences pollutant concentration in the breathing zone. In spaces with low air supply velocity, if the pollution source is located above the head of a standing/seated occupant (Brohus and Nielsen, 1996) or if the pollution is emitted in proximity of the nose of a supine body (Laverge et al. 2013), the CBL will not increase, or can even reduce, the pollutant concentration in the breathing zone. Therefore, in indoor spaces where air mixing is minimized and where occupants are predominantly standing and/or sitting, it is not imperative to focus on the pollution emitted at the head level or at the upper room levels.

Craven and Settles (2006) reported that understanding the behaviour and physics of the human convection flow is important for the control of inhaled air quality and thermal comfort, as well as the pollutant transport and the pollution concentration around the human body. Another set of studies found that convective flow around the human body is very important because it is active in bringing the air into inhalation zone and has a prominent role in dispersion of pollutants in the same zone (Brohus and Nielsen, 1996; Bjørg and Nielsen, 2002; Eisner et al. 2002). Melikov (2004) reported that the biggest portion of inhaled polluted air for sedentary person originated from the human CBL. Similarly, Zhu et al. (2005) reported that in a stagnant indoor environment, a person inhales air that mostly originates from the lower part of the CBL. Clark and Cox (1973) revealed that the biggest portion of inhaled air originates from the human CBL with 6,000 to 50,000 particles per litre of air that terminate its trajectory in the nose of an occupant. One CFD study showed that approximately one third of all the air inhaled by a standing occupant was transported from the region around the mouth, while two thirds came from the lower region of the human CBL (Murakami, 2004). Duguid and Wallace (1948) reported that dust particles originating from the clothing are important to consider from the point of view of respiratory tract airborne infection.

Spitzer et al. (2010) assessed the impact of a seated human rotational movement around its vertical axis on particle transport in the breathing zone by using Phase Doppler Anemometry (PDA) technique. They found that human CBL has an ability to transport particulate matter towards the head region. In addition, the human body rotation had a prominent impact on particle concentration in the breathing zone, with 56% concentration reduction compared to a non-moving body. Nevertheless, these results may not be reliable as the only particles moving in the vertical direction were taken into account, which in case of rotational movement may not a be predominant direction. A recent study conducted by Salmanzadeh et al. (2012) evaluated particle concentration levels around a human body and in the inhalation zone. A

probability of transporting particles from the floor to the breathing zone by means of human CBL was explored. Simulation results revealed that human CBL can substantially contribute to a high particle concentration levels in the breathing zone, which is especially the case in rooms with displacement ventilation. Furthermore, in densely populated indoor spaces, it has been shown that interaction between human convective flows exists even when occupants are positioned 0.4-0.5 m apart, which is important from the cross-infection point of view (Datla and Glauser, 2009; Clark and de Calcina-Goff, 2009). These interactions, however, do not necessarily result in cross-contamination, because the CBL may not always carry the source of pollution. The pollution source emitted from different body parts is not likely to spread equally within the CBL. Therefore, it is important to consider the extent to which pollution emitted from different body parts spreads across the CBL and whether it can be transmitted to the breathing zone of other occupants.

As mentioned before, the surrounding environment and airflow patterns can greatly modify the CBL and therefore, it is necessary to know its effect on the pollutant distribution around the human body. Rim and Novoselac (2009) investigated more deeply the transport of particulate and gaseous pollutants in the vicinity of a human body in two different types of environments. It was found that in the stratified environment, the inhaled concentration of pollutants located 0.5 m behind the occupant and 0.15 m above the floor was four times higher than the ambient concentration. In this case, the CBL at the lower leg entrained the pollution and transported it to the breathing zone. In the same study, the authors found that in a highly mixed environment, the role of the CBL diminished and the concentration around the occupant was uniform. Rim and Novoselac (2010) found that low (average room speed 0.036 m/s) and medium airflow mixing (0.084 m/s) caused up to nine and four times, respectively, higher concentration near occupant than present in the ambient air. Several studies have shown the importance of the occupant's orientation relative to the location of the pollution source for the exposure

prediction (Ge et al. 2013; Brohus and Nielsen, 1995). In the latter study (Brohus and Nielsen, 1995), an occupant was placed in the wind tunnel with a contaminant source located at 0.25 m in front of the body. The results showed that an optimal way to minimize exposure in a horizontal uniform flow field was with the occupant positioned with its side facing the invading airstream.

2.4.2 Infectious agents and their survival

Studies have shown that human respiratory activities such as breathing, talking, coughing and sneezing play a major role in dispersal of potentially infectious respiratory droplets in the indoor environment (Wells, 1934; Morawska, 2006; Nicas et al. 2005). Only limited number of droplets become airborne which is a function of their diameter and shape. Smaller droplets are known to be more infectious (in both infectivity and severity of disease) since they are smaller in size and can deeply penetrate into a lower human respiratory tract. As an example, highly dangerous respiratory diseases such as measles, chicken pox and pulmonary tuberculosis can be transmitted via droplet nuclei (Beggs, 2003; Qian et al. 2006). Furthermore, study done by Li et al. (2007) suggests the connection between the spread of diseases such as SARS and the airborne route of the infection.

Infectious disease can be defined as a clinically evident illness resulting from the presence and activity of pathogenic microbial agents in individual host organism. The source of infection can be an infected occupant, ventilation system, building materials and/or terrorist attack (intentional release). Once the particle is released from respiratory tract of infected occupant, it needs to survive under a different set of conditions outside the body (temperature, relative humidity, radiation) and terminate its trajectory in recipient's body in order to initialize the infection. These conditions pose challenges to microorganism survival, i.e. the viability of pathogenic microorganism decreases with time. The next hindrance for initiating an infection

is an ability of immune system of the host to naturally defend itself. For infants and elderly people, as well as immuno-compromised people, even a smaller amount of infected organisms is able to initialize a disease. In the case of airborne transmission, pathogens initially interact with mucosal surfaces of the host, such as mouth, eyes and nose. Once the pathogen enters the human body, it must initialize an infection in order to develop into a disease. Each pathogen has its own desired environment and cannot reproduce unless it finds its favourable conditions (for bacteria), i.e. the favourable host cell (for viruses). For instance, tuberculosis is unable to initiate infection unless it enters the human upper respiratory tract.

For a pathogen reproduction and growth in the indoor environment, they need to survive the temperature range of 20-40 ºC which includes both the ambient air temperature and the temperature of the human body core and skin surface, as reported by Greenwood et al. (2002). In general, a number of viruses are shown to die off much faster at a comfortable relative humidity range (40-60%), as in case of the human corona-virus (Ijaz et al. 1985). Viruses that contain more lipids, such as influenza (Fig. 2.2, left), tend to be more viable at lower relative humidity values (Assar and Block, 2000). Contrary to this, viruses with lower lipid content, such as SARS (Fig. 2.2, middle) are more conserved at higher relative humidity. Tuberculosis (Fig. 2.2, right) is also known as a bacteria that can persist for a long period of time due to its thick wall of cell (Fitzgerald and Hass, 2005), which makes it one of the most common causes of death from infectious diseases in adults. Studies have shown that viruses such as SARS coronavirus can remain viable in indoor environment for more than a week (Lai et al., 2005).

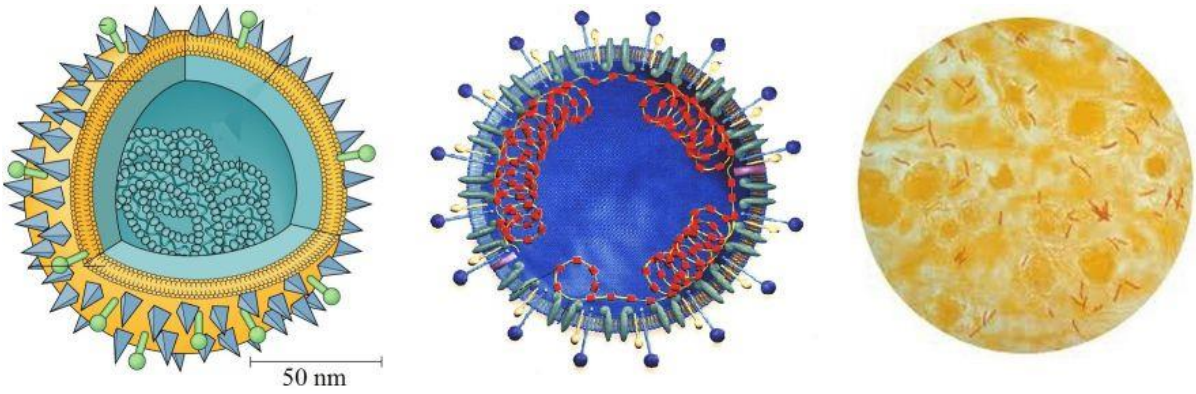

Figure 2.2 Structure of viruses: Influenza (left); SARS (middle) and Tuberculosis (right).

2.4.3 The mechanisms of airborne transmission

The transmission of infections agents may occur through several routes, depending on the type of organism: direct/indirect contact, large droplets or airborne route. The direct transmission route involves a direct contact with an infected person while the indirect route refers to a contact with a contaminated object and it will not be a part of this study. The airborne transmission (droplet nuclei) refers to the dispersion of airborne droplet nuclei or small potentially infectious particles that can be inhaled by a susceptible occupant. The susceptible occupant does not need to have a direct contact or share the same room with an infected occupant. In general, aerosols are a suspension of solid or liquid particles in the air, with a particle size range from 0.001 to 100 μm (Hinds, 1982). The droplet nucleus is the airborne residue of the aerosol from which most of the liquid has evaporated (Wells, 1934). Due to their small size, droplet nuclei remain airborne for a long period of time and could become a threat for the susceptible occupants.

Through different pulmonary activities people release particles of different sizes and different flow characteristics. Studies have shown that droplets generated from respiratory activities can range in diameter size from 0.01 - 500 μm depending on the factors such as mucus properties and relative humidity (Gralton et al. 2011), but majority of them are smaller than 100 μm (Papineni and Rosenthal, 1997). Wells (1934) reported that particles larger than 100 μm in

diameter can be considered as “large droplets”, while smaller than 100 μm in diameter “small droplets”. In addition, it is found that for droplets smaller than 100 μm in diameter, evaporation will fully take place before falling 2 m away. Duguid (1946) defined droplet nuclei as particles smaller than 5 μm. As proposed by Xie et al. (2007), particle size can be defined as: “Droplet nuclei” smaller than 10 μm in diameter; “Small droplets” smaller than 60 μm in diameter; and “Large droplets” larger than 60 μm in diameter. Hinds (1999) found that particles with 10 μm in diameter size or less are able to penetrate into human lungs. On the other hand, Nicas et al. (2005) summarized data on particle size distribution of respiratory aerosols and found that particle become twice smaller in diameter after evaporation, due to the difference in relative humidity between nearly saturated expelled droplets and less humid surroundings. This practically means that particle size of 20 μm or less need to be considered for airborne transmission investigation.

Not all pathogens can remain airborne which depends on their droplet nuclei diameter and their size. Large droplets are generally not affected by mechanical ventilation design since they cannot remain suspended in the air, but quickly deposit on the surrounding surfaces due to the gravity influence. Deposited droplets can eventually evaporate and become re-suspended. Droplets of smaller size quickly evaporate, forming droplet nuclei that remain suspended in the air for a longer period of time and scattered over the space by tracking the room airflow patterns. Xie et al. (2007) studied a distance that respiratory droplets can travel in the indoor environment. The findings show that large expelled droplets can travel more than 6 m through the exhaled air at initial velocity 50 m/s (sneeze), more than 2 m at initial velocity 10 m/s (cough) and less than 1 m at initial velocity 1 m/s (exhalation). More research has been carried out on coughing due to its more frequent occurrence and dispersal through the mouth (Morawska, 2006).

There have been several studies demonstrating the connection between the transmission of airborne diseases in the indoor environment and the airflow patterns generated by mechanical ventilation. Li et al. (2007) systematically reviewed 40 studies and found that 10 studies were conclusive in relation to the connection between building ventilation design and spread of airborne diseases. Study concludes that there is a strong evidence which supports association between room airflow patterns and the spread and transmission of airborne diseases, such as influenza, tuberculosis, SARS, measles, chickenpox and smallpox. In addition, several studies showed the connection between particle transport and airflows generated by building occupants (Bjørg and Nielsen, 2002; Murakami, 2004; Rim and Novoselac 2009; Salmanzadeh et al. 2012). This leads to the realization of the importance of room air distribution in the transmission of airborne diseases.

2.4.4 Coughing and breathing airflow characteristics

Human respiratory activities, such as breathing, talking, coughing, sneezing, etc., generate large number of airborne particles with attached pathogens (Morawska, 2006; Nicas et al. 2005; Yang et al. 2007). Therefore, it is important to understand the airflow characteristics and patterns of these flows for evaluation of airborne cross-contamination and personal exposure.

Coughing is a typical and most obvious syndrome of a respiratory disease that involves a sudden, often repetitive reflex which helps to clear the respiratory tract from foreign particles and irritants, as well as from secretions. It consists of three stages: inhalation, forced exhalation and forced release of air from the lungs. The human cough often has a sequential mode and generally occurs twice. Gupta et al. (2009) found that flow characteristics of the first cough closely resembles the one of a single cough, while the second cough makes 50-60% flow characteristics of a single cough. A cough jet has a very strong initial momentum of around 10 m/s (Xie et al. 2007) that can penetrate far before it has dissolved in the ambient air (Tang et

al. 2009). Zhao et al. (2005) found that the initial velocity of the cough of 20 m/s will cause droplets to travel over 3 m, while the higher initial velocity can disperse coughed droplets even further. The averaged cough velocity was found to be 11.7 m/s, obtained from 50 coughs generated by 11 male and female subjects (Chao et al. 2009).

At normal activity levels, the human respiratory tract handles around 6 l/min or air as a result of breathing (Hyldgaard, 1994). The main reason for the exhalation is to remove the carbon dioxide and other waste products from humans. The exhaled air may carry small organisms such as viruses that can cause airborne disease transmission (Nicas et al. 2005; Morawska, 2006). In reality, exhalation takes longer than inhalation, however, it is often approximated with 2.5 s inhalation, 1 s break, 2.5 s exhalation and 1 s break (Zhu et al. 2005). At comfortable state, most of the people exhale through their nose. In this case, two jets at an intervening angle of 30˚ are formed (without interaction with each other) and 45˚ inclination angle from the horizontal direction (Hyldgaard, 1994). Exhalation through the mouth creates a jet in horizontal direction that is more easily influenced by the buoyancy, compared to the nose exhalation (Özcan et al. 2005; Nielsen et al. 2009). Although an exhaled air has a low momentum, it can disrupt the convective flow around the human body and reach the distance up to 0.4 m (Bjørn and Nielsen, 2002).

Data on the number and size of expelled droplets are difficult to generalize, as they vary according to the person (Edwards et al. 2004). Yang et al. (2007) summarized the size distribution of cough droplets and droplet nuclei for people of different ages and gender. It is reported that the average size distribution of the coughed droplets was in a range 0.62 - 15.9 μm (8.35 μm average), while range of 0.58 – 5.42 μm was reported for the average droplet nuclei size. Chao et al. (2009) documented that the average droplet size expelled through the cough was 13.5 μm with 5.2 droplets per cm^3 per cough. According to Morawska et al. (2009), the majority of aerosolized particles released through the coughing are below 0.8 μm in size.

Coughing can generate as much as 3,000 droplet nuclei, which is equal to the number of droplet nuclei produced by 5 minutes of talking (CDC, 2003). On the other hand, exhaled particles are typically smaller in size with a mean diameter from 0.3 to 0.8 μm (Holmgren et al. 2011).

Despite a prominent role of the human cough and exhaled air in infectious disease transmission, only a limited knowledge is available on how they interact with room airflows and impact airflow characteristics in the breathing zone. Previous findings have shown that cough expelled droplets become influenced by the typical room airflows at the distance beyond 2 m from the release point due to large velocity drop (Pantelic et al. 2009; Pantelic and Tham, 2013). How the cough droplets interact with the ventilation flows and subsequently, with the convective flow around the body of a susceptible occupant is mostly unknown to date which makes personal exposure predictions challenging. These findings highlight the importance of understanding the interaction between the human respiratory flow and surrounding airflows generated by the ventilation system and buoyancy flows induced by the building occupants.

2.5 Measurement techniques of the human convective boundary layer

Despite its importance and continuous presence, a proper experimental characterization of the human CBL has not been carried out in the past. As mentioned, the CBL around a heated human body consists of laminar, transitional and fully developed turbulent region (Clark and Toy, 1975). To properly characterize this low velocity flow field, measurement techniques deployed have to be able to: (i) accurately measure velocities in the range of 0 - 1 m/s, (ii) conduct measurement close to the heated surface without disturbing it (non-intrusive) and (iii) capture unsteadiness of the flow field (or show that flow field is steady), and (iv) provide a sufficient range of measurement (high spatial resolution). Since the velocities close to the heated body are relatively small, any disturbance can cause substantial measurement error. In order to

examine if the flow field is steady, periodic or unsteady, the measurements have to be conducted in multiple points simultaneously with a sufficient measurement frequency.

Rotating vane anemometers, thermal anemometers (hot-wire, hot-film and hot-sphere), ultrasonic anemometers and Laser Doppler Velocimetry are commonly used point-wise airflow measurements techniques (Sun and Zhang, 2007). The Laser Doppler Velocimetry can be successfully employed for measurements of the unsteady nature of the CBL because it is a non-intrusive technique with a high measurement frequency (Melikov and Zhou, 1996; Johnson et al. 1996). This technique, however, has a limitation of performing only single-point measurements. Rotating vane anemometers, ultrasonic anemometers and constant temperature anemometers due to their size substantially disturb the flow, while the hot sphere anemometers do not provide information about airflow direction (Liu et al. 2012). All these instruments require a large number of measuring points to properly characterize the airflow field. Such limitations indicate that these techniques may not able to fulfil the entire list of requirements necessary for CBL measurements.

The measurement techniques with a high spatial resolution used to characterize indoor environments are: Particle Streak Velocimetry, Particle Image Velocimetry (PIV), and Particle Tracking Velocimetry (Sun and Zhang, 2007). The Particle Streak Velocimetry can identify if a flow is 2D or 3D (Gbamelé et al. 2000), but in some cases is not sufficient for the precise understanding of the flow (Singh et al. 2002). The Particle Tracking Velocimetry has high measurement accuracy for low velocity flows and can measure larger area than the PIV, but maintaining neutral buoyancy of tracers in buoyancy driven flows is a challenge and can increase measurement inaccuracy (Liu et al. 2012). The PIV can measure instantaneous velocity field and can provide high spatial resolution of the velocity data (Kühn et al., 2008). The standard PIV system has measurement frequency of 15 Hz, which is considered to be sufficient to resolve flow features encountered in the indoor environment (Hanzawa et al.,

1987). Since the PIV is a non-intrusive technique, it also has the capability of measuring velocity field very close to the heated body and represents a very good choice for airflow investigation (Poussou et al., 2010). A review of different measurement techniques with a high spatial resolution points out that the PIV is a preferred choice for human CBL investigation.

2.6 Knowledge gap and hypotheses

Throughout the literature review chapter a nexus has been established between the convective flows generated by occupants and the exposure to indoor pollutants that can be potentially harmful or may cause discomfort. Although several studies attempted to visualize and quantify the CBL around a human body, most of them lack comprehensive data on airflow characteristics obtained with the measurement technique with a high spatial resolution. In addition, numerous factors that influence the development of the human CBL have not been explored comprehensively enough in the past. For instance, how the body posture and room air temperature affect the shape and velocity around the human body is not well known. Furthermore, the influence of the clothing insulation, table positioning and chair design on the airflow characteristics at the breathing zone has not been quantified. As these factors influence the development of the CBL, it will also affect the pollutant transport from the source to the occupant. Therefore, understanding the extent to which each factor affects airflow characteristics around the human body is crucial for design of improved exposure mitigation measures. The following hypothesis is therefore proposed:

- Factors such as body posture, room air temperature, clothing insulation, table positioning and chair design alter the velocity and temperature profiles around the human body.

Previous research has shown that different airflow patterns exist in every room, hence any generalization is uncertain. Therefore, in order to understand how the human CBL interacts with the ventilation flow, a simplified approach is needed which is based on the physics of this airflow interaction. In such an approach, the interacting flows can be assisting, opposing or transverse to each other. So far, little is known about the true nature of the interaction between these flows. Some previous studies investigated only the local airflow interaction in the breathing zone (Bolashikov et al. 2011a; Bolashikov et al. 2011b; Yang et al. 2009) and did not focus on how airflow patterns in the occupied spaces globally (immediately surrounding the person) affect the development of the CBL. Others adopted more theoretical approach using wind tunnels (Johnson et al. 1996; Heist et al. 2003) that gives limited body orientation with respect to the free stream. Neither of the previous studies considered airflow interaction between the CBL and the assisting flow from below nor opposing flow from above. Previous experiments have also shown that increase of the free stream velocity decreases the relative importance of the buoyancy effect produced by the human body. Widely adopted velocity at which invading flow starts to disturb the CBL is 0.1 m/s or above (Melikov and Zhou, 1996; Bjørn and Nielsen, 2002). These findings, however, apply only to the disturbance due to a horizontal airflow or due to a walking person. None of the studies in the past considered the velocity magnitude at which opposing and assisting airflows create disturbance to the CBL. Therefore, the following hypothesis is proposed:

- Different velocities of supplied air are required to penetrate the human CBL, depending on a direction of invading flow.

From the literature review it has been well-established that the human CBL plays important role in pollution transport around a human body. Previous studies, however, focus on a single point measurement that gives limited information on the pollutant distribution around the human body. In order to well-understand the pollution transport phenomena within the CBL

and how much the pollution spreads around the human body, it is necessary to perform measurement in multiple points. In addition, influence of factors such as location of the pollution source, room air temperature, table positioning and seated body inclination angle on the pollutant distribution in the breathing zone is largely unknown. In densely occupied spaces, it has been shown that interaction among human convective flows exists when they are positioned at 0.4-0.5 m distance, which suggests that cross-infection can take place at that distance (Datla and Glauser, 2009; Clark and de Calcina-Goff, 2009). These interactions, however, do not necessarily result in cross-contamination, because the CBL may not always carry the source of pollution. It is, therefore, necessary, to understand how the pollution is distributed within the CBL in order to reduce the risk of cross-infection. Therefore, the following hypothesis is formulated:

- Pollution distribution in the breathing zone of an occupant depends on the factors such as location of the pollution source, room air temperature, table positioning and body posture.

Studies in the past demonstrated that the human CBL has the ability to alter personal exposure, which led to realization of its important role in the transport of pollutants in the indoor environment. Most of studies that involve personal exposure measurements were conducted in case specific environments, hence any generalization of the results is challenging. Cough expelled droplets become influenced by room airflows due to a large velocity drop at a distance beyond 2 m from the release point (Pantelic et al. 2009; Pantelic and Tham, 2013). How the cough droplets interact with the ventilation flows and subsequently, with the CBL is mostly unknown to date which makes personal exposure predictions uncertain. As mentioned earlier, some studies have challenged ventilation standards by showing that the increase of the ventilation rates can in some cases lead to the higher exposure and the increased risk of airborne disease transmission (Melikov et al. 2010; Bolashikov et al. 2012; Popiolek et al. 2012; Pantelic

and Tham, 2013). These studies emphasize the importance of understanding the complex airflow interaction in the rooms generated by mechanical ventilation and heat sources. Based on these studies, the following hypothesis is proposed:

- There is no direct correlation between the amount of the supplied ventilation air and the personal exposure to airborne particles.

2.7 Research objectives

This study is divided into two general research objectives. The two general research objectives are:

- To examine the extent to which the room air temperature, room airflow patterns, body posture, clothing insulation, table positioning and chair design affect the airflow characteristics (the velocity, turbulence and temperature) around the human body.
- To examine the pollution distribution within the CBL and personal exposure to gaseous and particulate pollutants under factors that influence the human CBL, as well as under different locations of the pollution sources.

The first general objective is addressed in chapters 3, 4 and 7; while the second general objective is addressed in chapters 5 and 6. Several specific research objectives are presented in chapters 3 – 7 of this thesis.

2.8 Study Design

Five independent but interrelated studies were designed to address the knowledge gap. These five studies represent five chapters in this thesis (Chapters 3 - 7), that are presented as five blue clusters in Figure 2.3. The five chapters are designed as follows:

Chapter 3: The velocity field of the human convective boundary layer in a quiescent indoor environment is investigated in this chapter. The results describe influence of parameters such as ambient air temperature, body posture, clothing insulation/design, chair design, table positioning and seated body inclination angle on the velocity field as well as the shape of the human convective boundary layer.

Chapter 4: This chapter investigates the velocity field of the human convective boundary layer which is exposed to airflows generated by ventilation system. Three airflow directions were studied with respect to the human convective boundary layer: opposing, transverse and assisting.

Chapter 5: Ability of the convective boundary layer around a human body to transport gaseous pollutants in a quiescent indoor environment is investigated in this chapter. The results show the dependence between pollutant distribution in the breathing zone and factors such as location of the pollution source, room air temperature, table positioning and seated body inclination angle.

Chapter 6: Impact of the human convective boundary layer on the personal exposure to human generated particles is examined in this chapter. The personal exposure of the occupant is investigated in quiescent and ventilated environments when pollution is released as a cough droplets and particles at the level of feet. Influence of five uniform airflow directions are examined with respect to the convective boundary layer flow.

Chapter 7: This chapter investigates temperature field of the human convective boundary layer in a quiescent indoor environment. The results describe influence of parameters such as ambient air temperature, table positioning, seated body inclination angle, and human respiratory cycle on the temperature profiles around a human body.

It should be emphasized that previous studies have not performed investigation of the human convective boundary layer to this stage of completeness, since this work examines both airflow characteristics (velocity, turbulence and temperature) and personal exposure (to gaseous and particulate pollutants).

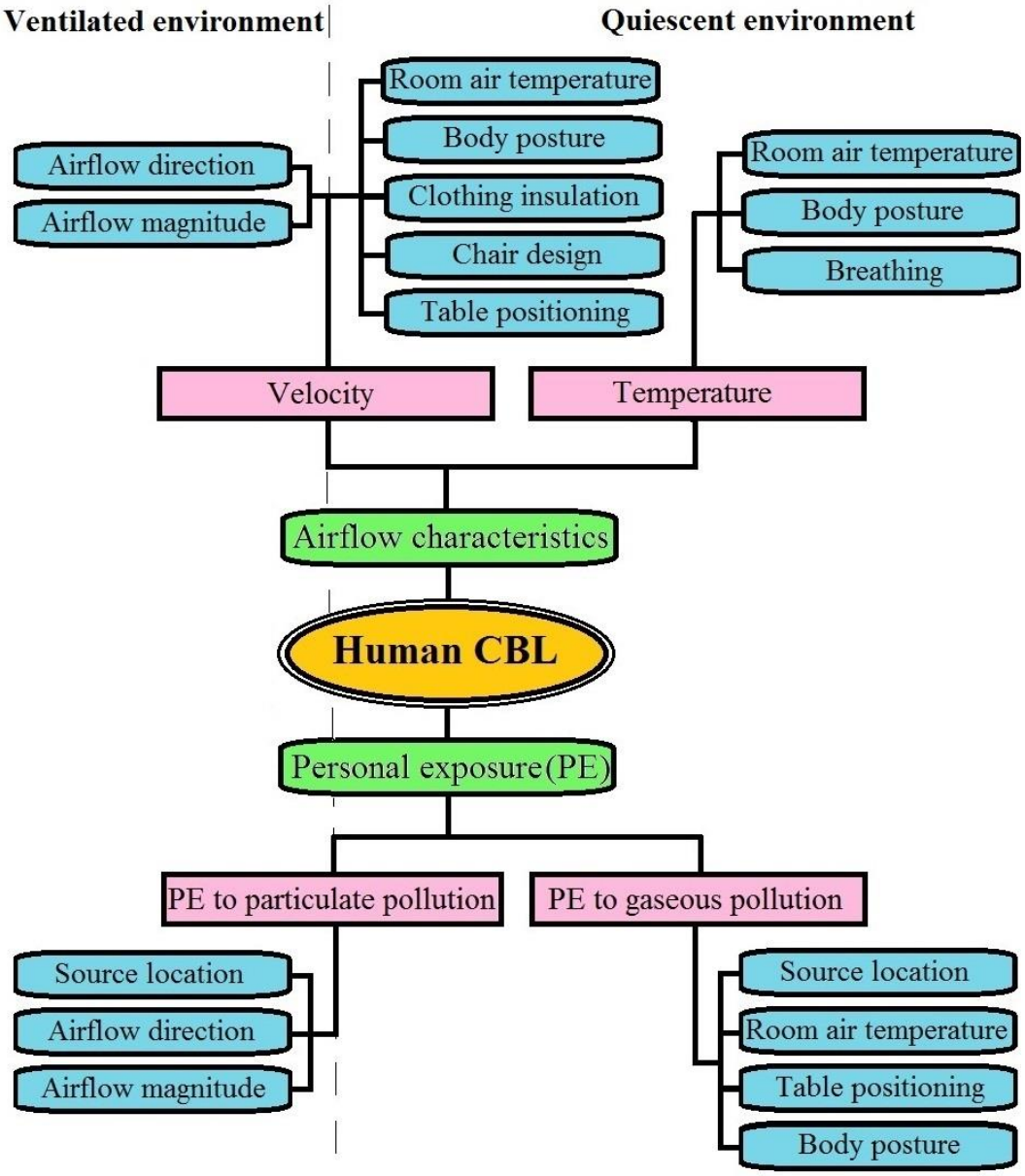

Figure 2.3 Study design.

CHAPTER 3: VELOCITY FIELD OF THE HUMAN CBL IN A QUIESCENT INDOOR ENVIRONMENT

3.1 Specific objectives

The first specific objective of this part of the study is to characterize the human CBL in the quiescent indoor environment under two ambient temperatures and body postures. The second specific objective is to study the impact of factors such as clothing insulation and design, chair design, table positioning and seated body inclination on airflow characteristics in the breathing zone of a seated manikin. Some of the parameters have already been studied in the past, but most of them lack comprehensive data on airflow characteristics obtained with measurement technique with a high spatial resolution. For the purpose of this study, the Particle Image Velocimetry (PIV) results are complemented with Pseudo Color Visualization (PCV) technique to improve overall understanding of airflow distribution around the human body. The PCV technique has not been previously used for CBL studies.

3.2 Research methodology

3.2.1 Experimental facility

An environmental chamber in the Department of Building at National University of Singapore with dimensions 11.1 (L) x 8.0 (W) x 2.6 (H) m was used for the purpose of this study. The chamber was equipped with displacement ventilation system composed of four supply diffusers located in the corner of the room and six ceiling mounted exhaust diffusers. To minimize radiant heat exchange with the surroundings, one external wall was insulated and heat sources

from the lighting fixtures were eliminated. The other three walls and the floor were adiabatic, while the ceiling was suspended below an insulated roof of the building.

3.2.2 Experimental equipment

The non-breathing and non-sweating thermal manikin (P.T. Teknik Limited, Denmark) with a complex female body shape of 1.68 m height in the standing and 1.23 m height in the sitting posture was used to thermally simulate a realistic human body. The body consisted of 26 independently heated and controlled segments that released 65 W/m^2 of heat which approximates the heat loss from the human body in a thermally comfortable state. During the experiments the manikin's body was kept at a constant surface temperature of 32 ºC. This theoretical scenario was chosen to precisely determine the effect of each parameter studied. Future studies will involve non-uniform temperature distribution of the manikin that resembles the skin temperature of an average person in a thermally comfortable state. The thermal manikin was calibrated prior to the experiments.

In this study, Particle Image Velocimetry (PIV) system was employed to capture and analyze the target flow field in front of the thermal manikin. It consists of dual YAG laser (New Wave Research, Inc., Fremont, CA, USA), double-pulse 190 mJ and a wavelength of 532 nm, synchronizer, computer and 2MP CCD camera with 28 mm lens that offers 1600 × 1200 pixel resolution. The image acquisition frequency of the CCD camera was set to 10 Hz which well exceeds typical frequencies of turbulent eddies found in ventilated spaces (Hanzawa et al. 1987). More details on the PIV are given in Appendix A.1. Atomized olive oil particles were (mean diameter of 1 μm) generated in a six-jet atomizer (Model 9306, TSI Inc., Shoreview, MN, USA) were used for seeding the flow around the thermal manikin. The degree of coupling between the particles and the fluid was high (Stokes number close to zero), which suggests that

the seeding particles behaved like tracers. More details related to the flow seeding, calibration and the measurement accuracy are discussed in Appendix A.3 and A.4.

The Pseudo Color Visualization (PCV) technique was employed to visualize the flow field around the thermal manikin. Both the PIV and PCV are image acquisition techniques which are similar with two differences: (i) in the area of the flow field captured by the camera; and (ii) the image processing algorithms. In the case of PCV technique, since the individual seeding particles need not be visible to the camera, it enabled a substantially larger field of view. The PCV technique has the ability to assign a spectrum of colors to the particles illuminated by the laser, depending on the pixel intensity obtained by the camera. For the purpose of this study, all PCV images have entirely qualitative character and the color spectrum does not have any quantitative content. More details on PCV technique can be found in the manual (Insight 3G^{TM}, 2004).

3.2.3 Experimental design

During the experiments, the ventilation system was turned off with the aim to provide quiescent indoor conditions. The chamber was periodically ventilated (i.e. between each measurement) in order to maintain the constant room air temperature and remove heat loads introduced by the manikin and measuring equipment. Prior to the experiments, tests were performed to establish how much time is necessary for environment to become quiescent from the moment air delivery was turned off. Results indicated that 5 min is enough for this transition and that time was adopted as a part of the experimental protocol. Velocity measurements were performed with DANTEC omnidirectional thermal anemometers (probe type 54T33) that are capable of measuring velocity higher than 0.05 m/s (±0.02 m/s accuracy) and the ambient temperature in a range from 0 to 45 ˚C (±0.2 K). Both velocity and temperature recordings took place at 4 locations around the thermal manikin at 1.2 m distance, vertically placed at 0.5 m, 1

m, 1.5 m and 1.9 m from the floor at each of the locations (Figure 3.1). The mean velocity was obtained as an average of 300 single measurements of instantaneous velocity. The magnitude of the mean velocity was low, below 0.05 m/s, indicating that quiescent indoor environment had been achieved, as suggested by Murakami et al. (2000). Measurement equipment was placed at far enough distances from the manikin in order not to interfere with the natural convection flow. All the external walls were insulated and heat from the light sources was eliminated, which made all surrounding walls adiabatic. Ambient temperature was measured to indicate that the effect of the thermal stratification on the CBL was acceptable. Temperature recordings closely followed the set point temperature with negligible level of thermal stratification compared to the vertical air temperature difference recommended by ISO (2005). The maximum thermal gradient between the lowest and the highest measurement point was about 0.5 ºC.

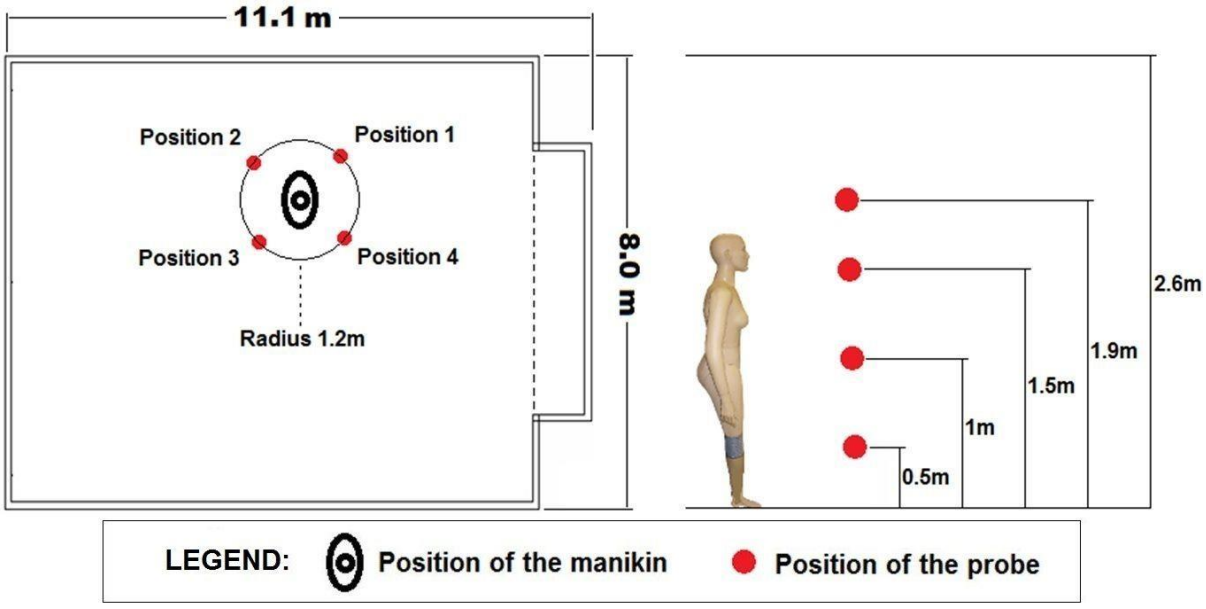

Figure 3.1 Velocity and temperature measurement locations in environmental chamber.

Given the objectives of this study, two sets of experiments were conducted:

- Set 1: The first set of experiments aimed to characterize the velocity field of the CBL around a thermal manikin under two ambient temperatures (20 and 26 ºC) at two body postures (sitting and standing). A nude (0 clo) thermal manikin with no hair was used as an experimental subject;
- Set 2: The second set of experiments aimed to examine the influence of clothing insulation/design, chair design, table positioning and seated body inclination on airflow characteristics of the CBL in the breathing zone of a seated manikin at 23 ºC ambient temperature.

Impact of clothing insulation/design on the airflow characteristics in the breathing zone was examined by studying different clothing levels (nude, thin and thick clothing) and design (tight and loose), as well as impact of the wig (Figure 3.2). Impact of tight versus loose clothing design for thin and thick clothing ensemble was studied under equal rate of heat loss from the body in order to eliminate additional variables. The effect of chair design was assessed with the manikin dressed in thin-tight clothing (reference case) that was seated in four different types of chair commonly used by the building occupants in Singapore, as shown in Figure 3.3.

Figure 3.2 Thermal manikin with different levels of clothing insulation/design.

Figure 3.3 Four chair designs used in the experiments.

Impact of table positioning on the strength of the CBL in the breathing zone was tested under three scenarios: First, without table that corresponds to the reference case; second, when the

abdomen of a seated manikin was positioned at horizontal distance of 10 cm from the front edge of the table; and third, when there was no gap between them, i.e. the edge of the table was contiguous to the abdomen of the manikin (Figure 3.4). Influence of seated body inclination angle on the airflow characteristics in the breathing zone was examined without the table, when the manikin was: Seated upright, leaned forward and leaned backwards.

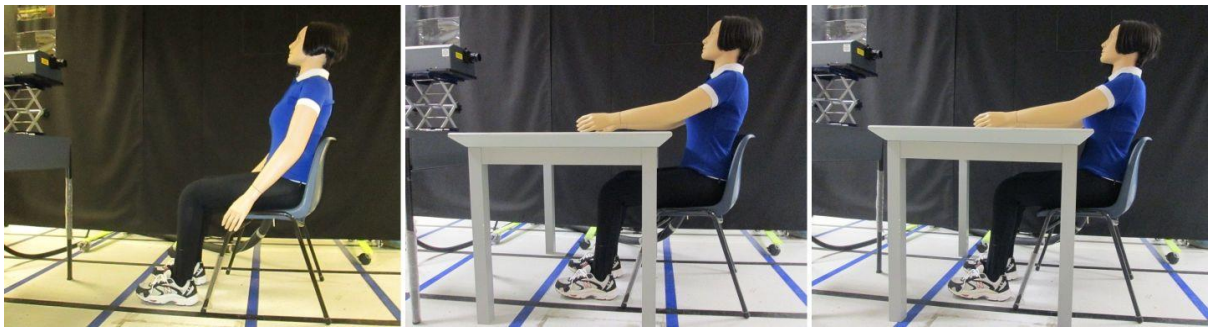

Figure 3.4 Table positioning: No table (left), Table 10 cm (middle) and Table 0 cm (right).

After all the body segments reached thermal equilibrium at 32 ºC (1 hour), manikin heat loss data were recorded during 30 min. For both sets of experiments, 20 different scenarios have been explored. Details for each scenario are enclosed in the Table 3.1.

Table 3.1 Summary of the two sets of experiments with 20 different scenarios.

	Parameter	Scenario	Details/Comments
Set 1	Ambient temperature	20 ºC	Nude manikin
		26 ºC	Nude manikin
	Body posture	Standing	Nude manikin
		Sitting	Nude manikin leaned back. 15 º from the vert. axis
Set 2	Clothing insulation/design * (Figure 3.1)	Nude	
		Thin-tight clothing	**Reference case** - Thin socks, thin tight trousers, thin tight short-sleeve T-Shirt
		Thin-loose clothing	Thin socks, thin loose trousers, thin loose short-sleeve T-Shirt
		Thick-tight clothing	Thick socks, thick tight trousers, thick tight long-sleeve T-Shirt, thick tight jumper
		Thick-loose clothing	Thick socks, thick loose trousers, thick loose long-sleeve T-Shirt, thick loose jumper
		No wig	Short hair wig, slightly below the ear level
	Chair design (Figure 3.2)	**Basic chair** **	
		Computer chair	
		Light meshed chair	Mesh only from the backside
		Executive chair	
	Table positioning (Figure 3.3)	**No table** **	
		Table 10 cm	Table dimensions 1x0.8x0.75 m (WxLxH)
		Table 0 cm	Table dimensions 1x0.8x0.75 m (WxLxH)
	Seated body Inclination	**Upright** **	
		Leaned forward	25 º from the vertical axis
		Leaned backwards	25 º from the vertical axis

* All clothing ensembles include underwear and shoes.
** Corresponds to the Reference case - "Thin-tight clothing".

3.2.3.1 PIV and PCV setup

The PIV laser was mounted in front of the thermal manikin to illuminate the seeding particles in the 2D plane perpendicular to the central vertical axis of the manikin. The thickness of the laser sheet was 1 mm. In the Set 1 experiments, CCD camera was positioned perpendicular to the laser sheet at 0.6 m distance, which yielded image frame size of 27.5 x 20 cm^2. To characterize the entire CBL in front of the manikin, the camera was positioned at 15 different locations (7 locations for the standing scenario), as shown by the dotted rectangles (Fig. 3.5, left). A traversing system has been employed to allow camera positioning with high precision. For each set of measurements at a single location, 540 image pairs were captured and averaged that corresponds close to one minute of the flow. More details related to obtaining the optimal number of image pairs are attached in the Appendix A.2. In the Set 2 experiments the same CCD camera was positioned 0.48 m away from the laser sheet, which produced 20 x 15 cm^2 image size. No traversing system was necessary since there was a single target image with limited focus in the breathing zone of the manikin (Fig. 3.5, right). The values of the velocity and root mean square (RMS) of fluctuating velocities reported in this study are resultant vectors from x and y components.

Seeding of the flow was achieved by atomizing olive oil that generated particles with a mean diameter around 1 μm. A proper seeding of the flow was a challenge. More information related to seeding of the flow, calibration, size of interrogation area and other PIV parameters can be found in the Appendix A.3. In addition, a comparison between PIV and a hot-wire anemometer was conducted as an attempt to compare measurement results and the details are enclosed with the Appendix A.4.

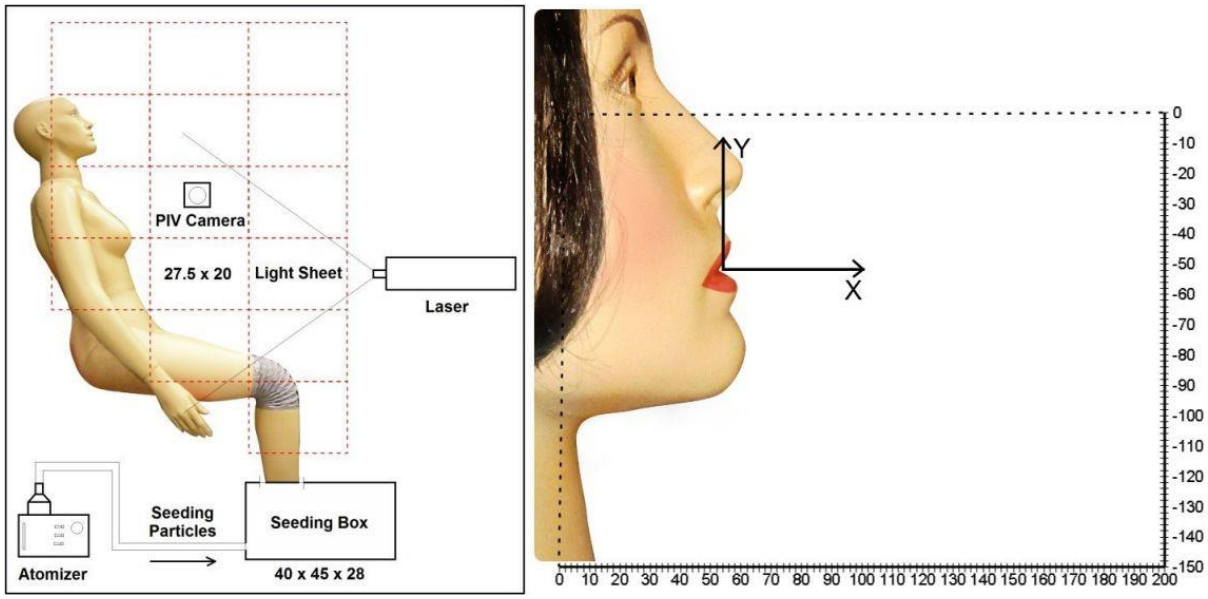

Figure 3.5 PIV setup – Set 1 Experiments (left) and Set 2 Experiments (right).

In addition to averaged quantitative vector fields in Set 1 experiment, qualitative features of the instantaneous CBL flow for standing and sitting body postures were obtained using PCV technique. This technique allows us to better understand the inherent unsteady nature of the human CBL. The PCV technique is able to assign different spectrum of colors to different pixel intensity obtained by the camera. In this study, all PCV images have completely qualitative character and the color spectrum does not have any quantitative meaning.

3.3 Results

3.3.1 Characterization of the velocity field around a nude thermal manikin

Experimental results based on PIV measurements show maximum mean velocity distribution with height, measured close to the surface of the standing and seated manikin (Figure 3.6). The maximum mean velocity is found to fall within a range of 1-3 cm from the surface at each height of the manikin. As seen, with increasing height, boundary layer flow accelerates up to the chin. At the height of the chin, a field of lower velocity exists, both in case of 20 and 26 ºC. The velocity reduction at the chin level is attributed to the contours of the head behaving like a physical obstacle, as described by Lewis et al. (1969). The upward free convection flow impinges on the mandible where it is divided into two parts: one part of the rising convective boundary flow deflects up the side of the cheeks, while the remaining part flows under the surface of the chin, thus causing velocity reduction in that region.

At 20 ºC ambient temperature, the standing manikin generates the maximum mean velocity of 0.22 m/s, at 3 cm from the chest (Figure 3.6). After collision with the chin, a region of equally high velocities is re-established at the forehead peaking at 0.23 m/s. At this point, rising convection flow is detached from the head and further developed into a human thermal plume. These results are in agreement with the ones documented by Lewis et al. (1969) who reported a maximum velocity in the human boundary layer of 0.25 m/s, measured 5 cm from the skin. Elevating the ambient temperature to 26 ºC weakened the thermal gradient, resulting in a maximum mean velocity of 0.16 m/s at the chest region, which is 27% lower than in the case of 20 ºC ambient temperature. At 20 ºC ambient temperature, seated manikin generated a maximum velocity of 0.24 m/s measured in the forehead region, which was 33% higher than in case of 26 ºC ambient temperature (0.16 m/s). We could observe that to some degree, a

sitting posture generates a higher peak velocity in the forehead region, compared to the standing posture. This is attributed to the chin of the seated manikin (leaned 15º backwards) that plays minor role in blocking the rising convection flow from beneath, compared to the standing manikin.

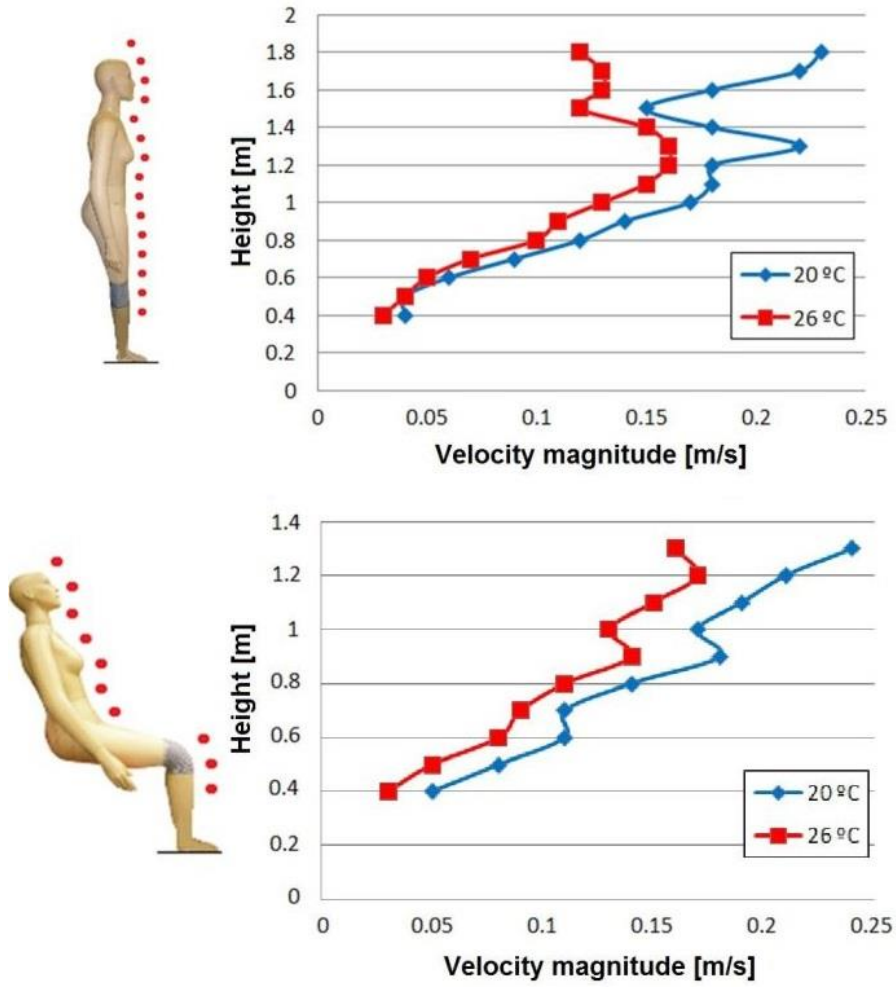

Figure 3.6 Maximum mean velocity distributions with height under two background temperatures: standing posture (top); b) sitting posture (bottom).

Figure 3.7 shows velocity contours in the front of the standing manikin at 20 and 26 ºC ambient temperatures. Velocity contours at 7 measurement locations were joined together manually to create an entire picture of the human CBL. The CBL flow starts in the lower leg region with a velocity of about 0.05 m/s at a height of 0.6 meters from the floor. With increasing height, boundary layer flow accelerates due to buoyancy effects and increase in thickness. As seen, a

higher velocity is obtained at 20 ºC ambient temperature. This difference becomes more prominent starting from the upper leg region at the height of 0.9 m, gradually increasing with height. In case of 26 ºC ambient temperature, it is observed that rising flow is not sufficiently strong to be quickly re-established just above the forehead, after detaching itself from the head. For the purpose of this study, the outer edge (thickness) of the CBL was defined by the velocity of 0.05 m/s, which corresponded to a peak velocity of the surrounding air under quiescent indoor conditions. The thickness of the CBL in the breathing zone of the standing manikin was rather similar between the two given temperatures, with 9 cm at 20 ºC and 11 cm at 26 ºC.

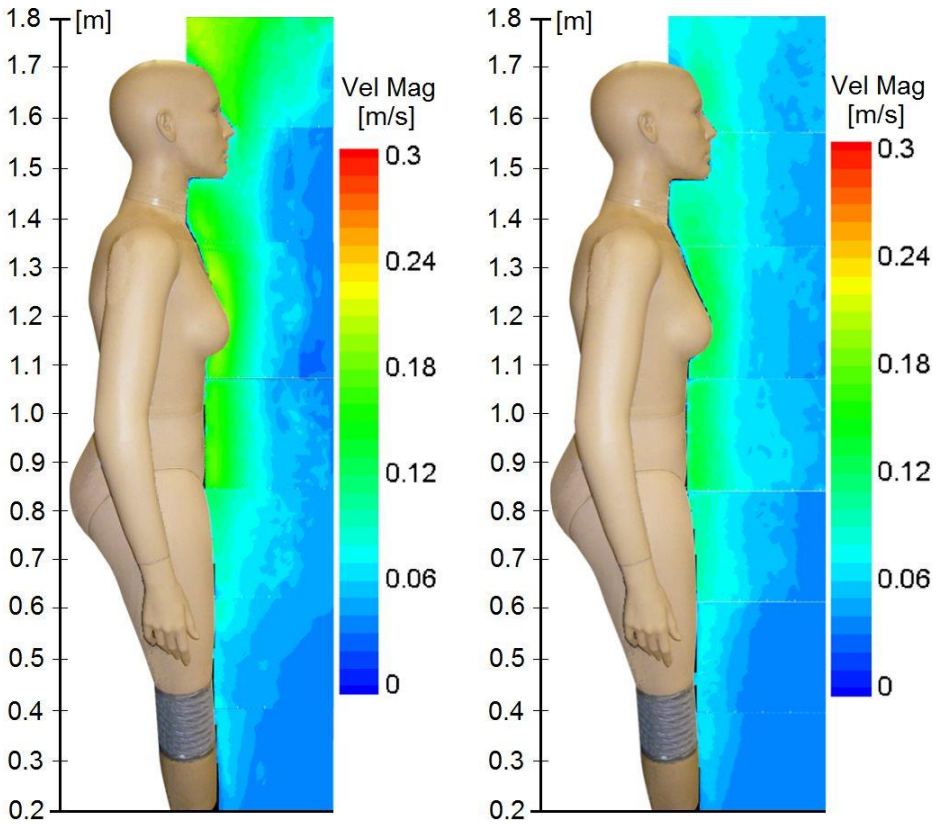

Figure 3.7 Velocity contours in front of the standing manikin: 20 ºC (left); 26 ºC (right).

Figure 3.8 shows the velocity contours in front of the seated manikin at 20 and 26 ºC ambient temperatures. Similar to the standing posture, a higher velocity was recorded when the ambient temperature was kept at 20 ºC due to a stronger thermal gradient. Unlike the standing posture, the shape of the CBL in front of a seated manikin was distinctly different between the two

ambient temperatures. Ambient temperature of 20 ºC induced a strong thermal gradient that creates a strong-convection flow at the upper body part of the manikin. This flow seems to be able to pull the rising convection flow from the thighs and lower legs towards itself and consequently, creates a more concentrated CBL flow with the thickness of 45 cm in the breathing zone. A similar phenomenon was observed by Salmanzadeh et al. (2012) in numerical study of the airflow adjacent to the heated manikin. At 26 ºC ambient temperature, flow separated from lower legs was less concentrated and unable to be redirected towards the breathing zone. The reason for this was the weakened thermal gradient that created a dissolved type of the flow with two distinct air regions; one starting from lower abdomen and the other, separated from lower legs (Fig. 3.8, right). As a result, a middle region of lower velocities exists between these two air regions. Observations indicated that shifting the laser plane from the centerline passing through the gap between the legs to plane that passes through the center of the thighs, eliminates the effect of the separate air streams and "joints" the two airflows.

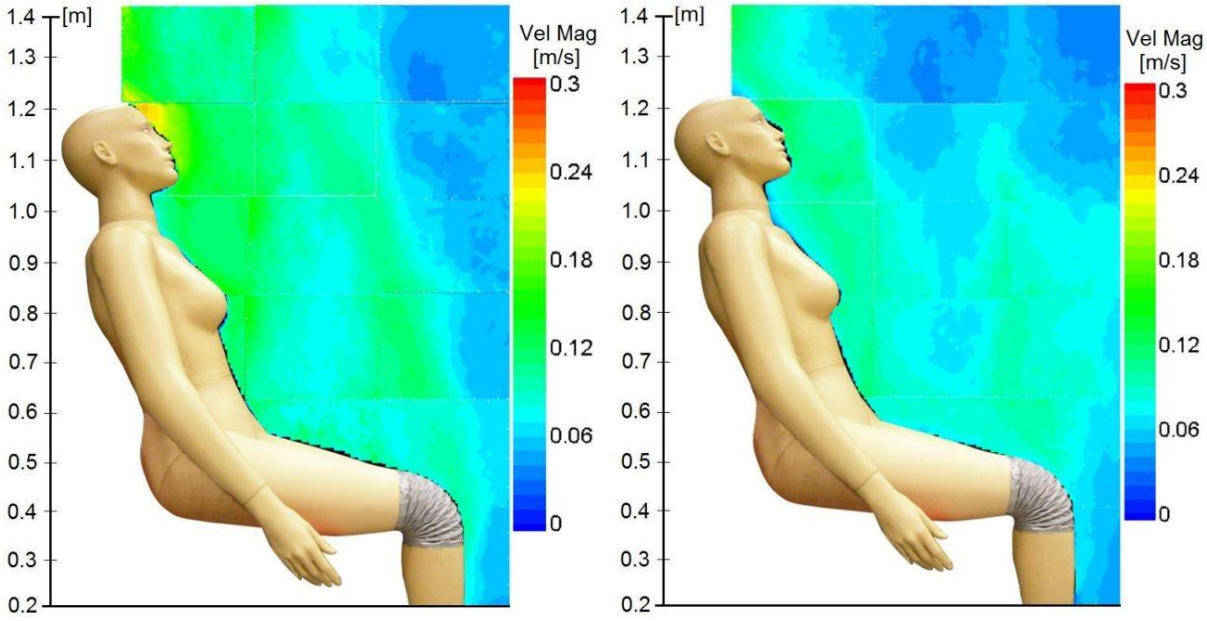

Figure 3.8 Velocity contours in front of the seated manikin: 20 ºC (left); 26 ºC (right).

The PCV technique that gives instantaneous images of the CBL in 2D plane has been employed in order to better understand the impact of the ambient temperature and body posture on the development of the human CBL, as well as to better understanding an unsteady nature of the human CBL overall. Figure 3.9 shows that at 20 ºC background temperature, the CBL flow in front of the seated manikin is deflected towards the facial zone due to a greater thermal gradient that generates a stronger convection flow at the upper body part, which is in line with Fig. 3.8. Visualization of the CBL in front of a standing manikin at 20 ºC is shown in Figure 3.10. No obvious difference in the CBL thickness in front of the standing manikin was perceived between two temperatures and therefore, only one scenario is shown. In Figures 3.9 and 3.10, color spectrum does not have the actual meaning and the figures have a purely qualitative character, as previously explained. For better understanding of an unsteady nature of the human CBL under two room air temperatures and body postures, three PCV videos are enclosed with this study (see Compact Disk, Videos 3.1 – 3.3).

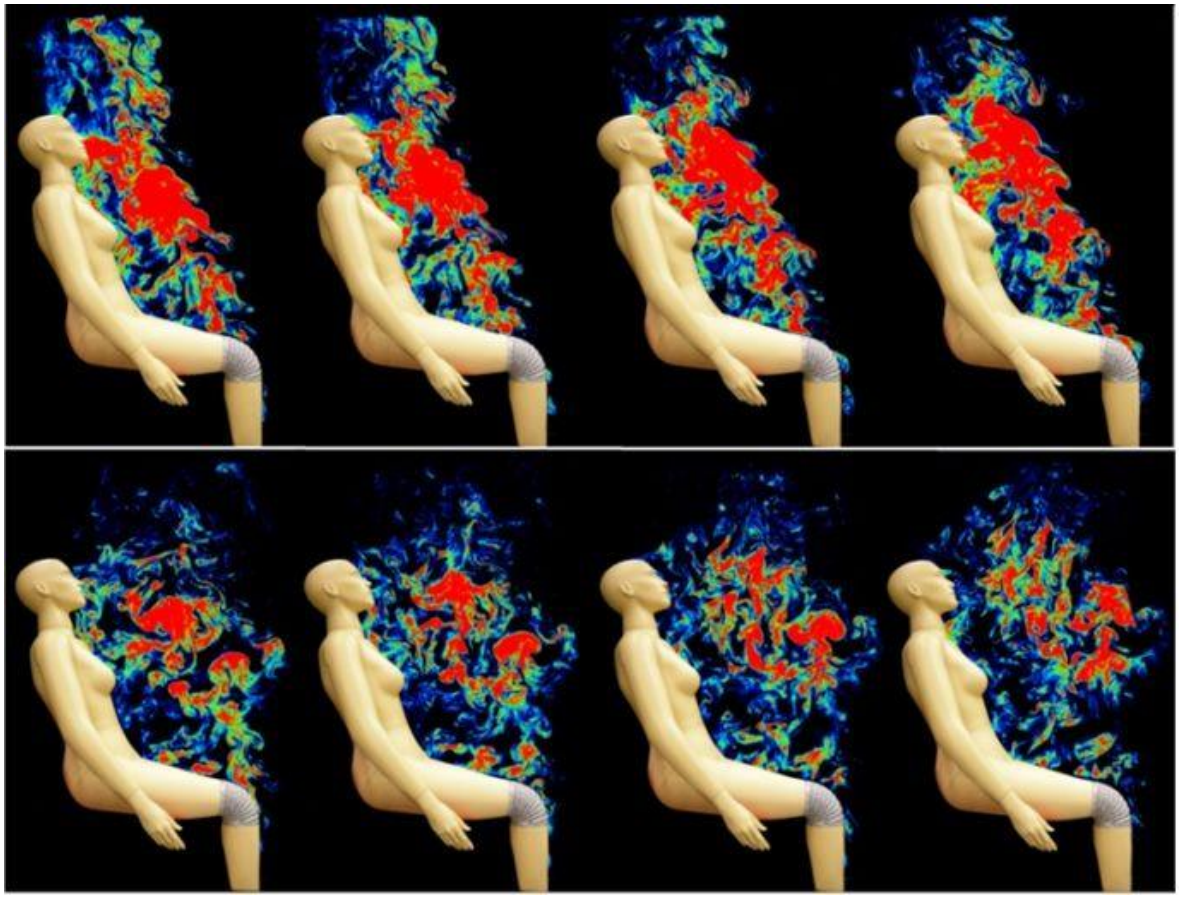

Figure 3.9 The PCV of the CBL at 0.5s interval: Sitting manikin at 20 ºC (top) and 26 ºC (bottom).

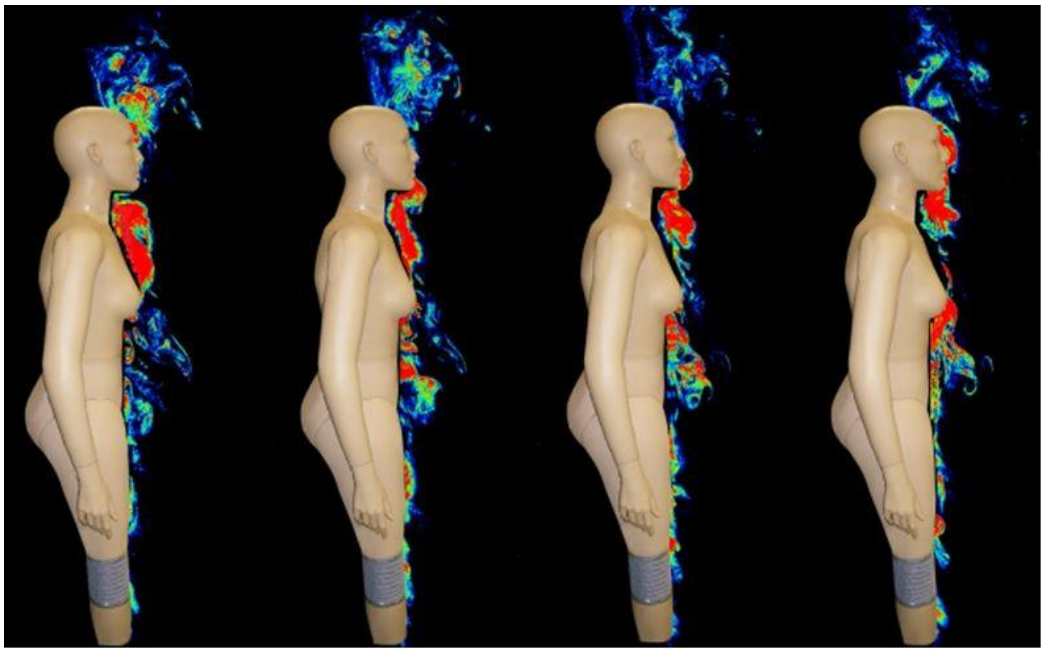

Figure 3.10 The PCV of the CBL at 0.5s interval: Standing manikin at 20 ºC.

3.3.2 Parameters influencing the velocity field in the breathing zone of a sitting thermal manikin

The results of Set 2 Experiments consist of absolute mean velocity plots in the breathing zone delimited with 20 x 15 cm^2 area, where the length of an arrow is proportional to the velocity magnitude of the flow. The mean velocity and RMS of fluctuating velocities are presented along the middle section of the mouth (along X-axis). It can be seen from Figs. 3.11-3.15 that typical velocity profile is developed that is inherent for flows near a vertical heated surface. Zero velocity at the skin surface sharply increased to a peak value and subsequently steadily decreased. Further away from the skin surface velocity of the CBL approached the velocity of the surrounding air (not shown). The RMS of fluctuating velocity along the X-axis was always the lowest in region close to the surface and uniform further away from the body, which, together with velocity profile that steadily decreased after reaching a peak value, indicated that turbulence gradually increased with increasing distance from the surface.

Figure 3.11 shows the influence of different clothing insulation/design levels on the velocity magnitude in the breathing zone. It is observed that different clothing insulation/design altered the velocity magnitude and relative turbulence intensity primarily within 5 cm from the surface of the body, while further away from the body this effect was low. The convection flow in front of the nude manikin (89 W/m^2) had the highest velocity with respect to other cases, with 0.24 m/s in front of the nose. The mean peak velocity in the breathing zone of the nude manikin (along X-axis) of 0.205 m/s was measured at 0.012 m distance from the surface (see also Fig. 3.12). Expectedly, an increase of clothing insulation decreased heat loss from the body due to increase of the surface temperature of the clothing, which decreased the velocity of the CBL in the facial region. Thin clothing ensemble reduced total heat loss from the body from 89 to 65 W/m^2 and shifted the peak velocity further away from the body, compared to an unclothed

case. The peak velocity reduction of 17% occurred in the breathing zone in the case of thin-tight ensemble (0.17 m/s), while thick clothing further decreased heat loss to 49 W/m^2 and the peak velocity in the breathing zone up to 40% (0.124 m/s).

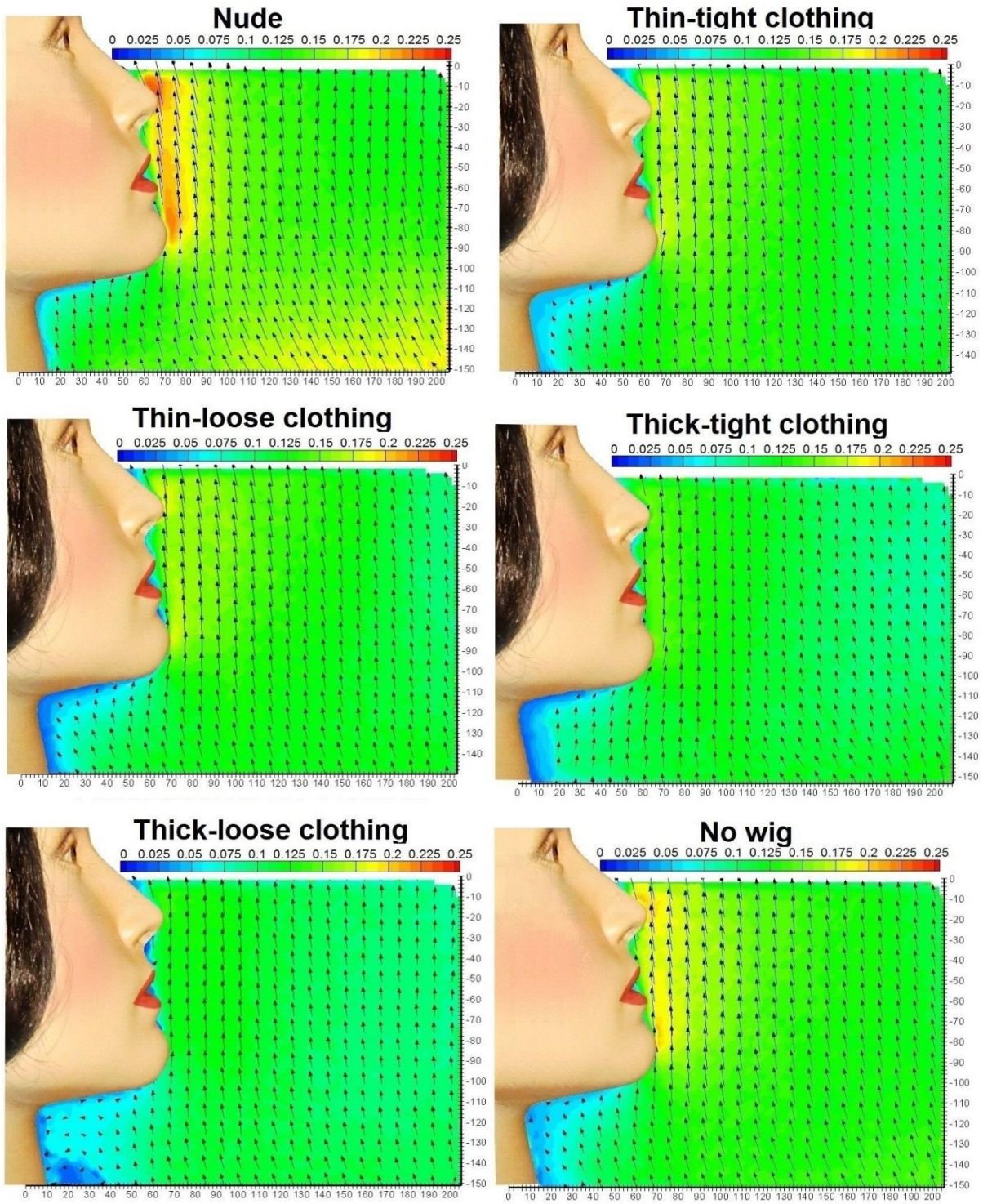

Figure 3.11 Influence of clothing insulation/design on the airflow characteristics in the breathing zone.

From Fig. 3.12, it can be seen that different clothing design (tight versus loose) had a different effect on the velocity profile in the breathing zone under two different levels of clothing insulation. In case of the thin clothing insulation, tight and loose clothing design generated the same velocity profile in the breathing zone. On the other hand, with increasing the clothing insulation the effect of clothing design became more prominent. Compared to the reference case (thin-tight clothing), thick-tight clothing decreased the peak velocity in the breathing zone by 28% (0.148 m/s), while thick-loose clothing reduced the peak velocity by 40% (0.124 m/s). With increasing distance from the body, the effect of clothing design on airflow characteristics diminished. In our case, loose clothing design contained many folds and a thick collar that acted as a physical barrier for the rising convection flow. This decreased the velocity in the neck region of the manikin, as clearly seen in Figure 3.11 (Thick-loose clothing). Removing the wig from the manikin created a prominent effect by increasing the heat loss from the skull from 22 to 89 W/m^2, i.e. total heat loss from 65 to 75 W/m^2. This led to increase of the peak velocity from 0.17 m/s (reference case - Thin-tight clothing) to 0.187 m/s, as shown in Figs. 3.11, 3.12 and 3.16. This is contributed to the convection flow above the bald head that strongly pulls the rising flow from beneath, thus inducing a higher velocity range in the facial region. Another reason is that the presence of the wig intensifies mixing of the convection flow with the surrounding air (Zukowska et al. 2012).

The influence of four different chair designs on the velocity profile in the facial region of the thermal manikin along X-axis is shown in Fig. 3.12. Similar to different clothing insulation/design, the major effects are observed in the region up to 5 cm from the surface of the body. The basic chair (denoted as Thin-tight clothing in Fig. 3.11) generated a mean peak velocity of 0.17 m/s close to the mouth, which was 13, 16 and 24% higher than the scenarios with light-meshed chair; computer chair and executive chair, respectively (see also Fig. 3.16). A small contact area between the body and the basic chair, as well as backrest porous structure

of the light-meshed chair allowed a higher convection heat loss from the back of the manikin. An increase of heat loss from the back presumably generated a stronger convection flow above the head that pulled the rising airflow from the facial region, thus inducing a higher velocity compared to the computer and executive chairs. Executive chair provided a highest degree of thermal insulation reducing the heat loss from the back, buttocks and thighs by 40% compared to the basic chair and peak velocity to 0.129 m/s. Beyond 5 cm distance from the face, four chair types generated a marginal difference in the CBL velocity field.

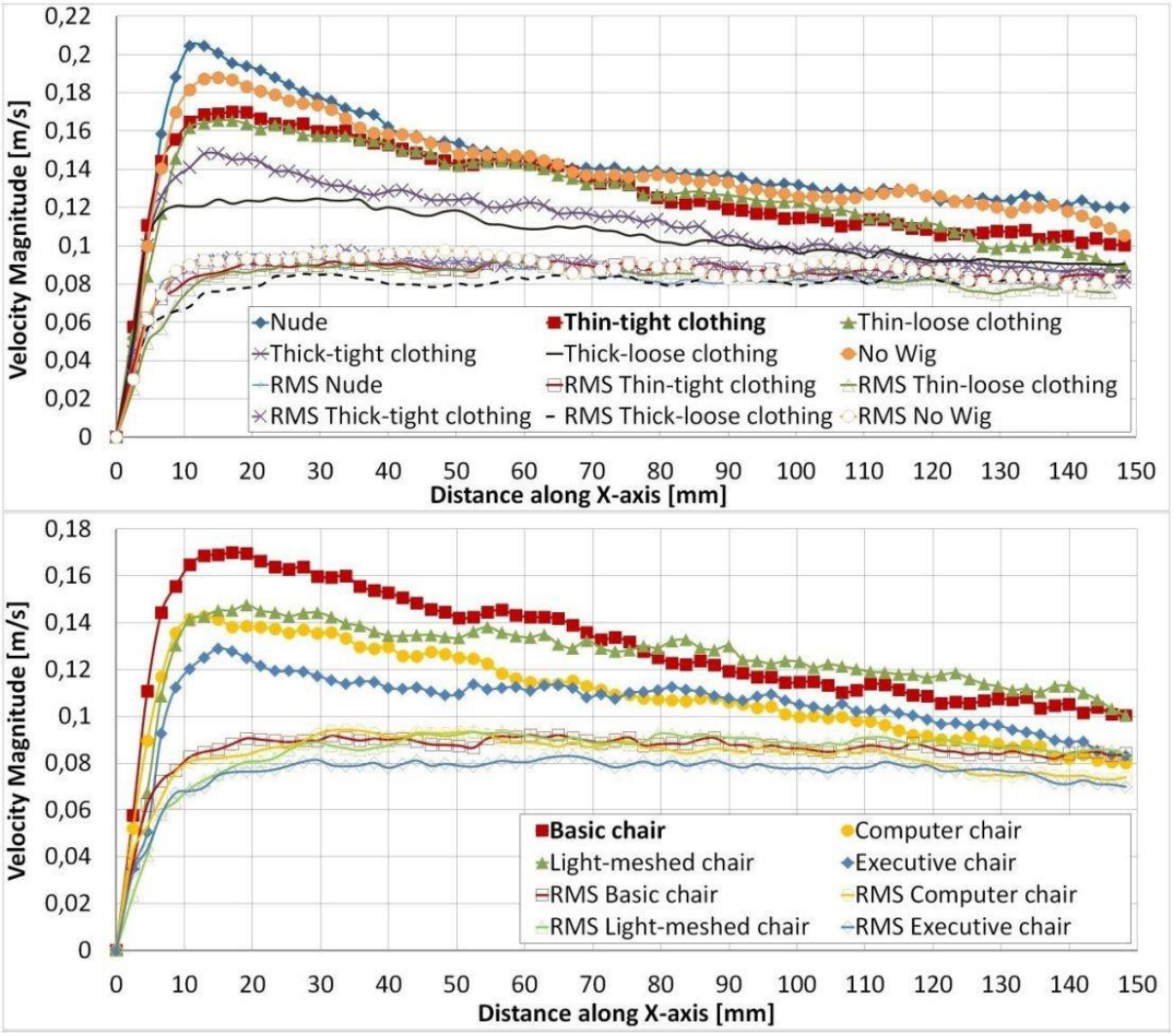

Figure 3.12 Average velocity and RMS of fluctuating velocities in the breathing zone: Impact of the clothing insulation/design and chair design.

The results indicate that airflow characteristics substantially differ for the cases when there was no table in front of the manikin (Fig. 3.11, Thin-tight clothing), compared to when the front edge of the table was positioned 10 cm from the manikin and with no gap between the table and the manikin (Fig. 3.13). Positioning the table 10 cm in front of the manikin caused reduction of the mean peak velocity in the mouth region from 0.17 m/s measured at 0.018 m to 0.141 m/s measured at 0.011 m (see also Fig. 3.15-3.16). Closing the gap between the table and abdomen of the manikin created a barrier for the rising convection flow from the legs and groins. This resulted in creation of a new CBL starting from the top surface of the table that was weaker in nature and more sensitive to the obstacles in the form of clothing. A mean peak velocity in this case was 0.111 m/s measured at 0.007 m distance, which was 21% lower than when the table was 10 cm away, and 34.5% lower compared to the reference case with no table. At about 0.15 m from the face of the manikin, when there was no gap between the table and the manikin, convection flow barely existed and it originated mainly from the arms of the manikin that were placed on the table. As a result, the velocity dropped at some distance from the surface with constant RMS of fluctuating velocities values which suggest extremely high turbulence intensity levels of up to 100% in that region (Fig. 3.15). It can also be seen that adding the table in front of the manikin shifts the peak velocity point closer to the surface the body.

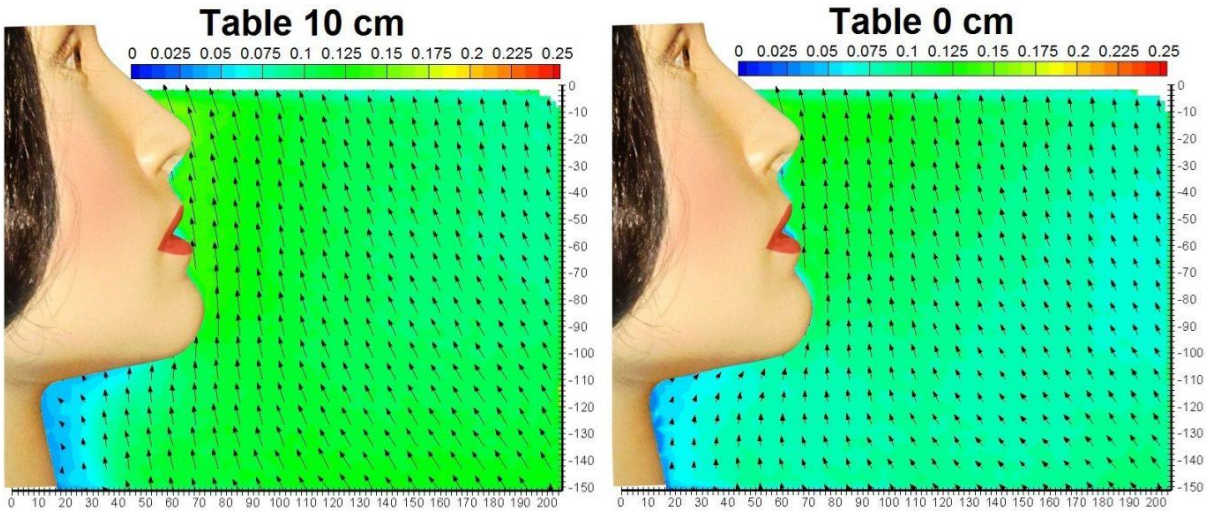

Figure 3.13 Influence of table positioning on the airflow characteristics in the breathing zone.

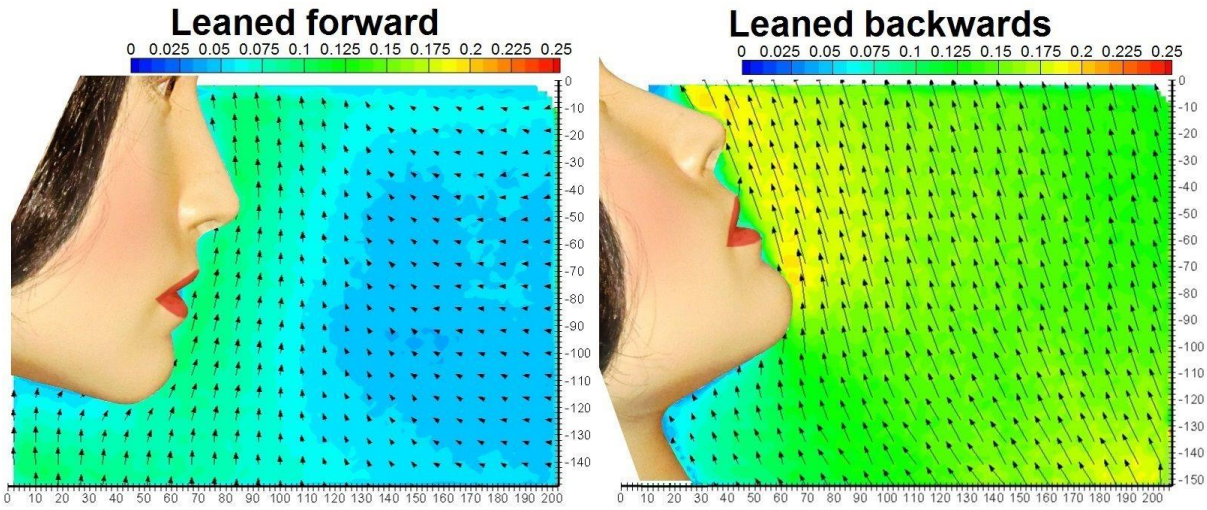

Figure 3.14 Influence of sitting body inclination angle on the airflow characteristics in the breathing zone.

The comparison of the results in Figures 3.11 and 3.14 show the influence of different seated body inclination angles on the airflow characteristics in the breathing zone of the thermal manikin. Three postures were explored: Upright (Fig. 3.11, Thin-tight clothing); leaned forward and leaned backwards (Fig. 3.14). Manikin leaned backwards induced the strongest flow in the breathing zone with maximum mean velocity of 0.185 m/s compared to 0.17 m/s in the upright posture. Relative difference in the mean velocity between two cases along X-axis was 17.5%. When the manikin was leaned forward, the thickness of the CBL in the facial region

was only 6.5 cm with literally no air movement further away from the face, which explains the high turbulence levels of about 100% in that region (Fig. 3.15). In this case, the mean peak velocity of the CBL dropped to 0.093 m/s which was 45% below the reference case, and 50% below the case when manikin was leaned backwards (see also Fig. 3.16). This measurable difference is attributed to the fact that when the manikin was leaned forward, a vertical axis that normally passes through the center of the head and the thermal plume was shifted 35 cm from the head towards the back of the manikin. Therefore, the convection flow in front of the manikin was pulled by the thermal plume characterized by the highest velocity, which resulted is thinner boundary layer in the breathing zone. Another reason for lower velocity in this zone was the chin, which in this case, had a stronger blocking effect for the rising flow from beneath.

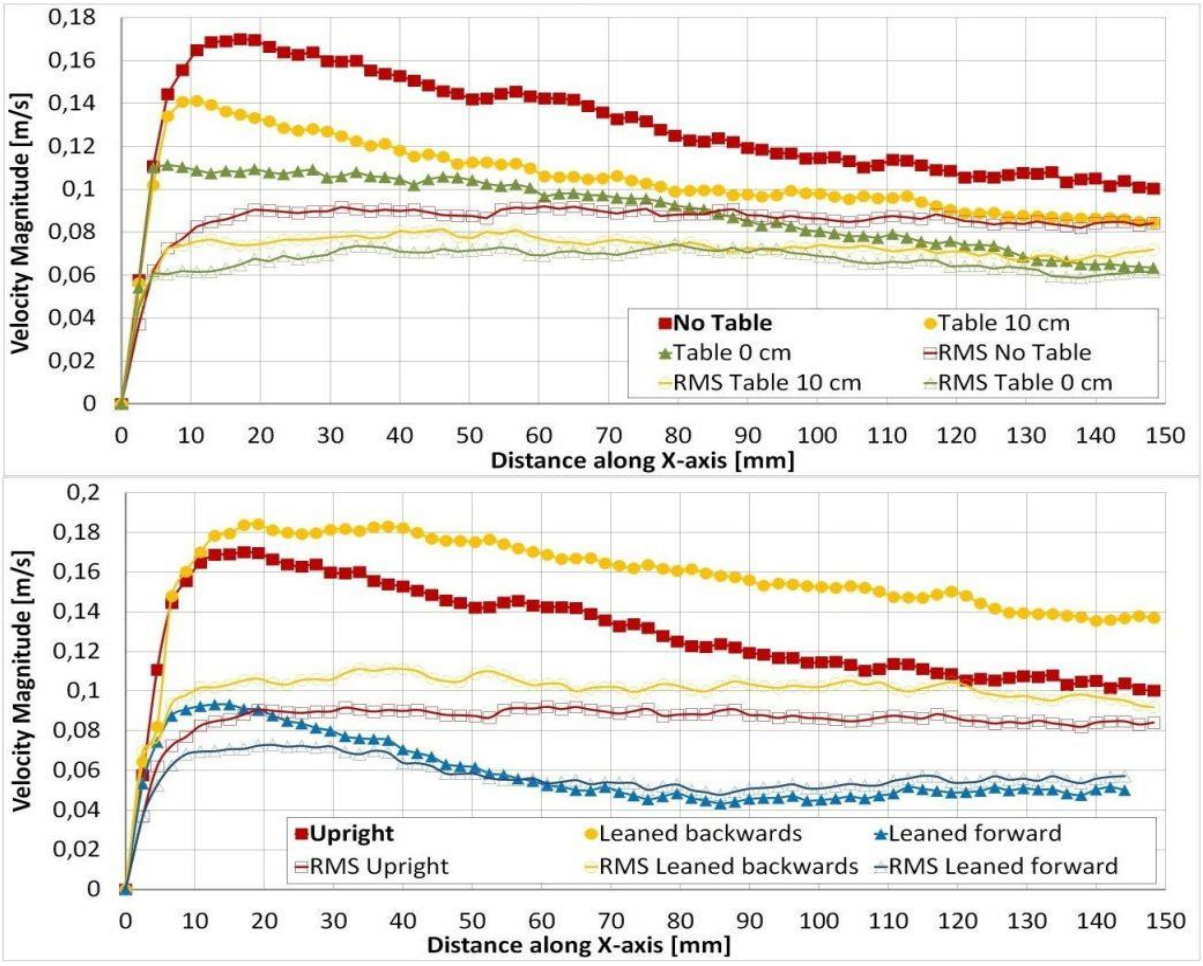

Figure 3.15 Average velocity and RMS of fluctuating velocities in the breathing zone: Impact of table positioning and seated body inclination angle.

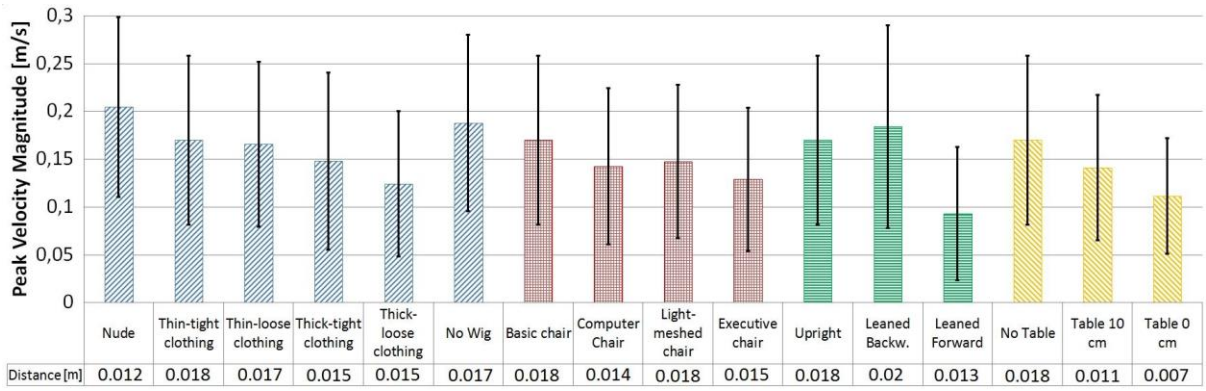

Figure 3.16 Peak velocity and RMS of fluctuating velocities in the breathing zone with distance from the surface.

3.4 Discussion

The results of this study can provide a fundamental knowledge of airflow distribution around the human body. Practical implications are further discussed in relation to an optimal ventilation design, transport of pollutants within and against CBL flow, and accuracy of experiments and numerical predictions. The findings reported in this chapter confirm previous findings that the velocity of the human CBL decreases at the lower temperature difference between the surface of the body and ambient air. Since in these experiments purely buoyancy driven flow took place, Rayleigh number (*Ra*) is used to describe flow field around the human body (Tavoularis, 2005):

$$Ra = \frac{g\beta\Delta T L^3}{v\alpha}$$

where v is kinematic viscosity, β is thermal expansion coefficient and α is thermal diffusivity. Rayleigh number below 10^8 indicate a laminar flow regime, while transition to a turbulent regime occurs within a range $10^8<Ra<10^{10}$. A simple approximation of a standing thermal manikin with a vertical heated cylinder shows that transition to turbulence occurs at the body height of 0.9 m at 20 ºC room air temperature and height of 1.1 m at 26 ºC room air temperature.

The calculated transition height is in agreement with the one reported by Clark and Toy (1975) who documented that at 20 ºC room air temperature and 33 ºC skin temperature, transitional regime starts at 0.9 m height. Therefore, in the rooms with elevated air temperature set point, transition to a turbulent flow regime is expected to occur at the higher body level. This implies that entrainment of the surrounding air into the CBL is likely to occur at the higher body level and that the higher percentage of inhaled air will originate from the CBL.

Sedentary occupants generate wider convection flow due to additional air stream from the thighs and lower legs, which makes it challenging to be characterized. The PIV measurements complemented with the PCV technique demonstrated the ability to characterize the complex flow interaction in front of the thermal manikin. The results showed that at 26 ºC room air temperature, seated occupants generate wider type of the CBL with larger entrainment area for the surrounding air. This wider CBL around the seated body may enhance cross-flow and cross-contamination between occupants. On the contrary, a narrower convection flow around the seated body generated at 20 ºC room air temperature is expected to reduce the probability of cross-contamination from the feet level. The importance of cross-flow becomes even greater if we consider that microenvironment around the human body contains substantially more microorganisms (30-400%) than the ambient air (Lewis et al. 1969). The implication of such a flow on exposure to different pollutants/diseases remains to be studied in the future.

The outer surface temperature of the human clothing is about 27-28 °C. An increase in clothing insulation reduces the power supplied to the manikin and temperature of the clothing surface which is reflected in lower velocities in the breathing zone. In parallel, RMS of fluctuating velocity remains nearly equal under different clothing insulation level. This implies that in quiescent environments or rooms with low turbulent mixing, increased clothing insulation generates more turbulent and complex convective flows enveloping the human body, compared to the nude or lightly dressed people. For instance, a change from thin to thick clothing outfit

increased the turbulence intensity from 52 to 62 %, measured at the point with the highest velocity in the breathing zone. In addition, for each of the clothing ensembles studied, relative turbulence intensity increases with increasing the distance from the body. The increased turbulence, in turn, may differently affect the exposure to indoor pollution due to faster entrainment of surrounding airflows.

Under the conditions studied, the results indicate that, as the level of clothing insulation decreases, the impact of clothing design becomes less important. Overall, parameters such as clothing and chair design have a minor influence on the velocity and turbulence profile at some distance from the surface, which suggests that it may not be crucial to precisely simulate their geometry. These findings are similar to those documented by Zukowska et al. (2012). Nevertheless, since the clothing and the chair design can modify airflow characteristics very close to the surface of the body, they may be important for the transport of pollution emitted from the surface of the human body. This is especially the case in rooms with quiescent indoor conditions or those with low velocity ventilation such as displacement air distribution where the CBL is more prominent. On the other hand, in the rooms with high turbulent mixing where strong air currents exist in the occupant zone (up to 0.5 m/s), chair design should be carefully simulated because its presence may disturb the surrounding airflows, and thus modify room air distribution. The findings in subsequent chapter indicate that the chair substantially alter velocity field in front of a seated manikin when the air is vertically supplied from the floor. More comprehensive study requires investigation of other chair types, materials and chair deformation properties in order to achieve better air distribution.

Closing the gap between the table and abdomen of the manikin, results in creation of new CBL of a lower velocity and reduced thickness, with corresponding peak velocities of 0.17 m/s and 0.111 m/s. Velocity profiles reported in this study are in line with the ones documented by Bolashikov et al. (2011), who reported the peak velocity reduction from 0.19 m/s to 0.10 m/s,

when the board was used to block the rising convection flow. From the personalized ventilation optimal design point of view, closing the gap between table and manikin is useful because it allows easier penetration of the personalized jet into the breathing zone and thus, enhances inhaled air quality with a lower energy penalty. In addition, airborne pollutants originating/entrained at lower leg region and/or detached from the skin may be prevented from reaching the breathing zone. Instead to the breathing zone, the pollution may be directed towards the sides of the body rejoining the thermal plume above the head. This would not be the case if the table is moved 10 cm away because it only partially blocks the rising convection flow from below. From the protection point of view against invading droplets released by the neighboring person, reducing the horizontal distance between the table and the occupant might not be an optimal solution. In rooms with displacement ventilation, closing the gap between the table and the occupant will likely limit the transport of clean air into the breathing zone. This is further explored in subsequent chapters. In practice, the occupants are not expected to constantly keep a certain distance from the edge of the table; however, it is possible to design and position the table in such a way to be optimized for the desired application.

As shown, seated body inclination angle creates substantially different air currents around the human body which may have different practical implications. For instance, pollutants originating/entrained at the level of lower legs will presumably terminate their trajectory in the inhalation zone when the body is inclined backwards, as they are pulled by the strong plume rising above the head. The same body posture may reduce the level of cross-infection among occupants that typically exhale at the velocity of 1.4 m/s through the nose and 1.3 m/s through the mouth (Tang et al. 2013). Thereby, a warm flow of exhalation is drawn upwards not only due to the lesser density, but also due to a strong convection flow rising from beneath. In contrast, forward body inclination may pull the pollution from beneath up along the back of an occupant, thus avoiding the breathing zone, which is studies in the following chapters.

Nevertheless, level of cross-infection may increase as there would be little air barrier for the flow of exhalation. The results obtained suggest that seated body inclination angle may have different implications relative to exposure levels and/or the performance of personalized ventilation system; however, this parameter is difficult to control in practice.

Implications discussed above clearly suggest that a thoughtful understanding of the human CBL is useful, especially with regard to exposure to indoor pollutants. Results from several recent studies (Bolashikov et al. 2012; Popiołek et al. 2012; Pantelic and Tham, 2013) that investigated indoor exposure to the expiratory released aerosols showed that increase of the air change rate can lead to the exposure increase. These studies conclusively show that complex flow interactions between the CBL, expiratory flows and airflow patterns generated by the air delivery systems are the key factors in determining exposure to the expiratory aerosols. Although investigation of this phenomenon is in its early stage, current findings imply that air change rate is an inadequate parameter for predicting exposure. More research on this topic is provided in the subsequent chapters.

3.5 Conclusions

The results of experimental investigation of the human CBL performed in a quiescent indoor environment reveal the following:

- Room air temperature of 20 ºC created a concentrated flow around the seated human body with the peak velocity of 0.24 m/s, while 26 ºC air temperature dissolved the convection flow with the peak velocity of 0.16 m/s;
- Increasing the room air temperature from 20 to 26 ºC reduced the peak velocity in front of the standing manikin from 0.23 m/s to 0.16 m/s, but did not influence the shape of the CBL;

- Clothing insulation and wig should be carefully considered in numerical simulations since the thin and thick clothing ensemble reduced the peak velocity from 0.205 m/s to 0.166 m/s and 0.124 m/s, respectively, while removing the wig increased the peak velocity from 0.17 m/s to 0.187 m/s;
- With decrease of the clothing insulation the effect of clothing design diminished. Under the conditions studied, clothing and chair design had a minor influence on the velocity and turbulence profile beyond 5 cm distance from the body;
- Table contiguous to the body and forward inclination of a seated body weakened the convection flow and reduced its thickness with respective peak velocities of 0.111 m/s and 0.093 m/s compared to the 0.17 m/s reference case; and
- Particle Image Velocimetry (PIV) and Pseudo Color visualization (PCV) techniques can be adequately employed for the human CBL investigation.

Practical implications of the present study should be carefully interpreted because there is an inherent difference between the highly mixed and quiescent indoor conditions. To further understand a behavior of the CBL around the human body, it is necessary to study its interaction with surrounding airflows generated by ventilation system. Since the present study exclude the influence of respiratory cycle flow, the future work will also be focused on how human CBL interact with the airflow of exhalation.

CHAPTER 4: VELOCITY FIELD OF THE HUMAN CBL IN VENTILATED SPACES

4.1 Specific objectives

The specific objective of this part of the study is to investigate airflow interaction between the CBL and the opposing flow from above, transverse flow from front and assisting flow from below for three different velocities of the ventilation flow. Measuring techniques employed for this study consist of Particle Image Velocimetry (PIV) complemented with Pseudo Color Visualization (PCV) technique, which have been shown in the previous chapter to provide a good synergy between quantitative and qualitative airflow characteristics and can be adequately employed for the CBL investigation. Findings of this chapter contribute to the fundamental knowledge of how the human CBL interacts with the airflow in the occupied spaces of the room.

4.2 Research methodology

4.2.1 Experimental facility

Measurements were performed in an environmental chamber with a displacement air distribution system. The dimensions of the chamber as well as the heat gains from the walls and lighting fixtures have been already described in Chapter 3. A thermal manikin was positioned in the center of the chamber. Air from a dedicated air handling unit was supplied via six low-momentum floor standing diffusers and room air was exhausted through six ceiling mounted grills. All supply and exhaust devices were located at far enough distance from the

thermal manikin to eliminate the supply airflow from affecting the CBL, as shown in Figure 4.1 (left). Furthermore, supply diffusers were sealed on the side facing the manikin to prevent any such interference.

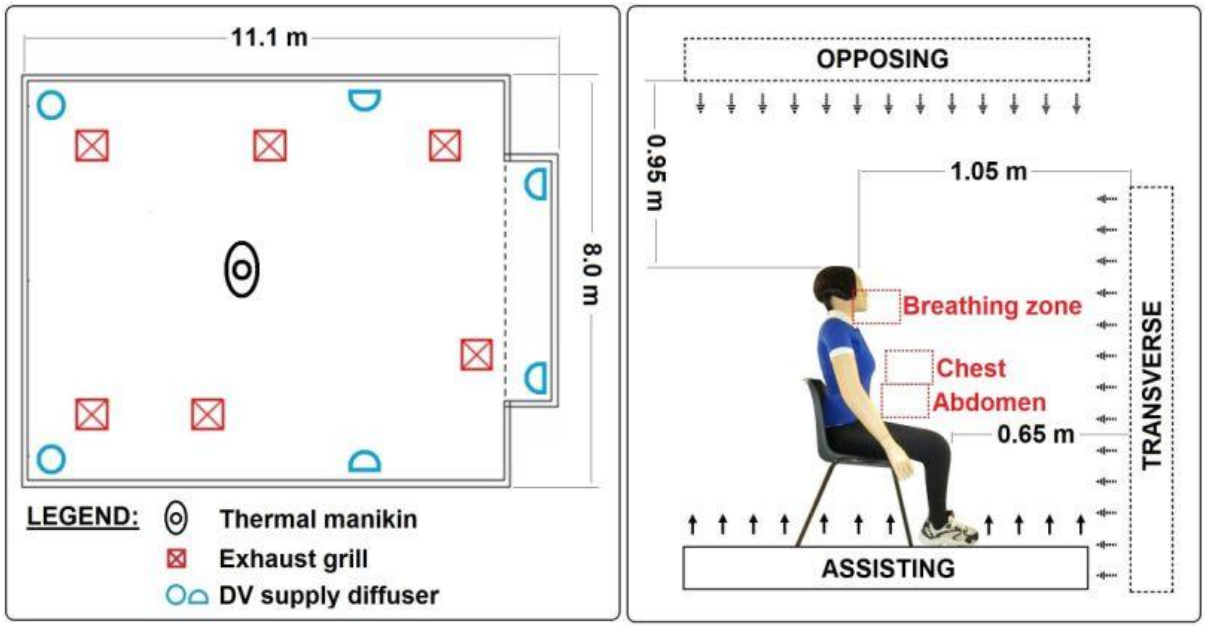

Figure 4.1 The Environmental chamber (left) and experimental setup for the seated manikin (right).

4.2.2 Experimental equipment

A specially designed rectangular box with dimensions 1.8 m x 1 m x 0.2 m (L x W x H) was used to generate a uniform forced-convection flow around the thermal manikin. The top plate of the box was perforated with 18000 holes of 5 mm diameter. The box (in further text airflow generator) contained 66 DC fans that were controlled with a fine-tuning frequency regulator capable of providing a velocity range from 0 to 1 m/s. The amount of heat added to the airstream by the fans was negligible. The uniformity test performed with omnidirectional thermal anemometers (Dantec Dynamics) with ±0.02 m/s and ±0.5 K accuracy, at 0.7 and 1 m distances from the outlet of the airflow generator showed that at both distances: (i) the velocity of the airflow did not change; and (ii) the velocity of the airflow cross-section remained

relatively constant within 10% among the corresponding 32 horizontal grid-points. Test was performed in accordance with the standard (ASHRAE, 2012) that uses the coefficient of variation as an indicator of the flow uniformity. These findings suggested that the airflow generator delivered a uniform flow of room air before reaching the CBL of the manikin. In addition, the velocity was measured at 0.2 m around the cross-section of the airflow at distances of 0.7 and 1 m from the outlet. At both distances, the velocity was low (about 0.05 m/s) which suggest that the generated airflow was unidirectional and did not spread towards the side.

Figure 4.2 Perforated box design for the uniform airflow distribution.

The non-breathing and non-sweating thermal manikin, whose dimensions were described in Chapter 3, was used to thermally simulate a realistic human body. During the experiments the manikin released 65 W/m^2 of heat which approximates the heat loss from the human body in a thermally comfortable state. The recorded temperature of the manikin's surface was in the range of 30.5˚C to 34.5˚C. The tight-fitted clothing of the manikin, consisting of trousers, t-shirt, shoes, socks and underwear, corresponds to a typical attire level of occupants in tropical buildings. Tight clothing ensemble enabled an easier reproduction of the measurement results. The thermal manikin was calibrated prior to the experiments.

In this study, the Particle Image Velocimetry (PIV) system was employed to capture and analyze the target flow field in front of the thermal manikin. For the flow visualization around

the thermal manikin the Pseudo Color Visualization (PCV) technique was used. Both the techniques were previously described in details in Chapter 3.

4.2.3 Experimental design

The CBL of the seated thermal manikin and its interaction with surrounding airflows was examined under three different scenarios: (i) opposing airflow from above; (ii) transverse airflow from front and (iii) assisting airflow from below. In the three scenarios, the airflow generator was positioned above, in front and below the thermal manikin at the distances indicated in Figure 4.1 (right). For scenarios of opposing and assisting flows, the airflow generator was positioned 12 cm away from the surface (respectively ceiling and floor) to allow air suction from its bottom plate. The results were compared to the case obtained in a quiescent indoor environment, which was taken as the reference (and henceforth referred as "pure CBL"). Interaction between the CBL and assisting flow was performed primarily for the sitting body posture. The manikin was seated in a basic type of the plastic chair shown in the Figure 4.1 (right), which is better described in Chapter 3. In the case of assisting flow, in response to the finding that the chair created interference that substantially altered the airflow patterns that impacted the breathing zone, additional experiments were conducted for the standing posture. In all scenarios, uniform airflow was supplied through the airflow generator to achieve velocities of 0.175 m/s, 0.3 m/s and 0.425 m/s at the surface of the manikin when the manikin was not heated (i.e. adiabatic with the room temperature). Velocities of 0.175 m/s and 0.3 m/s were chosen to represent typical velocities occurring in most occupied indoor spaces (Baldwin and Maynard, 1998), while a velocity of 0.425 m/s is similar to one induced by the mechanical fan and/or personalized ventilation (Melikov et al. 2003).

Minimizing the total heat gain in the chamber facilitated a constant room air temperature of 23 ˚C to be maintained at the minimum ventilation rate (1 h^{-1}). The low ventilation rate minimized

interference between the CBL and ventilation flow. Velocity and temperature measurements were obtained with Dantec thermal anemometers at 4 locations around the thermal manikin at 1.2 m distance, vertically placed at 0.5 m, 1 m, 1.5 m and 1.9 m from the floor at each of the locations. Based on 300 recordings obtained during 5 min of the instantaneous velocity obtained during 5 min, the mean velocity magnitude measured was below 0.05 m/s, which indicated that quiescent indoor environment had been achieved, as suggested by Murakami et al. (2000). Air temperature at the highest measurement point was 0.5 ˚C higher than the air temperature near the floor, which suggested a low degree of vertical thermal stratification.

To achieve a good mixing between the olive oil particles and air, seeding was performed through the bottom side of the airflow generator, simultaneously at four locations. Uniformly distributed seeding particles were discharged through the perforated plate of the box by the mechanical fans. Particles were illuminated by the PIV laser that was aligned with the centerline of the manikin. In the case of the transverse flow, the PIV laser was mounted at the top of the airflow generator in order to avoid interference with the flow discharged from it. To capture instantaneous flow field in the breathing zone delimited with 20 x 15 cm area, the CCD camera was positioned at 0.48 m orthogonal distance from the laser sheet.

4.2.4 Data analysis

After performing an optimal number of images independence test, it was found that variation in the average velocity distribution beyond 540 image pairs becomes negligible (<3%). Therefore, for each measurement 540 image pairs were analyzed that is equivalent to 54 s of the flow. Captured images were analyzed using Insight 3G software (Version 9.1.0.0. TSI Inc.). A processor type "Recursive Nyquist", that starts with 64 x 64 pixels^2 and ends with 32 x 32 pixels^2 interrogation area, was used to analyze instantaneous images. As a result, 2-3% of

spurious vectors per image were detected and rejected. Image post-processing functions or filters were not applied in the data analysis.

Analyzed data are presented as a mean velocity plot along with the velocity vectors where the length of an arrow is proportional to the velocity magnitude and the direction of the arrow corresponds to the flow direction at the point. In addition, the velocity and RMS of fluctuating velocity are presented as a function of the horizontal distance from the middle section of the mouth. The magnitudes of the velocity and RMS represent the resultant vectors from the X and Y components. The relative turbulence intensity was obtained as the ratio of the standard deviation of velocity fluctuations (RMS) and the mean velocity at each measurement point.

4.3 Results

Three sets of experiments were carried out, that describe the interaction between the CBL with mutually opposing, transverse and assisting flows.

4.3.1 Interaction with opposing flow from above

Figure 4.3 shows the mean velocity contours in the breathing zone of the CBL in a quiescent environment, as well as its interaction with the opposing flow from above. Figure 4.4 shows the influence of the opposing flow on the CBL mean velocity profiles and the RMS of fluctuating velocities as a function of the horizontal distance from the mouth. In the case of no surrounding airflow, the thermal manikin created a velocity profile that is characteristic of airflows adjacent to a vertical heated plate. The peak velocity in the mouth region was 0.185 m/s, recorded at a distance of 14 mm, while at 150 mm distance from the mouth the velocity dropped nearly by half (0.095 m/s). Adding an opposing (downward) flow at 0.175 m/s created negligible effect on the airflow characteristics in the breathing zone, as shown in Figures 4.3

and 4.4 (top). Further velocity increase created substantial disturbances to the CBL at the height of the head. A downward velocity of 0.30 m/s was not able to completely offset the plume; however, it reduced the peak velocity by 46% (from 0.185 m/s to 0.10 m/s), while at 150 mm distance from the mouth the velocity dropped down to 0.06 m/s. As the velocity of the CBL close to the surface is naturally higher, stronger disturbances of the CBL are expected to occur at some distance from the surface. As seen in Figure 4.3, at 120 mm distance in front of the nose, the downward flow collided with the CBL, thus creating the vortex in that region. Opposing flow at 0.425 m/s was able to completely break away the human thermal plume, and created a predominantly downward velocity in front of the face. In this case, invading downward flow followed the natural curvature of the skull peaking at 0.26 m/s at 90 mm distance in front of the mouth (Figure 4.4, top). As the top of the head created a physical barrier for the downward flow, the region below the chin and very close to the mouth preserved the upward air movement.

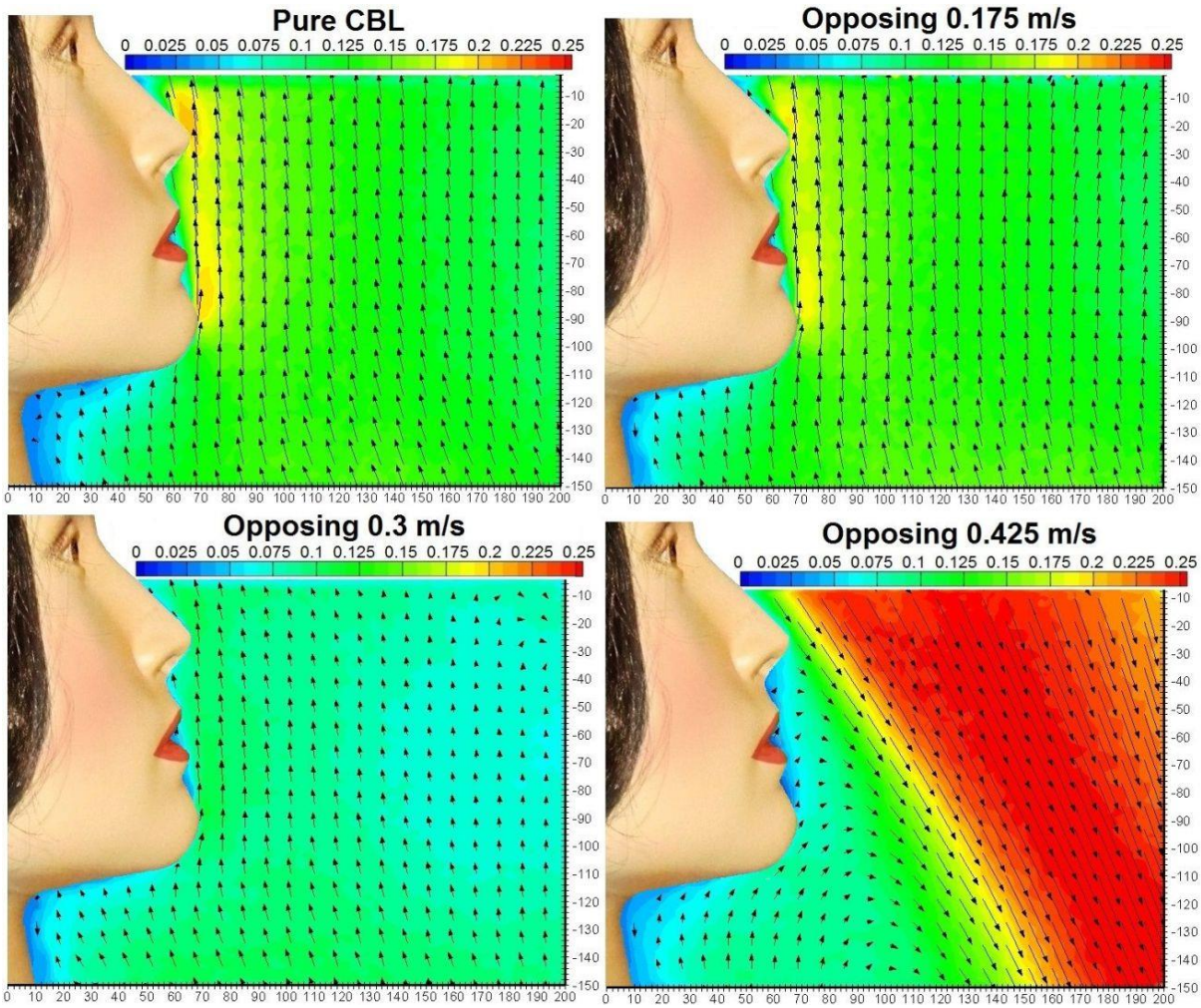

Figure 4.3 PIV of the CBL and its interaction with opposing flow from above.

Although the results of the RMS of fluctuating velocities are presented (Figure 4.4, bottom), the results were discussed based on the relative turbulence intensity values. In case of the pure CBL, the RMS of fluctuating velocity remained relatively constant further from the body surface, which indicated that the relative turbulence intensity gradually increased with increasing the distance from the surface, reaching 85% at 150 mm distance from the mouth. Due to the small disturbance in case of the opposing flow at 0.175 m/s, similar relative turbulence intensity profile was observed. The opposing flow at 0.30 m/s created a collision point between two flows at the nose level, thus causing a high degree of turbulence intensity up to 110%. When downward flow of 0.425 m/s was applied, a change in the flow direction

occurred within 20-30 mm from the mouth which resulted in a region of higher turbulent intensity with turbulence levels of 110%. Further ahead of the mouth, the relative turbulence intensity declined progressively to 27% at 150 mm from the mouth due to a single predominant airflow direction.

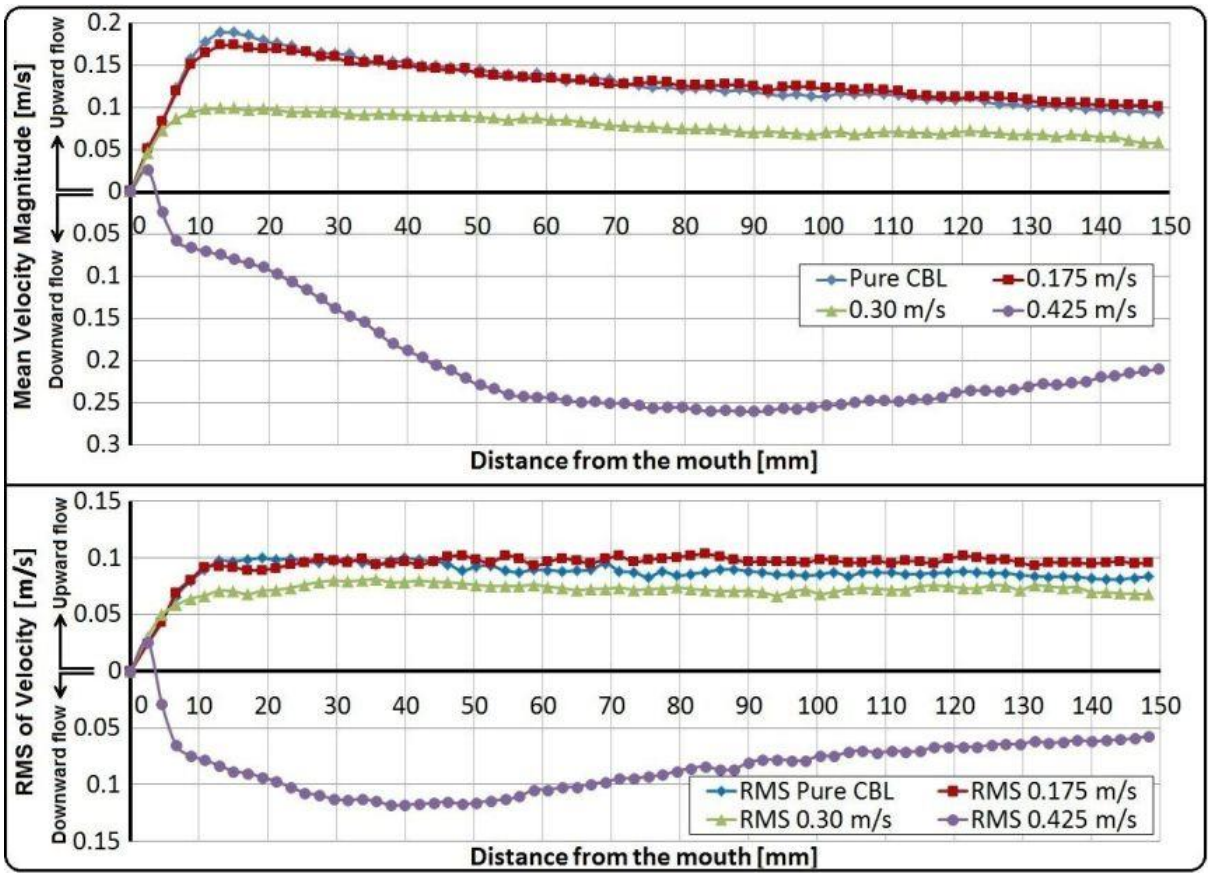

Figure 4.4 Mean velocity (top) and RMS of fluctuating velocities (bottom) in the mouth region: Impact of the opposing flow from above.

To fully comprehend how the uniform downward airstream impinges upon the thermal plume above the head and the CBL in front of an occupant, PCV technique was employed (Figure 4.5). The top part of the Figure 4.5 displays a pure thermal plume produced from the manikin's body heat. As there were no mechanically driven airflows in the surroundings, the plume rose vertically upwards. The thermal plume and mutually opposing flow at 0.175 m/s collided at the height of about 0.4 m above the head (Figure 4.5). At this height, the rising thermal plume is

spread in the horizontal direction, similar to the effect of the jet impinging on an orthogonal plate. A study in which locally supplied airflow opposes the thermal plume showed that the airflow of 4 l/s, which corresponds to the target velocity of 0.24 m/s, creates a collision point at a similar height (Yang et al. 2009). Downward flow at 0.30 m/s further penetrated the rising plume creating a collision point at the height of approximately 0.15 m above the head. Due to a stronger CBL, the thermal plume above the head remained upward. Finally, when the opposing flow approached the manikin at the velocity of 0.425 m/s, the thermal plume did not exist as it was fully overpowered by the invading flow. Four additional videos that describe interaction between the human thermal plume and downward flow at three velocities are enclosed as supplementary information (Compact Disk, Videos 4.1 – 4.4).

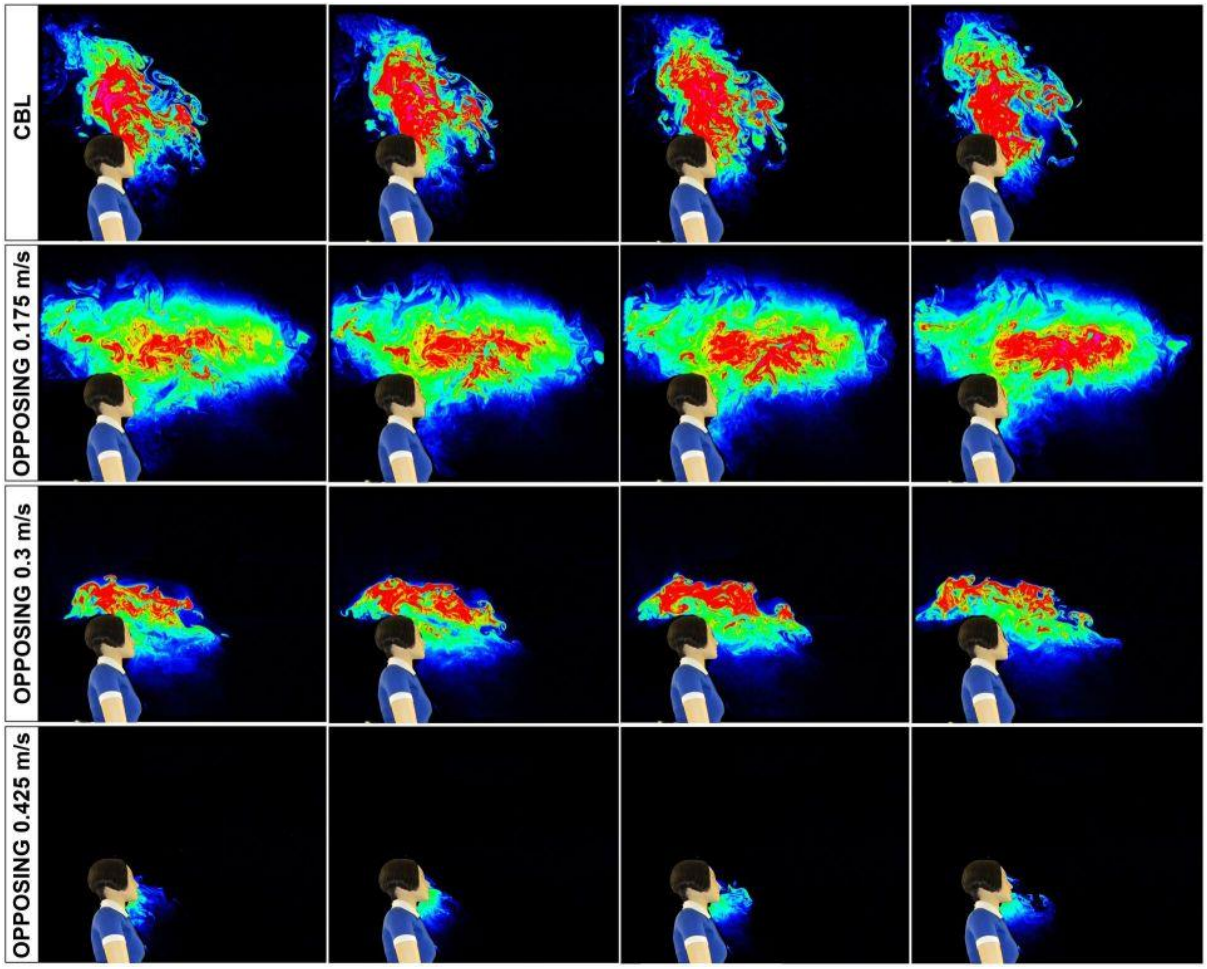

Figure 4.5 PCV of the CBL at 0.5s interval: Influence of opposing flow from above.

4.3.2 Interaction with transverse flow from front

Figure 4.6 shows the mean velocity contours of the CBL under its interaction with the transverse flow from the front. Figure 4.7 shows the change of the mean velocity and standard deviation of velocity fluctuations (RMS) as a function of the distance at the level of the mouth. The results indicate that the pure CBL flow was strongly disturbed by invading transverse flow at a relatively low velocity of 0.175 m/s (see also Figure 4.3 – for comparison with pure CBL). In this case, the maximum velocity of the CBL dropped sharply from 0.185 m/s (for the pure CBL) to 0.08 m/s at 15 mm horizontal distance from the mouth. Further increase of the invading flow velocity to 0.30 m/s and 0.425 m/s completely replaced the upward CBL flow with horizontal airstreams, generating mean velocities of 0.10 m/s and 0.125 m/s at 15 mm distance from the mouth, respectively. When each of the three invading velocities was applied, the mean velocity at 15 mm horizontal distance from the mouth was lower than in the case of the pure CBL (Figure 4.7, top). The velocity of invading flow steadily decreased as it approached the manikin, which is partially due to its collision with the manikin's surface (Yang et al. 2009) and partially due to the collision with the upward CBL.

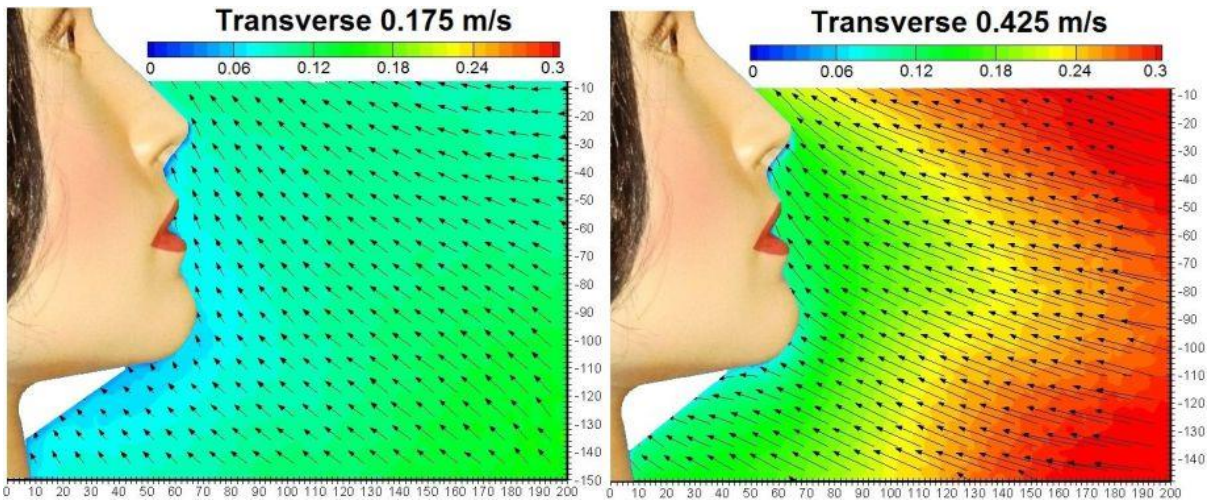

Figure 4.6 PIV of the CBL and its interaction with transverse flow from front.

Exposing the manikin to horizontal airstream from the front at 0.425 m/s induced higher velocity close to the surface of the manikin, compared to those introduced at 0.30 m/s and 0.175 m/s. Since the CBL was completely replaced by the invading flow at 0.425 m/s, the flow maintained a predominantly horizontal flow direction. This predominant flow direction resulted in the lowest values of the standard deviation of velocity fluctuations (RMS) and consequently, the lowest relative turbulence intensity levels. At 100 mm distance in front of the mouth, the relative turbulence intensity values for the free stream velocities of 0.425 m/s, 0.30 m/s and 0.175 m/s were 35%, 45% and 60%, respectively.

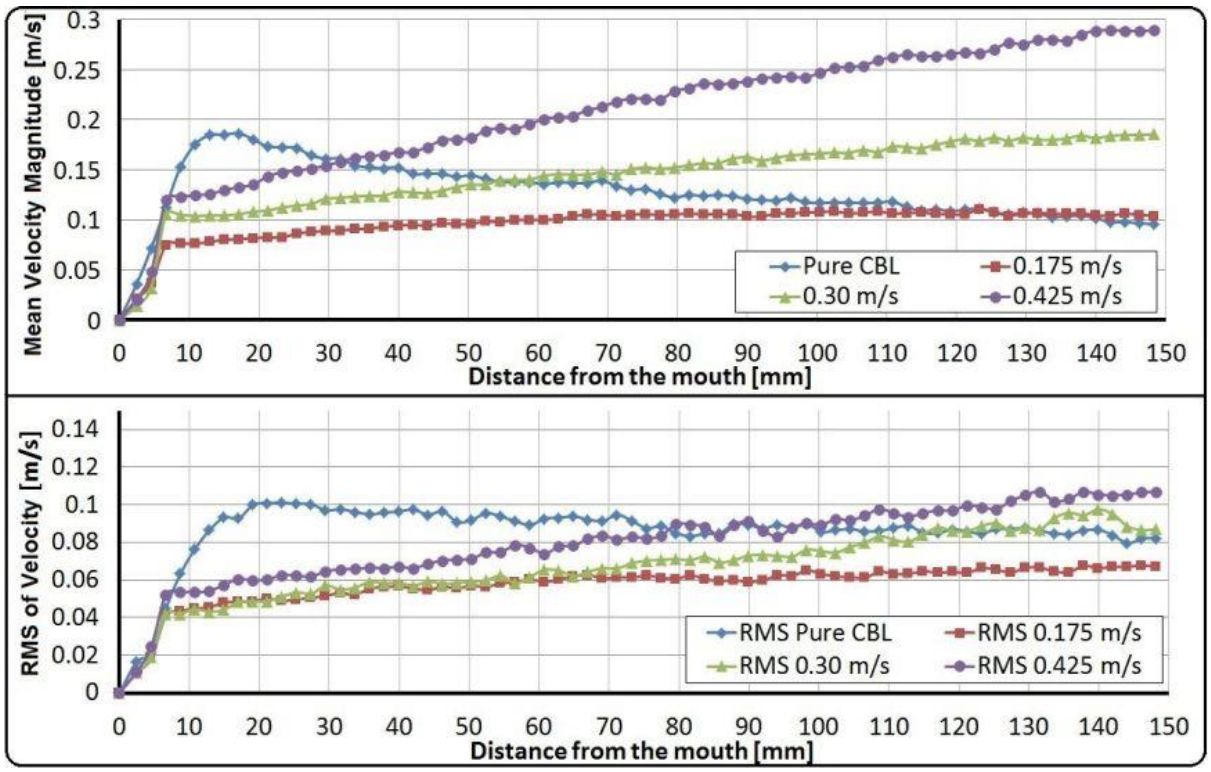

Figure 4.7 Mean velocity (top) and RMS of fluctuating velocities (bottom) in the mouth region: Impact of the transverse flow from front.

4.3.3 Interaction with assisting flow from below - seated manikin

Airflow interaction between the CBL and assisting flow from below was investigated when the thermal manikin was standing or seated in the chair. The velocity contours in front of the seated

manikin exposed to a uniform upward airflow at 0.175 m/s, 0.30 m/s and 0.425 m/s are presented in Figure 4.8. Expectedly, assisting flow at 0.175 m/s resulted in increased mean velocity in the breathing zone, relative to the case of the pure CBL (see also Figure 4.3). Although, assisting flow at 0.175 m/s reduced the peak velocity from 0.185 m/s to 0.165 m/s, the velocity along the horizontal distance from the mouth was higher and remained constant at 0.16 m/s, as shown in Figure 4.9 (top). The RMS of fluctuating velocities in the same region was reduced and remained relatively steady at 0.065 m/s, which corresponds to a turbulence intensity of 40%. In contrast to expected results, further increase of the upward velocity to 0.30 m/s and 0.425 m/s reduced the velocity in the breathing zone and changed the direction of the flow. The velocity reduction occurred up to 70 mm distance from the mouth compared to the pure CBL scenario, and across the whole breathing zone compared to the case of assisting flow at 0.175 m/s (Figure 4.9, top). The velocity profile for assisting flow at 0.30 m/s and 0.425 m/s was rather similar, starting from 0.12 m/s at 10 mm in front of the mouth and steadily increasing to 0.14 m/s at 150 mm distance. The upward vector direction was replaced with vectors approaching the face at 45˚ angle, which will be discussed in the following paragraphs. Unlike the velocity, the level of the relative turbulence intensity in front of the mouth was considerably higher for the case of assisting flow at 0.425 m/s (85%), compared to the turbulence intensity at 0.30 m/s (55%), as shown in Figure 4.9 (bottom).

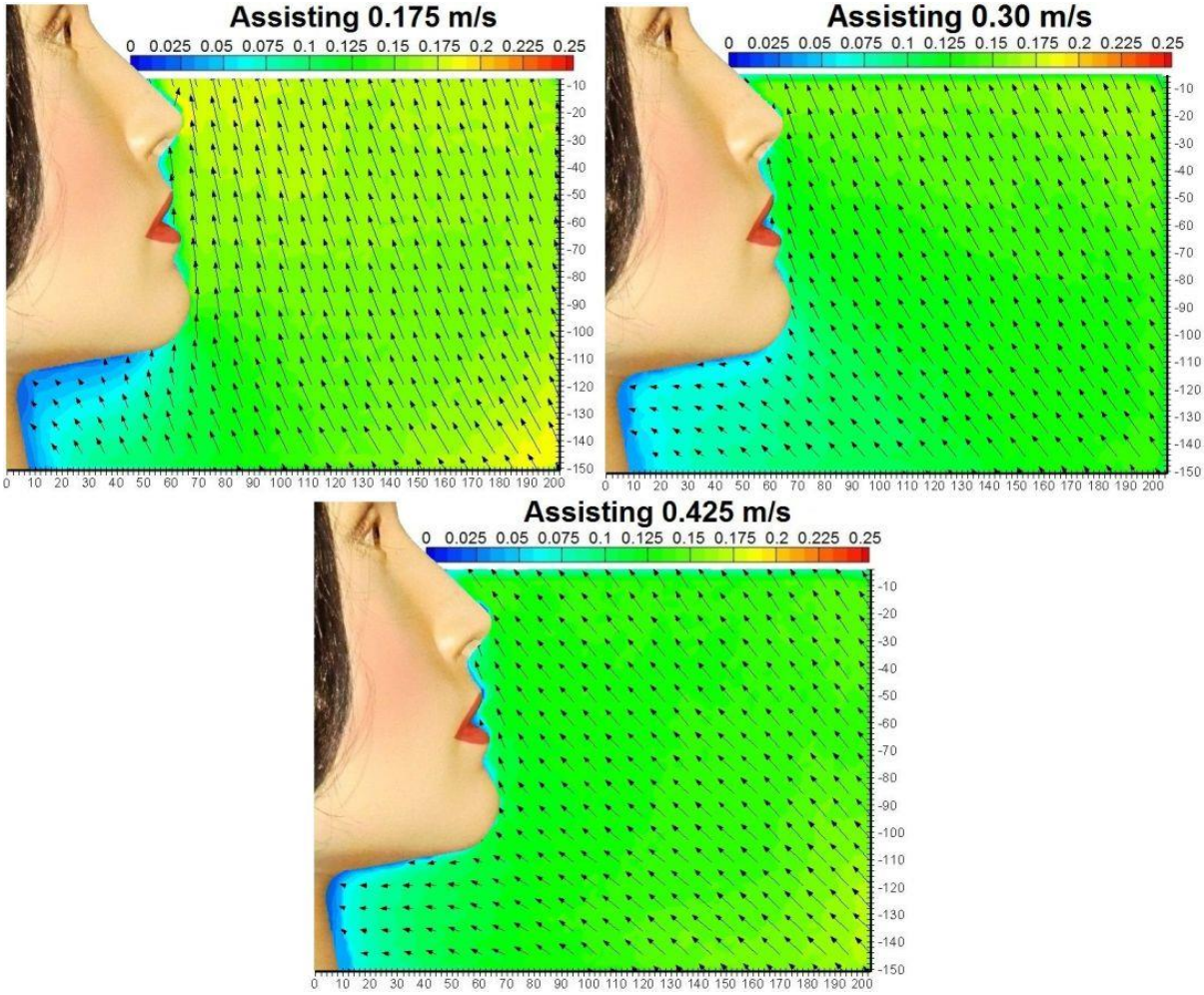

Figure 4.8 PIV of the CBL and its interaction with assisting flow from below – seated manikin.

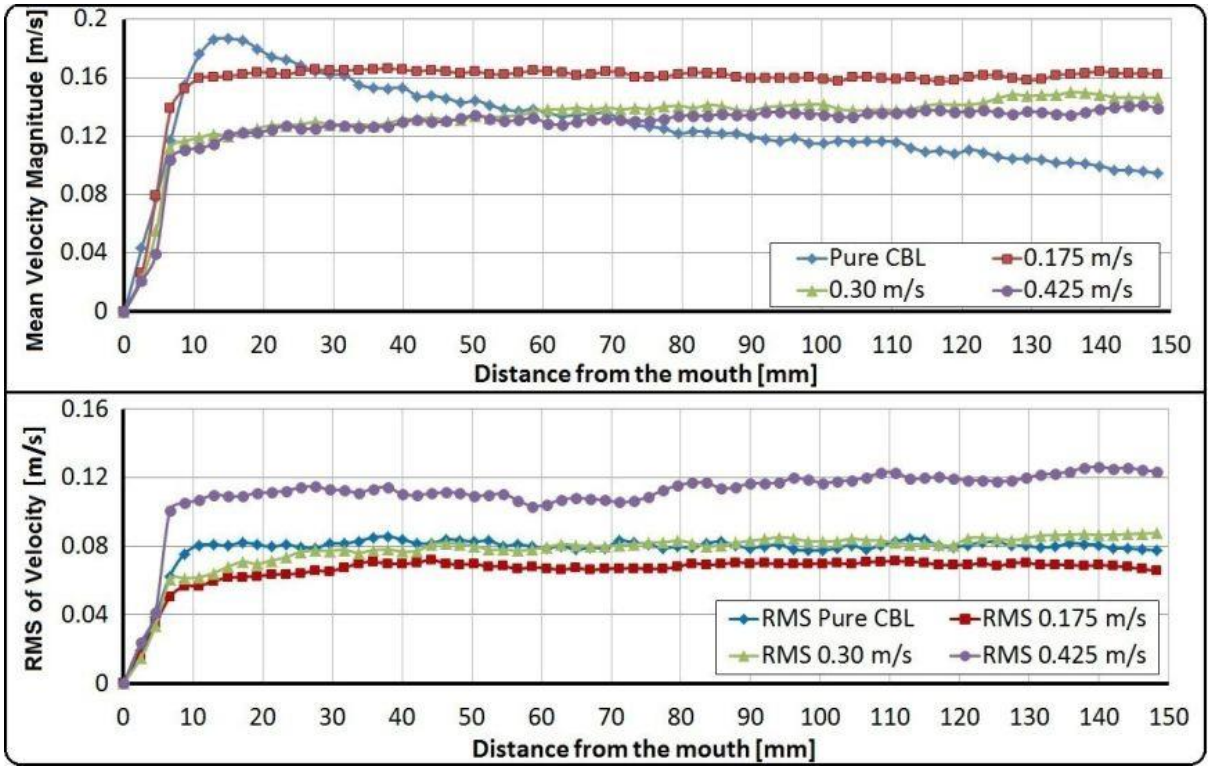

Figure 4.9 Mean velocity (top) and RMS of fluctuating velocities (bottom) in the mouth region of a seated manikin: Impact of assisting flow from below.

To understand the effect of velocity reduction in the breathing zone due to velocity increase of the assisting flow, additional PIV experiments were performed. The target measurement area was positioned in the chest and abdominal zone of the manikin, as indicated in Figure 4.1 (right). Due to the space limitation, the results in Figure 4.10 show only the velocity contours in case of assisting flow at 0.175 m/s and 0.425 m/s; however, scenarios of the pure CBL and assisting flow at 0.30 m/s are also discussed. Thermal manikin placed in a quiescent environment induced an upward air movement of approximately 0.10 m/s in the abdominal region that steadily accelerated towards the chest (not shown). As seen in Figure 4.10, adding the assisting flow at 0.175 m/s created an area of low velocities at 0.03 m/s in abdominal region. Further in front of the abdomen, at the distance that precisely matched the horizontal edge of the chair (X= 160 mm), there was a strong upward movement that corresponds to the flow induced by the airflow generator. After passing the edge of the chair, this flow did not separate

much from the chair and maintained a confluent character with respect to the rising CBL flow, as shown in the chest region. The confluent character between the CBL and mutually assisting flow at 0.175 m/s clearly explains the velocity increase in the breathing zone.

After its collision with the chair, the assisting flow at 0.425 m/s separated from the edge of the chair, forming a large vortex in front of the chest with a downward airstream in the abdominal region, as shown in Figure 4.10 (right). From the fluid dynamics view point, this problem is typical for bluff body flow where the passing flow experiences frictional and pressure drag force. In this case, pressure drag was predominant and related to the cross-section of the chair and flow separation. As the upward velocity from the airflow generator increased, Reynolds number increased and consequently, the pressure gradient on the bottom side of the chair increased in magnitude. Once the adverse pressure gradient became sufficiently strong, it produced separation of the flow. This separation from the edge of the chair increased the size of a wake, which explains the existence of a large vortex in the chest region. This vortex was responsible for change of the airflow direction in the breathing zone resulting in vectors 45˚ inclined towards the face. A similar effect was observed in case of assisting flow at 0.30 m/s, where the only difference was the size and location of the vortex. The vortex was smaller and shifted closer to the body due to the lower velocity from the airflow generator and respective pressure drag. Four additional videos that describe interaction between the human CBL and upward flow at three velocities are enclosed with this thesis (see Compact Disk, Videos 4.5 – 4.8).

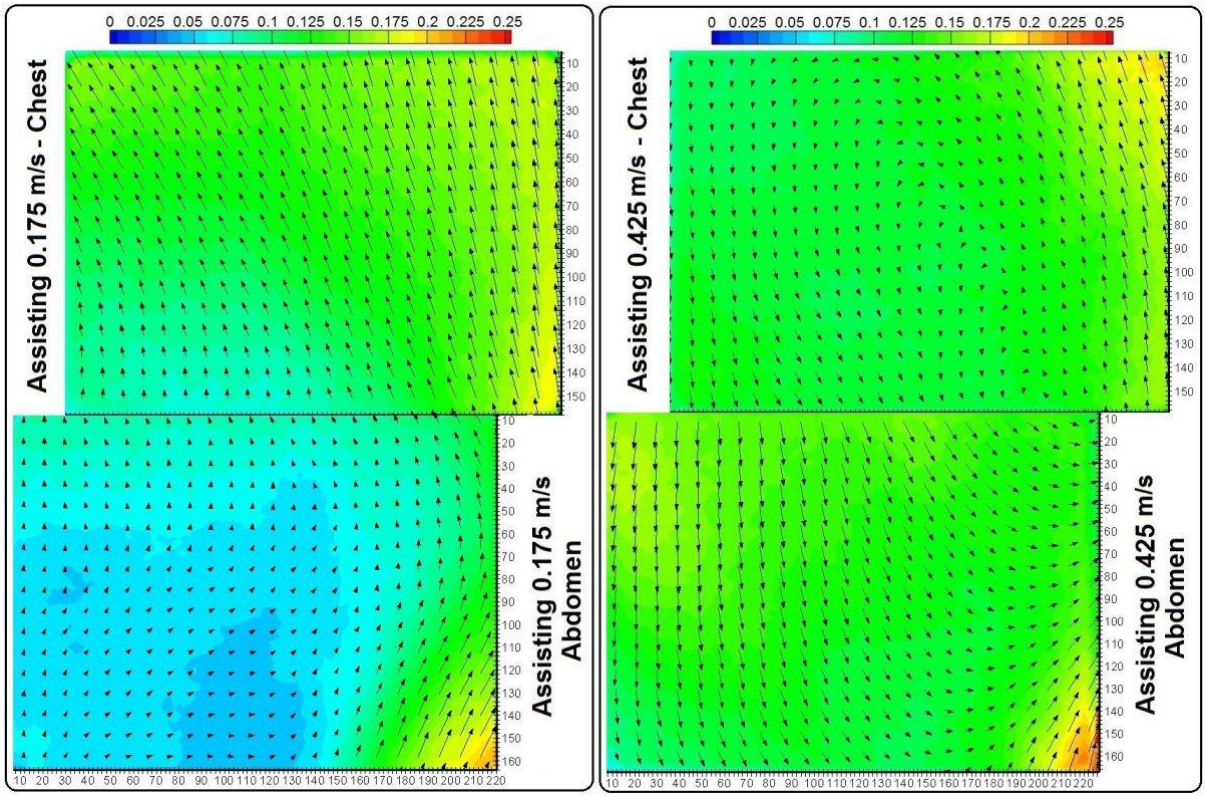

Figure 4.10 PIV of the CBL and its interaction with assisting flow from below at 0.175 m/s (left) and 0.425 m/s (right) – chest (top) and abdominal (bottom) region in front of the seated manikin.

4.3.4 Interaction with assisting flow from below - standing manikin

Findings that velocity increase of the assisting flow decreases the velocity in the breathing zone led to further investigations that involve a standing body posture. Figure 4.11 shows the mean velocity contours in front of the standing manikin under its interaction with the assisting flow from the airflow generator. Unlike the sitting posture where the chair created a blocking effect to the rising flow from the airflow generator, a standing manikin created no obstruction for the assisting flow. Consequently, the higher velocity of the assisting flow generated higher velocities in the breathing zone of the manikin. In the case of a pure CBL, after peaking at 0.165 m/s the velocity profile steadily decreased to 0.125 m/s at 130 mm horizontal distance from the mouth (Figure 4.12, top). Assisting flow at 0.175 m/s created the same velocity pattern in a higher magnitude range, peaking at 0.245 m/s and continually decreasing down to 0.21

m/s. Relative turbulence intensity along the horizontal distance from the mouth substantially dropped when assisting flow at 0.175 m/s was applied, from 55% down to 30% (Figure 4.12, bottom). Assisting flow at velocities of 0.30 m/s and 0.425 m/s created a lower turbulence intensity of about 30% and the velocity profile that gradually increased with the horizontal distance from the mouth, reaching 0.32 m/s and 0.38 m/s at 100 mm distance, respectively.

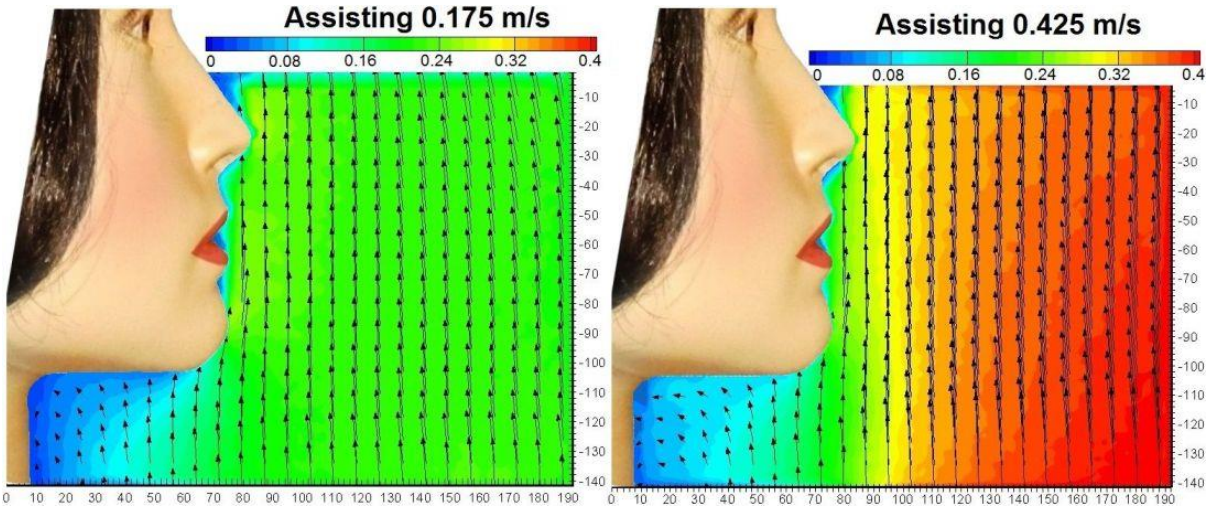

Figure 4.11 PIV of the CBL and its interaction with assisting flow from below – standing manikin.

A comparison of the velocities in the breathing zone when the thermal manikin was standing and sitting in a quiescent environment (Figure 4.9 and 4.12), confirms the previous findings that the sitting posture generates a higher peak velocity (Chapter 3). Moving the manikin from seated to standing posture reduced the peak velocity from 0.185 to 0.165 m/s (by 11%). This is probably because of the chin of a seated manikin that plays lesser role in blocking the rising CBL from beneath, as well as due to the additional flow stream that detaches from the tights and lower legs that accelerate the convection flow induced by the front part of the torso. Nevertheless, at 10 cm horizontal distance from the mouth, standing manikin generated higher velocity of 0.125 m/s compared to 0.105 m/s for the sitting posture, which suggest a milder velocity decay profile in the case of a standing manikin.

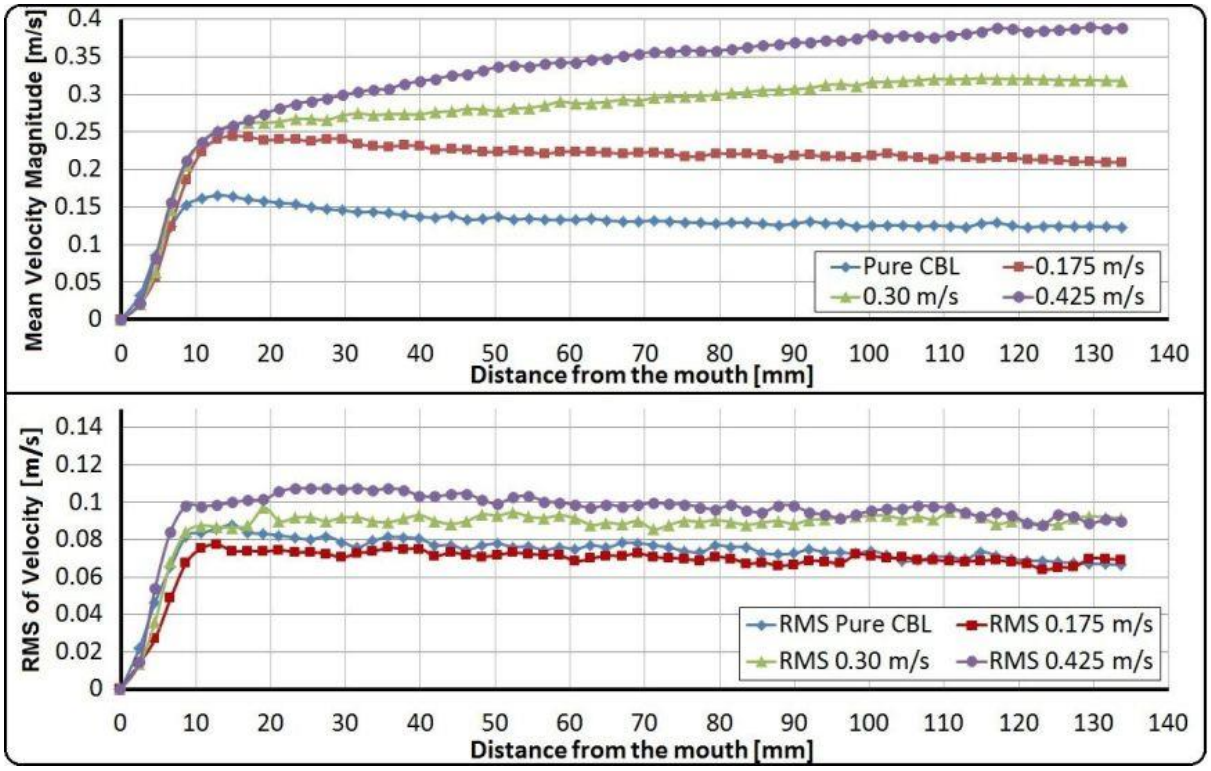

Figure 4.12 Mean velocity (top) and RMS of fluctuating velocities (bottom) in the mouth region of a standing manikin: Impact of assisting flow from below.

4.4 Discussion

This part of the study is designed to enhance understanding of the convection flow enveloping the human body and its interaction with mutually opposing, transverse and assisting airflow. The results are discussed with respect to personal exposure to ambient pollutants, thermal comfort and optimal ventilation design.

Ventilation with a vertically downward air distribution is recommended as an efficient pollutant removal strategy that reduces the risk of airborne cross-infection (ASHRAE, 2013b; CDC, 2003). In this approach, however, a uniform downward airflow generated by the ceiling mounted air terminal devices is disturbed in the regions above the heat sources that intensify the air mixing (Nielsen et al. 2007). Our results show that the downward uniform flow at the velocity of 0.30 m/s penetrates the human thermal plume to the breathing zone causing

intensive air mixing resulting in a high degree of turbulence intensity up to 110%. This is well above the turbulence intensity of 27% recorded when the plume was offset by downward flow at a velocity of 0.425 m/s, which highlights the importance of the velocity magnitude of the ventilation flow and airflow interaction in general. Other examples of flow opposing the CBL are downward diffuse ventilation, downward flow induced by the ceiling mounted personalized ventilation or ceiling mounted fan that is commonly found in residential and other non-conditioned spaces. The level of penetration to the breathing zone depends on characteristics and interaction of the downward flow and the thermal plume. Our finding that downward flow of 0.175 m/s does not affect the CBL is different from widely adopted assumption that invading flow of 0.1 m/s starts to disturb the CBL. In terms of optimal ventilation design that is aimed to deliver conditioned outdoor air to the occupant's inhalation zone without draught discomfort, downward flow approach may have several issues. The downward flow confronts the upward thermal plume and hence, a higher momentum is necessary to reach the breathing zone, compared to assisting and transverse flow scenarios. Concerning the ability of the CBL to entrain and transport potentially infectious pollutants from the lower room level to the breathing zone, the magnitude of the opposing flow can have different implications on the human exposure. Downward flow at 0.425 m/s peels of the CBL in the breathing zone and protects from pollution located in the middle or lower room level, or in the case that an occupant is a pollution source itself. In this case, however, special attention must be paid to avoid thermal discomfort, especially due to draught at the head, as the velocity of 0.425 m/s exceeds the comfortable velocity range recommended by the standard (ISO 7730, 2005). Increased velocity also poses an additional energy penalty. At 0.30 m/s, downward flow reduces the draught risk but collides with the CBL close to the head which may easily increase particle dwell time in the same region and thus increase the exposure to such particles. Opposing flow at 0.175 m/s has a negligible impact on the CBL; thus the pollution at the floor level near the human body

may end up in the breathing zone unobstructed. Our finding that a complete destruction of the thermal plume occurs at a downward velocity of 0.425 m/s differs from the one found by Yang et al. (2009). They reported that the downward personalized airflow supplied from ceiling mounted nozzle destroys the plume at an airflow above 16 l/s, which corresponds to the velocity of 0.8 m/s in the target area. This discrepancy may be due to the difference in the cross-section area of the local invading flow (diameter 0.35 - 0.5 m) and in our case, a cross-sectional area generated by the airflow generator (1.8 m^2). Comparison of these two studies emphasizes that the CBL may interact differently with global airflow patterns in the occupied spaces and locally supplied airflows.

Occupants exposed to traversing flows can be commonly found in practice, e.g. desktop fan, personalized ventilation, stratum ventilation, etc. In contrast to opposing flow, transverse flow penetrates the CBL at the breathing zone at a relatively low velocity of 0.175 m/s. This finding can be useful for an optimal design of personalized ventilation system, because transverse flow from front can deliver fresh air to the breathing zone within comfortable velocity limits and with lower energy penalty, compared to the opposing flow scenario. The ability of transverse flow to penetrate to the breathing zone at a lower flow rate can also be important from the protective point of view against ambient pollutants entrained by the CBL or those shed from the clothing and skin. The latter ones apply to products of chemical reactions of bio-effluents from the body. In this case, invading transverse flow from the front easily pushes the rising pollution towards the side of the body and prevents them from reaching the breathing zone. In this case, special attention must be paid to reduce cross-infection risk since the pollutants from the occupant, including the potentially infected exhaled air if he/she is sick, may be discharged towards the other occupants. One way is to combine supply with personalized exhaust that could serve as a source control and mitigate fraction of pollution from the infected occupant that is inhaled by other occupants (Melikov and Dzhartov, 2013; Yang et al. 2013). Occupants

exposed to a uniform transverse flow from the front are likely have to a higher draught discomfort level compared to opposing flow at equal flow rate, as there is no need to offset the thermal plume, but also improved perceived air quality (Melikov and Kaczmarczyk, 2012).

Occupants exposed to an upward air movement create another commonly encountered airflow interaction in an indoor environment. Typical examples are occupants exposed to an upward flow generated by displacement or under-floor air distribution, as well as upward piston flow from the perforated floor customary met in clean rooms. The results of this study reveal the importance of furniture arrangement that augment the complexity of interaction between the CBL and mutually assisting flow. The blocking effect of the chair creates a vortex in abdominal and chest region and completely alters the airflow patterns around the seated manikin at the velocities above 0.175 m/s. In another study it was found that presence of the table in front of an occupant can reduce the peak velocity in front of the mouth by 45% (Chapter 3). On the other hand, increasing the airflow of assisting flow supplied vertically upwards from the table to 10 l/s increased the velocity in the breathing zone up to 0.34 m/s, since there were no obstacles encountered (Bolashikov et al. 2011b). These findings clearly imply that the chair, the table and other furniture play an important role in formation of airflow patterns around the human body and should be carefully considered in numerical predictions and optimal ventilation design. More research is needed on the topic of different furniture design and arrangement in order to achieve a desired air distribution around the human body. Airflow patterns in front of the manikin placed in a uniform upward airstream substantially differ between sitting and standing body postures. The upward airflow induced by the airflow generator and the CBL of a standing manikin are mutually confluent and do not cause substantial air mixing. On the other hand, downward air distribution within the comfortable velocity range is disturbed by the manikin's plume which makes it difficult to create a uniform downward air distribution due to high mixing of air and high turbulence intensity levels.

Increased turbulence intensity of the flow adjacent to the human body may cause an increase of the heat transfer from the body (Melikov and Zhou, 1996). These findings show that the body posture and its orientation relative to the airflow direction are important for airflow distribution in the microenvironment around the human body. Considering the pollution from the floor that is brought up to the breathing zone via the CBL, adding the clean assisting flow would probably reduce the exposure in both the cases of standing and seated manikin, due to a dilution effect. The same apply for the other pollutants generated close to the occupant such as bio-effluents from the body or formaldehyde from the table that are expected to be diluted by the upward uniform flow and reduce the exposure. Pollutants located at some distance from the body would be transported to the upper room level where they can be exhausted. The impact of the critical distance at which the pollution would not be transported to the breathing zone needs to be studied in the future.

Although briefly discussed, this part of the study does not show the results of how interaction between the CBL and mutually opposing, transverse and assisting flow affects personal exposure to surrounding pollutants. These personal exposure results are investigated and discussed in Chapter 6. It should be noted that the practical implications of this study are valid at a surrounding air temperature of 23 ˚C and may be different at higher or lower temperatures. The effects of other air movements, such as created by other occupants or heat sources, have also not been studied. In addition, room geometry such as increasing the ceiling height modifies the CBL. This part of the study does not consider a human respiratory airflow. Future research and design trends are expected to go through the paradigm shift from the coarse total volume description and design to the description and design that consider the airflow distribution in the microclimate around the occupants and its impact on personal exposure. This shows the necessity for a thoughtful understanding of the airflow physics enveloping the human body and its interaction with airflows generated by the air delivery systems.

4.5 Conclusions

The PIV, complemented with PCV technique was employed to investigate the resultant velocity vectors generated by the complex interaction between the CBL around human body and mutually opposing, transverse and assisting flows. The results reveal the following:

- The airflow interaction in occupied spaces depends on the direction and the magnitude of the ventilation flow and should be carefully considered in order to reduce personal exposure to ambient pollutants and thermal discomfort and achieve optimal ventilation design;
- Under the conditions studied, the downward flow at the velocity of 0.175 m/s was unable to modify airflow patterns in the breathing zone, which was very different from assisting flow that alters the CBL at the same velocity. Increasing the velocity of downward flow to 0.30 m/s reduced the peak velocity in the breathing zone from 0.185 m/s to 0.10 m/s, while downward flow of 0.425 m/s destroyed the thermal plume;
- In the case of transverse flow supplied from the front, the CBL was strongly disturbed already at the velocity of 0.175 m/s;
- The CBL of a standing manikin exposed to the uniform upward airflow did not cause extensive mixing of flow patterns, such as in case of opposing flow from above that was disturbed by the occupant's thermal plume. A higher velocity of the assisting flow increased the velocity in front of the standing manikin. In case of the seating manikin, however, increasing the upward velocity above 0.175 m/s reduced the peak velocity in the breathing zone and changed the flow direction, attributable to the blocking effect of the chair; and
- These findings imply that furniture plays an important role in formation of airflow patterns and should be carefully considered in numerical predictions and for an optimal ventilation design.

CHAPTER 5: GASEOUS CONCENTRATION FIELD OF THE HUMAN CBL IN A QUIESCENT INDOOR ENVIRONMENT

5.1 Specific objectives

The previous studies on pollution transport around the human body focused on a single point measurement. These are not sufficient to understand the pollution transport phenomena within the CBL and pollutant distribution in the breathing zone. In addition, influence of factors such as location of the pollution source, room air temperature, table positioning and seated body inclination on the pollutant distribution in the breathing zone is unknown. The first specific objective of the part of the study is to determine pollutant distribution in the breathing zone as a function of the source location in quiescent indoor environment. The second specific objective is to quantify the same effects as a function of: i) room air temperature; ii) table positioning, and iii) seated body inclination angle. The findings of this part of the study will contribute to understanding of the pollution distribution in the breathing zone of a person and are useful for better control of personal exposure.

5.2 Research methodology

5.2.1 Experimental facility

The measurements were conducted in a climate chamber at the Technical University of Denmark with dimensions 4.7 x 6.0 x 2.5 m^3. The chamber was well insulated and the vinyl sheets covered the inner walls. The chamber was continuously ventilated with a low velocity

upward piston flow (100% outdoor conditioned air) that was supplied through the floor at constant temperature and exhausted through the perforated area of the ceiling. The floor was built of a porous sheet with a steel floor grating placed on the top. Most of the air (85%) was supplied vertically upwards through the whole area of the floor, while the remaining air was introduced through the space between the wall and the vinyl sheets. This kind of construction ensured that the room air temperature is equal to the mean radiant temperature and the absence of radiant temperature asymmetry. In addition, a low vertical thermal stratification (<0.1 K/m) was measured during the experiments at numerous locations across the chamber. The air temperature measured at the floor supply was always equal to the supply air temperature monitored by the air handling unit control system. The supply air temperature and velocity were stable during the experiments and did not fluctuate with time.

5.2.2 Experimental equipment

A calibrated non-breathing and non-sweating thermal manikin (P.T. Teknik Limited, Denmark) with a complex female body shape of 1.23 m height in the sitting posture was used to thermally simulate a realistic human body. The manikin was positioned in the center of the chamber and it was dressed in the tight-fitting summer attire (t-shirt, trousers, underwear, socks and shoes) with is equivalent to clo value 0.7. The manikin's body consisted of 17 independently heated and controlled body parts with the surface temperature close to that of an average human body in a state of thermal comfort under a given clothing insulation and thermal environment. The manikin heat output at 23 ˚C room air temperature was 65 W/m^2, which is equal to the dry heat loss from a human body in a thermally comfortable state. The air introduced to the room was supplied at such a low velocity so as to minimally disturb the natural convection around the thermal manikin. In addition, a horizontal plate (2.0 x 1.54 m^2) was placed below the manikin in a way shown in Figure 5.1 (left) to prevent the supply airflow

from affecting the natural convection induced by the thermal manikin (CBL). In this way, the air movement in the vicinity of the manikin was induced solely due to the manikin's body heat. The velocity measured with omnidirectional thermal anemometers (SENSOR, ±0.02 m/s accuracy) at numerous locations around the unheated manikin was below 0.05 m/s, which indicated that quiescent indoor conditions had been achieved, as suggested by Murakami et al. (2000). For sampling of the pollution source, two calibrated Innova multi-gas samplers (Model 1303) and analyzers (Model 1312) were used, which were placed outside the chamber. In addition, the Pseudo Color Visualization (PCV) technique was employed to better understand how the CBL interacted with the surface of the table. More details about this technique can be found in Chapter 3.

5.2.3 Experimental design

The air was exhausted from the chamber through the reduced free flow area of the ceiling (2.4 x 2.4 m^2) located directly above the manikin. This was done to ensure that the rising thermal plume of the manikin would not spread across the chamber causing additional air circulation, but to be directly exhausted above. During the experiments the thermal manikin was the only heat source present in the chamber. A minimal vertical thermal stratification of < 0.1 K/m was recorded during the experiments.

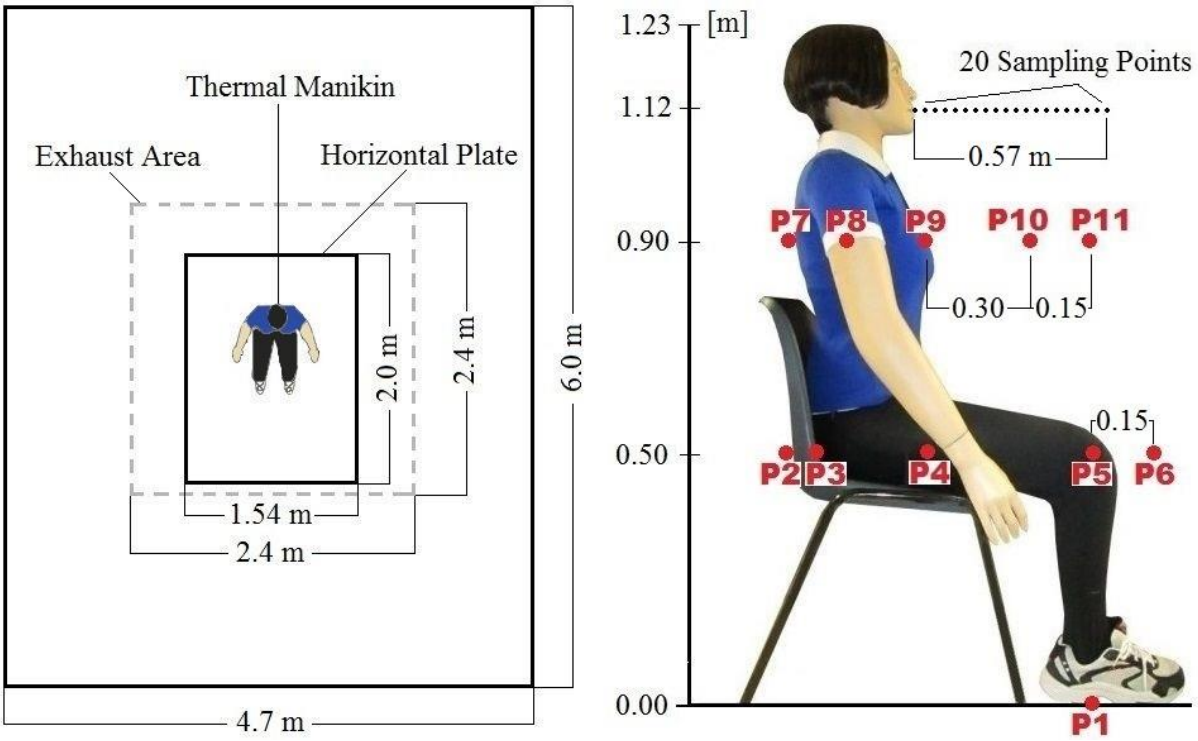

Figure 5.1 Top projection of the climate chamber (left) and pollution dosing/sampling locations (right).

Two sets of experiments were conducted as follows:

- Set 1: The first set of experiments aimed to examine the impact of the source location on the pollutant distribution in the breathing zone. The gaseous pollution was supplied isothermally with negligible initial velocity at eleven different locations around the manikin, as shown in Figure 5.1 (right). Each pollution source was aligned with the vertical plane of symmetry of the manikin, except P8 that was located in the armpits. Seven locations were chosen to simulate pollution emitted from the occupant's body, e.g. human bioeffluents (P1, P3, P4, P5, P7, P8, P9), while the remaining four locations resembled the pollution released in occupant's proximity, e.g. emissions from indoor surfaces and other airborne pollutants (P2, P6, P10, P11). The room air was kept at a constant temperature of 23 ˚C.

- Set 2: The second set of experiments aimed to examine the influence of room air temperature (20, 23 and 26 ºC), table positioning and seated body inclination angle on the pollutant distribution in the breathing zone. The influence of the table positioning was examined when the abdomen of the seated manikin was located at horizontal distances of 0 and 10 cm from the front edge of the table, in the same way described in Chapter 3 (Figure 3.4). The influence of a seated body inclination angle was examined when the manikin was leaned 25˚ forward and backwards. In each case of Set 2 experiments, the pollution was located at the chest and groins only. A summary of both sets of experiments is enclosed in the Table 5.1.

A pollution source was simulated by tracer gas Nitrous oxide (N_2O) that was injected through a sponge ball (diameter 0.05 m) at a steady emission rate. The N_2O is approximately 1.5 times heavier than the room air which may introduce uncertainty in studies with minimized air movement. In our study, the resulting density difference was considered negligible when the pollution source was located within the CBL. When released in the region of still air (e.g. P2), the effect of density difference on personal exposure presumably increased but was still considered reasonably small. The tracer gas was successively sampled in the breathing zone at 20 locations along the horizontal line in front of the mouth, with a distance between two consecutive points of 0.03 m (Figure 5.1, right). The first sampling point was located at the upper lip of the manikin (Melikov and Kaczmarczyk (2007) at 0 mm distance from the surface, to represent the sampling of inhaled air. The tracer gas was sampled through the sampling tubes and sent to two Innova multi-gas samplers (Model 1303) and analyzers (Model 1312) placed outside the chamber. The successive sampling from two instruments indicated that the tracer gas was sampled at two locations at the time, before sampling through another two neighboring sampling tubes. This assured a small flow rate (130 ml/min) through the sampling tubes and minimal impact of the CBL flow. Total sampling time took three hours, which corresponded

to 45 samples of gas in each point, and the results were averaged. It was found that 45 samples was a representative number above which the variation in the concentration became negligible (< 5%). A low level of N_2O was found in the supply air due to leakage in ducts that was subsequently deducted from the results to minimize measurement inaccuracy.

Table 5.1 Transport of the pollution around a thermal manikin - Summary of the two sets of experiments

	Parameter	Case	Details
Set 1	Pollution source location	Skin/clothing surface	P1, P3, P4, P5, P7, P8, P9
		Surroundings	P2, P6, P10, P11
Set 2 *	Room air temperature	20 ºC 23 ºC 26 ºC	
	Table positioning	No table Table 10 cm Table 0 cm	Table dimensions 1 x 0.6 x 0.75 m (W x L x H)
	Seated body inclination	Upright Leaned forward Leaned backwards	 25 º from the vertical axis 25 º from the vertical axis

* Pollution released from the chest and the groins.

5.2.4 Data analysis

As a measure of the pollution spread within the CBL, a new term was introduced named human body pollution boundary layer (PBL). The thickness of the PBL was defined to determine the extent to which the pollution spreads horizontally from the mouth. It was assumed that the thickness of the PBL extended to a distance where the concentration of the tracer gas reached 10% of the maximum sampled concentration along the horizontal line in front of the mouth. In addition, the cumulative concentration of the pollution was determined based on the amount of tracer gas transported to horizontal measurement locations in the breathing zone (Figure 5.1, right). The cumulative concentration was calculated by the total area below the concentration curve along the horizontal line in front of the mouth.

5.3 Results

The experimental results demonstrate a relationship between pollutant distribution in the breathing zone and: (i) the source location; (ii) room air temperature, table positioning, and body inclination angle.

5.3.1 Impact of the source location

Figure 5.2 shows the results of an average tracer gas concentration distribution in the breathing zone of the thermal manikin for different pollution source locations. These results are also presented in a tabular form (Table 5.2), up to a distance of 450 mm from the mouth. Overall, the large amount of the pollution was transported towards the breathing zone by means of the manikin's CBL. As seen, the pollutant concentration in the breathing zone of the manikin varied with the source location. The pollution concentration close to the mouth (<100 mm) was always higher than the concentration further from it, regardless of the source location. This suggests that the CBL has a strong entrainment ability and the ability to transport the pollution to the mouth not only in the vertical, but also in the horizontal direction. The concentration decay profile was more prominent when the pollution was located at the surface of the body, compared to pollutants emitted further away, which showed milder concentration gradients. The high concentration gradients close to the surface formed because the body heat attracted the pollution towards the manikin, as similarly found by Salmanzadeh et al. (2012).

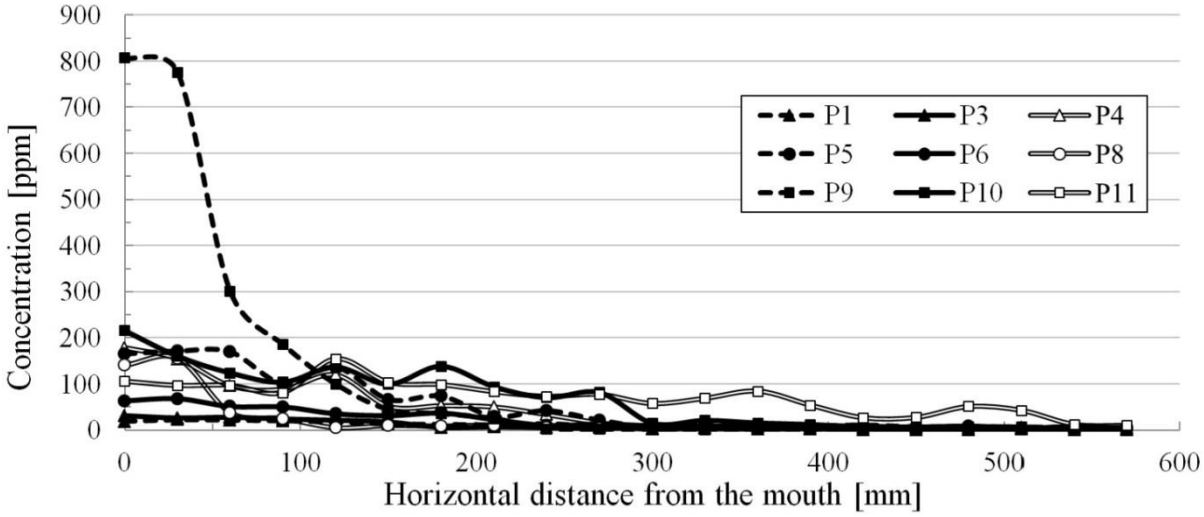

Figure 5.2 Concentration of tracer gas in the breathing zone - Impact of the source location.

Table 5.2 Concentration of tracer gas [ppm] in the breathing zone for different source locations

	Horizontal distance from the mouth [mm]															
	0	30	60	90	120	150	180	210	240	270	300	330	360	390	420	450
P1	19	22	22	20	18	13	13	11	14	9	10	11	7	8	11	7
P3	31	26	28	24	21	18	6	7	6	6	2	3	2	3	1	2
P4	179	155	96	88	120	52	53	50	34	16	5	6	8	4	5	5
P5	165	171	170	101	136	67	74	30	42	21	6	9	7	4	2	2
P6	63	68	51	50	35	31	37	23	10	13	9	8	7	9	8	7
P8	141	156	38	25	5	10	9	11	5	4	4	3	4	3	4	3
P9	807	776	301	186	100	45	36	25	3	2	2	1	1	0	2	2
P10	216	160	124	104	136	99	138	94	70	81	15	21	15	12	7	6
P11	106	97	97	81	155	104	99	83	73	77	58	69	85	54	27	28

Among all source locations, the highest breathing zone concentration was achieved with the source located at the chest (P9), peaking at 807 ppm at zero distance from the mouth. Moving the pollution source 0.3 and 0.45 m away from the chest (P10 and P11) reduced the pollution concentration at the mouth by 73.5% and 87%, respectively. This substantial reduction is attributed to the increased distance between the source and the mouth, as well as to a weaker CBL further from the heated body surface (Chapter 3) that intensifies mixing, i.e. dilution of the pollution. When the pollution was released at the upper back (P7) or behind the chair (P2), the concentration in the breathing zone was equal to zero (not shown). Additional measurements at different locations in the room showed that the pollution released behind the

chair (P2) spread across the room, while the pollution released at the upper back (P7) moved up along the back joining the thermal plume. The majority of the pollution located at the lower back (P3) was transported upwards along the back; however, a small portion ended up in the breathing zone, which was 96% lower than in case of the chest release (P9). This occurred because the rising pollution from the lower back had more time to mix within the CBL and part of it could reach the front side of the manikin. A similar amount of the pollution was transported to the breathing zone when the pollution was released at the feet (P1). When located close to the knees (P6), some pollution was entrained by the CBL, which is relatively thin at the height of the knees as shown in Chapter 3 and by Homma and Yakiyama (1988). As a result, a small amount of pollution was transported to the breathing zone. More substantial amount of the pollution released at the knees (P5) was transported to the breathing zone, which was approximately 2.6 times higher than when the source was located at P6. The breathing zone concentration of pollution released from the groins (P6) was equal to that from the knees (P4). Three additional videos that show visualization of the pollution emitted from the chest (Video 5.1), knees (Video 5.2) and groins (Video 5.3) are enclosed as supplementary information (see Compact Disk).

Figure 5.3 shows the impact of the source location on normalized personal exposure (concentration at 0 mm distance from the mouth) and the thickness of the PBL in the breathing zone. Normalized personal exposure was calculated as the ratio of the concentration measured at the mouth divided by the concentration measured at the mouth when the pollution was located at the chest. The thickness of the PBL and personal exposure for the source locations P1, P2 and P7 were not determined because of their low concentration in the breathing zone. As seen, both the thickness of the PBL and personal exposure change with the source location. The smallest thickness of the PBL was when the pollution was released at the armpits (P8 – 107 mm) and chest (P9 – 130 mm). Increasing the distance between the manikin and the

pollution source at 0.9 m height (from P9 to P10, P11) and at 0.5 m height (from P4 to P5, P6) increased the thickness of the PBL. This was especially the case for the pollution released at 0.9 m height, where the thickness of the PBL for the source located at P11 increased 4.3 times compared to the source located at P9. When the source was located at the groins and knees, the thickness of the PBL was higher and personal exposure was lower, compared to the source emitted at the chest. The opposite effect was observed when the pollution originated from behind of the manikin as the pollution emitted at the lower back (P3) caused higher personal exposure then the one emitted at the upper back (P7). This result indicates the importance of the side of the body at which the pollution was released. The standard deviation of personal exposure was generally high, which suggests the unsteady nature of the CBL in the breathing zone. Overall, when the pollution was released from in front of the manikin, personal exposure was indirectly proportional to the thickness of the PBL, i.e. the increased thickness of the PBL was always followed by the reduction of personal exposure. Table 5.3 summarizes the percentage of personal exposure reductions in relation to the results obtained with source located at the chest (P9).

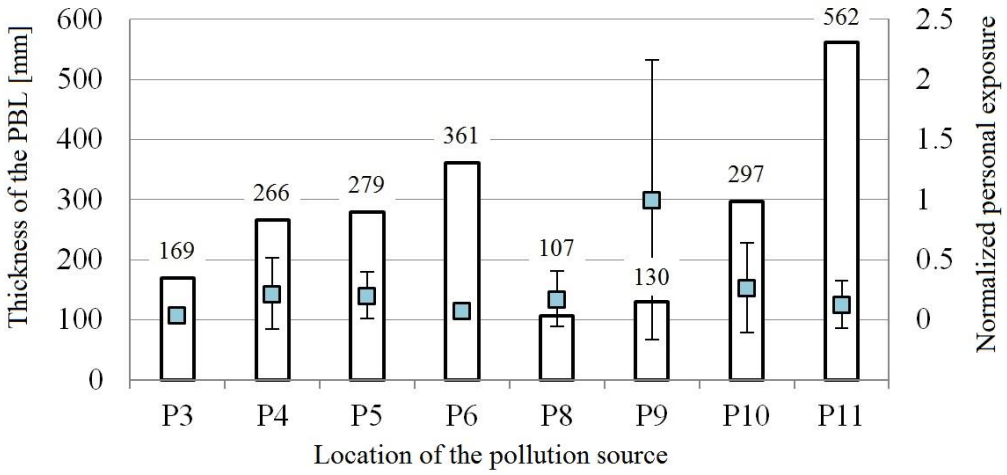

Figure 5.3 Normalized personal exposure and the thickness of the PBL - Impact of the source location.

Table 5.3 Personal exposure percentage reduction - Influence of the source location

Pollution location	P1	P2	P3	P4	P5	P6	P7	P8	**P9 ***	P10	P11
% reduction	97.5	99.5	96	78	79.5	92	100	82.5	0	73.5	87

* Refers to the reference case at the chest.

The results in Figure 5.4 show the cumulative pollution concentration in the breathing zone of the manikin and personal exposure for different source locations. With the exception of armpits (P8), the cumulative pollution concentration increased with the height from which the pollution was released. This is because the pollution released at the lower height had more time to diffuse within the CBL before it reached the breathing zone. This result shows the importance of the height at which the pollution was released. In case of armpits, a part of the pollution was transported behind the manikin, which reduced the cumulative pollution concentration in the breathing zone. The results also show that for a different source location, there is no direct correlation between the cumulative concentration and personal exposure. Although personal exposure decreased when the distance between the body and the source location increased, this was not the case with the cumulative pollution concentration.

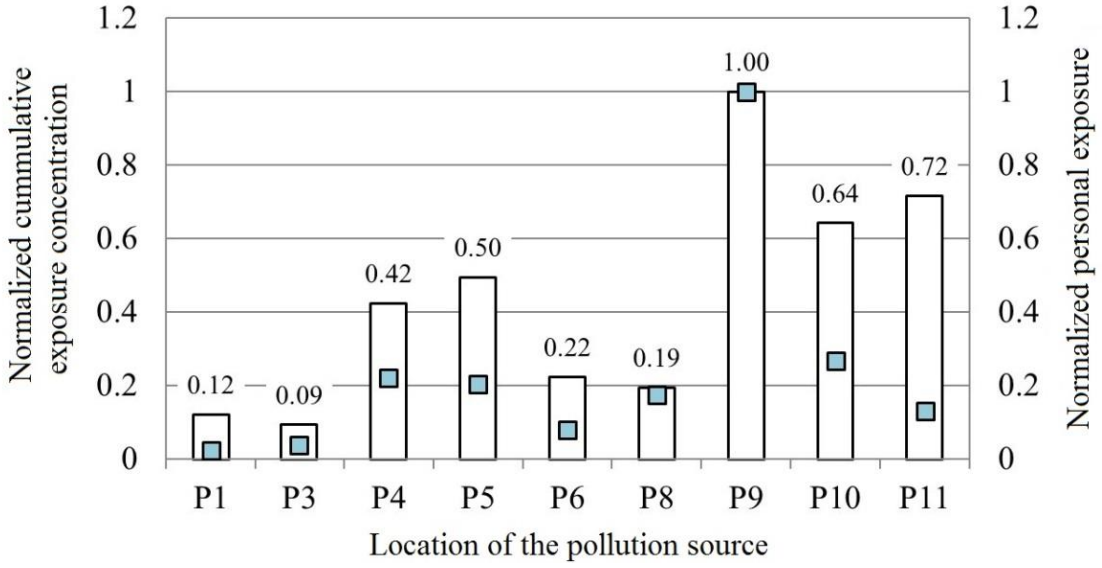

Figure 5.4 Normalized cumulative pollution concentration in the breathing zone and personal exposure - Impact of the source location.

5.3.2 Impact of the room air temperature

The impact of the room air temperature on the breathing zone concentrations when the pollution was located at the chest and groins is shown in Figure 5.5. For both source locations, reducing the room air temperature from 23 to 20 ˚C increased the pollutant concentration in the breathing zone. As the lower room air temperature strengthened the CBL and increased its velocity (Chapter 3), it also intensified the transport of the pollution to the breathing zone. The opposite effect can be seen when the room air temperature increased from 23 to 26 ˚C, as shown in Figure 5.5.

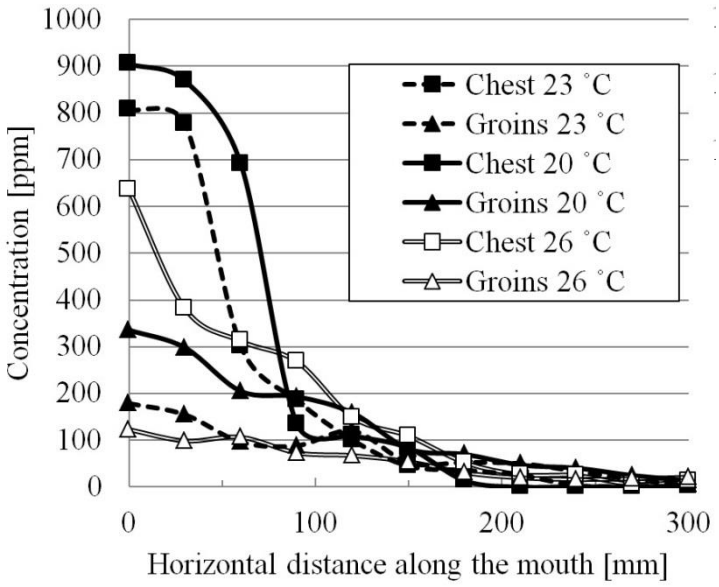

Figure 5.5 Concentration of tracer gas in the breathing zone - Impact of room air temperature.

Figure 5.6 shows the normalized personal exposure and the thickness of the PBL at three room air temperatures. As seen, the pollution emitted at the groins spread more compared to the pollution from the chest, for all three temperatures studied. Elevating the room air temperature from 23 to 26 ˚C increased the thickness of the PBL for both the source locations; however, it also reduced personal exposure. When the room air temperature was changed from 23 to 20 ˚C the opposite effect occurred, which suggests that there is an indirect correlation between the

thickness of the PBL and personal exposure under various room air temperatures. Furthermore, increasing the room air temperature from 20 to 26 ˚C reduced personal exposure by 30% for the pollution emitted from the chest. This can be correlated with the peak velocity decrease of 33% in the breathing zone, when the same temperature change was applied, as shown in Chapter 3. Table 5.4 summarizes the percentage of personal exposure change in relation to the source released at 23 ˚C.

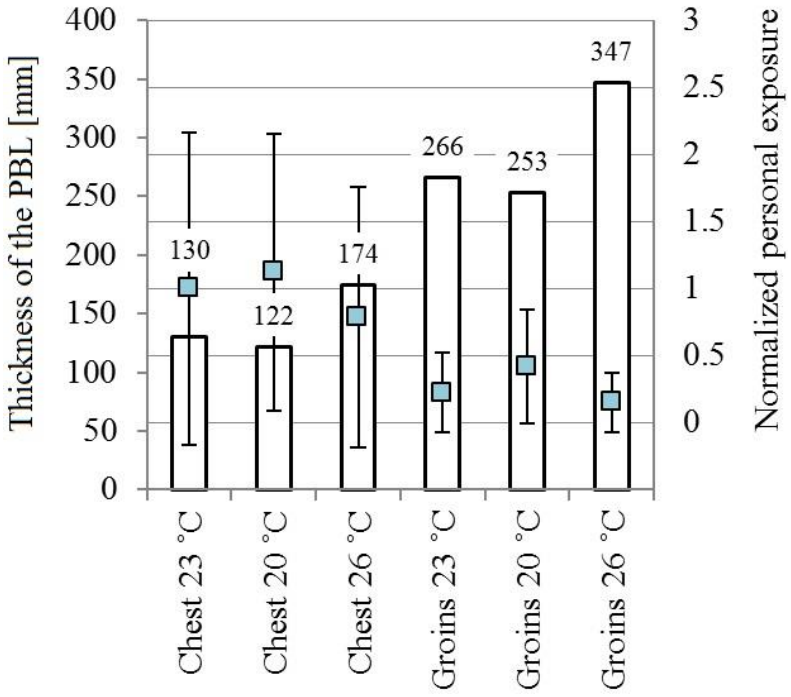

Figure 5.6 Normalized personal exposure and the thickness of the PBL - Impact of room air temperature.

Table 5.4 Personal exposure percentage change - Influence of room air temperature

	Chest			Groins		
Room air temperature	20 ºC	**23 ºC ***	26 ºC	20 ºC	**23 ºC ***	26 ºC
% change	+12	0	-21	+88	0	-31

* Refers to the reference case.

The results in Figure 5.7 show the cumulative pollution concentration in the breathing zone of the manikin and personal exposure for three room air temperatures. Analogously to personal exposure, increasing the room air temperature reduced the cumulative concentration for both source locations. The opposite effect occurred when the room air temperature increased,

suggesting a direct correlation between the cumulative concentration in the breathing zone and the room air temperature.

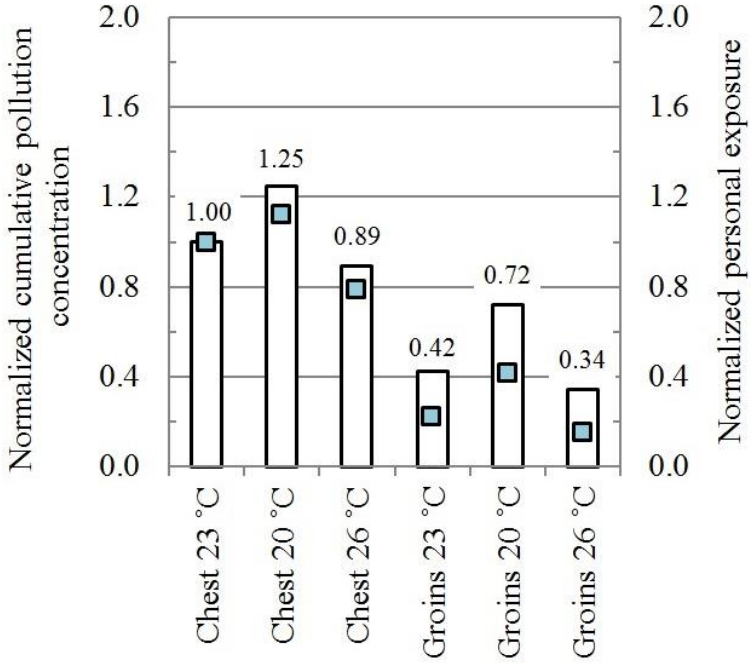

Figure 5.7 Normalized cumulative pollution concentration in the breathing zone and personal exposure - Impact of room air temperature.

5.3.3 Impact of the table positioning

The impact of the table positioning on the breathing zone concentrations when the pollution was located at the groins and chest is presented in Figure 5.8. It could be seen that the presence of the table substantially disturbed the transport of the pollution to the breathing zone. The table positioned at the distance of 10 cm from the manikin's abdomen increased the pollutant concentration at the mouth of the manikin. The concentration further away from the surface, however, dropped more compared to the case without the table. Closing the gap between the manikin's abdomen and the front edge of the table notably reduced the concentration of the pollutants released from the groins and chest.

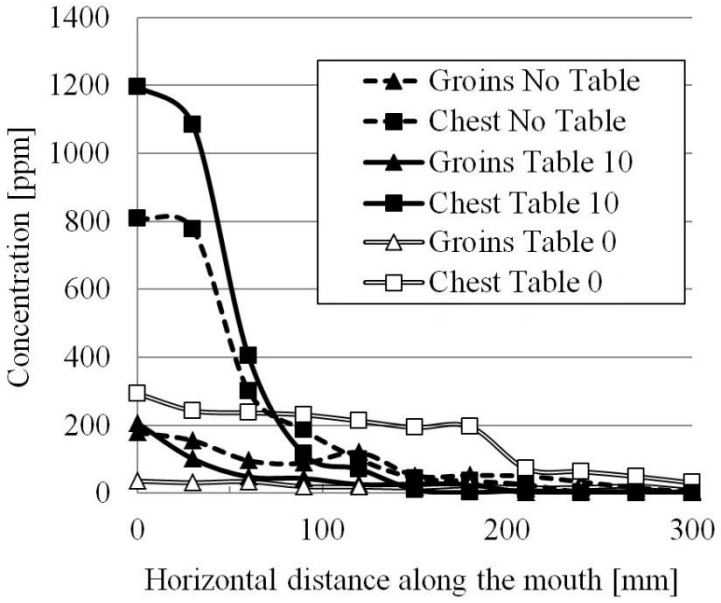

Figure 5.8 Concentration of tracer gas in the breathing zone – Impact of table positioning.

Figure 5.9 shows results of the thickness of the PBL and personal exposure, as a result of different table positioning. At 10 cm distance between the manikin and the front edge of the table, the thickness of the PBL was reduced by 31% in case of the chest and 30% in case of the groins, compared to the reference case (No Table). In the same case, personal exposure increased by 48% in case of the chest release and 15.5% in case of the groins release. Figure 5.10 presents the PCV visualization of the CBL flow when the table was present and not present, and when the seeding particles were released at the feet of the manikin. The CBL was naturally thinner due to the table presence, which also explains the reduced thickness of the PBL. While the pollution released at the groins and chest was less spread and the amount of the injected pollution was kept constant, the pollution in the breathing zone was more concentrated, which increased personal exposure. On the other hand, with zero distance between the manikin and the table, the peak velocity of the CBL dropped from 0.17 to 0.111 m/s, as shown in Chapter 3. This reduced personal exposure by 63.5% when the pollution was released at the chest, compared to the case with no table. In addition, the personal exposure dropped by 80% in case pollution generated at the groins (see Table 5.5) because most of the

pollution was physically prevented from reaching the breathing zone (see Figure 5.10). When there was no gap between the table and the manikin, the thickness of the PBL was very high for both source locations, as shown in Figure 5.9. This probably occurred because of the low velocity of the CBL that diffused and spread the pollution extensively in front of the manikin. Nevertheless, the results of the PBL thickness in this case should be carefully interpreted because of the low cumulative concentration, as shown in Figure 5.11.

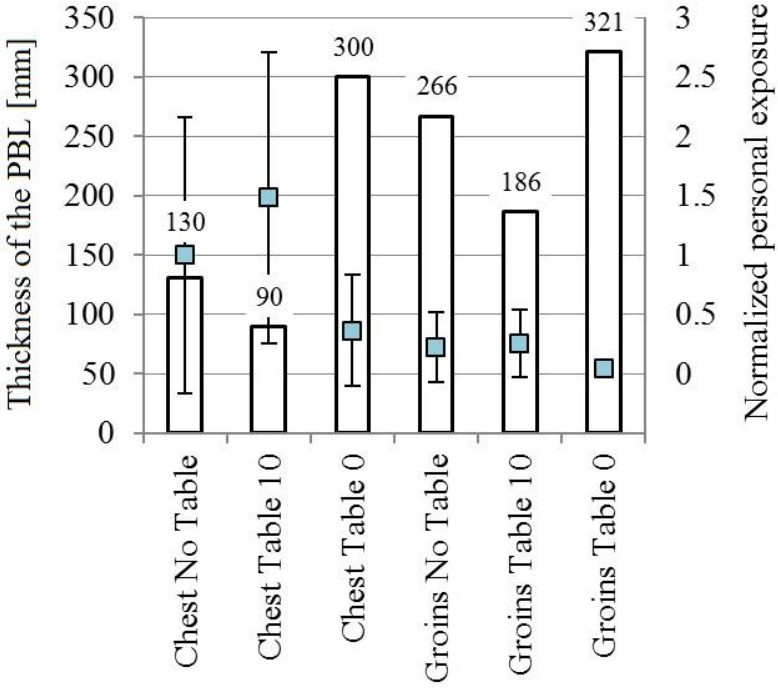

Figure 5.9 Normalized personal exposure and the thickness of the PBL – Impact of table positioning.

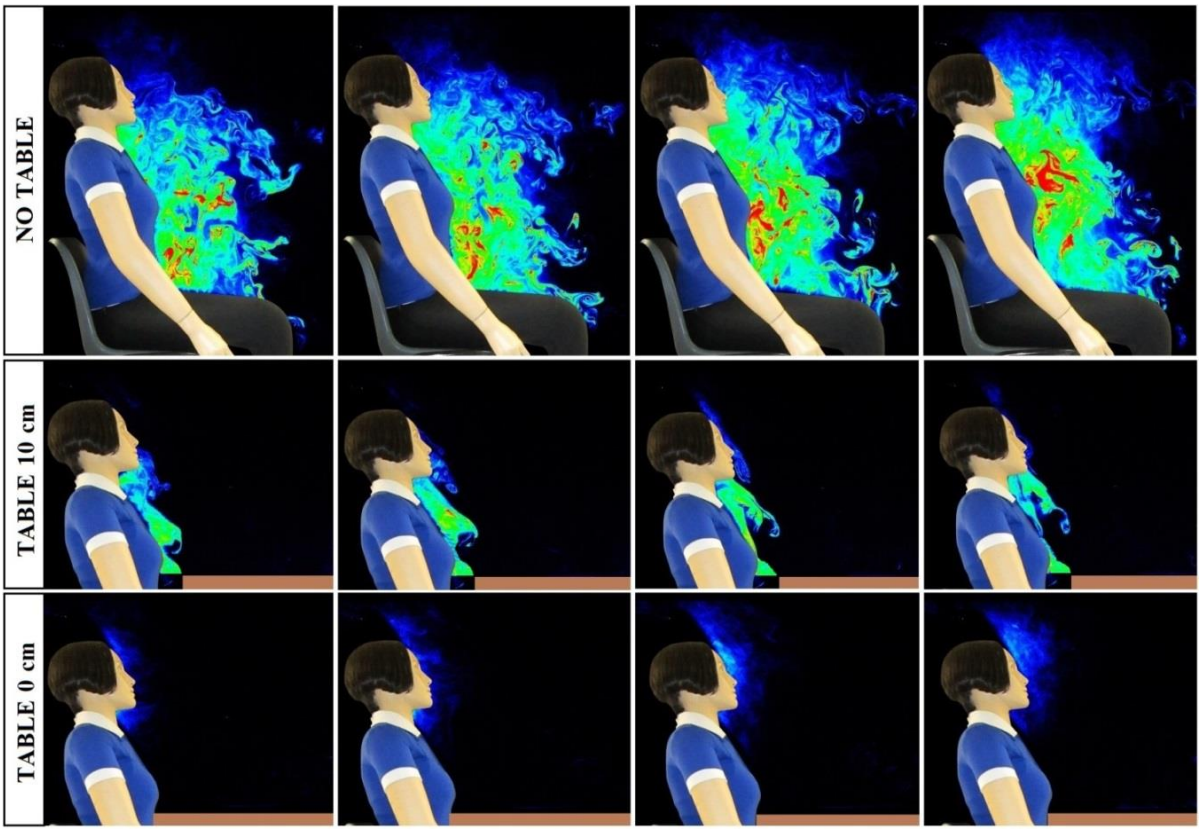

Figure 5.10 Pseudo Color Visualization of the CBL when the seeding particles were released at the feet of the manikin: Impact of the table positioning at 0.5s interval.

Table 5.5 Personal exposure percentage change - Influence of the table positioning

	Chest			Groins		
Table positioning	**No table***	Table 10 cm	Table 0 cm	**No table***	Table 10 cm	Table 0 cm
% change	0	+48	-63.5	0	+15.5	-80

* Refers to the reference case.

The results in Figure 5.11 show the cumulative pollution concentration in the breathing zone of the manikin and personal exposure for different table positioning. As seen, the profile of the cumulative exposure followed personal exposure profile when the pollution was released at the chest. On the other hand, the presence of the table blocked the transport of pollution from the groins, which reduced the cumulative pollution concentration in the breathing zone.

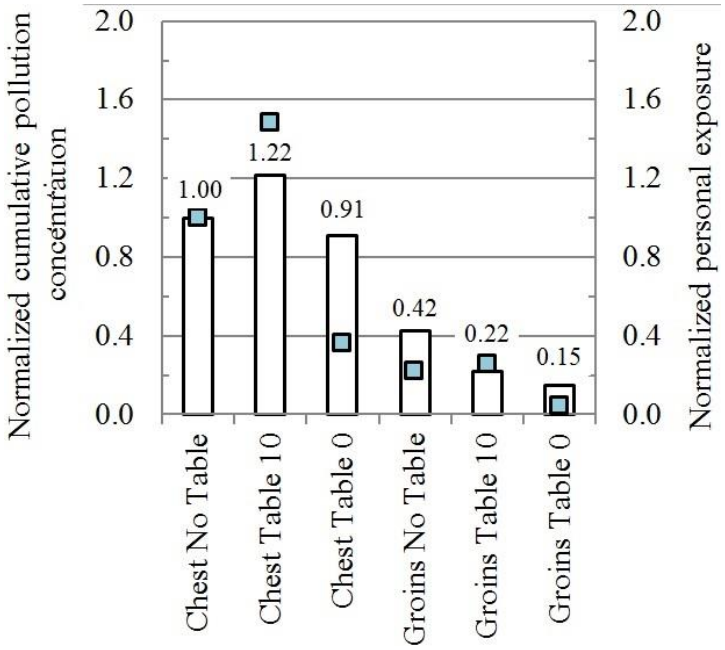

Figure 5.11 Normalized cumulative pollution concentration in the breathing zone and personal exposure – Impact of table positioning.

5.3.4 Impact of the seated body inclination angle

The impact of a seated body inclination angle on the breathing zone concentrations is shown in Figure 5.12. The results show that forward body inclination decreased the pollution concentration in the breathing zone as much as 82.5% in case of the chest and 74% in case of the groins. The opposite but milder effect was observed in case when the manikin was leaned backwards. As seen, when the manikin was inclined backwards the pollution decay profile was milder compared to the case with no inclination. This occurred because the pollution could not "stick to" the body and follow its contours as easily as it was the case with the straight body posture, causing more detachment from the surface. The manikin, when leaning forward, caused most of the pollution from the groins and chest to avoid the mouth region because of the blocking effect of the chin that acted as a physical obstacle to the rising pollution. The pollution impinged onto the chin and passed up the side of the cheeks, which was especially

prominent when the manikin was leaning forward. This type of airflow was previously described in more details in Chapter 3 and by Lewis et al. (1969).

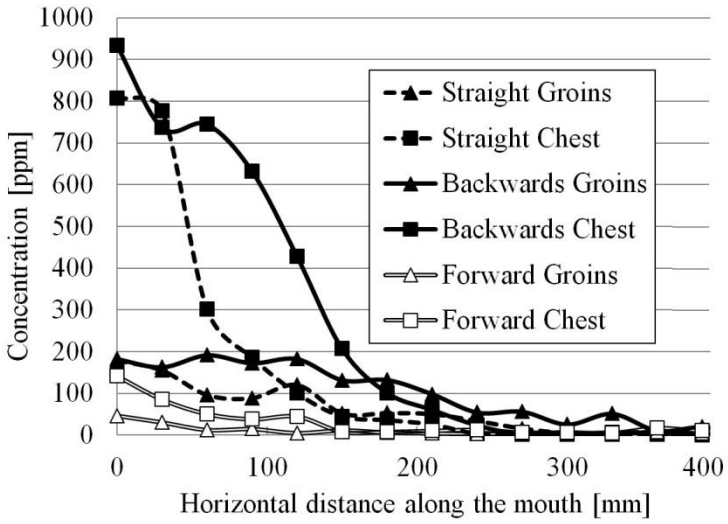

Figure 5.12 Concentration of tracer gas in the breathing zone – Impact of a seated body inclination.

Figure 5.13 shows the normalized personal exposure and the thickness of the PBL for different seated body inclination angles. In general, the pollution emitted from the groins was more spread, compared to pollution from the chest. It can be seen that the backward body inclination increased the thickness of the PBL and personal exposure. The forward body inclination decreased both the thickness of the PBL and personal exposure. The personal exposure changed in the same way as the velocity in the breathing zone, as the occupant leaned backwards increases the velocity, while forward body inclination decreases the velocity (Chapter 3). The results also suggest a direct correlation between personal exposure and spread of the pollution, which is opposite to the case of different room air temperatures and table positioning. Table 5.6 summarizes the percentage of personal exposure change in relation to the upward body posture.

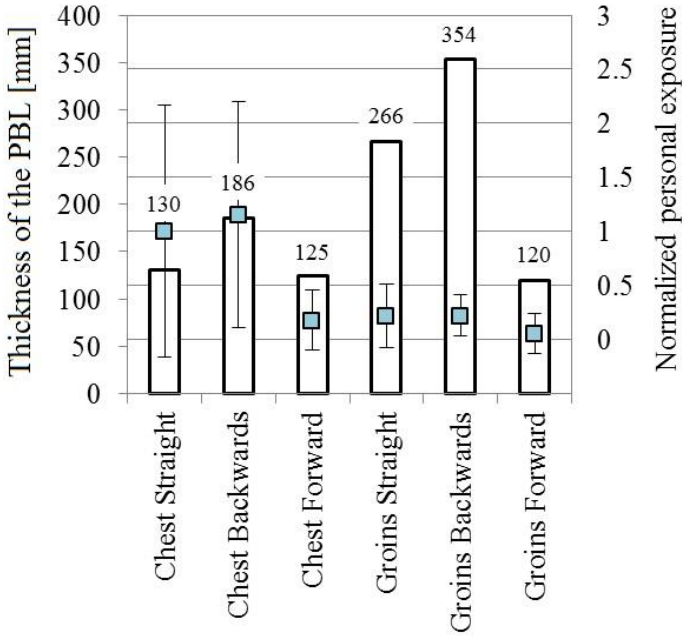

Figure 5.13 Normalized personal exposure and the thickness of the PBL - Impact of a seated body inclination.

Table 5.6 Personal exposure percentage change - Influence of seated body inclination

	Chest			Groins		
Seated body inclination	**Upright ***	Leaned forward	Leaned backwards	**Upright ***	Leaned forward	Leaned backwards
% change	0	-82.5	+15.5	0	-74	+2

* Refers to the reference case.

The results in Figure 5.14 show the cumulative pollution concentration in the breathing zone of the manikin and personal exposure for different seated body inclination angle. Similar to different room air temperatures, the profiles of the cumulative exposure followed personal exposure profiles, suggesting a direct correlation between them. In other words, the backward inclination increased the cumulative pollution concentration, while the opposite was the case for the forward body inclination.

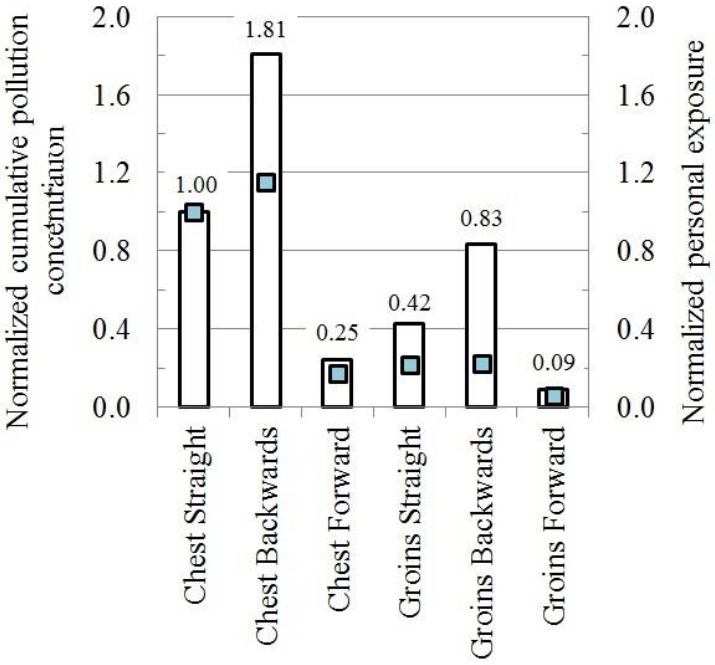

Figure 5.14 Normalized cumulative pollution concentration in the breathing zone and personal exposure - Impact of a seated body inclination.

5.4 Discussion

This part of the study was designed to enhance understanding of the pollution distribution around the human body and influence of parameters such as the source location, room air temperature, table positioning and seated body inclination angle. The results are discussed in relation to personal exposure, cross-contamination and optimal ventilation design.

The results in this chapter demonstrate the ability of the CBL to increase personal exposure when the pollution is located in the vicinity of a human body. Considering gaseous pollutants that originate from the human body (bioeffluents), and those released in occupant's proximity, the results show the CBL can entrain and transport the pollution to the breathing zone and that concentration is the highest close to the surface of the body. The concentration decays with increasing the distance from the surface approaching the average room concentrations. Therefore, the conventional methods for indoor pollution measurements based on a "well-

mixed" assumption would underestimate the realistic exposure to the pollution. There are, however, cases when the conventional exposure estimation methods can lead to overestimation of personal exposure, such as in a case when ozone reacts with the human surfaces (hair, skin, skin oils, clothing, etc.). In this case, the CBL becomes depleted of ozone with the lowest concentrations very close to the surface and the highest concentrations in the bulk air region (Rim et al. 2009).

Among different source locations studied, the pollution emitted from the chest has the highest contribution to the breathing zone pollution concentration. This result is in a general agreement with the CFD simulation findings reported by Rim and Novoselac (2010), which showed that in room with low air mixing when the source is located in front of chest region, the concentration in the breathing zone is nine times higher than the one obtained in the room with a perfect mixing. The results generally show that different source locations create large discrepancies in personal exposure and spread of the pollution in the breathing zone. Besides the sources located at the human body, it is also important to consider a horizontal distance between the source and the body because it affects the thickness of the PBL. The thickness of the PBL is an important factor for the exposure of other occupants in the room. Although the pollutants originating from the human body are more easily transported by the human CBL, the results on Figure 5.3 suggest that they are spread less compared to the pollutants released in the vicinity of the body. Pollutants from the human body are likely to be transported to the upper room levels via the thermal plume where they can be exhausted or mixed with the room air. The ability of the CBL to transport the pollution is reduced when the source is located at some distance from the body, because part of the pollution is entrained by the CBL, while the rest is mixed with the surrounding air. Such pollutants can originate from the exhaled breath of a neighboring occupant or from other pollutants in the surrounding that can mix with the CBL and travel to the breathing zone.

The previous studies generalized that when the source is located near the occupant, high breathing concentrations occur (Brohus and Nielsen, 1996; Rim and Novoselac, 2009). In this part of the study, however, the same effect is observed only for the pollutant locations from the front side of the manikin. The pollutants released from the occupant's back are transported upwards via the CBL, mostly avoiding the breathing zone. This can be advantageous when the source of clean air is located in front of the person, since the CBL can transport more clean air from the front, than from the back of the person. Ventilation efficiency will therefore, be higher if the air supply diffuser (in case of displacement or underfloor air distribution) is located in front of the person, than behind of the person. If the pollution source is, however, located behind the chair, it could be important for exposure of other occupants in the room. The results also suggest that pollutants emitted at the lower part of the body cause lower personal exposure, but are likely to increase exposure of other occupants because they spread more compared to the pollutants emitted at the upper part of the body. The opposite effect occurs when the pollution is located at higher body heights. This underlines the need to adopt a holistic approach that considers both personal exposure and exposure of other occupants.

Removing the pollution away from the human body reduced the concentration in the breathing zone, which suggests that this could be a possible way to reduce personal exposure. In addition, other control strategies to reduce the exposure to airborne pollutants can be introduced such as blocking the rising CBL with the table (Bolashikov et al. 2011; Chapter 3), weakening the CBL with the personalized ventilation jet to provide more clean inhaled air (Pantelic et al. 2009; Bolashikov et al. 2010) or optimizing the room airflow patterns (see Chapter 6). These techniques, however, usually do not consider how the pollution spreads upon being removed from the occupant which may easily increase the cross-contamination. Therefore, an implementation of the local exhaust could be a viable solution (Bolashikov et al. 2010; Yang et al. 2013; Bolashikov et al. 2014; Bivolarova et al. 2014). The exhaust terminal sucks the

pollution before it reaches the breathing zone or before it spreads across the room which could improve the inhaled air quality of all occupants in the room. This pollution removal technique could be effectively applied for different source locations in the room.

The velocity measurements of the CBL in the breathing zone (Chapter 3) show a solid correlation with the pollution concentration in the same zone, when the variables are room air temperature and seated body inclination angle. The two studies, performed under the similar experimental conditions, show that increase of the room air temperature from 20 to 26 ˚C reduced the peak velocity at the forehead by 33%, while personal exposure at the mouth dropped by 30% when the source was located at the chest. Analogously, a backward leaning occupant increased the peak velocity at the mouth by 8.1% (Chapter 3), compared to the straight body posture, while personal exposure increased by 15.5%. In addition, the thickness of the CBL and PBL changes in a similar pattern, as the increased room air temperature dissolves both the airflow around the human body and the pollution. Even though, the room air temperature usually aims to accommodate thermal comfort needs, the results show that it can be also used to control the pollutant distribution in the breathing zone.

In terms of optimal positioning of a table, the results of this part of the study can be used to control the transport of the pollution or clean air from the lower room levels to the breathing zone. The results suggest that if the pollution source is located at the lower room levels, closing the gap between the occupant and the table would interrupt the CBL and reduce personal exposure. In turn, if the source of clean air is located below the occupant (e.g. displacement ventilation diffuser), having a gap of 10 cm between the occupant and the edge of the table would improve the inhaled air quality. Both the table positioning and the seated body inclination angle are difficult to control in practice as building occupants have different physical preferences. Nevertheless, in spaces where the source of the pollution/clean air is known, it is possible to provide an optimal distance between an occupant and the edge of the

table. For instance, if the source of pollution originates from the carpet, it is possible to block the rising pollution by attaching a flexible board with spring system to the table which softly presses the occupant's abdomen (Bolashikov et al. 2010).

The results obtained in this chapter demonstrate the dependency of personal exposure on such factors as the source location, room air temperature, table positioning and body inclination. It should be noted that the practical implications of this part of the study may be changed under different room conditions. This part of the study does not consider room ventilation flow, human respiratory flow and movement, which are likely to modify pollutant distribution around the human body. Nevertheless, the results are applicable to indoor spaces with low air mixing and where people are predominantly seated during the day. The results may also be applied to smaller particles, such as smoke/household dust and different inhalable particles that naturally follow the room airflows. Due to a strong pressure to reduce building energy consumption, a low velocity ventilation design is gaining popularity where personal exposure is a major concern. Hence, the findings of this study tend to become even more important in the future.

5.5 Conclusions

This part of the study investigated a distribution of gaseous pollution in the breathing zone of a thermal manikin in a quiescent indoor environment. The impact of the source location, room air temperature, table positioning and body inclination was evaluated. The experimental results revealed the following:

- When the pollution source originated from the human body or was released in its vicinity, the CBL contributed, to a great extent, to an increase of personal exposure by transporting the pollution to the breathing zone;

- The location of the source had a considerable influence on personal exposure and thickness of the PBL. The source located at the human body caused higher personal exposure and lower level of spread into the room air, compared to the pollution emitted further away. The source emitted at the lower body parts reduced personal exposure, but spread more across the room, compared to the pollutants from the upper body parts;
- Reducing the room air temperature intensified the transport of the pollution to the breathing zone, which increased personal exposure and reduced the pollution spread. The personal exposure increase was found when the occupant was leaned backwards in the chair;
- Closing the gap between the edge of the table and the occupant can be used to reduce the pollution transport to the breathing zone. Keeping the distance between the table and the occupant of 10 cm caused higher personal exposure compared to that in case without the table; and
- In a room with little air movement, a "well-mixed" mass balance assumption can lead to underestimation of the exposure. The future studies should therefore, focus on a detailed understanding of the pollutant distribution in the vicinity of a human body.

CHAPTER 6: IMPACT OF THE HUMAN CBL AND VENTILATION FLOW ON THE PERSONAL EXPOSURE TO HUMAN GENERATED PARTICLES

6.1 Specific objectives

Chapter 4 presented the results of the interaction between the CBL and three idealized flows (opposing flow from above, transverse flow from in front and assisting flow from below). That work provides a basis for the present chapter, which focuses on the impact of the resulting complex flows on personal exposure. The specific research objective of this part of the study is to investigate personal exposure of an occupant to particles released at feet level and cough released droplets in: (i) a quiescent environment; and (ii) a uniform flow field. The results presented in this chapter will contribute to better understanding of the effects of room airflow patterns and their intensities on personal exposure.

6.2 Research methodology

6.2.1 Experimental facility

The experimental facility used for the measurements was the same as described in Chapter 4.

6.2.2 Experimental equipment

As the results in this Chapter 6 are a direct continuation of the measurements discussed in Chapter 4, an airflow generator and the thermal manikin created an identical set of experimental conditions and thus, they will not be further described.

Particles released from the manikin's feet were generated by atomizing polydispersed olive oil (extra virgin) particles (mean diameter of 1 μm) in a Six-Jet Atomizer (Model 9306A, TSI Inc., Shoreview, MN, USA). The particle generator created a seeded flow that closely followed the density of air (Stokes number was close to zero) which implied that particles behaved like tracers. The injected pollution had the same temperature as surrounding air. By adjusting the input pressure to 34.5 kPa above the atmospheric, the aerosol output was minimized to 2.4 l/min. The outlet of the particle generator was connected to a flexible pipe (0.05 m diameter) whose other end was positioned between the manikin's feet and through which the particles were released without the initial velocity. For an accurate comparison of the results, the aerosol generation flow rate in terms of particle number and size distribution was kept constant throughout the experiments.

A cough machine (Chao and Wan, 2006) was used to approximate the human cough. The liquid used in the cough machine contained a mixture of water (94%) and glycerin (6%) to closely resemble the properties of human saliva and particularly its evaporative properties. This equipment has been used and described in several studies (Chao and Wan, 2006; Pantelic et al. 2009). The mixture of two fluids was discharged through an air-atomizing nozzle that generated puffs of droplets of different size and velocity distribution. It is important to note that number and size of expelled droplets are difficult to generalize, as they vary according to the person (Edwards et al. 2004). In our case, the repeatability test was performed to assure that the number and size distribution of the cough droplets do not vary substantially between two consecutive releases. The results showed a very small discrepancy among repeated measurements (up to 5%). By a fine adjustment of the desired flow rate and pressure of the mixture of air and liquid, the cough machine replicated the initial droplet-size distribution reported by Chao et al. (2009) with the initial velocity of the cough of around 10 m/s, as similarly reported by Zhu et al. (2006). The Pseudo Color Visualization technique (see Chapter

3) was used to visualize the cough released from 2 and 3 m distances from the manikin and to acquire the data of the cough velocity by image processing. At 0.45 m distance in front of the manikin, the velocity of the cough released from 2 m was 3 m/s; and 5 m/s when the cough was released from 3 m distance. These values were obtained in quiescent indoor environment and the input parameters of the cough machine were kept constant throughout the experiments. Due to the absence of heating elements, the temperature of the discharged flow was equal to the room air temperature (23 ˚C), which was lower than would be the case in a real cough.

Aerosol spectrometer (Model Grimm 1.108, Aerosol Technik GmbH, Ainring, Germany) was used to measure the real-time aerosol concentration in the breathing zone of the thermal manikin. A previously calibrated aerosol spectrometer with 16 size channels, sampling rate of 1.2 L/min, 1 Hz measurement frequency and reproducibility rate of ±2% was able to count particles in the size range from 0.30 µm to 20.0 µm. For the purpose of this study, pollutant transmission was considered only through airborne particles within the optical diameter range from 0.5 to 0.65 µm, and the results reported are applicable only to particles that strictly follow the airflow. These particles belong to the fine particle range (diameter 0.1 – 2 µm) such as those found in household dust/smoke and in different respirable particles.

6.2.3 Experimental design

By minimizing the total heat gains in the chamber it was possible to maintain a constant room air temperature of 23˚C and 60% relative humidity at the minimum air exchange rate (1 ACH). The purpose of the background ventilation was to maintain a constant air temperature in the chamber without disturbing the manikin's CBL. Disturbance by the ventilation system was assessed by measuring the velocity (Dantec omnidirectional thermal anemometers; accuracy ±0.02 m/s; ±0.5 K) at 16 locations around the manikin, all at 1.2 m distance. The recorded velocity at each point was below 0.05 m/s which indicated that quiescent indoor conditions had

been achieved, as suggested by Murakami et al. (2000). In addition, the maximum air temperature difference between points near the floor and the ceiling was not above 0.5 K.

Firstly, personal exposure was studied when the manikin was heated and unheated. Secondly, personal exposure was examined in relation to the direction of the uniform airflow, i.e. when the heated manikin was exposed to: (i) assisting airflow from below; (ii) opposing airflow from above; (iii) transverse airflow from in front; (iv) transverse airflow from one side and (v) transverse airflow from behind. To generate such flows, the airflow generator was positioned in five different positions relative to the manikin, as shown in Figure 6.1, left (Transverse flow from side not shown). Finally, the impact of a uniform flow field on personal exposure was examined for three velocities supplied through the airflow generator: 0.175, 0.30 and 0.425 m/s as determined near the surface of an unheated manikin (see Chapter 4). The lower two velocity bands (0.175 and 0.30 m/s) are velocities typically occurring in majority of occupied indoor spaces (Baldwin and Maynard, 1998), while the velocity of 0.425 m/s is commonly induced by personalized ventilation (Melikov et al. 2003). In the experiments when the manikin was heated, the velocities at these locations were altered after collision with the CBL of the manikin.

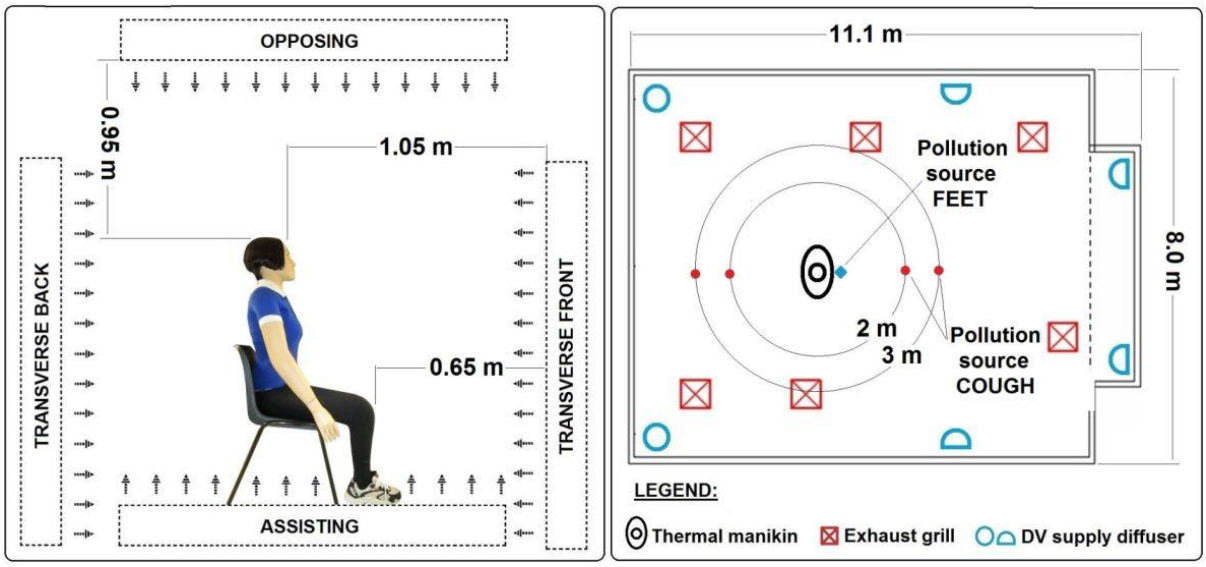

Figure 6.1 Experimental design: Invading flow directions (left); the environmental chamber with pollution location (right).

The pollution source location at the feet was chosen to simulate fine particles from the floor/carpet or shoes which become re-suspended through human activities such as walking or sitting on furnishings (Qian et al. 2014). The nozzle of the cough machine was positioned at either 2 or 3 m distance from the manikin at the height of the mouth (1.12 m) to examine the impact of the distance between coughing and exposed person on personal exposure. In the case when the airflow generator was positioned in the front of the manikin, the cough machine was positioned at 2 and 3 m behind the manikin in order to avoid the blockage caused by the physical presence of the airflow generator (Figure 6.1, right). In all other cases, the cough machine was positioned in front of the manikin. Samples of particles/droplets were drawn from a single point in the breathing zone of the manikin and personal exposure was calculated based on their average concentration. An isokinetic sampling probe was located at the upper lip of the manikin at a distance of 1 cm from the surface to accurately represent the sampling of inhaled air, as recommended by Melikov and Kaczmarczyk (2007).

Detailed sampling and dosing procedure for both pollutants is shown in Figure 6.2. As seen, in both cases total sampling time was 210 s, while the time interval for the analyzed data was shortened. When the pollution originated from the feet, the results were recorded and averaged over 120 seconds (sampling rate 1 Hz), while for the cough release over 150 seconds, 10 coughs (denoted by C1, C2, etc.) were recorded and averaged. For the particles released at the feet, a relatively short measurement time was adopted to prevent any possible re-entrainment of the particles into the uniform flow field. The cough droplets were released every 15 seconds, since that was the time required to reach the initial background concentration after the release. Between two consecutive measurements, the chamber was flushed with the outdoor air to remove all injected particles and to return to initial background concentration. In both scenarios, the background concentration was recorded 60 s prior to pollutant release which was subsequently deducted from the results to minimize measurement inaccuracy due to initial

background concentration. The initial background concentration was several orders of magnitude lower than the average concentration of released particles. The personal exposure measurements were repeated 10 times in each case in order to reduce the bias caused by flow unsteadiness within the human CBL and the measurements were averaged before analysis. The total measurement uncertainty (random and systematic) was 7% for the pollutant released at the feet and 10.5% for the cough released droplets, at a level of confidence interval of 95%. The result differences below or equal to the uncertainty values were considered negligible, i.e. within the uncertainty limits.

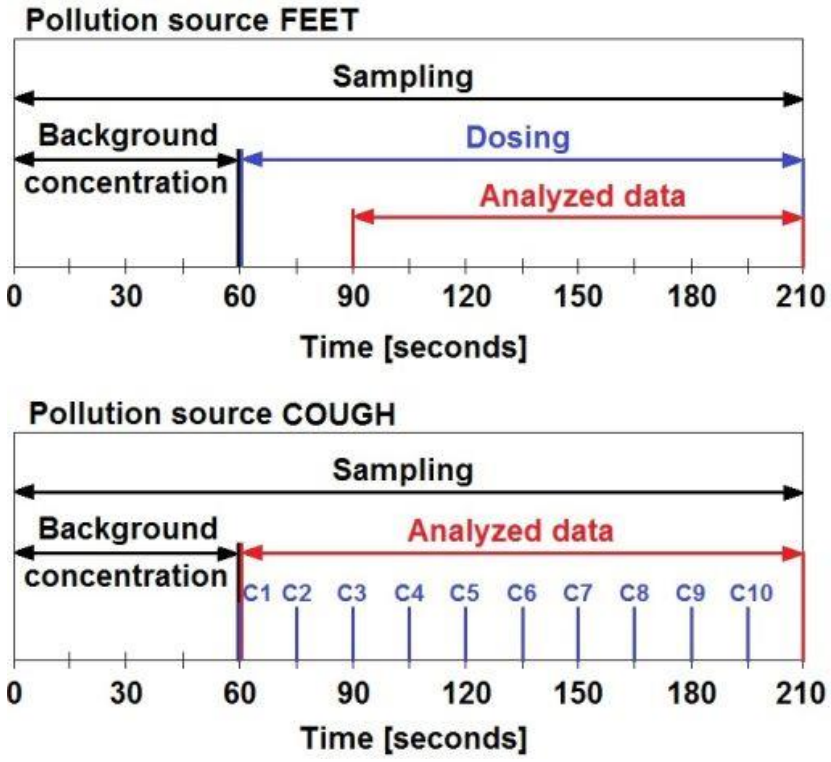

Figure 6.2 Detailed sampling and dosing procedure for two pollution sources.

6.3 Results

The experimental results demonstrate the effects of airflow patterns and their intensities on personal exposure.

6.3.1 Personal exposure to pollutants released from the feet

Figure 6.3 shows the results of the averaged personal exposure to feet released particles, as a result of the CBL flow and its interaction with mutually assisting, opposing and transverse flow (from in front, back and side). The results were normalized with respect to the averaged concentration obtained with the heated manikin in quiescent environment (CBL). When the manikin was heated in quiescent indoor conditions (reference case), the CBL was able to pull the particles from the feet to the breathing zone resulting in 5.8 times higher averaged exposure compared to the case with no CBL. This result is aligned with the results of other studies (Brohus and Nielsen, 1996; Eisner et al. 2002) which showed that the CBL was able to increase inhaled concentration of pollution compared to the ambient concentration when the pollution source was located near the occupant. In case of the unheated manikin in quiescent indoor conditions (No CBL), a small portion of particles ended up in the breathing zone due to the absence of the CBL. In this case, it was observed that the particles released at the feet were naturally spread in all directions and mixed with the surrounding air. One part of them rose upwards towards the breathing zone, probably pulled by the heated aerosol spectrometer (4.5 W) located near the manikin's head. However, due to its very low power (4.5 W) its effect was considered negligible.

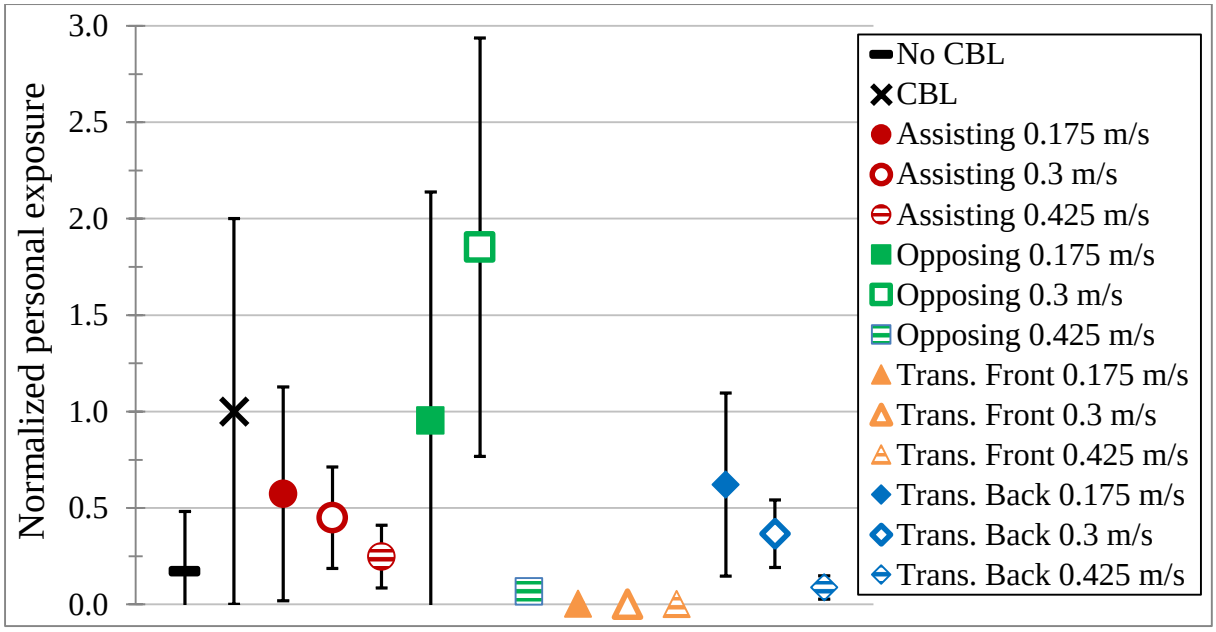

Figure 6.3 Normalized cumulative exposure to the pollution released from the feet - Influence of the CBL, the direction of the invading airflow and the airflow velocity.

The results in Figure 6.3 reveal that personal exposure decreased when the manikin was exposed to assisting and transverse flow from front, side and back. All of the measurements of the personal exposure of the manikin exposed to invading uniform airflow were compared to the reference case (CBL). Assisting flow from below at the velocity of 0.175 m/s reduced the exposure by 43% compared to the reference case. This exposure reduction was attributed to the effect of particle dilution from the feet by the upward unpolluted flow. Higher velocities of 0.3 and 0.425 m/s further reduced the exposure by 55% and 75% respectively, compared to the reference case. When the manikin was exposed to the transverse flow from the back, the increased velocity of the invading flow easily overcame the upward CBL flow and displaced the pollution towards the surroundings. The respective personal exposure reductions at the velocities of 0.175, 0.3 and 0.425 m/s were 38%, 63% and 91%. The manikin exposed to transverse flow from in front created the same effect on personal exposure as when it was exposed to the transverse flow from side (not shown in Figure 6.3). In both cases, transverse flow completely eliminated the exposure already at 0.175 m/s.

When the manikin was exposed to the opposing flow from above, the personal exposure showed a non-monotonic dependence on the velocity of the invading flow. Since it was unable to penetrate the thermal plume, the opposing flow from above at 0.175 m/s created a negligible effect on personal exposure. Airflow with the velocity of 0.3 m/s generated the peak personal exposure level that was 85% above the reference case. In this case, downward flow collided with the upward CBL at the level of forehead (Chapter 4), thus maximizing the pollutant residence time in the breathing zone. This finding is different from commonly adopted assumption that with increased magnitude of the surrounding flows, the ability of the CBL to transport the pollution upwards deteriorates. Further increase of the velocity of the downward flow to 0.425 m/s reduced the number of particles in the breathing zone by 93% with respect to the reference case. In this case, most of the pollution from the feet was prevented of reaching the breathing zone, since the downward flow was able to break away the CBL, as documented in Chapter 4.

6.3.2 Personal exposure to cough droplets – Impact of the CBL and the cough release distance

Figure 6.4 shows the results of the personal exposure to cough released droplets from 2 and 3 m distance when the manikin was heated and unheated in quiescent environment. As is apparent, when the cough was released from 2 and 3 m distance, the results differed substantially both in terms of the peak exposure and delay time of exposure after the cough release. From 2 m distance, the cough droplets impinged on the manikin 3 s after their release, causing a peak particle number of $1.14x10^6$ (per m^3). When the cough was released from 3 m distance, droplets that reached the breathing zone were more dispersed and had less momentum, resulting in a peak particle number of $0.54x10^6$ (per m^3), which was 53% lower compared to the previous case. In this case the peak exposure was reached 6 s after the release, which explains why after that time droplet concentration in the breathing zone was higher for 3 m release than for 2 m release.

Figure 6.4 shows that the CBL of the manikin was unable to reduce the peak exposure to cough droplets from either of the two distances studied. The peak exposure of the heated and unheated manikin remained unchanged, which suggests that the initial puff generated by the cough machine had a sufficiently strong momentum to completely blow away the CBL. Nevertheless, after the initial collision between the cough droplets released from 2 m and the manikin's body, i.e. the initial penetration of the CBL, it quickly re-establishes, as reported by (Pantelic and Tham, 2013). In this way, the CBL diluted the droplet concentration in the breathing zone (see Figure 6.4) and reduced the cumulative personal exposure by 16% compared to the case with no CBL. From 3 m, the droplets were spread more around the manikin (conical dispersion) and the concentration over 15 seconds remained equal to that of the unheated manikin (within uncertainty limits). In this case, it was probable that some of the droplets directed towards the

face were transported upwards upon the initial impingement, while part of droplets that fell downwards after impingement and those dispersed more around the manikin were transported back up to the breathing zone by the CBL. Additional videos obtained with Pseudo Color Visualization technique that describe interaction between the human CBL and cough droplets released from 2 m (Video 6.1) and 3 m (Video 6.2) are enclosed as supplementary information (see Compact Disk). This visualization technique has been previously introduced in Chapters 3 and 4.

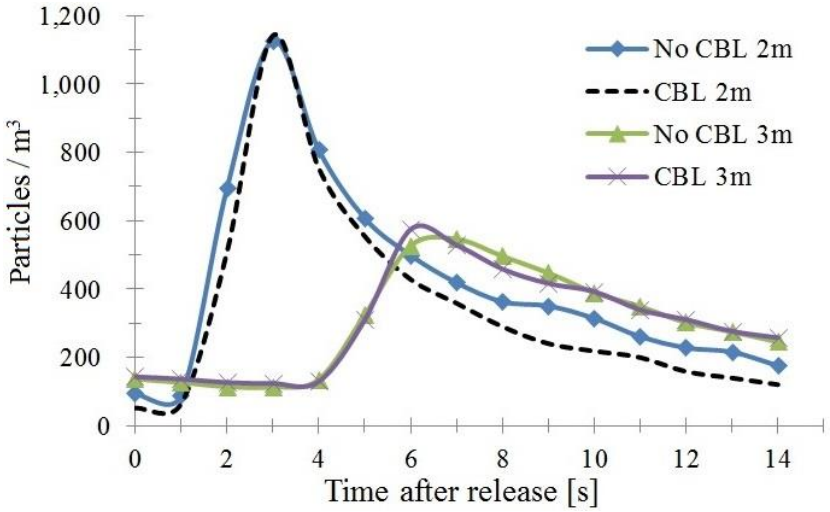

Figure 6.4 Averaged personal exposure of heated/unheated manikin to cough droplets released from 2 and 3 m.

6.3.3 Personal exposure to cough droplets released from 2 m – Impact of the direction of the invading airflow and its magnitude

Figure 6.5 shows the measured personal exposure to cough droplets released from 2 m distance from the manikin, as a result of the CBL flow and its interaction with mutually assisting, opposing and transverse flow (from in front, back and side). Figure 6.6 shows the shape of the averaged personal exposure over 15 s after the cough release, for the same scenarios. As seen in all cases, the surrounding airflows had a positive or neutral influence on personal exposure, while the influence of the flow velocity on personal exposure was dependent on the airflow

direction. Assisting flow around the manikin at the velocity of 0.175 m/s was able to disturb and redirect the approaching cough from 2 m distance from in front and reduce the cumulative personal exposure by 50% (Figure 6.5). An increase of the velocity to 0.30 and 0.425 m/s further displaced the cough, reducing personal exposure by 63 and 70%, respectively. An identical effect on the personal exposure was obtained when transverse flow from the side was applied. When the manikin was exposed to transverse flow from in front and the cough took place 2 m from the back, the effect on personal exposure was different. In this case, the head/back of the manikin created an obstacle for the cough droplets which, together with the invading flow from in front, further reduced personal exposure by 75, 82 and 92% for the velocities of 0.175, 0.30 and 0.425 m/s, respectively. It may be seen that for all three airflow directions, increasing the velocity from the airflow generator almost linearly decreased the cumulative personal exposure; however in none of the cases it was reduced to zero.

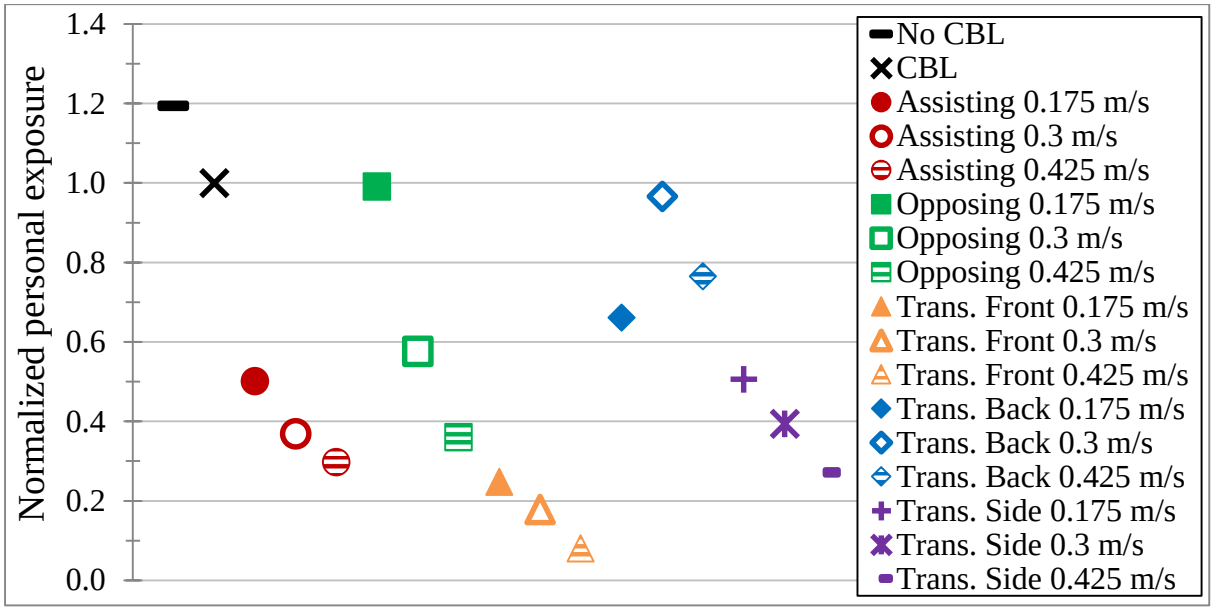

Figure 6.5 Normalized cumulative exposure to the cough released from 2 m distance from the manikin - Influence of the CBL, the direction of the invading airflow and the airflow velocity.

The personal exposure when the manikin was exposed to the cough from 2 m from in front and with an opposing flow from above is also presented. As when the pollution originated at the feet, the downward flow at a velocity of 0.175 m/s caused negligible reduction in the cumulative exposure (Figure 6.5) and the peak exposure (Figure 6.6). The initial puff released by the cough machine was able to penetrate the breathing zone at the velocity of 0.30 m/s without changing the peak exposure (Figure 6.6). After impingement, however, the downward jet effectively removed the droplets from the breathing zone, reducing the cumulative exposure by 42%. Airflow at the velocity of 0.425 m/s pushed away part of the cough, which reduced the peak exposure by half and the cumulative exposure by 64%. Finally, when the cough was released 2 m from in front of the manikin with transverse flow from the back, the velocity had a crucial influence on the exposure. The lowest velocity of 0.175 m/s was unable to reduce the peak exposure (Figure 6.6) but was effective in removing the droplets after impingement, which resulted in a 34% reduction of personal exposure (Figure 6.5). A more complex flow structure was created in the breathing zone when the airflow velocity was increased to 0.30 m/s, due to collision of two opposing flows at that height. Flow from the back interacted with the cough approaching from front, which caused the droplets to reside longer in the breathing zone and increased peak exposure by 9%, while the cumulative exposure reduction was again negligible. Increasing the velocity to 0.425 m/s partially deflected the cough jet, reducing both peak exposure and cumulative exposure by 23%.

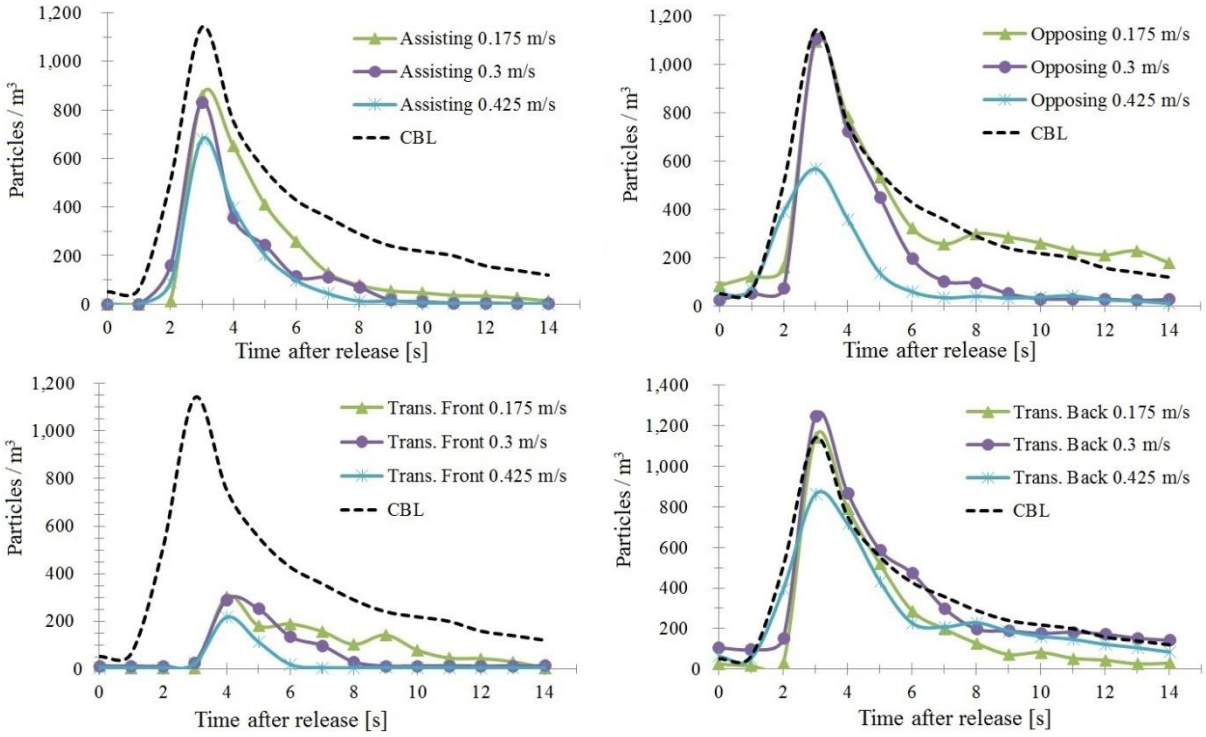

Figure 6.6 Averaged personal exposure to the cough released from 2 m distance from the manikin – Influence of the CBL, the direction of the invading airflow and the airflow velocity.

6.3.4 Personal exposure to cough droplets released from 3 m – Impact of the direction of the invading airflow and its magnitude

The results of the cumulative exposure of the manikin exposed to a cough released from 3 m distance and the uniform surrounding airflows are shown in Figure 6.7. In this case, the cough flow was more dispersed and unable to dominate the flow around the manikin, as it did at 2 m distance. This enabled the surrounding airflows from any direction to substantially reduce the level of personal exposure even at the minimum velocity. In each case, the peak level of personal exposure dropped with increasing the velocity from the airflow generator, as shown in Figure 6.8. Unlike the case when the transverse flow from the back at 0.30 m/s collided with the cough from 2 m in the breathing zone and increased the peak exposure, the cough from 3 m was successfully offset by the same flow, reducing cumulative exposure by 85%. The respective cumulative personal exposure reductions at the velocities of 0.175 and 0.425 m/s

were 51 and 88%. Comparing the results from 2 and 3 m releases show the importance of the pollution location relative to the exposed person and the direction of the surrounding airflows. A similar effect on personal exposure was detected when the uniform surrounding airflow approached the manikin from the side, below or above. The transverse flow in from front effectively eliminated the invading cough from the back even at the lowest velocity of 0.175 m/s. Further increasing the velocity did not change personal exposure. Table 6.1 summarizes the percentage of cumulative exposure reductions under the influence of uniform surrounding airflows and their magnitude, for all the pollutant scenarios.

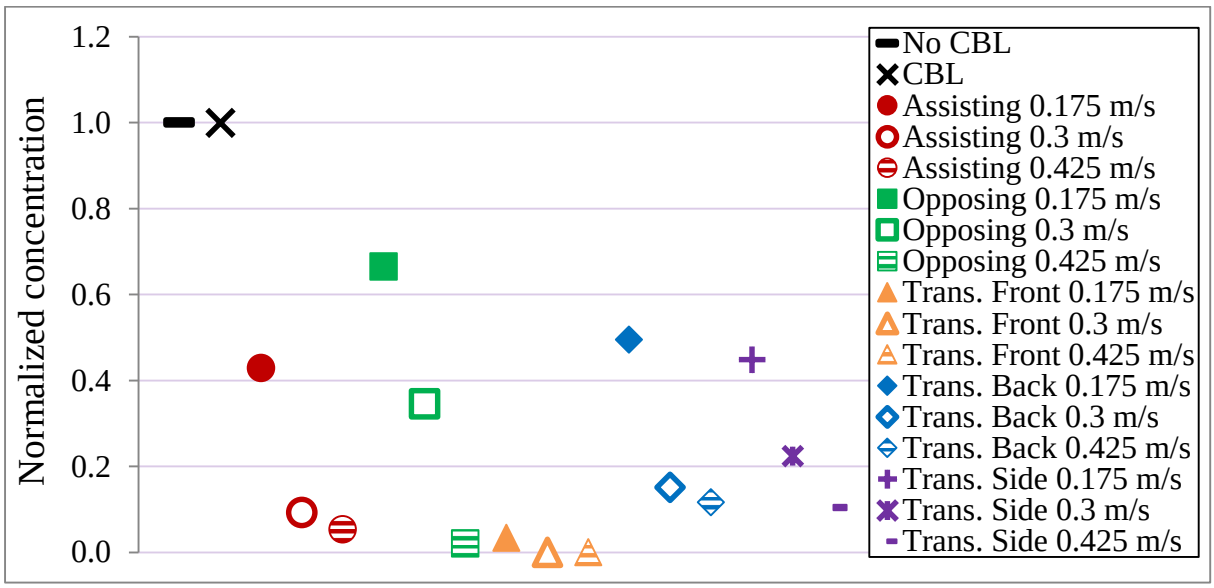

Figure 6.7 Normalized concentration of the cough released from 3 m distance from the manikin – Influence of the CBL, the direction of the invading airflow and the airflow velocity.

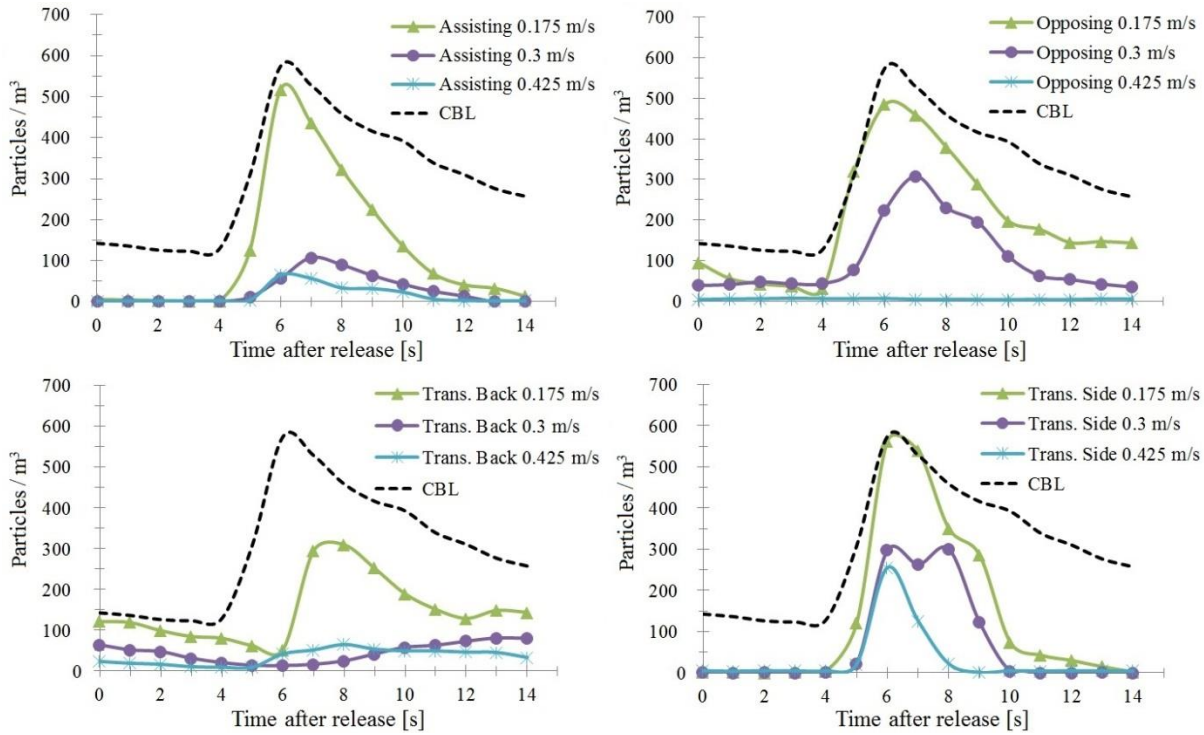

Figure 6.8 Averaged personal exposure to the cough released from 3 m distance from the manikin – Influence of the CBL, the direction of the invading airflow and the airflow velocity.

Table 6.1 Personal exposure percentage reduction - Influence of the direction of the invading airflow and its magnitude

	Velocity [m/s]	Assisting	Opposing	Transverse Front	Transverse Side	Transverse Back
Feet	0.175	43	-*	100	100	38
	0.30	55	**-85**	100	100	63
	0.425	75	93	100	100	91
Cough 2 m	0.175	50	-	75	49	34
	0.30	63	42	82	61	-
	0.425	70	64	92	73	23
Cough 3 m	0.175	57	34	97	55	51
	0.30	91	66	100	78	85
	0.425	95	98	100	90	88

*The percentage differences ≤7% (feet) and ≤10.5% were considered negligible (within uncertainty limits).

6.4 Discussion

The present chapter was designed to examine the relationship between personal exposure and air distribution in occupied spaces. The results are discussed in relation to the optimal design of different ventilation systems, thermal comfort and energy.

In current ventilation design, it is commonly accepted that an increase in the amount of air supplied to the room reduces exposure to all pollutants. However, in the majority of the cases the room air distribution is not taken into account. Based on our experiments, it is apparent that personal exposure can be minimized by proper design of airflow patterns alone. The results of this study clearly demonstrate that in some cases, increasing the amount of supplied air does not always reduce the exposure. For instance, flow opposing the CBL at a velocity of 0.175 m/s is unable to reduce exposure to cough droplets released 2 m from in front or to pollutants released from the feet. Furthermore, when the cough droplets are released from 3 m or if the pollution comes from the feet, increasing the velocity of the transverse flow from in front above 0.175 m/s does not provide any additional benefit in terms of reducing personal exposure. These results show that there is a non-linear ratio between personal exposure and the amount of air supplied to the room. Knowing the lowest supply velocity required to minimize exposure is important for reducing the risk of draft discomfort and the energy input. The results of the present study reveal that the transverse flow from in front at 0.175 m/s will be sufficient to reduce personal exposure. At the room air temperature below 23 ˚C, a further increase of the velocity will not affect personal exposure, but it may cause thermal discomfort (ISO 7730, 2005; ASHRAE, 2013a). The elevated velocity of the flow would also increase energy consumption.

Several existing standards recommend a vertical downward ventilation approach to contaminant removal, stating that it is able to reduce the cross-contamination risk (CDC, 2003; ASHRAE 2013b). Examples of such an air distribution are downward ceiling diffuse ventilation or downward flow generated by ceiling mounted fans, chilled beams or personalized ventilation with ceiling installed air supply devices. The findings of the present study indicate that in cases when the pollution originates from the occupants' feet, a downward ventilation approach can maximize personal exposure by as much as 85%. It is apparent that disregarding

the CBL flow when a downward flow is applied, will bring personal exposure equal to zero, which indicates the importance of considering human generated airflows in an indoor environment. The same finding could be applied to other human body parts, especially those from the front side, since the CBL is able to bring emitted pollution to the breathing zone. This is important to consider because shedding rate of the human skin is large and equivalent to 0.2 – 1 billion skin cells per day (Roberts and Marks, 1980). In addition, potentially infectious airborne pollutants from the surroundings such as those from exhaled breath or cough can easily be entrained by the CBL and increase personal exposure. Increasing the discharge velocity of the downward flow to 0.425 m/s reduces the exposure, but it could also cause thermal discomfort (ISO 7730, 2005) and carries an energy penalty. In addition, it is important to consider where particles go after being removed by the downward flow. If removed downwards, they can remain suspended in the lower regions, below the breathing zone, and then accumulate sufficiently to have adverse consequences. In addition, the downward flow that opposes the CBL can increase the settling rate, depositing more droplets onto the floor. In rooms where IAQ is a major concern, a change of the supply airflow direction that does not directly oppose the human thermal plume is recommended.

Transverse flows are commonly encountered in naturally/hybrid ventilated spaces where fans are used to enhance the comfort of the occupants or in rooms equipped with personalized ventilation, stratum ventilation, etc. Our results show that transverse flow from the back is less effective in reducing personal exposure compared to transverse flow from in front or from the side, when the pollution originates from the feet or released as a cough from 2 m. These results are in line with findings that person facing the free stream with its back intensifies the transport of the pollution to the breathing zone (Welling et al. 2000; Ge et al. 2013). When the pollution source approaches from behind, as in the case when one person breaths/coughs while facing the back of another person (as in classrooms, offices, transport, etc.), transverse flows from in

front and from the side are likely to be the most favorable. The same flows show the advantage over other airflow directions in case when the pollution originates at the floor (such as polluted carpet, smelly feet and other small re-suspended particles). The results indicate the potential advantages of personalized ventilation supplied from in front or from one side over other air supply directions, when properly designed. In transverse flows, however, it is likely that the pollution that is removed will increase the risk of cross infection of other occupants, since it can easily spread across the room. For instance, the exhaled air an occupant can be moved to the occupant sitting behind, if transverse flow from in front is applied. This issue could be overcome by careful positioning of the exhaust or by employing personalized exhaust devices (Melikov and Dzhartov, 2013; Yang et al. 2014).

In terms of effective contaminant removal from the room, the assisting flow from below would be a better strategy than the opposing flow, as the particles can more easily be transported above the occupancy zone and then removed or treated. Rooms ventilated with upward piston flow, displacement or under-floor ventilation are typical representatives of such an air distribution. The results of the study demonstrate that the assisting flow from below substantially reduces the personal exposure to any of two pollutants studied. Comparing the effectiveness in reduction of exposure to pollution that originates from the human body or to droplets released through coughing, a uniform upward flow would be more preferred air distribution strategy than a downward flow from the ceiling.

The experimental results demonstrate the dependency of personal exposure on such factors as pollutant location, airflow direction and airflow velocity. In should be noted that the results may not be applicable to larger particles that do not strictly follow the airflow. Although the CBL has been shown to have effect on personal exposure, in reality, a person does not always keep still which is likely to modify personal exposure. Nevertheless, there are many spaces where occupants perform sedentary tasks and move little during the day, which makes findings

of this study relevant. Apart from the occupants' movement, the effect of the human breathing creates velocities that can be comparable to the tested airflow velocities studied (Gupta et al. 2010). In addition, Chao et al. (2009) found that average expiration air velocity during talking is 3.1 m/s, which can alter air distribution in the occupied spaces and personal exposure. Study done by Melikov and Kaczmarczyk (2007) reported that the temperature, the relative humidity and the concentration of tracer gas measured in the air inhaled by the breathing thermal manikin were almost the same as those measured close to the upper lip of the non-breathing thermal manikin. Nevertheless, the human respiratory activities should also be taken into account in future studies. Although some of these topics require further investigation, several important conclusions can be drawn.

6.5 Conclusions

This chapter investigated personal exposure of an occupant to airborne particles released at the feet and cough released droplets from a seated infected source, both in a quiescent indoor environment and in a uniform airflow from different directions. The findings of this part of the study are the following:

- Personal exposure depends on the location of the pollution source, the airflow direction relative to the person and relative to the pollutant source and the airflow velocity;
- The human CBL substantially influenced personal exposure when the pollution originates at the feet, unlike the case of a human cough;
- The presence of the CBL was not sufficient to disturb the cough flow released from 2 or 3 m distance to the level that would cause measurable peak concentration reduction;
- Increasing the distance between the cough and the exposed occupant from 2 to 3 m, reduced peak exposure by half;

- For the two types of the pollution sources studied, the most favorable airflow patterns are transverse flow from in front and the side, as they could minimize, or sometimes eliminate, the exposure at the minimum velocity studied. These directions should therefore be considered in the design of ventilation, when the source location is unknown;
- When the pollution was located at the feet, interaction between the CBL and opposing flow from above created unfavorable velocity field and increased personal exposure. Increasing the velocity of the transverse flow from behind from 0.175 to 0.30 m/s could actually increase personal exposure, when the cough was released from 2 m. In some cases, increasing the velocity above 0.175 m/s did not provide any additional benefit in terms of reducing personal exposure; and
- There may be no direct correlation between the amount of the supplied air and personal exposure. Rather than relying on the outdoor air supply rate as a sole indicator of indoor air quality, more attention should be paid to room air distribution.

CHAPTER 7: TEMPERATURE FIELD OF THE HUMAN CBL IN A QUIESCENT INDOOR ENVIRONMENT

7.1 Specific objectives

This part of the study presents the experimental investigation of the air temperature field of the human CBL in the quiescent indoor environment. The specific objective is to examine the air temperature and standard deviation of air temperature fluctuations distribution in the CBL as a function of the room air temperature, body posture and human respiration flow. Some of the results are compared with the results obtained with a real human subject to determine the accuracy of measurements with a thermal manikin. The findings of this part of study contribute to better understanding of microenvironment around a human body which is useful in areas of indoor air quality, thermal comfort and airborne disease transmission. The results can be also used for improving the accuracy of CFD simulation predictions.

7.2 Research methodology

7.2.1 Experimental facility

The experimental facility was the same as described in Chapter 5. In the absence of internal heating elements, the velocity in the chamber was measured to assure that quiescent environmental conditions had been achieved. The velocity measured with omnidirectional thermal anemometers (SENSOR; accuracy ±0.02 m/s) at numerous locations in the chamber

was below 0.05 m/s, which provides evidence that quiescent conditions had been attained (Murakami et al. 2000).

7.2.2 Thermal manikin

A heated, clothed and non-sweating thermal manikin (P.T. Teknik Limited, Denmark) was used to simulate a realistic human body. The size and the shape of thermal manikin are discussed in Chapter 5. The manikin was seated in the chair positioned in the center of the chamber. In most of the experiments the manikin was dressed in the tight summer outfit (T-shirt, trousers, underwear, socks and shoes) which is equivalent to clo value 0.7. The manikin's body consisted of 17 independently heated and controlled body segments with a dry heat loss and the surface temperature close to that of an average human body in a state of thermal comfort under a given thermal environment and clothing insulation. In the case when the breathing was studied, the thermal manikin was connected to a system of artificial lungs, previously described by (Melikov and Kaczmarczyk, 2007). A typical respiration flow cycle was adopted (2.5 s inhalation, 2.5 s exhalation, 1 s break), with the breathing frequency of 10 times/min and the pulmonary ventilation of 6 liters/min. The exhalation flow was heated to 34 ˚C (Höppe, 1981) to provide a density of exhaled air close to that of a human being (1.14 kg/m^3). The flow was discharged horizontally in case of mouth exhalation and deflected 40˚ downwards from the horizontal axis in case exhalation though the nostrils. Overall, the respiratory boundary conditions corresponded to breathing parameters of an average occupant performing light sedentary tasks. More details can be found in Melikov (2004). The thermal manikin was calibrated prior to the experiments.

7.2.3 Experimental equipment

The air temperature measurements were performed with thermistors with time constant of 0.16 s (63% value). The sensors were not overheated by the measuring current (5 μA), which gave

dissipation power of 2.4 μW. The sensors were carefully calibrated prior to the experiments with a reference to the medical thermometer and the measuring error was less than ±0.1 K. The mean sampling frequency of the sensors (16 Hz) was above typical frequencies of turbulent eddies in various indoor spaces (Hanzawa et al. 1987). The thermal manikin was used to accurately measure the surface temperature of each body segment. Each body segment had independent control system which calculated the average surface temperature of the entire segment by measuring resistance of the nickel wire placed below the skin. Therefore, the surface temperature at particular point of interest was determined based on the average surface temperature of that body segment. To measure the carbon dioxide (CO_2) concentration from exhaled air, the CO_2 instruments (PS331) were used that have a high sampling rate of 4 Hz (Bolashikov et al. 2012). The CO_2 sensors were used to measure concentration in exhaled air of a real human subject.

7.2.4 Experimental conditions

Below the thermal manikin, a wooden horizontal plate (dimensions 2.0 x 1.54 m^2) was placed in order to prevent the low-velocity supply air from affecting the CBL induced by the thermal manikin (Figure 7.1). The purpose of the ventilation system was, therefore, to maintain the constant room air temperature without affecting the airflow in the vicinity of the manikin. The measurements, performed at several locations around the unheated manikin with omnidirectional thermal anemometers (SENSOR; ±0.02 m/s accuracy), showed that the natural free convection around the manikin was induced only due to the manikin's convective heat release, without disturbances by the surrounding flows. As all the measuring equipment was placed outside the chamber, the manikin was the only active heat source present in the chamber.

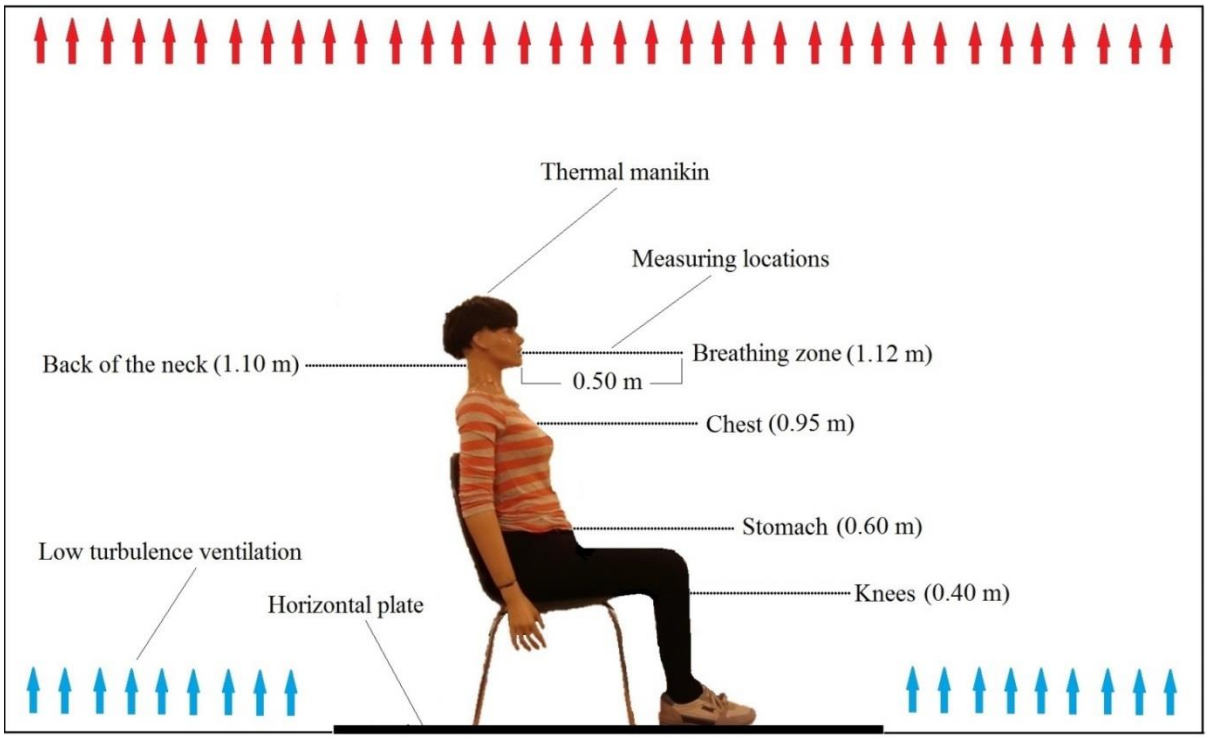

Figure 7.1 Cross section of the climate chamber and measurement locations.

Firstly, the impact of the room air temperature on the air temperature distribution in the CBL was examined for three cases: 20, 23 and 26 ºC. The air temperature was measured at five locations around the unclothed surface of the thermal manikin: breathing zone, chest, stomach, knees and back of the neck, as shown in Figure 7.1. Secondly, the impact of a seated body inclination angle was examined when the thermal manikin was leaned 25 ˚ forward and 25 ˚ backwards, and the results were compared with that of an upright seated posture. This experimental setup was previously adopted in Chapter 3. In this case, the measurements were performed in the breathing zone and at the back of the neck of the manikin, while the air temperature in the chamber was maintained at 23 ºC. Thirdly, the impact of the respiration flow was examined in relation to the air temperature distribution in front of the thermal manikin and in relation to the air temperature and CO_2 distribution in front of a real human subject. Two breathing modes were examined: exhalation through the nose and exhalation through the mouth; and the air temperature in the chamber was again kept at 23 ºC. Lastly, to determine the extent to which experiments with breathing thermal manikin were realistic, the additional

measurements were performed with a real human subject. The experimental conditions were kept identical in both cases. Both the manikin and the human subject had a very similar body shape and size (height: manikin – 1.70 m; human subject – 1.69 m), the same attire design (equal clo value), and seated in the same posture. The human subject was asked to keep as still as possible during the measurements and during achieving steady state conditions. A summary of air temperature measurements is enclosed in the Table 7.1.

Table 7.1 Summary of the air temperature measurements with 10 scenarios of TBL in front of the seated thermal manikin

Parameter	Scenario	Measuring site	Details
Room air temperature	20 ºC	Breathing zone, Chest, Stomach, Knees, Back of the neck	Nude unwigged manikin
	23 ºC	Breathing zone, Chest, Stomach, Knees, Back of the neck	Nude unwigged manikin
	26 ºC	Breathing zone, Chest, Stomach, Knees, Back of the neck	Nude unwigged manikin
Seated body posture	Upright	Breathing zone, Back of the neck	
	Leaned forward	Breathing zone, Back of the neck	25 º from the vertical axis
	Leaned backwards	Breathing zone, Back of the neck	25 º from the vertical axis
Breathing	Manikin nose exhalation	Breathing zone, Chest, Stomach	
	Manikin mouth exhalation	Breathing zone, Chest, Stomach	
	Person nose exhalation	Breathing zone, Chest, Stomach	Supported by CO_2 measurements
	Person mouth exhalation	Breathing zone, Chest, Stomach	Supported by CO_2 measurements

Figure 7.2 The outlook of the thermal manikin and a real human subject.

The air temperature measurements were simultaneously recorded: (i) at one point at a given body height; and (ii) at several body heights. The measurements took place along 0.5 m horizontal distance from the surface (Figure 7.1). This distance was chosen to exceed the thickness of the CBL of an occupant, as shown in Chapter 3 and in several other studies [Datla and Glauser, 2009; Clark and de Calcina-Goff, 2009]. Each measurement location was aligned with the central vertical plane of the manikin, except in case of the knees where the sensor was aligned with the vertical axis of one leg. At each measurement height, the sensor was positioned in total at 34 locations along the horizontal line. At the first measurement point, the temperature sensor was positioned at 2 mm distance from the surface of the manikin. When the manikin was dressed in a tight clothing outfit the temperature was measured starting from the clothing surface and there was no gap between the skin and the clothing. When the air temperature was measured in the breathing zone, the first measurement point of the sensor was placed between the upper and the lower lip of the manikin. Close to the manikin's surface where the highest thermal gradients occurred, fine measurements were performed with the following distances from the surface in millimeters: 2, 4, 6, 8, 10, 13, 16, 19, 22, 25, 30, 35, 40, 45 and 50. As the

sensor was moved further from the surface, the distance between two measurement points was set to be progressively coarser due to a smaller thermal gradient. In this region, the measurement intervals ranged from 10 mm (from 50 to 100 mm distance from the surface); 20 mm (from 100 to 300 mm) and 50 mm (from 300 to 500 mm). In the experiments that involve CO_2 concentration measurements, an identical experimental design was adopted.

The temperature sensors were precisely moved from the manikin by means of a custom-built traverse system controlled from outside of the chamber through a small opening in the wall. In this way, the experimental time was drastically shortened since the experimenter does not need to enter the chamber between two consecutive measurements and disturb the steady conditions.

7.2.4 Data analysis and measurement error

The air temperature measuring time at each point was 150 s and the results were averaged. As the sampling frequency was relatively high (16 Hz), this was more than sufficient time above which variation in air temperature between two repeated averaged measurements became negligible (<1%). In addition, the standard deviation of the air temperature fluctuations was determined in each measurement point based on 2400 air temperature recordings. For the experiments that involve the real human subject, the CO_2 data were recorded simultaneously with the air temperature measurements. Given the high sampling frequency of CO_2 sensors (4 Hz), the measuring time of 150 s at each point (600 recordings) was sufficient to provide a relatively low variation in the repeated measurement results (15%).

The thickness of the TBL was defined to determine the rate of the temperature drop from the surface to the region of undisturbed room air. For the purpose of this study, it was assumed that the outer edge of the TBL (thickness) extends to a distance where the air temperature drops 90% from the temperature of the surface of the body to the temperature of the room air. The air temperature at the outer edge of the TBL was determined as follows:

$$T_{TBL} = T_{surf} - 0.9 \cdot (T_{surf} - T_{amb})$$

The results of air temperature obtained with temperature sensors and the manikin were validated with a medical (mercury) thermometer which is considered the most accurate thermometer available on the market. The temperatures obtained with temperature sensors and thermal manikin had minimal discrepancy with that obtained with medical thermometer (<0.1 ˚C). The measurement error in the experiments where a real human subject was involved was estimated based on repeatability of the results (15%).

7.3 Results and discussion

Occupant's thermal sensation depends on the skin temperature and the rate at which it is changed. The skin temperature and the rate of its change depends on the air temperature enveloping a human body which further depends on number of factors such as room air temperature, thermal stratification, air distribution and magnitude in the vicinity of an occupant, clothing insulation, body posture, breathing, etc. The following paragraphs present the findings on the TBL investigation as a function of the room air temperature, seated body inclination angle and the human respiratory flow.

7.3.1 Impact of the room air temperature

Figure 7.3 shows the impact of the room air temperature and the clothing insulation on the average surface temperature distribution for 17 body segments of the thermal manikin. As seen, at the elevated temperature of the room air, the surface temperature increased. Increasing the room air temperature from 20 to 23 and 26 ˚C, linearly increased the average surface temperature from 31.7 to 32.6 and 33.5 ˚C, respectively. Thereby, the total heat output changed from 87 to 70 and 55 W/m^2, respectively. The tight summer clothing and the wig increased the

temperature of body surfaces where the additional insulation was introduced, especially at the feet and the top of head. Adding the clothing insulation reduced the heat output from the manikin from 70 to 56 W/m^2, at 23 ˚C room air temperature. It should be noted that the results of surface temperature distribution will be different for the manikins with different number of body segments.

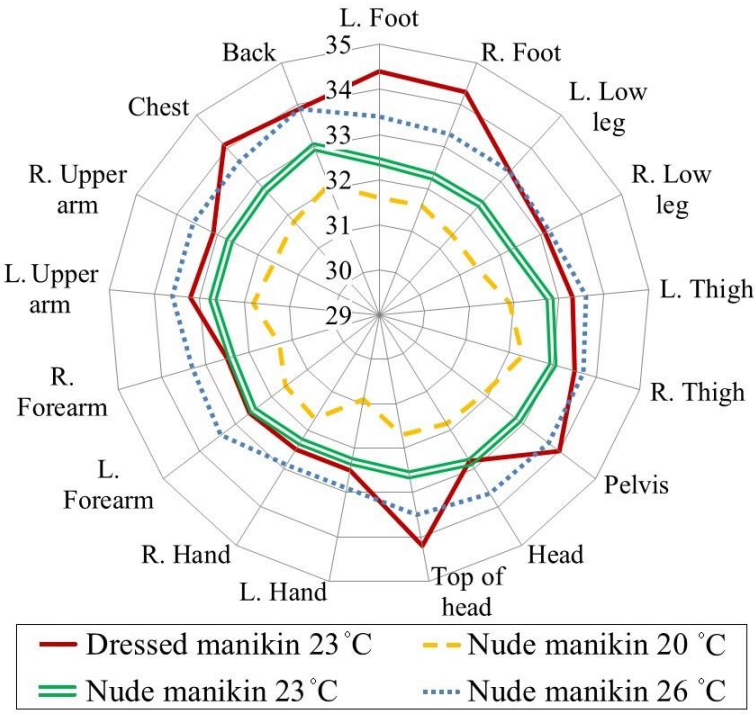

Figure 7.3 Manikin surface temperature distribution – Impact of the room air temperature and clothing.

Figure 7.4 shows the average air temperature (left) and the standard deviation of the temperature fluctuations (right) profiles of the TBL along the horizontal line in front of the mouth (top) and the chest (bottom) at different room air temperatures. In both cases, the air temperature was the highest very close to the surface and dropped rapidly as the distance from the manikin increased. Reducing the room air temperature from 23 to 20 ˚C decreased the manikin's surface temperature by 0.9 ˚C, but the temperature difference between the warm surface of the body and the room air increased by 2.1 ˚C. The standard deviation of temperature fluctuations was the highest at lower room air temperature. This is attributed to increased

turbulence and instability of the convection flow at the lower room air temperatures (Voelker et al. 2014; Chapter 3). The finding that standard deviation of temperature fluctuations becomes lower at increased room air temperature can be directly correlated with the finding that the velocity of the CBL decreases at elevated room air temperature. The peak velocity in the breathing zone of a nude sitting manikin drops by 27% (from 0.22 to 0.16 m/s) when the room air temperature increases from 20 to 26 ˚C (Chapter 3). At the same room air temperature change, the peak standard deviation of temperature fluctuations measured in the breathing zone dropped by 25% (from 0.76 to 0.57 ˚C), which suggest a solid correlation between the flow velocity and standard deviation of temperature fluctuations.

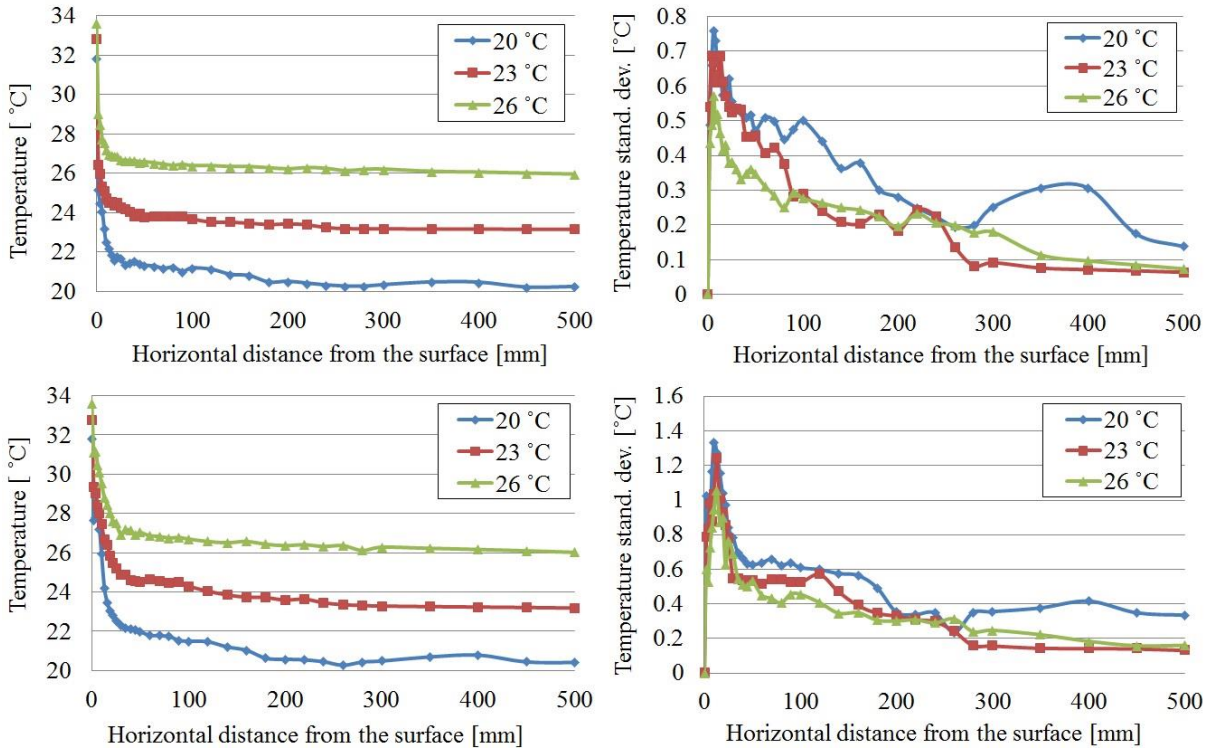

Figure 7.4 Average air temperature (left) and standard deviation of air temperature fluctuation (right) distribution in the breathing zone (top) and at the chest (bottom) – Impact of the room air temperature.

Figures 7.4 also shows that the standard deviation of the temperature fluctuations was the highest near the surface of the manikin and it decreased with increased distance from the surface. The recordings of air temperature fluctuations measured at different distances from the

chest are presented in more detail in Figure 7.5. As seen, the large air temperature fluctuations of were recorded at 10 mm from the chest, which decreased with increased distance from the surface, as shown for 50 and 500 mm distances. These findings are in line with the findings of Melikov and Zhou (1996) that the highest air temperature fluctuations occur close to the surface of the body, both in quiescent and ventilated environment. Apart from air velocity fluctuations, the increased air temperature fluctuations may be generally important to consider for occupant's draught sensation and its assessment (Madsen and Popiolek, 1994; Melikov et al. 1997). The dynamic discharge of the cold thermo-receptors that are located just below the human skin depends on the temperature fluctuations of the receptors. The temperature fluctuations of the receptors depend on the air temperature fluctuations near the skin. Therefore, the large unsteadiness of the air temperature increases the temperature fluctuations of the receptors and activates their dynamic response, which can increase the sensation of draught discomfort (Fanger et al. 1988).

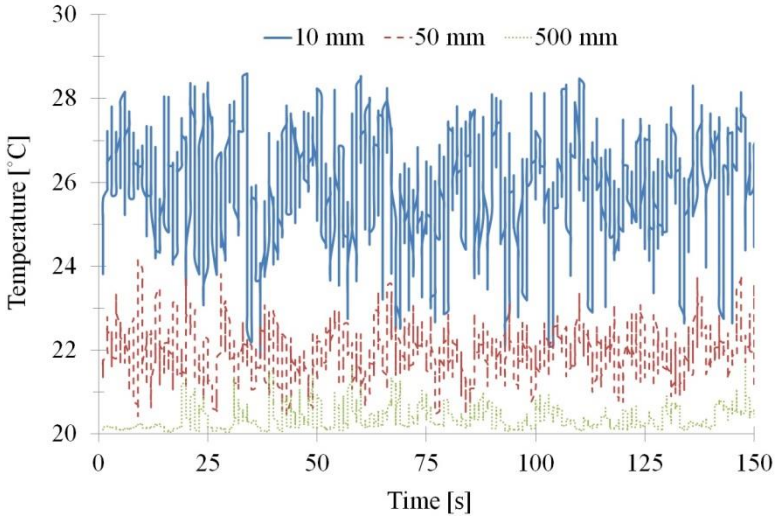

Figure 7.5 Air temperature fluctuations in front of the chest of a thermal manikin at 20 ˚C room air temperature measured at distances from the surface: 10, 50 and 500 mm.

The air temperature decay (left) and the standard deviation of the temperature fluctuations (right) profiles measured at different heights of the thermal manikin are compared in Figure 7.6. Figure 7.7 compares the thickness of the TBL for different locations of the thermal manikin

and is enclosed as supplementary information. At the height of the knees, the air temperature reached the room air temperature outer edge of the temperature boundary layer at the minimal distance from the surface compared to other body segments (Figures 7.6 and 7.7), which supports the findings of Murakami et al. (1997). This can be explained with understanding the nature of the convection flow around the human body. At the lower leg region, the CBL is laminar and closely follows the contours of the legs with the velocity of about 0.05 m/s (Lewis et al. 1969; Chapter 3). Therefore, the air that takes away the convective heat from the knees spreads little, which explains the sharp air temperature drop and the lowest standard deviation of temperature fluctuations in that region. With increasing the height, the CBL accelerates due to buoyancy effects and increase in thickness (Homma and Yakiyama, 1988), which explains less sharp air temperature decay profile in front of other body parts, especially in front of the chest and in front of the stomach. In this case, the additional airstream detached from the thighs and lower legs (Chapter 3), which warmed the air in front of the manikin and increased the standard deviation of temperature fluctuations and the thickness of the TBL. The air temperature at 50 mm in front of the stomach was 25 ˚C, which was 1.7 ˚C above the air temperature measured at the same distance in front of the knees. The large peak standard deviation up to 1.2 ˚C was recorded in the region of the chest, while in the region of the knees it dropped to 0.4 ˚C. The distance from the surface of the knees at which the peak standard deviation of temperature fluctuations were was achieved was at 6 mm at the level of the knees, which was less compared to 13 mm distance in case of the chest and knees. This can be explained with a laminar flow regime near the surface of the knees and highly turbulent airflow at the height of the chest.

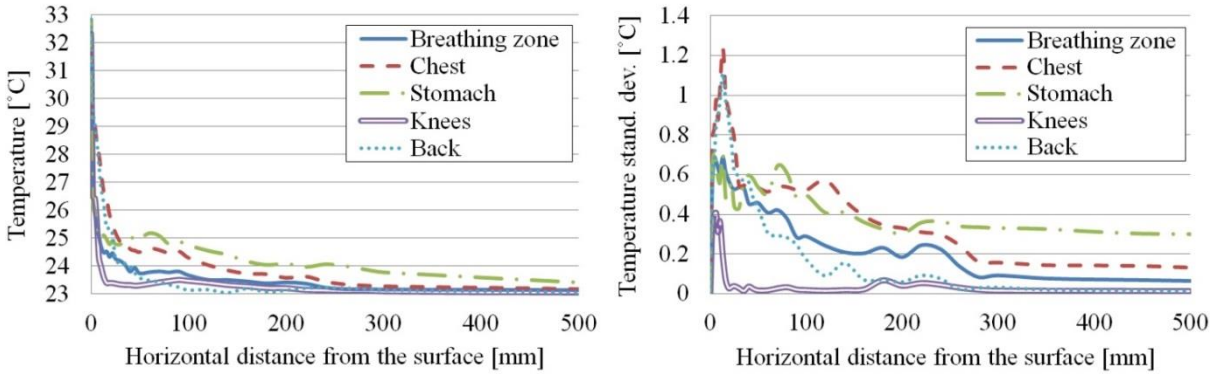

Figure 7.6 Average air temperature (left) and the standard deviation of air temperature fluctuations (right) distribution at different heights of the body at 23˚C room air temperature.

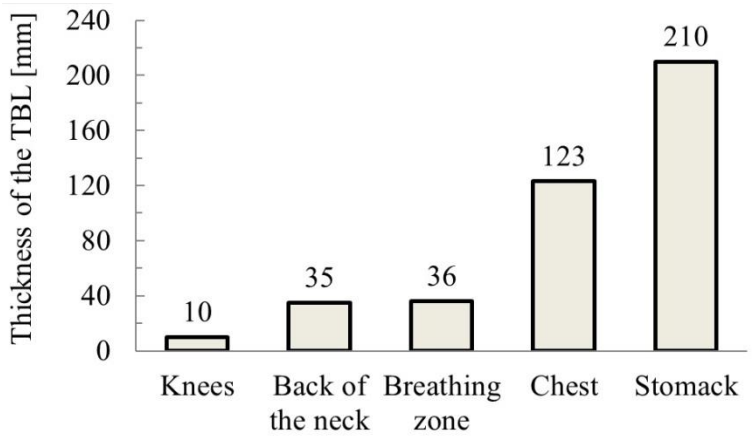

Figure 7.7 Thickness of the TBL for different location of the thermal manikin.

7.3.2 Impact of the seated body inclination angle

Figure 7.8 shows the impact of a seated body inclination angle on the air temperature distribution and the standard deviation of temperature fluctuations in the breathing zone and at the back of the neck of the manikin. The manikin, when leaning backwards, caused the lowest air temperature drop and the highest standard deviation of temperature fluctuations in the breathing zone, compared to the case of an upward or forward body posture. These findings can be explained by the velocity distribution in the CBL under the same experimental conditions, described in Chapter 3. As explained, the manikin leaned backwards increases the velocity in the breathing zone, since the blocking effect of the chin for the rising CBL is reduced. In addition, the body inclined backwards at the angle of 25 ˚ increases flow

detachment from the front surface of the body which inevitably lead to increased air temperature and its standard deviation in the breathing zone. As seen on Figure 7.8, in case of backward leaning, the temperature of undisturbed room air of 23 ˚C was approached only at 0.5 m distance from the surface. The opposite but milder effect was present when the air temperature and its standard deviation were measured at the back of the neck of the manikin.

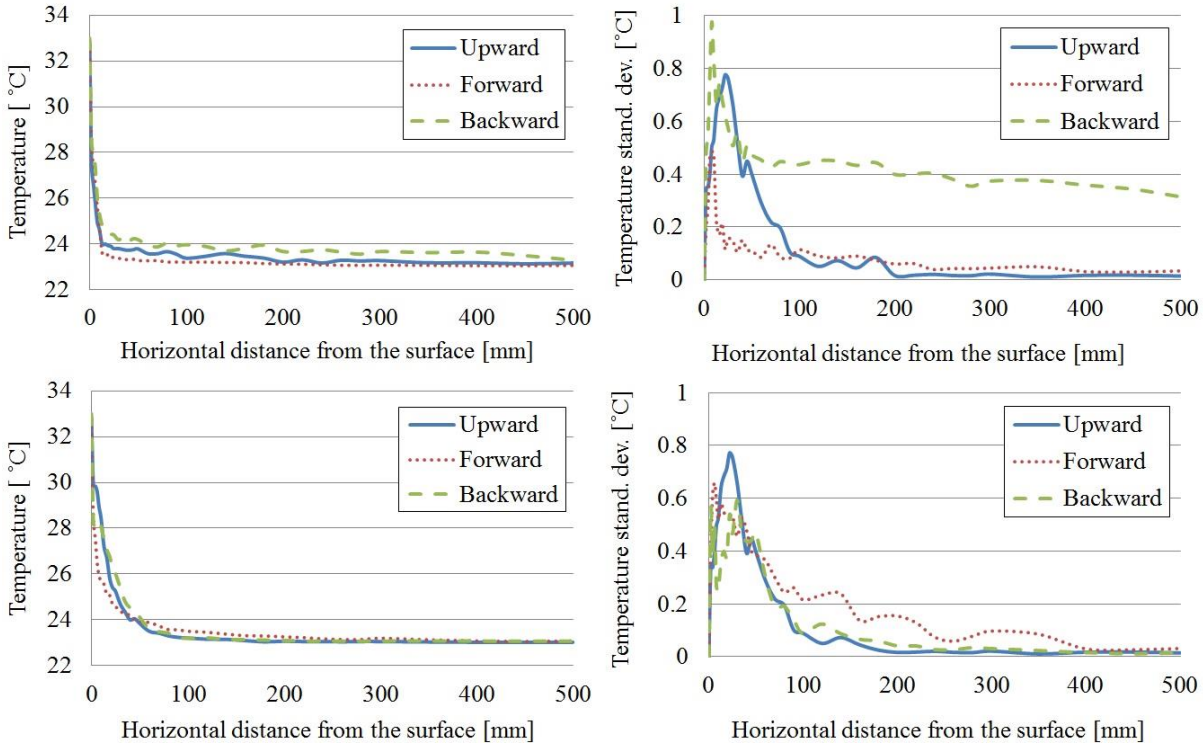

Figure 7.8 Average air temperature (left) and standard deviation of air temperature fluctuation (right) distribution in the breathing zone (top) and the back of the neck (bottom) – Impact of seated body inclination angle.

In Chapter 3 it was reported that changing the body posture from leaned forward to leaned backwards increases the peak velocity in the breathing zone by 99% (from 0.093 to 0.185 m/s). In the present chapter, the peak standard deviation of temperature fluctuation in the breathing zone increased by 104% (from 0.49 to 1.0 ˚C), which again demonstrate a good correlation between the standard deviation of temperature fluctuations and the velocity of the flow. This finding is in line with that reported by Melikov et al. (1997). Similar to the air temperature fluctuations, the velocity of the flow and the frequency of the velocity fluctuations are also

important because they change the heat flux through the skin and modify the temperature of receptors below the skin.

Figure 7.9 shows the calculated thickness of the TBL as a function of the room air temperature, clothing and seated body inclination angle. At the given room air temperature, the higher thickness of the TBL was recorded in the chest region than in the breathing zone, which is in line with the findings of Homma and Yakiyama (1988). The thickness of the TBL increased when the room air temperature decreased. This finding suggests that at different room air temperatures, the thickness of the TBL changes in an opposite manner from the thickness of the CBL, which expands at elevated room air temperature, as suggested in Chapter 3. At the lower room air temperature, the temperature difference between the thermal manikin and the room air was higher, and therefore, the air temperature approached the outer edge of the TBL at increased distance from the surface, i.e. the thickness of the TBL increased. Analogously, as the clothing insulation naturally decreased the temperature difference between the warm surface and the surroundings, it also decreased the thickness of the TBL. At both locations studied (breathing zone and chest), the thickness of the TBL showed the same pattern change. In the case of backwards-seated body inclination, the thickness of the TBL increased due to reduced decay rate of the air temperature in front of the manikin. The opposite effect was found in case of the forward body inclination.

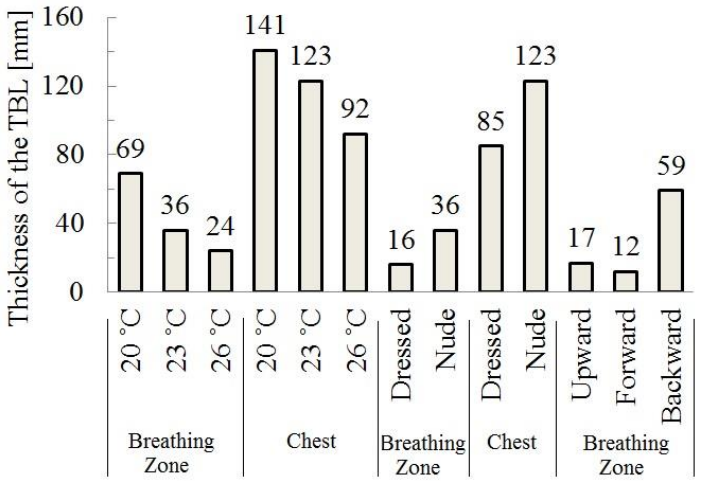

Figure 7.9 Thickness of the TBL as a function of the room air temperature, clothing and seated body inclination angle.

7.3.3 Impact of the human respiratory cycle

The impact of two respiratory cycle modes (nose and mouth exhalation) on the air temperature and the standard deviation of the temperature fluctuations profiles are presented in Figure 7.10. In addition, the Figure 7.10 shows the relative difference in results obtained with a breathing thermal manikin and a real human subject. Figure 7.11, in addition, shows the recordings of air temperature fluctuations measured at 25 mm distance in front of the manikin's mouth for two breathing modes. As seen on Figure 7.10, the respiratory cycle increased the air temperature in the breathing zone in front of the manikin and the human subject. The differences in the results between the manikin and a real person were small and within measurement accuracy due to increased measurement error in experiments that involve both the manikin and the human subject. In the breathing zone where the air temperature was measured at the height of the mouth, the exhalation through the mouth created a continuous air temperature drop with increased distance from the surface. This effect was present in both cases of the thermal manikin and a real person. The exhalation through the nose, however, generated the peak air temperature at 20-30 mm distance from the surface, as the exhalation jets by-passed the region very close to the mouth. This is obvious from Figure 7.11, that shows larger air temperature

fluctuations at 25 mm distance from the mouth of the manikin exhaling through the nose (standard deviation = 2.44 °C), compared to the manikin exhaling through the mouth (standard deviation = 1 °C). It can also be observed from Figure 7.10 that the respiratory cycle disturbed both the air temperature and the standard deviation at the breathing zone height far greater than at the height of the chest. This finding is expected in the case of mouth exhalation, since the exhaled flow forms a single jet that quickly rises after being expelled (Özcan et al. 2005; Nielsen et al. 2009). In the case of nose exhalation, however, the two separate jets are discharged downwards from the nostrils at 40˚ angle from the horizontal axis and at an intervening angle of 30˚ (Hyldgaard, 1994). This suggests that jets from the nostrils did not interact with each other and their separation explains why the air temperature change was not detected at the height of the chest. The standard deviation of the temperature fluctuations showed a similar trend to the air temperature profile, as shown in Figure 7.10 (right). The exhalation through the nose generated the large standard deviation of temperature fluctuations of up to 2.9 ˚C close to the mouth of the person, while in the chest region it was less than 1 ˚C.

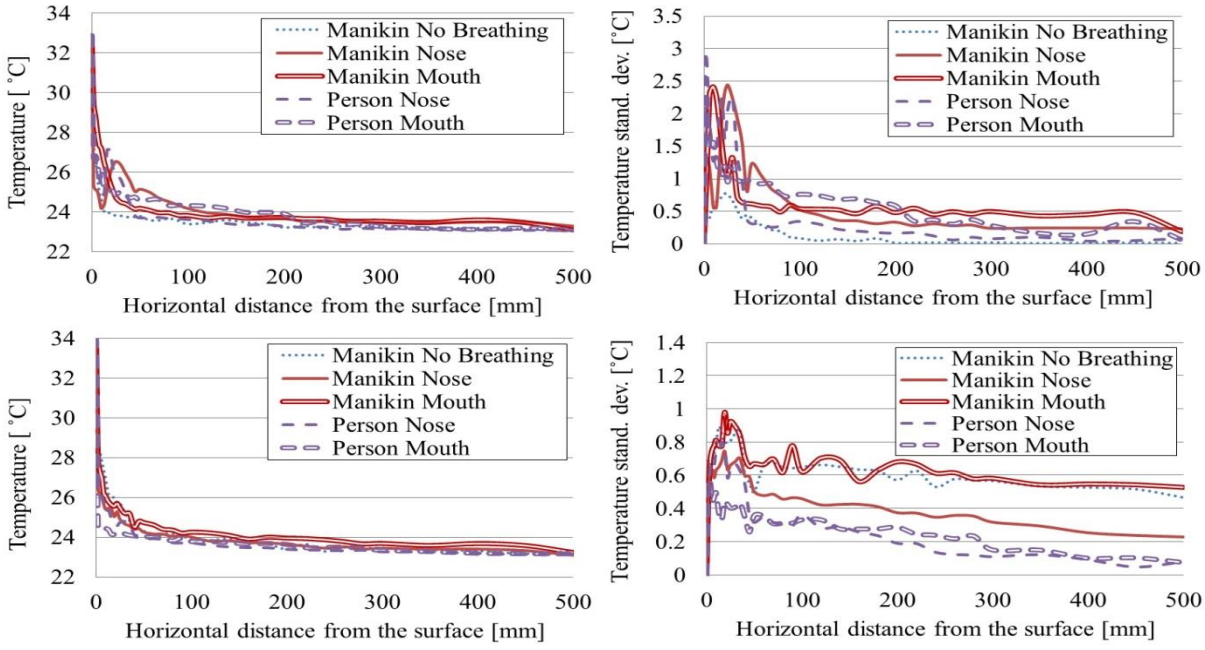

Figure 7.10 Average air temperature (left) and standard deviation of air temperature fluctuation (right) distribution in the breathing zone (top) and at the chest (bottom) of the breathing thermal manikin and a real human subject – Impact of the human respiratory cycle.

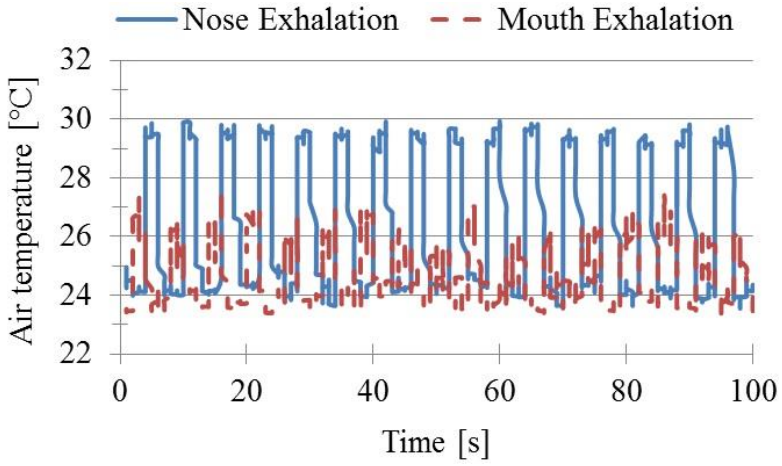

Figure 7.11 Air temperature fluctuations measured at 25 mm in front of the mouth of the thermal manikin for two breathing modes: Nose exhalation and mouth exhalation.

Simultaneously with the air temperature measurements in front of a real human subject, the CO_2 measurements were performed under the identical experimental conditions. Figure 7.12 shows the average CO_2 concentration distribution in front of a real person as a result of airflow interaction between the CBL and the human respiration. On the top of Figure 7.12, it can be seen that the average CO_2 concentration had the same profile as the air temperature (shown in Figure 7.10, top) for both breathing modes. Similar to the air temperature, the CO_2 level steadily dropped when the person exhaled through the mouth. In case of nose exhalation, the flow reached the peak concentration at the distance of 20-30 mm from the surface. At the chest of a person exhaling through the nose (Figure 7.12, bottom left), a detectable CO_2 concentrations were observed, peaking at 690 ppm at 0.28 m distance from the surface. This suggests that part of the exhaled jet could reach that region, even though this could not be detected with the air temperature measurements. The CO_2 concentration in the stomach region was minimally disturbed (Figure 7.12, bottom right), which suggest that the exhalation jets could not penetrate to that region. Based on the obtained results (Figures 7.10 and 7.12), it may be suggested that the exhalation jets from the nose by-passed the central vertical plane in front of the chest and mixed with the free convection flow below the height of the chest, reaching

the temperature of the mixed airflow. This explains the undisturbed air temperature profile and the increased concentration of CO_2 at the height of the chest.

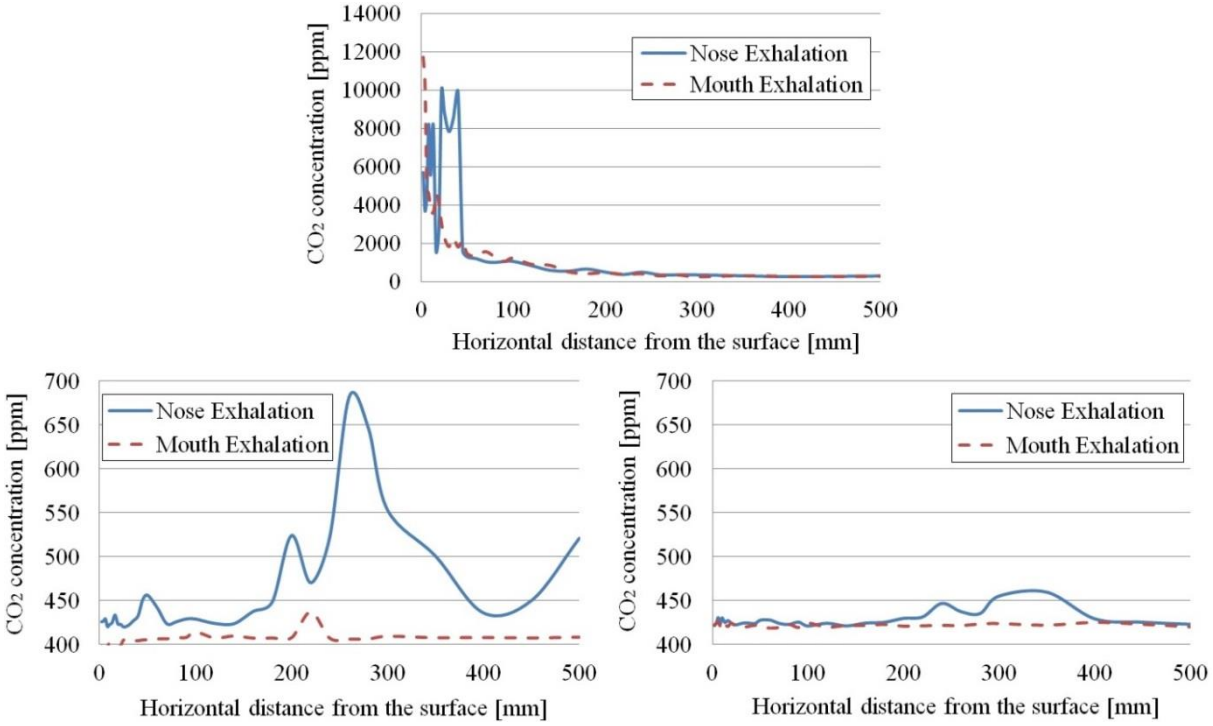

Figure 7.12 Average CO_2 concentration distribution in front of a real person at three different heights: breathing zone (top); chest (bottom, left) and stomach (bottom, right) – Impact of a human respiratory cycle.

7.4 Conclusions

This part of study investigated air temperature field around the human body in a quiescent indoor environment. The air temperature distribution around the human body was examined in relation to the room air temperature, seated body inclination angle and the human respiratory flow. The experimental results reveal the following:

- The standard deviation of the air temperature fluctuations increased when the room air temperature decreased. The air temperature fluctuations also increased closer to the surface of the body. The large standard deviation of air temperature fluctuations tends to be present when the velocity in the convective boundary layer increases;

- The air temperature and the standard deviation of the air temperature fluctuations at the level of stomach and chest were higher than at other body parts, due to additional convection flow that rises from the thighs and lower legs. The respiratory flow caused the highest standard deviation of temperature fluctuations up to 2.9 ˚C;
- The thickness of the TBL was wider at the level of the chest than in the breathing zone. The TBL also increased at elevated room air temperatures, reduced clothing insulation and when the body was leaned backwards;
- The person leaned backwards increased the air temperature and the standard deviation of air temperature fluctuations in the breathing zone;
- Coupling the air temperature and concentration measurements indicate that the exhaled jets from the nose by-passed the central vertical plane in front of the chest and penetrated the region below the chest; and
- The results recorded in front of the thermal manikin showed a good agreement with the results obtained with a real human subject.

CHAPTER 8: OVERALL DISCUSSION

This chapter is designed to discuss the relationships between airflow characteristics in the occupied spaces and personal exposure. These relationships are discussed as a function of several parameters studied such as the room air temperature, body posture, thermal insulation, table positioning and ventilation flow. The practical implications are discussed in relation to the optimal air distribution in occupied spaces with emphasis on indoor air quality, thermal comfort and energy.

Figure 8.1 presents temperature, velocity and concentration profiles in the breathing zone of a seated thermal manikin at the room air temperature of 23 ˚C. The results are taken from Chapters 3, 5 and 7 and merged for the purpose of direct comparison of main parameters investigated in this study. As seen on Figure 8.1 (top), typical velocity and temperature profiles are developed that are inherent for airflows near a vertical heated surface. The highest velocity gradients occured within 10-20 mm distance from the mouth due to the increased convective heat transfer. After reaching its peak at 17 mm distance from the surface, the velocity steadily dropped until it reached the velocity of undisturbed room air (not shown), which is defined with a value of 0.05 m/s in our study. The temperature decrease was also the highest within 10-20 mm next to the surface due to increased heat exchange, but dropped at substantially slower pace beyond that distance. This suggests that the thickness of the velocity boundary layer (i.e. CBL) is bigger than the thickness of the temperature boundary layer. For instance, the measured thickness of the CBL in front of a nude manikin at the room air temperature of 20 ºC was 0.45 m, while the thickness of the temperature boundary layer was 0.069 m in the same case. The results of this study show that both the velocity and temperature profiles near the heated surface can be modified by number of factors such as height of the body, room air temperature, body posture, thermal insulation, table positioning and ventilation flow.

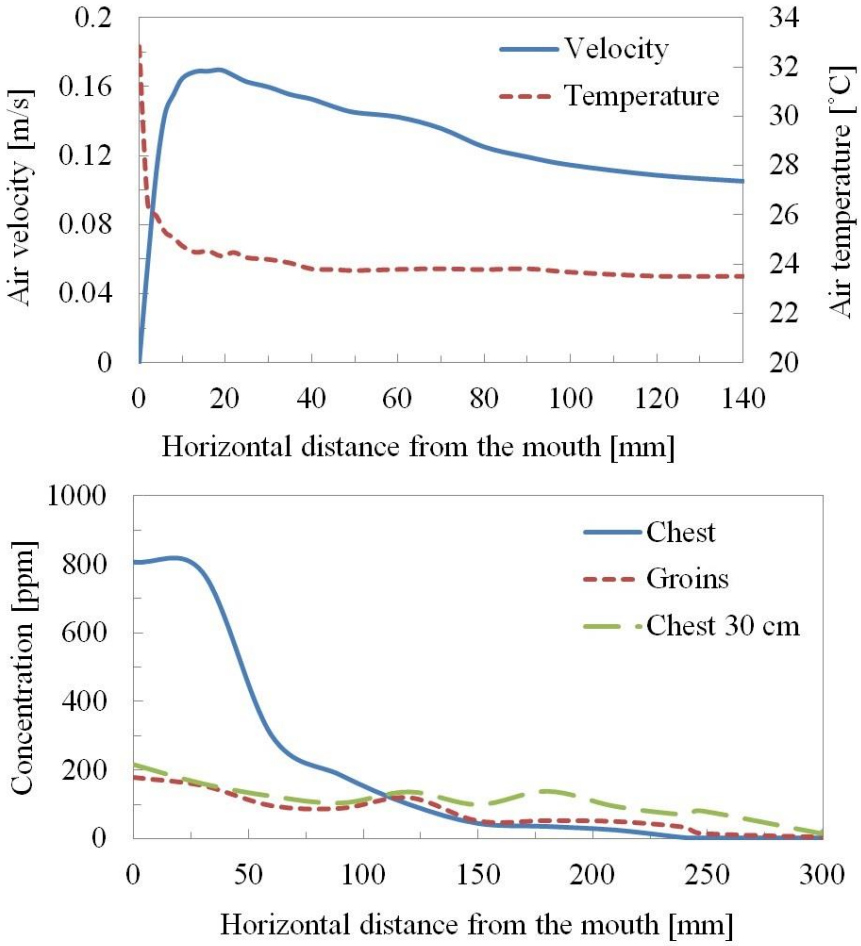

Figure 8.1 Temperature and velocity profile (top) and concentration profile for different source locations (bottom) in the breathing zone.

Figure 8.1 (bottom) compares the three concentration profiles of the tracer gas in the breathing zone of the thermal manikin, when the source is located at the chest, at 30 cm distance in front of the chest and at the groins. For the each source location, the highest concentration is achieved at the surface of the mouth. As seen, the concentration profile cannot be easily defined, which is not the case with the velocity and temperature profiles. This is because the pollution concentration profile depends on both the airflow characteristics of the CBL and the location of the pollution source. As seen in Figure 8.1 (bottom), when the pollution is emitted at the chest, the sharp concentration decay profile occurred near the mouth. When the pollution originated at 30 cm distance from the chest or at the groins, the concentration was the highest in the breathing zone and dropped relatively little until it reached the region of unpolluted

surrounding air. The results suggest that the human CBL has the ability to transport the pollution not only in vertical direction from the groins/chest to the breathing zone, but also in horizontal direction (from Chest 30 cm). These results are also important from the cross-contamination point of view because there is a discrepancy between the thickness of the CBL and the extent to which the pollution spreads within the CBL. The thickness of the CBL in the breathing zone of the nude manikin at the room air temperature of 20 ºC was 0.45 m, while the thickness of the PBL changed with the source location and can vary from 0.122 m when emitted from the chest, to 0.253 m when emitted at the groins. Therefore, as the extent to which pollution spreads within the CBL can vary, the interaction between convection flows of occupants positioned close by may not cause cross-contamination. These findings could be crucial to consider in densely occupied environments (hospitals, schools, offices, vehicles, etc.), where people are physically close to one another.

8.1 Room air temperature

The room air temperature is important not only from the point of view of thermal comfort, but also because it impacts the airflow characteristics around the human body and the pollution distribution. In previous chapters it has been established that at the lower room air temperature, the CBL has a higher velocity which increases its ability to transport the pollution to the breathing zone. The increase of the room air temperature from 20 to 26 ºC reduced the peak velocity in the breathing zone of a nude seated person by 33% (from 0.24 to 0.16 m/s). The same temperature change reduced the ability of the CBL to transport the pollution from the chest by 30%, since the inhaled concentration dropped from 908 to 639 ppm, as shown in Chapter 5. Analogously, the elevated room air temperature dissolved the CBL more compared to the lower temperatures (see Figure 3.9), which also caused more extensive spread of the

pollution. When the room air temperature increased from 20 to 26 ºC, the thickness of the PBL expanded from 122 to 174 mm, when the pollution is located at the chest. Although increased room air temperature reduced personal exposure to pollutants released from occupant's body, it also increased the thickness of the PBL which can increase the probability of cross-flow and cross-contamination among occupants. This is especially important to consider in densely occupied indoor environments such as schools, theatres, public transports, etc., where occupants come into closer physical proximity. In practical terms, the pollution emitted from the feet of a seated occupant is pulled upwards by the CBL and, due to its increased diffusion to the surroundings at elevated air temperatures, it may more easily end up in the inhalation zone of an occupant seated nearby.

On the other hand, if the source of clean air resides in the lower room levels, the CBL can entrain it and increase the amount of clean air being inhaled. Rooms equipped with displacement air distribution are designed based on this principle. Thereby, lower temperature of the supply air will induces the stronger CBL which will further increase the inhaled air quality. In practice, however, the displacement ventilation systems are often coupled with chilled ceilings (Riffat et al. 2004), that allow higher dry bulb temperature design without compromising thermal comfort (Jeong and Mumma, 2006). As a result, the ability of the CBL to transport the clean air to the breathing zone decreases, as the chilled ceiling increases the radiant heat loss from the human body up to 50% (Kulpmann, 1993). This reduces the human convective heat loss (weaker CBL), which further reduces the amount of the clean air transported to the breathing zone. These findings suggest that the room air temperature can be used to control the amount of the transported pollution or clean air to the breathing zone. In practice, however, the room air temperature set point usually aims to satisfy the thermal comfort requirements without considerations given to human exposure.

8.2 Body posture

As shown in Chapter 3, the standing manikin created a narrow CBL in front of the body (0.09 m) which is 5 times less thick compared to seated manikin (0.45 m) at 20 ˚C room air temperature. The narrower CBL has a smaller entrainment area for the surrounding air which suggests that it is likely to entrain smaller amount of polluted/clean surrounding air and transport it to the breathing zone. In parallel, due to a narrow CBL of a standing person, the transient flow of exhalation could more easily penetrate the CBL and spread across the space. Understanding the airflow and pollution transport around a seated person is more beneficial as most of the building occupants are predominantly seated during the day (Pokora and Melikov, 2014).

The inclination angle of a seated body is important factor for optimal design of microenvironment at the table because it affects the velocity, temperature and pollution distribution in the breathing zone of a person. Changing the posture from upright to 25˚ backward body inclination simultaneously increased the peak velocity in the breathing zone by 8.8%; the peak air temperature fluctuations in the breathing zone by 25%; the personal exposure by 15.5% and the thickness of the PBL in the breathing zone by 43% when the pollution is located at the chest. In practical terms, for an optimal design of the personalized ventilation located in front of the occupant, the backward seated body inclination will require a higher supply flow rate to penetrate the breathing zone, compared to the forward body inclination. In addition, the pollutants that origin from the human body, or that are entrained by the CBL, will be more easily transported to the breathing zone if the occupant is leaned backwards. The finding suggests that the seated body inclination angle can be used to control the amount of the transported pollution/clean air to the breathing zone.

The seated body inclination angle is challenging to control in practice. Since the workstations' computers and furniture are predominantly static, most of the occupants need to adapt to them visually and physically. Occupants doing computer-related work spend about 75% of the time in forward-leaning or upright seated position (Dowell et al. 2001). On the other hand, the research has shown that leaning backwards is the most preferred sitting posture because it offers several health benefits (Andersson and Ortengren, 2004). In practice, it is possible to design a dynamic workstation with an ability to position the furniture and computers at the distance that will optimally control the strength of the convection flow as the occupant changes its posture. For instance, the occupant that is inclining backwards moves the table surface towards itself, along with the computer display, keyboard and personalized ventilation air terminal device. For an optimal design of the personalized ventilation, the supply diffusers can be designed in such a way to follow the occupants' body movement at the table in order to continuously create a desired microclimate around the human body.

8.3 Thermal insulation

Similar to the room air temperature, the clothing insulation usually aims to satisfy thermal comfort requirements, as well as cultural aspects which sometimes can be counterproductive to thermoregulation. As shown in Chapter 3, the clothing insulation and the hair on the head reduced the heat loss from the human body, which also reduced the velocity of the CBL. These findings, however, need to be carefully interpreted since the results of this study are obtained at fixed room air temperature. In practice, clothing insulation decreases at elevated room air temperatures, while increase in clothing insulation occurs when the indoor temperature set point is decreased. As also shown in Chapter 3, lowering the room air temperature from 26 to 20 ˚C increased the peak velocity in the breathing zone by 50% (from 0.16 to 0.24 m/s). This

contradicts the velocity reduction due to increase of the clothing insulation. The results show that increase of the clothing insulation from thin to thick outfit reduced the peak velocity in the breathing zone drops by 26% (from 0.165 to 0.122 m/s), for the loose clothing design. In addition, the posture of the body and the presence of the chair can change the insulation level provided by the clothing. For instance, a seated occupant has lower thermal insulation due to compression of air layers within the clothing (ASHRAE, 2013a). This decrease in insulation can be compensated by the additional insulation provided by the chair. In addition, body movement decreases clothing insulation by increasing air movement within the clothing, which was not the focus of this study. Therefore, more research on this topic is needed that focus on a mutual influence of factors such as clothing and chair insulation and design, room air temperature, body posture, activity level, etc.

The clothing insulation and the wig can also be important for personal exposure considerations. As the increase of the clo value decreased the strength of the CBL, the ability of the CBL to transport the pollution diminished. This suggests that the additional clothing and hair on the head can serve as a protection against the pollutants detached from the human body/clothing, or other pollutants located at the lower room levels (e.g. polluted carpet and other re-suspended particles) that can become entrained by the CBL. This statement should be carefully interpreted since the clothing itself can be a source of pollution through the shedding process (McDonagh and Byrne, 2014). In some cases, the clothing surface can reduce concentration of some pollutants in the breathing zone, such as in case of chemical reactions between ozone and skin/clothing surfaces (Rim et al. 2009). In this case, ozone reacts with the clothing and the CBL becomes depleted of ozone and enriched with ozone reaction products. On the other hand, as the thickness of the CBL increases with increase of clothing insulation (Homma and Yakiyama, 1988), this may intensify mixing of the pollution within the CBL and increase the pollution spread across the room. The same effect may easily occur if the pollution is located

below the clothing (skin oils, bioeffluents, etc.), where the pollution can diffuse within clothing and spread more equally around the body and across the room. Although the clothing and chair design have smaller impact on the CBL than the level of clothing insulation, the results suggest that they should be considered for the pollution transport since they modify the airflow characteristics close to the surface.

Although the thermal insulation provided by clothing and the wig are parameters that cannot be controlled in practice, the results indicate they are important to be carefully considered in full-scale experiments. These results are also important for numerical predictions, since many researches tend to neglect simulating clothing insulation level and the hair on the head, and thus disregard its impact on the CBL formation. The results also suggest that the chair should also be carefully simulated, as its presence disturbed the surrounding airflows and modified air distribution in occupied spaces, especially in rooms with high turbulent mixing when the air is supplied from below. In the future, it is reasonable to expect appearance of multipurpose clothing design that apart from reducing the heat loss by providing an additional insulation, it can also cools and disinfects the surrounding air and provide thermal comfort and enhance inhaled air quality.

8.4 Table positioning

Similar to the chair, the presence of the table is important for air distribution in the room, especially in the occupied spaces. Based on the results, the table positioned in front of an occupant influenced the CBL to a greater extent than the clothing or the chair and it can be used to control block the convection flow from beneath. The presence of the table can be also used to control personal exposure and the extent to which pollution spreads across the room.

The results show that adding the table in front of an occupant at 10 and 0 cm distance, reduced the velocity from 0.17 m/s to 0.141 and 0.111 m/s, respectively. Although the velocity decreased due to the presence of the table, the ability of the CBL to transport the pollution may not decrease. The table located at 10 cm distance from the occupant increased personal exposure regardless if the pollution is located below or above the table height. This suggests that for personal exposure it is important to consider not only the velocity of the CBL, but also how the pollution is distributed within the CBL, i.e. to understand how the PBL develops. Closing the gap between the table and the occupant created a new and weaker CBL which reduced the transport of pollution released from the chest (by 63.5%) and especially the transport of pollution released from the lower body parts (by 80%). A table contiguous to occupant's body can be also beneficial from the point of view of indoor air quality, if the source of clean air is designed to approach the breathing zone from the front of the body (e.g. personalized ventilation, stratum ventilation, etc.) or from the above (e.g. downward ceiling diffuse ventilation, active chilled beams, etc.). This is because a weaker CBL allows easier penetration of clean air to the breathing zone. On the other hand, having a source of clean that entrains the CBL at the lower leg region (e.g. upward piston ventilation flow, displacement ventilation, underfloor ventilation), the distance of 10 cm between the edge of the table and occupant's abdomen would enhance the air quality, compared to the case with no table or especially if the table touches occupant's abdomen.

Based on findings in this study, it is possible to design and position the table in such a way to be optimized for the desired application, especially in rooms where the location of the pollution or clean air is known. In practice, occupants are not expected to be positioned in a way that their abdomen keeps a fixed distance from the desk all the time. It is possible, however, to control the rising convection flow by attaching the additional board with spring system or sponge/foam plate to the edge of the table that gently presses the abdomen of the occupant

(Bolashikov et al. 2010). In the offices of the future, it is reasonable to expect evolution of the furniture and equipment design that will make the workstations more dynamic and capable of providing individual micro-environmental control that can be used for enhanced airflow and pollutant distribution around the human body.

8.5 Ventilation flow

As earlier mentioned, in most of indoor spaces that operate with high turbulent mixing, the knowledge on the airflow patterns is poor which results in impaired air quality, since the pollutants from unoccupied spaces can be transported to occupied spaces (Melikov, 2011). In addition, the results show that the furniture and other obstacles can substantially alter the air distribution in occupied spaces. Their presence, however, is generally not taken into account in ventilation design practice. The findings of this study show that personal exposure can be minimized by understanding and controlling airflow interaction in occupied spaces, while providing thermal comfort and saving energy.

In chapter 6, it is outlined that the downward ventilation approach may be inefficient in terms of reducing personal exposure, providing thermal comfort and reducing the energy input. The uniform ventilation flow supplied horizontally from behind of the person can also be inefficient as it can increase the exposure to pollutants approaching from in front of a person (e.g. pollution from talking, coughing, sneezing, etc.). The results indicate that regardless whether the airborne pollution is located on the human skin/clothing, or if pollution is entrained by the CBL from the lower room levels or whether if approaches from the surroundings, supplying the clean air horizontally in front of the person can most effectively reduce personal exposure. If the supplied airflow is maintained at the velocity of 0.175 m/s, this airflow direction can also provide thermal comfort at minimum energy input. A further increase of the velocity at the

room air temperature below 23 ˚C may also cause thermal discomfort (ISO 7730, 2005; ASHRAE, 2013a). Nevertheless, at increased room air temperatures, the flow supplied horizontally from the front can provide thermal comfort even at elevated air movement, which is one of the strategies to save energy recommended by some standards. An exception that allows even higher supply air velocity is granted if the velocity of the supplied air can be individually controlled.

The results of this study demonstrate that in some cases increasing the velocity of the supply air can increase personal exposure, if the airflow interactions in occupied spaces are not taken into account. The results also show that a further increase of the velocity beyond certain threshold may not provide additional benefit in terms of personal exposure reduction. This suggests an existence of a non-linear relationship between the amount of supplied air to the room and personal exposure in indoor environments. To minimize personal exposure without compromising thermal comfort and energy savings, it is necessary to understand airflow interaction in the occupied spaces and to be able to control it. The current total volume air distribution principles commonly used in buildings are not able to satisfy these requirements. Therefore, a change in the approach how rooms are ventilated is clearly needed. Based on results of this study, there is a need for an advanced air delivery system that can supply the air from the front side of the person at the velocity that can be optimally controlled to satisfy the requirements for inhaled air quality, thermal comfort and energy. One such system that can be implemented in practice is personalized ventilation system that can supply the air with optimal direction and quantity to the breathing zone for enhanced inhaled air quality and minimized energy input.

CHAPTER 9: CONCLUSIONS, LIMITATIONS AND RECOMMENDATIONS

This study presented the results of experimental investigation of the relationships between airflow characteristics around the human body and personal exposure to airborne pollutants. These relationships were examined in relation to the room air temperature, body posture, clothing and chair insulation/design, table positioning, location of the pollution source and ventilation flow. From the findings stated below, all the study hypotheses have been found to be supported. The main findings of this study can be summarized as follows:

- The human CBL substantially influences the airflow and pollution distribution in occupied spaces. When the pollution source originated from the human body when released in its vicinity, the CBL contributed, to a great extent, to an increase of personal exposure by transporting the pollution to the breathing zone. The presence of the CBL, however, was not sufficient to disturb the cough flow to the level that would cause measurable peak concentration reduction.
- The room air temperature impacts the airflow characteristics around the human body and the pollution transport. At the low room air temperature of 20 ˚C, the CBL around the seated human body became more concentrated with the peak velocity of 0.24 m/s, while the increasing the room air temperature to 26 ˚C dissolved the CBL and reduced its peak velocity to 0.16 m/s. Reducing the room air temperature increased the standard deviation of air temperature fluctuations in the occupied spaces. It also intensified the transport of the pollution to the breathing zone, which increased personal exposure and reduced the pollution spread across the room.

- Standing thermal manikin creates a narrow CBL which is approximately 5 times less thick compared to seated manikin. A backward inclination of a seated body increased the velocity, air temperature and the standard deviation of temperature fluctuations in the breathing zone. In addition, personal exposure increased when the pollution originated from the human body leaned backwards in the chair. The opposite effect was observed when the seated occupant was leaned forward.
- Clothing insulation and hair on the head have a measurable influence on the airflow in the occupant's breathing zone and they should be carefully considered in CFD simulations and in physical experiments on exposure. The thin and thick clothing ensemble reduced the peak velocity from 0.205 m/s to 0.166 m/s and 0.124 m/s, respectively, while removing the hair increased the peak velocity from 0.17 m/s to 0.187 m/s. Under the conditions studied, clothing and chair design had a minor influence on the velocity and turbulence profiles beyond 5 cm distance from the body. In ventilated spaces, the furniture plays an important role in formation of airflow patterns and should be carefully considered for an optimal ventilation design.
- The presence of the table blocks the rising human convection flow which affects both airflow characteristics in the breathing zone and personal exposure. Closing the gap between the edge of the table and the occupant can be used to reduce the pollution transport to the breathing zone. Keeping the distance between the table and the occupant at 10 cm can increase the amount of pollution/clean air transported from beneath, compared to that in case without the table.
- The location of the source has a considerable influence on personal exposure and the extent to which is spreads. The source located at the human body caused higher personal exposure and lower level of spread into the room air, compared to the pollution emitted further away. The source emitted at the lower body parts reduced personal exposure, but spread more

across the room, compared to the pollutants from the upper body parts. Increasing the distance between the coughing and exposed occupant from 2 to 3 m, reduced the peak exposure by half. In rooms with little air movement, a "well-mixed" mass balance assumption leads to underestimation of the exposure.

- The direction and magnitude of ventilation flow play an important role for airflow distribution in the occupied spaces and it can be used to reduce personal exposure to airborne pollutants while assuring thermal discomfort and saving energy. The downward airflow from above and the transverse from behind of a person created the most unfavourable velocity field that increased personal exposure by 85%, increased draught discomfort and energy use. The upward airflow from below reduced personal exposure, but caused extensive mixing of flow patterns in the breathing zone, attributable to the blocking effect of the furniture. For the pollution sources examined, the most favorable airflow patterns are transverse flow from the front and the side, as they can minimize, or sometimes eliminate, the exposure at the minimum supply air velocity. These airflow directions should therefore be considered in the design of ventilation, when the source location is unknown.
- An increase of the supply air velocity can actually increase personal exposure, depending of the direction of the supplied airflow. In some cases, increasing the velocity of the supplied flow did not provide any additional benefit in terms of reducing personal exposure. There may thus be a non-linear dependence between the amount of the supplied air to the room and personal exposure. Rather than relying on the outdoor air supply rate as a sole indicator of indoor air quality, more attention should be paid to room air distribution.

Practical implications of those results obtained in quiescent indoor environment should be carefully interpreted, since the buoyant flows in occupied spaces and a non-uniform pollutant concentration is less prominent in spaces with higher degree of air mixing. Although the CBL has been shown to have effect on personal exposure, in reality, a person does not always keep

still which is very likely to modify personal exposure. Nevertheless, there are many spaces where occupants perform sedentary tasks and move little during the day, which makes findings of this study relevant. Apart from the occupants' movement, the effect of the human respiration flow have been disregarded is some cases. Study done by Melikov and Kaczmarczyk (2007) reported that the temperature, the relative humidity and the concentration of tracer gas measured in the air inhaled by the breathing thermal manikin were almost the same as those measured close to the upper lip of the non-breathing thermal manikin. Nevertheless, our measurements cannot directly indicate to what extend the results would be changed if the respiratory flow was applied. The expiration would certainly disturb the airflow in the breathing zone; however, the same would presumably quickly re-establish during the inhalation phase. Hence, the airflow distribution, and thus, the pollution concentration in the breathing zone during the inhalation phase would presumably not differ substantially from the results that we reported. Future research should therefore focus more on the human respiratory flow and body movement that may modify airflow and pollutant distribution around a human body.

Another limitation of the present study is that is considers human exposure only to gases and to those small particles that naturally follow the room airflows. Although it gives valuable information on small particle transport mechanisms around a human body, it is difficult to draw a general conclusion about the role of the human CBL in transporting large particles. In addition, our results may not be applicable to all gaseous pollutants, such as ozone. When ozone reacts with the human surfaces (hair, skin, skin oils, clothing, etc.), the CBL becomes depleted of ozone with the lowest concentrations very close to the surface and the highest concentrations in the bulk air region (Rim et al. 2009). Therefore, chemical reactions between the human skin/clothing and pollutants should also be identified as a direction for the future work. Apart from these limitations, the direction for the future work should also include more comprehensive set of indoor environmental conditions and factors, such as: room air

temperatures, ratios between convective and radiant heat exchange from the human body including the effect of skin wetness, clothing levels and body postures, velocities and airflow directions provided by mechanical ventilation, physical room configurations and furniture design, building occupancy types, exposure routes such as the one through dermal absorption, types and location of pollution sources. When studying these factors, it is important to consider their mutual influence since some of them can be mutually contradicting. Although some of these topics require further investigation, several important conclusions can be drawn.

For an adequate exposure description, future studies need to go through the paradigm shift from the coarse total room volume description of the environment to the description that takes into account flow interactions in the human microclimate. In addition, the paradigm shift is needed from a total volume to advanced air distribution that can minimize personal exposure, remove the pollution at the source and provide each occupant possibility to control its own micro-environment, as suggested by Melikov (2012). For the advanced air delivery systems, understanding the CBL will be especially important since they can substantially modulate microclimate and create environments that are not well-mixed. Future research directions should therefore include developing technologies for enhanced micro-environmental control that can control the airflows and pollution distribution around the human body; locally exhaust or clean the pollution, enhance occupant-system interaction; create dynamic furniture/equipment; and provide detached/wearable micro-environmental systems.

BIBLIOGRAPHY

-Andersson, B.J. and Ortengren, R. (1974) Lumbar disc pressure and myoelectric back muscle activity during sitting. 1. Studies on an office chair, Scandinavian Journal of Rehabilitation Medicine;

-ASHRAE (2009) Handbook-Fundamentals (SI), American Society of Heating, Refrigerating and Air-Conditioning Engineers, Inc;

-ASHRAE (2012) Method of Testing General Ventilation Air-Cleaning Devices for Removal Efficiency by Particle Size, ASHRAE Standard 55–2012, Atlanta, Georgia, American Society of Heating, Refrigerating and Air-Conditioning Engineers;

-ANSI/ASHRAE Standard 55 (2013a), Thermal environmental conditions for human occupancy, American Society of Heating, Refrigerating and Air-Conditioning Engineers, Inc;

-ASHRAE (2013b) HVAC Design Manual for Hospitals and Clinics, Atlanta, Georgia, American Society of Heating, Refrigerating and Air-Conditioning Engineers, Inc;

-Anttonen, D.H. (2001) Thermal Manikin in the tests of sleeping bags, Proceedings of the Fourth International Meeting on thermal manikins, Switzerland, September 27-28;

-Assar, S.K. and Block, S.S. (2000), Survival of microorganisms in the environment, In: Disinfection, sterilization, and preservation. Lippinkott-Williams;

-Awbi, H. (2003) Ventilation of buildings, Spon Press;

-Baldwin, P.E.J. and Maynard, A.D. (1998) A survey of wind speeds in indoor workspaces, The Annals of Occupational Hygiene, 42, 303-313;

-Bauman, F.S., Zhang, H., Arens, E.A. and Benton, C.C. (1993) Localized comfort control with a desktop task conditioning system: Laboratory and field measurements, ASHRAE Transactions, 99, 733–749;

-Beggs, C.B. (2003) The airborne transmission of infection in hospital buildings: fact or fiction, Indoor Built Environment, 12, 9–18;

-Bivolarova, M., Melikov, A., Kokora, M., Mizutani, C. and Bolashikov Z. (2014) Novel bed integrated ventilation method for hospital patient rooms, Proceedings of Roomvent 2014, Pages 49-56;

-Bjørn, E., Mattsson, M., Sandberg, M. and Nielsen, V. (1997) Displacement ventilation – effects of movement and exhalation, Proceedings of Healthy Buildings 1997, 163‑8. Washington DC, USA;

-Bjørg, E. and Nielsen, P.V. (2002) Dispersal of exhaled air and personal exposure in displacement ventilation rooms, Indoor Air, 12(3):147-64;

-Bolashikov, Z.D., Melikov, A.K. and Kernek, M. (2009) Improved performance of Personalized Ventilation by Control of the convection flow around occupant body, ASHRAE Transactions;

-Bolashikov, Z.D., Melikov, A. and Krenek, M. (2010) Control of the free convective flow around the human body for enhanced inhaled air quality: Application to a seat-incorporated personalized ventilation unit, HVAC&R Research, volume 16, number 2;

-Bolashikov, Z.D., Nagano, H., Melikov, A.K., Velte, C. and Meyer, K.E. (2011a) Airflow characteristics at the breathing zone of a seated person: passive control over the interaction of the free convection flow and locally applied airflow from front for personalized ventilation application, Roomvent 2011, Norway, Trondheim, Paper ID: 268;

-Bolashikov, Z., Melikov, A., Velte, C., Meyer, KE. (2011b) Airflow characteristics at the breathing zone of a seated person: interaction of the free convection flow and an assisting locally supplied flow from below for personalized ventilation application, Proceedings of Roomvent 2011, Norway, Trondheim;

-Bolashikov Z.D., Melikov A.K., Kierat W., Popiolek Z. and Brand M. (2012a) Exposure of health care workers and occupants to coughed airborne pathogens in a double-bed hospital patient room with overhead mixing ventilation, HVAC&R Research, 18(4):602–615;

-Bolashikov, Z., Nagano, H., Melikov, A.K., Velte, C. and Meyer, K.E. (2012b), Airflow characteristics in the breathing zone of a seated person using desk incorporated pair of confluent jets as personalized ventilation - effect of supply velocities, Proceedings of Healthy Buildings 2012, 8-12 July 2012, Brisbane, session 7A, paper 7A.1;

-Bolashikov, Z., Barova, M. and Melikov, A. (2014) Control of exposure to exhaled air from sick occupant with wearable personal exhaust unit, Proceeding of Indoor Air 2014, Paper ID: HP0876;

-Brohus, H. and Nielsen, P.V. (1995), Personal Exposure to Contaminant Sources in a Uniform Velocity Field, Proceedings of Healthy Buildings, 1555-1560;

-Brohus, H. and Nielsen, P.V. (1996) Personal Exposure in Displacement Ventilated Rooms, Indoor Air, 6, 157–167;

-CDC (2003) Guidelines for environmental infection control in health-care facilities. Atlanta, GA: Center for Disease Control and Prevention;

-Cermak, R. and Melikov, A. (2006) Air quality and thermal comfort in an office with underfloor, mixing and displacement ventilation, International Journal of Ventilation, 5, 323-332;

-Chao, C.Y.H. and Wan, M.P. (2006) A study of the dispersion of expiratory aerosols in unidirectional downward and ceiling-return type airflows using multiphase approach. Indoor Air 16, 296–312;

-Chao, C.Y.H., Wan, M.P., Morawska, L., Johnson, G.R., Ristovski, Z.D., Hargreaves, M., Mengersen, K., Corbett, S., Li, Y., Xie, X. and Katoshevski D. (2009), Characterization of expiratory air jets and droplet size distributions immediately at the mouth opening, Journal of Aerosol Science, 40, 122–33;

-Cho, Y. and Awbi H.B. (2002) Effect of heat source location in a room in the ventilation performance, Proc. Air Distribution in Rooms, Proceedings of Roomvent 2002, Copenhagen, pp.445-448;

-Clark, R.P., and Cox, R.N. (1973) The generation of aerosols from the human body; in Airborne Transmission and Airborne Infection: Concepts and Methods, Wiley, New York, Chap.95, pp. 413-426;

-Clark, R.P., and Edholm, O.G. (1985) Man and his thermal environment, E. Arnold, London;

-Clark, R.P. and Toy N. (1975) Natural convection around the human head, Journal of Physiology 1975, 244:283–93;

-Clark, R.P. and de Galcina-Goff, M.L. (2009) Some aspects of the airborne transmission of infection, Journal of the Royal Society Interface; 6, S767-S782;

-Craven, B.A. and Settles G.S. (2006) A computational and experimental investigation of the human thermal plume, Journal of Fluids Engineering, Vol.128/1251;

-Datla, B.V. and Glauser, M. (2009) Flow Measurements in Indoor Office Environment, Proceedings of Healthy Buildings 2009, Syracuse, USA, Paper 809;

-Dowell, Green, Yuan (2001) Office Seating Behaviors: An Investigation of Posture, Task, and Job Type, Proceedings of the Human Factors and Ergonomics Society 45th Annual Meeting, HFES, Santa Monica, CA;

-Duguid, J.P. (1946) The size and duration of air-carriage of respiratory droplets and droplet nuclei, Journal of Hygiene (London), 44:471-9;

-Duguid, J.P. and Wallace, A.T. (1948) Air infection with dust liberated from clothing, Lancet 2: 845;

-Edwards, D.A., Man, J.C., Brand, P., Katstra, J.P., Sommerer, K., Stone, H.A., Nardell, E. and Scheuch, G. (2004) Inhaling to mitigate exhaled bioaerosols, Proceedings of the National Academy of Sciences, 101, 17383–17388;

-Eisner A.D., Heist D.K., Drake Z.E., Mitchell W.J., Wiener R.W. (2002) On the impact of the human (Child) Microclimate on passive aerosol monitor performance, Aerosol Science and Technology, 36, 803-813;

-Ernst, A. and Zibrak, J.D. (1998) Current concepts - Carbon monoxide poisoning, New England Journal of Medicine 339, 1603 -1608;

-Etheridge D. and Sandberg M. (1996) Building Ventilation: Theory and Measurement, John Wiley and Sons Ltd, Chichester, England;

-Fanger, P.O., Melikov, A.K., Hanzawa, H. and Ring, J. (1988) Air turbulence and sensation of draught, Energy and Buildings, 12, 21-39;

-Ferro, A.R., Kopperud, R.J. and Hildemann, L.M. (2004) Elevated personal exposure to particulate matter from human activities in a residence, Journal of Exposure Analysis and Environmental Epidemiology, 14, S34–S40;

-Fisk, W.J. (2000) Health and productivity gains from better indoor environments and their relationship with building energy efficiency, Annual Review of Energy and Environment 25, 537-566;

-Fitzgerald D. and Haas D.W. (2005) Mycobacterium tuberculosis. In: Mandell GL, Bennett JE, Dolin R, editors. Principles and practice of infectious diseases, 6th edition. Philadelphia: Churchill Livingstone; p. 2852-2886;

-Gbamelé, Y.M., Desevaux, P. and Prenel, J.P. (2000) A method for validating two-dimensional flow configurations in particle streak velocimetry, Journal of fluids engineering, 122(2):438;

-Ge Q., Li X., Inthavong K., Tu J. (2013) Numerical study of the effects of human body heat on particle transport and inhalation in indoor environment, Building and Environment, 59, 1-9;

-Gralton J., Tovey E., McLaws M., and Rawlinson W. (2011) The role of particle size in aerosolised pathogen transmission: A review, Journal of Infection, 62, 1-13;

-Greenwood D., Slack R.C.B., Peutherer J.F. (2002) Medical microbiology, 6th ed. Churchill Livingstone;

-Gupta J.K., Lin C.- H., Chen Q. (2009) Flow dynamics and characterization of a cough, Indoor Air; 19, pp. 517-525;

-Gupta, J.K., Lin, C.-H. and Chen, Q. (2010) Characterizing exhaled airflow from breathing and talking, Indoor Air, 20, 31-39;

-Halvonova B., Melikov A.K. (2010) Performance of “ductless” personalized ventilation in conjunction with displacement ventilation: Impact of disturbances due to walking person(s), Indoor Air, pp. 427-436;

-Hanzawa H., Melikow A.K., Fanger P.O. (1987) Airflow characteristics in the occupied zone of ventilated spaces. ASHRAE Transactions, 93: 524–539;

-Heist, D.K., Eisner, A.D., Mitchell, W. and Wiener, R. (2003) Airflow around a child-size manikin in a low-speed wind environment, Aerosol Science and Technology, 37:303-14;

-Hinds, W.C. (1982) Aerosol Technology, New York, John Wiley & Sons;

-Hinds W.C. (1999) Properties, behaviour and measurement of airborne particles, John Wiley & Sons, Inc.;

-Holmgren H., Bake B., Olin A.C. and Ljungström E. (2011) Relation Between Humidity and Size of Exhaled Particles. Journal of Aerosol Medicine and Pulmonary Drug Delivery 24:5, 253-260;

-Homma, H. and Yakiyama, M. (1988) Examination of free convection around occupant’s body caused by its metabolic heat. ASHRAE Transactions, 94(1):104–24;

-Höppe, P. (1981) Temperature of expired air under varying climatic conditions. International Journal of Biometeorology, 25, 127–132;

-Hyldgaard, C.E. (1994) Humans as a source of heat and air pollution, Proceedings of Roomvent 1994, 4th International Confefence on Air Distribution in Rooms, Krakow, Poland, pp. 414-433;

-Hyldgaard, C.E., Thermal Plumes above a Person. In: Proceedings of the 6th International Conference on Air Distribution in Rooms – Roomvent, Stockholm, Sweden, Vol. 1, p. 407-413, (1998);

-Ijaz M.K., Brunner A.H., Sattar S.A., Nair R.C. and Johnson-Lussenburg C.M. (1985) Survival characteristics of airborne human coronavirus 229E, Journal of General Virology 66, 2743-8;

-INSIGHT 3G^{TM} TSI software platform. Instruction manual 2004;

-ISO, International Standard ISO/DIS/7730 (2005) Moderate Thermal Environments-Determination of PMV and PPD Indices and Specification of the Conditions for Thermal Comfort: International Standard Organization for Standardization, Geneva, Switzerland;

-Jeong, J.W. and Mumma, S. (2006) Designing a Dedicated Outdoor Air System with Ceiling Radiant Cooling Panels, ASHRAE Journal Vol. 48;

-Johnson, A.E., Fletcher, B. and Saunders, C.J. (1996) Air movement around a worker in a low-speed flow field, Annals of Occupational Hygiene, 40:57-64;

-Kofoed, P. (1991) Thermal plumes in ventilated rooms, Ph.D. Thesis, Department of Building Technology and Structural Engineering, Aalborg University, Denmark;

-Kulpmann, R.W. (1993), Thermal comfort and Air Quality in Rooms with Cooled Ceilings – Results of Scientific Investigation, ASHRAE Transactions 99 (2): 488-502;

-Kühn, M., Ehrenfried, K., Bosbach, J. and Wagner, C. (2008) Feasibility study of tomographic Particle Image Velocimetry for large scale convective airflow, Proceedings 14th International Symposium on Applications of Laser Techniques to Fluid Mechanics, Lisbon, Portugal;

-Lai, M.Y, Cheng, P.K and Lim, W.W. (2005) Survival of severe acute respiratory syndrome coronavirus. Clinical Infectious Diseases; 41:67-71;

-Laverge, J., Novoselac A., Corsi R. and Janssens A. (2013) Experimental assessment of exposure to gaseous pollutants from mattresses and pillows while asleep, Building and Environment, 59, 203‑210;

-Lewis, H.E., Foster, A.R., Mullan, B.J., Cox, R.N., and Clark, R.P. (1969) Aerodynamics of the Human Microenvironment, The Lancet, 322 (7609), pp.1273–1277;

-Li, Y., Leung, G. M., Tang, J. W., Yang, X., Chao, C. Y. H., Lin, J. Z., Lu, J. W., Nielsen, P. V., Niu, J., Qian, H., Sleigh, A.C., Su, H.-J. J., Sundell, J., Wong, T. W. and Yuen, P. L. (2007) Role of ventilation in airborne transmission of infectious agents in the built environment – a multidisciplinary systematic review, Indoor Air 17, 2–18;

-Li, X., Inthavong, K, Ge, Q. and Tu, J. (2013) Numerical investigation of particle transport and inhalation using standing thermal manikins. Building and Environment; 60:116-125;

-Liu, W., Mazumdar, S., Zhang, Z., Poussou, S.B., Liu, J., Lin, C-H. and Chen Q. (2012) State-of-the-art methods for studying air distributions in commercial airliner cabins, Building and Environment, 47:5-12;

-Louis M.E.S. and Hess J.J. (2008) Climate Change: Impacts on and Implications for Global Health, American Journal of Preventive Medicine, 35(5);

-Madsen, T. L. and Popiolek, Z. (1994) An instrument for draught measurements caused by fluctuations in air temperature and/or velocity, Proceedings of Roomvent 1994, Volume 2, Cracow, Poland, 1994, pp. 336-345.

-Marr D., Khan T., Glauser M., Higuchi H. and Jianshun Z.D. (2005) On Particle Image Velocimetry (PIV) Measurements in the Breathing Zone of a Thermal Breathing Manikin, ASHRAE Transactions, Vol. 111 Issue 2, p299;

-McCullough E.A, Jones B.W. and Tamura T. (1985) A comprehensive database for estimation clothing insulation. ASHRAE Transactions, 91 (2):29-47;

-McCullough E.A., Zibokowski P.J. and Jones B.W (1987) Measurement and prediction of the insulation provided by bedding system, ASHRAE Transactions, 93 (1):1055-1068;

-McCullough E.A., Olesen B.W. and Hong S. (1994a) Thermal insulation provided by chairs. ASHRAE Transactions, 88 (2):791-805;

-McCullough E.A., Hong S. (1994b) A database for determining the decrease in clothing insulation due to body motion. ASHRAE Transactions, 100 (1):765-775;

-McDonagh, A. and Byrne, M.A. (2014) A study of the size distribution of aerosol particles resuspended from clothing surfaces. Journal of Aerosol Science, 75, 94-103;

-McGinley, K.J., Marples, R.R. and Plewig, G. (1969) A method for visualizing and quantitating the desquamating portion of the human stratum corneum. Journal of Investigative Dermatology, 53 (2), 107–11;

-Melikov, A.K. and Langkilde, G. (1990) Displacement ventilation - Airflow in the near zone. Proceedings of ROOMVENT'90, Session B1- 3, Paper 23, Oslo, Norway, June 13-15, 1990;

-Melikov, A.K., and Zhou, G. (1996) Air movement at the neck of the human body. Proceedings of Indoor Air 1996, Nagoya, Japan (1):209–14;

-Melikov, A.K., Kruger, U., Zhou, G., Madsen, T.L. and Langkilde, G. (1997), Air Temperature Fluctuations in Rooms, Building and Environment, 32, 101-114;

-Melikov, A.K., Cermak, R., Kovar, O. and Forejt, L. (2003) Impact of airflow interaction on inhaled air quality and transport of contaminant in rooms with personalized and total volume ventilation, Proceedings of Healthy Building 2003, Singapore, 2, 592–597;

-Melikov, A.K. (2004) Breathing thermal manikins for indoor environment assessment: important characteristics and requirements, European Journal of Applied Physiology, 92: 710–713;

-Melikov, A.K. (2004) Personalized ventilation. Indoor Air 14(Suppl. 7), 157–167;

-Melikov A.K. and Kaczmarczyk, J. (2007) Measurement and prediction of indoor air quality using a breathing thermal manikin. Indoor Air, 17(1):50-9;

-Melikov A.K., Ivanova T. and Stefanova G. (2007) Seat incorporated personalized ventilation, Proceedings Roomvent 2007:1318;

-Melikov, A.K. and Dzhartov V. (2009) Control of the free convection flow around human body by radiant cooling, Proceedings of Healthy Building 2009, Syracuse, Paper: 620;

-Melikov, A.K., Bolashikov, Z.D., Kierat, W., Popiolek, Z. and Brand, M. (2010) Does increased ventilation help reduce cross-infection in isolation hospital wards? In: Proceedings of Clima 2010, Antalya, Turkey, Paper R7-TS39-OP02;

-Melikov A.K., Bolashikov Z.D. Nagano H., Velte C. and Meyer K.E. (2011) Airflow characteristics at the breathing zone of a seated person: Active control over the interaction of the free convection flow and locally applied airflow from front for personalized ventilation application, Roomvent 2011, Norway, Trondheim, Paper ID: 278;

-Melikov, A.K. (2011) Advanced air distribution, ASHRAE Journal, pp. 73-78;

-Melikov, A.K. and Kaczmarczyk, J. (2012) Air movement and perceived air quality, Building and Environment, 47, 400–409;

-Melikov, A.K. (2012) Creating benefits for all in the design of the indoor environment, Yearly report of the Department of Civil Engineering, Technical University of Denmark, p. 19;

-Melikov, A.K. and Dzhartov, V. (2013) Advanced air distribution for minimizing airborne cross-infection in aircraft cabins, HVAC&R Research, 19, 926-933;

-Morawska, L. (2006) Droplet fate in indoor environments, or can we prevent the spread of infection? Indoor Air, 16: 335–347;

-Morawska, L., Johnson, G.R., Ristovski, Z.D., Hargreaves, M., Mengersen, K., Corbett, S., Chao, C.Y.H., Li Y. and Katoshevski, D. (2009) Size distribution and sites of origin of droplets expelled from the human respiratory tract during expiratory activities, Journal of Aerosol Science, vol. 40, issue 3, pp. 256-269;

-Mundt, E. (1995) Displacement ventilation systems - convection flows and temperature gradients, Building and Environment; 30(1):129-33;

-Murakami, S., Kato, S. and Zeng, J. (1997) Flow and temperature fields around human body with various room air distribution, CFD study on computational thermal manikin - Part 1. ASHRAE Transactions 103 (1), S.3-15;

-Murakami, S., Ohira N. and Kato S. (1999) CFD analysis of a thermal plume and the indoor airflow using k-epsilon models with buoyancy effects, Flow, Turbulence and Combustion, 63:113-134;

-Murakami, S., Kato, S., and Zeng, J. (2000) Combined Simulation of Airflow, Radiation and Moisture Transport for Heat Release From a Human Body, Building and Environment 35, 6, pp. 489–500;

-Murakami, S. (2004) Analysis and design of micro-climate around the human body with respiration by CFD, Indoor Air, 14 (Suppl 7): 144–156;

-Nicas M., Nazaroff W.W. and Hubbard A. (2005) Toward understanding the risk of secondary airborne infection: mission of respirable pathogens. Journal of Occupational and Environmental Hygiene; 2:143-54;

-Nielsen P.V., Displacement Ventilation - Theory and Design. AUC, 1993;

-Nielsen P.V., Bartholomaeussen N.M., Jakubowska E., Jiang H., Jonsson O.T. and Krawiecka K. (2007) Chair with integrated personalized ventilation for minimizing cross infection, Proceedings of Roomvent 2007:1078;

-Nielsen, P.V., Hyldgaard, C.E., Melikov, A., Andersen, H. and Soennichsen, M. (2007) Personal exposure between people in a room ventilated by textile terminals: with and without personalized ventilation, HVAC&R Research, 13, 635–643;

-Nielsen P.V., Jensen R.L., Litewnicki M. and Zajas J. (2009) Experiments on the Microenvironment and Breathing of a Person in Isothermal and Stratified Surroundings, Proceedings of Healthy Buildings 2009, Syracuse, USA, Paper 374;

-Noble, W.C., Habbema, J.D.F., van Furth, R., Smith, I. and de Raay, C. (1976) Quantitative studies on the dispersal of skin bacteria into the air, Journal of Medical Microbiology, 9, 53–61;

-Olesen B.W., Sliwinska E., Madsen T.L. and Fanger P.O. (1982) Effect of Body Posture and Activity on the Thermal Insulation of Clothing: Measurements by a Movable Thermal Manikin. ASHRAE Transactions, 88(2), 791-805;

-Özcan, O., Meyer, K.E. and Melikov A. (2003) Turbulent and stationary convective flow field around the head of a human, Proceedings of International Symposium on Turbulence, Heat and Mass Transfer — THMT-03, Antalya, Turkey;

-Özcan, O., Meyer, K.E. and Melikov A. (2005) A visual description of the convective flow field around the head of a human, Journal of Visualization 8(1): 23–31;

-P.T. Teknik Limited, Denmark, http://pt-teknik.dk/;

-Pantelic J, Sze To G.N., Tham K.W., Chao C.Y.H. and Khoo Y.C.M. (2009) Personalized ventilation as a control measure for airborne transmissible disease spread, Journal of Royal Society Interface, 6, pp. 715-726;

-Pantelic, J. and Tham, K.W. (2013) Adequacy of air change rate as the sole indicator of an air distribution system's effectiveness to mitigate airborne infectious disease transmission caused by a cough release in the room with overhead mixing ventilation: A case study, HVAC&R Research, 19, 947-961;

-Papineni, R.S. and Rosenthal, F.S. (1997) The size distribution of droplets in the exhaled breath of healthy human subjects, Journal of Aerosol Medicine, 10, 105–116;

-Pokora P. and Melikov A. (2014) Occupant body movement and seat occupancy rate for design of desk micro-environment, In: Proceedings of Roomvent 2014, Sao Paolo, Brazil, Paper ID 130;

-Popiolek, Z., Bolashikov Z., Kostadinov K., Kierat W. and Melikov A. (2012) Exposure of health care workers and occupants to coughed air in a hospital room with displacement air distribution: impact of ventilation rate and distance from coughing patient. Proceedings of Healthy Buildings 2012, June 8–12, Brisbane, Australia;

-Poussou S.B., Mazumdar S., Plesniak M.W., Sojka P.E., Chen Q. (2010) Flow and contaminant transport in an airliner cabin induced by a moving body: model experiments and CFD predictions. Atmospheric Environment; 44:2830–2839;

-Qian H., Li Y., Nielsen P.V., Hyldgaard C.E., Wong T.W., Chwang A.T.Y. (2006) Dispersion of exhaled droplet nuclei in a two-bed hospital ward with three different ventilation systems, Indoor Air, 16:111-128;

-Qian, J., Peccia, J. and Ferro, A.R. (2014), Walking-induced particle resuspension in indoor environments, Atmospheric Environment, 89, 464-481;

-Riffat, S.B., Zhao, X. and Dohert, P.S. (2004) Review of research into and application of chilled ceilings and displacement ventilation systems in Europe, International Journal of Energy Research 2004; 28: 257-286;

-Rim D. and Novoselac, A. (2009) Transport of particulate and gaseous pollutants in the vicinity of a human body, Building and Environment, 44, 1840-1849;

-Rim, D. and Novoselac, A. and Morrison, G. (2009) The influence of chemical interactions at the human surface on breathing zone levels of reactants and products, Indoor Air, 19, 324–334;

-Rim, D. and Novoselac, A. (2010) Occupational exposure to hazardous airborne pollutants: effects of air mixing and source characteristics, Journal of Occupational Environmental Hygiene, 7, 683-692;

-Roberts, D., Marks, R. (1980) The determination of regional and age variations in the rate of desquamation: a comparison of four techniques, Journal of Investigative Dermatology, 74:13-6;

-Salmanzadeh, M., Zahedi, Gh., Ahmadi, G., Marr, D.R. and Glauser, M. (2012) Computational modeling of effects of thermal plume adjacent to the body on the indoor airflow and particle transport, Journal of Aerosol Science, 53, 29–39;

-Settles, G. (2001) Schlieren and shadowgraph techniques: Visualizing phenomena in transparent media, Berlin, Germany, Springer-Verlag;

-Singh, A., Hosni, M.H. and Horstman, R.H. (2002) Numerical simulation of airflow in an aircraft cabin section, ASHRAE Transactions, 108(1):1005–1013;

-Sørensen, D.N. and Voigt, L.K. (2003) Modelling flow and heat transfer around a seated human body, Building and Environment 38, 753-762;

-Spengler, J.D. and Sexton, K. (1983) Indoor air pollution: A public health perspective. Science 221:9-17;

-Spitzer, I.M., Marr, D.M. and Glauser, M.N. (2010) Impact of manikin motion on particle transport in the breathing zone, Journal of Aerosol Science, 41, 373–383;

-Sun, Y. and Zhang, Y. (2007) An overview of room air motion measurement: Technology and application. HVAC&R Research, Volume 13, Number 6;

-Sundell, J., Levin, H., Nazaroff, W. W., Cain, W. S., Fisk, W. J., Grimsrud, D. T., Gyntelberg, F., Li, Y., Persily, A. K., Pickering, A. C., Samet, J. M., Spengler, J. D., Taylor, S. T. and Weschler, C. J. (2011) Ventilation rates and health: multidisciplinary review of the scientific literature, Indoor Air, 21, 191–204.

-Sze, To, G.N., Wan, M.P., Chao, C.Y.H., Fang, L. and Melikov, A.K. (2009) Experimental study of dispersion and deposition of expiratory aerosols in aircraft cabins and impact on infectious disease transmission. Aerosol Science and Technology 43, 466–485;

-Tang, J.W., Liebner, T.J., Craven, B.A. and Settles, G.S (2009) A Schlieren optical study of the human cough with and without wearing masks for aerosol infection control, Journal of the Royal Society Interface, Vol.6, Supplement 6, S727-S736;

-Tang, J.W, Nicolle, A.D., Klettner, C.A., Pantelic, J., Wang, L. (2013) Airflow Dynamics of Human Jets: Sneezing and Breathing - Potential Sources of Infectious Aerosols. PLoS ONE 8(4): e59970. doi:10.1371/journal.pone.0059970;

-Tavoularis S. (2005) Measurement in Fluid Mechanics, Cambridge University Press, New York, NY;

-Tham K.W. and Pantelic J. (2010) Performance evaluation of the coupling of a desktop personalized ventilation air terminal device and desk mounted fans. Building and Environment 45, 1941–1950;

-Tham K.W., Pantelic J. (2012) Adequacy of air exchange rate as a sole indicator of air delivery system's protective effectiveness against airborne infections disease transmission, Proceedings of Healthy Buildings;

-Thatcher, T.L. and Layton, D.W. (1995) Deposition, resuspension, and penetration of particles within a residence, Atmospheric Environment, 29, 1487–1497;

-TSI INSIGHT 3G^{TM} software platform (2004) Instruction manual;

-Voelker, C., Maempel, S. and Kornadt, O. (2014) Measuring the human body's microclimate using a thermal manikin, Indoor Air; DOI: 10.1111/ina.12112;

-Wallace, L. (2000) Correlations of personal exposure to particles with outdoor air measurements: A review of recent studies, Aerosol Science and Technology, 32, 1, 15-25.

-Welling, I., Andersson, I., Rosen, G., Raisanen, J., Mielo, T., Marttinen, K. and Niemela R. (2000), Contaminant Dispersion in the Vicinity of a Worker in a Uniform Velocity Field, Annals of Occupational Hygiene, 44, 219-225;

-Wells, W.F. (1934) On air-borne infection study: II – droplets and droplet nuclei, American Journal of Hygiene, 20, 619–627;

-Wysocki, C. and Preti, G. (2004) Facts, fallacies, fears, and frustrations with human pheromones, The anatomical record, Discoveries in molecular, cellular, and evolutionary biology, 281, 1201-1211;

-Xie, X., Li, Y., Chwang, A.T.Y., Ho, P.L. and Seto, E.H. (2007) How far droplets can move in indoor environments: revisiting the Wells evaporation-falling curve. Indoor Air, 17, 211-225;

-Yang, S., Lee, G.W.M., Chen, C-M., Wu, C.C. and Yu K.P. (2007) The size and concentration of droplets generated by coughing in human subjects. Journal of Aerosol Medicine, 20(4):484–94;

-Yang, B., Melikov, A. and Sekhar, C. (2009) Performance evaluation of ceiling mounted personalized ventilation system, ASHRAE Transactions, 115, 395-406;

-Yang, J., Sekhar, C., Cheong, D.K.W. and Raphael, B. (2013) Computational fluid dynamics study and evaluation of different personalized exhaust devices, HVAC&R Research, 19, 934–946;

-Yang, J., Sekhar, C., Cheong, D.K.W. and Raphael, B. (2014) Performance evaluation of a novel personalized ventilation–personalized exhaust system for airborne infection control. Indoor Air, DOI: 10.1111/ina.12127;

-Zhao, B., Zhang, Z. and Li, X. (2005) Numerical study of the transport of droplets or particles generated by respiratory system indoors, Building and Environment, 40, 1032–1039;

-Zhu, S., Kato, S., Murakami, S. and Hayashi, T. (2005) Study on inhalation region by means of CFD analysis and experiment, Building and Environment, 40, 1329-1336;

-Zhu, S.W., Kato, S. and Yang, J.H. (2006) Investigation into airborne transport characteristics of air-flow due to coughing in a stagnant room environment, ASHRAE Transactions, 112, pp. 123-133;

-Zukowska, D, Melikov, A and Popiolek, Z (2007) Thermal plume above a simulated sitting person with different complexity of body geometry. In: Proceedings of the 10th International Conference on Air Distribution in Rooms - Roomvent 2007, Helsinki, Vol. 3, pp. 191-198;

-Zukowska, D., Popiolek, Z. and Melikov, A. (2010) Determination of integral characteristics of an asymmetrical thermal plume from air speed/velocity and temperature measurements, Experimental Thermal and Fluid Science, 34, pp. 1205-1216;

-Zukowska, D., Melikov, A.K. and Popiolek, Z. (2012) Impact of personal factors and furniture arrangement on the thermal plume above a sitting occupant, Building and Environment 49, 104-116.

APPENDICES

Appendix A. Supplementary PIV data

Appendix A.1 PIV system description

The PIV system consists of dual YAG laser (New Wave Research, Inc., Fremont, CA, USA), double-pulse 190 mJ and a wavelength of 532 nm, 2MP CCD camera (28 mm lens) that offers 1600 × 1200 pixel resolution and possibility to generate 32 frames per second, synchronizer and the computer. The f-number of the camera (ratio of the lens's focal length and effective diameter of the aperture) was set to 5.6 to reduce light scattering from the surface of the manikin. PIV images were processed and analyzed using INSIGHT 3G software (Version 9.1.0.0. TSI Inc.). No filters or image post-processing functions were applied.

Appendix A.2 Optimal number of images - independence test

Independence test was performed to ensure the optimal number of image pairs necessary to be captured and averaged for this study. A set of 360, 450, 540, 630 and 720 image pairs was averaged and mutually compared. It was found that for each set of measurements, 540 image pairs was a representative number above which variation in velocity became negligible (<3%). This number of images corresponds close to one minute of the flow. Considering an inherent unsteadiness of the turbulent flow around the thermal manikin, a higher number of image pairs would be desirable to obtain a smoother velocity profile, which was impracticable due to a long image processing time.

Appendix A.3 Details on the PIV parameters.

Optimal seeding particle diameters need to be large enough with respect to pixel size to be visible to the camera and small enough to trace a natural fluid motion without altering any fluid properties. In addition, seeding must be uniform to obtain an accurate velocity data. Stokes number that determines the degree of coupling between the particle phase and the fluids was close to zero (density of air and olive oil seeding flow is very similar), which suggested that the particles behaved like tracers, i.e. tracking error was assumed to be negligible. As shown in Fig. 5, manikin's feet were placed through an elliptical hole in the top surface of the seeding rectangular box (0.4 x 0.45 x 0.28 m). Prior to each set of measurements, seeding box was filled with seeding particles. To ensure the optimal seeding, characteristics of the seeding flow in lower leg region were compared with the flow characteristics in the same region before the seeding took place. This was done by measuring the velocity with omnidirectional anemometers positioned in a way to minimally disrupt a natural convection flow. No signs of forced convection were observed. To further ensure that the seeding particles rose solely due to buoyancy forces, the thermal function of the manikin was switched off. In this scenario, seeding particles did not rise, which suggests that the particle movement were induced by natural convection in all the experiments.

Prior to velocity measurements, a calibration process was performed to ensure accurate results in case that camera shifts occurred in between measurements. This involves a metric ruler as a calibration target (accuracy within 0.5 mm), to obtain geometrical data necessary to compute the flow velocity. In order to protect the camera CCD chip from unwanted laser reflections, a thin black piece of paper that precisely followed the contours of the manikin was used to block the reflective surface of the manikin. Black paper was positioned 10 cm away from the measurement plane in order to avoid obstruction of the natural flow. This caused a velocity

data loss in the vicinity of the manikin surface (2 mm in width). Another reason for data loss in the same region is the inability to obtain velocity measurements closer to the surface than half of the width of the interrogation cell (1 mm), since PIV vectors are local averages over the cell of interrogation. Two pieces of black cloth were placed 2 m behind the manikin and behind the measurement plane to minimize hazardous light scattering and better visualization of the seeding particles.

Increasing the image field of view generates a higher velocity standard deviation. A higher value of velocity standard deviation (36.5%) for the larger target field of view (20 x 27.5 cm) was obtained, compared to standard deviation of 20.5% for a smaller field of view (20 x 15 cm). This is attributed to the fact that the flow is steadier closer to the human body due to lower local Reynolds number which stabilized the flow field (as shown in results section), compared to an increased unsteadiness (turbulence levels) that exists further away from the body that is associated with a larger field of view. Another reason for this is that further away from the body surface the flow is highly unsteady causing less seeding uniformity, and thus higher SD compared to the smoother velocity fields in the regions closer to the body surface. Furthermore, the larger the interrogation area, the lower percentage of spurious vectors and processing time exist. This is at the expense of lower spatial resolution, which is required to accurately represent the nature of the flow. For the purpose of characterization of the whole CBL in front of the thermal manikin, 64 x 64 pix^2 interrogation area was considered sufficiently accurate, while the more detailed, Recursive Nyquist processor, was used in the Set 2 experiments, starting with 64 x 64 pix^2, and ending with 32 x 32 pix^2 interrogation area. In both scenarios on average, less than 3% of spurious vectors were detected. Details about PIV parameters are shown in Table A.3.

Table A.1 PIV parameters for Set 1 and Set 2 experiment

	Number of image pairs	Field of view	Interrogation area	Number of vectors per image	Velocity Standard Deviation
Set 1	540	27.5 x 20 cm	64 x 64 pix^2	49 x 36	36.5%
Set 2	540	20 x 15 cm	32 x 32 pix^2	96 x 72	20.5%

Appendix A.4 Comparison between PIV and a hot-wire anemometer

PIV results validation is a challenge since there is no other non-intrusive technique capable of performing instantaneous measurements in a large area. For the purpose of this study, comparison between PIV and a hot-wire anemometer (Anemomaster Model A031) was conducted as an attempt to compare measurements along X-axis in the breathing zone of the manikin, in the same manner as described in Set 2 experiments. A calibrated anemometer (±0.02 m/s accuracy, taking into account temperature fluctuations along X-axis), mounted on the traversing system, recorded the velocity in multiple points along X-axis during 5 min period and 1 second recording interval. The results were found to be in a good agreement with PIV velocity data that correspond to 540 time-averaged image pairs. A relative difference between PIV and anemometer velocity data along X-axis was less than 8% (Figure A.4).

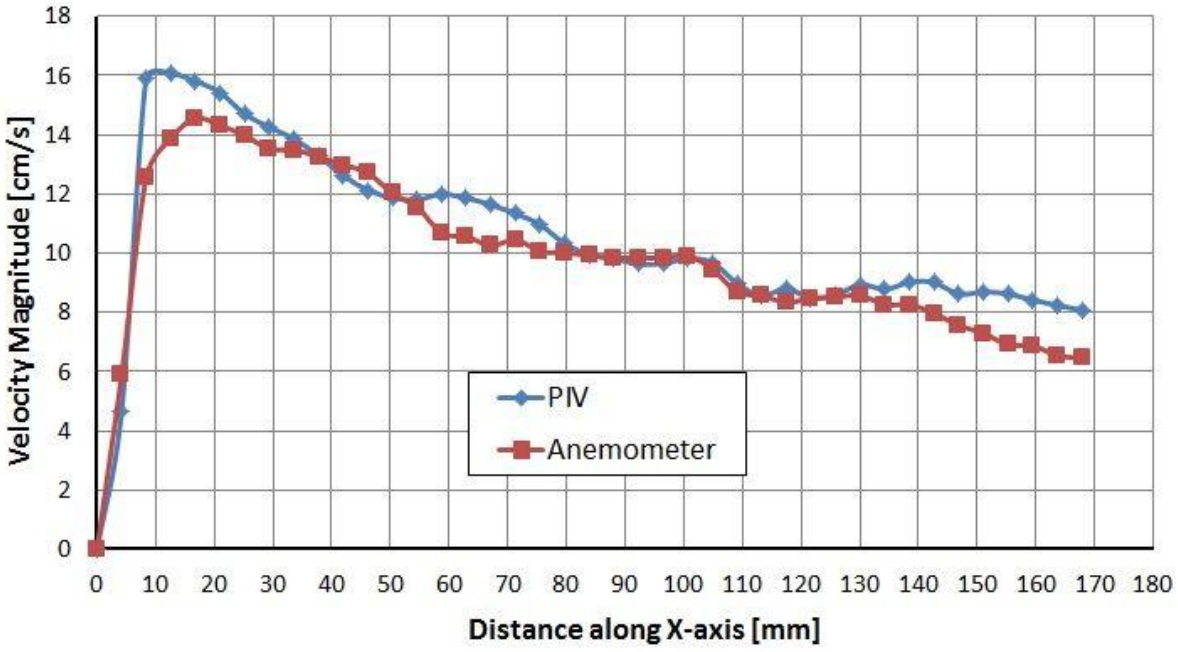

Figure A1 Comparison of PIV results with a hot-wire anemometer in the breathing zone of the thermal manikin.

Appendix B. Peer-reviewed publications from this PhD thesis

1. **Licina, D., Melikov A., Sekhar, C., Tham, K.W.** (2015) Air temperature investigation in microenvironment around a human body, Building and Environment, 92, 39-47.

2. **Licina, D., Melikov A., Sekhar, C., Tham, K.W.** (2015) Transport of Gaseous Pollutants by Convective Boundary Layer around a Human Body, Science and Technology for the Built Environment, DOI: 10.1080/23744731.2015.1060111.

3. **Licina, D., Melikov A., Pantelic J., Sekhar, C., Tham, K.W.** (2015) Human convection flow in spaces with and without ventilation: Personal exposure to floor released particles and cough released droplets, Indoor Air, DOI: 10.1111/ina.12177.

4. **Licina, D., Melikov A.K., Sekhar, C., Tham, K.W.** (2015) Human convective boundary layer and its interaction with room ventilation flow, Indoor Air, 25, 21-35. DOI: 10.1111/ina.12120.

5. **Licina, D., Pantelic, J., Melikov, A., Sekhar, C., Tham, K.W.** (2014) Experimental investigation of the human convective boundary layer in a quiescent indoor environment, Building and Environment, 75, 79-91.